

NMR HYDROPHILIC METABOLOMIC ANALYSIS OF BACTERIAL RESISTANCE
PATHWAYS USING MULTIVALENT QUATERNARY AMMONIUM
ANTIMICROBIALS IN *ESCHERICHIA COLI* AND *BACILLUS CEREUS*
EXPOSED TO DABCO AND MANNOSE FUNCTIONALIZED
DENDRIMERS

by

Michelle Lynne Aries

A dissertation submitted in partial fulfillment
of the requirements for the degree

of

Doctor of Philosophy

in

Biochemistry

MONTANA STATE UNIVERSITY
Bozeman, Montana

December 2021

©COPYRIGHT

by

Michelle Lynne Aries

2021

All Rights Reserved

ACKNOWLEDGEMENTS

I would like to thank my advisor, Professor Mary Cloninger for all of her help and support all these years. I am grateful to have been able to learn and conduct research under such a smart, caring, and knowledgeable person I would also like to thank Professor Mary Cloninger for guidance, funding (NIGMS 62444), and the use of equipment and supplies. For providing the bacterial stocks and mutants used in this research, I would like to thank Professor Mary Cloninger, the Cloninger Lab, and Dr. Harrison VanKoten. I am thankful for the help and advice Dr. Candace Goodman gave me when I was starting out. I grateful to Dr. Brian Tripet and Dr. Mary Cloud Ammons, who helped to develop the procedures for metabolite extraction and analysis. Dr. Brian Tripet also helped with NMR procedures. I would like to thank Dr. Valérie Copié and the Copié Lab for use of equipment. I am thankful to Professor Mike Franklin and the Franklin Lab for instruction and for the use of their NanoDrop and Bioanalyzer. I would especially like to thank Dr. Kerry Williamson from the Franklin Lab for teaching me how the NanoDrop and Bioanalyzer function, for answering my questions, and for giving me time on the Bioanalyzer. I am thankful to Professor Ed Dratz and the Dratz lab for use of their lab equipment and for advice. I would like to thank my committee members, Dr. Mary Cloninger, Dr. Ed Dratz, Dr. Brian Bothner and Dr. Sandra Halonen, for all their time and effort. I would like to thank Donna Negaard for all of her assistance, support, and advice. I greatly appreciate the use of equipment and assistance provided by all these people throughout my time here; this research would not have been possible without them.

TABLE OF CONTENTS

1. INTRODUCTION	1
Organization and Summary	11
References	14
2. NMR METABOLOMIC ANALYSIS OF BACTERIAL RESISTANCE PATHWAYS USING MULTIVALENT QUARTERNARY AMMONIUM FUNCTIONALIZED MACROMOLECULES.....	20
Contribution of Authors and Co-Authors	20
Manuscript Information Page	21
Abstract	22
Introduction.....	23
Methods.....	28
Results.....	33
Discussion	39
Conclusion	43
References.....	46
3. NMR HYDROPHILIC METABOLOMIC ANALYSIS OF BACTERIAL RESISTANCE PATHWAYS USING MULTIVALENT ANTIMICROBIALS WITH CHALLENGED AND UNCHALLENGED WILD TYPE AND MUTATED GRAM-POSITIVE BACTERIA.....	51
Contribution of Authors and Co-Authors	51
Manuscript Information Page	52
Abstract	53
Introduction.....	54
Methods.....	62
Results.....	67
Discussion	91
General Comparisons between Metabolite Levels	92
Significance of Metabolite Changes	97
Metabolomic Comparison of Gram-Positive and Negative Bacterial Exposure to DABCOMD	99
Conclusion	101
References.....	105

TABLE OF CONTENTS CONTINUED

4. DISCUSSION AND COMPARISON OF BOTH THE <i>ESCHERICHIA COLI</i> AND THE <i>BACILLUS CEREUS</i> RESULTS.....	111
<i>Escherichia coli</i>	112
<i>Bacillus cereus</i>	115
Comparison of Gram-Negative and Gram-Positive Bacteria Metabolomics Data.....	119
References.....	122
5. CONCLUSIONS.....	125
DABCOMD likely Mechanism of Action	127
Gram-negative: <i>Escherichia coli</i>	127
Gram-positive: <i>Bacillus cereus</i>	129
Future Work.....	131
References.....	133
APPENDICES	136
APPENDIX A: Supplementary Materials for Chapter 2: <i>E. coli</i> Manuscript.....	137
Table of Contents.....	138
Methods.....	139
Data.....	145
References.....	157
APPENDIX B: Supplementary Materials for Chapter 3: <i>B. cereus</i> Manuscript	158
Table of Contents	159
Methods.....	160
Data	164
References.....	224
APPENDIX C: RNA Project	225
RNA Work Overview	226
Zymo Research RNA Extraction Procedures and Modifications	229
Starting Procedures	230
Final Procedure Modifications.....	235

TABLE OF CONTENTS CONTINUED

Qiagen RNA Extraction Procedures and Modifications	239
Starting Procedures	239
Viable RNA Data.....	243
Final Procedure Modifications.....	244
References.....	249
CUMULATIVE REFERENCES CITED	250

LIST OF TABLES

Table	Page
2.1. Fold change of statistically significant metabolites in their corresponding metabolic pathway for the mid log and the stationary phase.....	38
3.1. Sample sets used in this study.....	62
3.2. Fold change of statistically significant metabolites in their corresponding metabolic pathways for the mid log phase of mutant versus wild type.....	80
3.3. Fold change of statistically significant metabolites in their corresponding metabolic pathways for the mid log phase of DABCOMD challenged mutant versus DABCOMD challenged wild type	81
3.4. Fold change of statistically significant metabolites in their corresponding metabolic pathways for the stationary phase of mutant versus wild type.....	82
3.5. Fold change of statistically significant metabolites in their corresponding metabolic pathways for the stationary phase of DABCOMD challenged mutant versus DABCOMD challenged wild type	83
3.6. Fold change of statistically significant metabolites in their corresponding metabolic pathways for the mid log phase of DABCOMD challenged wild type versus unchallenged wild type.....	84
3.7. Fold change of statistically significant metabolites in their corresponding metabolic pathways for the stationary phase of DABCOMD challenged wild type versus unchallenged wild type.....	85
3.8. Fold change of statistically significant metabolites in their corresponding metabolic pathways for the mid log phase of DABCOMD challenged mutant versus unchallenged mutant	87

LIST OF TABLES CONTINUED

Table	Page
3.9. Fold change of statistically significant metabolites in their corresponding metabolic pathways for the stationary phase of DABCOMD challenged mutant versus unchallenged mutant	88
3.10. Fold change of statistically significant metabolites in their corresponding metabolic pathways for the mid log phase of DABCOMD challenged wild type versus unchallenged mutant	90
3.11. Fold change of statistically significant metabolites in their corresponding metabolic pathways for the stationary phase of DABCOMD challenged wild type versus unchallenged mutant	91
A1. All Metabolites Identified using the Chenomx NMR Suite 8.2 Software Profiling Program and Metabolite Library.....	149
B1. All Metabolites Identified using the Chenomx NMR Suite 8.4 Software Profiling Program and Metabolite Library.....	165
B2. Fold change of statistically significant metabolites in their corresponding metabolic pathways for the mid log phase of DABCOMD challenged mutant versus unchallenged wild type.....	175
B3. Fold change of statistically significant metabolites in their corresponding metabolic pathways for the stationary phase of DABCOMD challenged mutant versus unchallenged wild type.....	176
B4. The Identification Number Corresponding to Pathways Found in Pathway Analysis for Figures B25 – B36	195
C1. Concentration and absorbance NanoDrop data demonstrating nonviable RNA	232

LIST OF TABLES CONTINUED

Table	Page
C2. Demonstrates the improvement in concentration and more pure samples, but the RNA is still nonviable as determined by the NanoDrop.....	233
C3. Demonstrates the RNA is nonviable as determined by the NanoDrop.....	241
C4. Demonstrates viable RNA as determined by the NanoDrop.....	243

LIST OF FIGURES

Figure	Page
1.1. Structure of C ₁₆ -DABCO Mannose Functionalized Dendrimer (DABCOMD)	3
1.2. Illustration of DABCOMD attacking bacteria	13
2.1. Structure of C ₁₆ -DABCO Mannose Functionalized Dendrimer (DABCOMD)	27
2.2. Overview of procedures	29
2.3. A Example ¹ H NMR spectra B Hierarchical Clustering.....	34
2.4. A 2D sPLS-DA plot and B PCA biplot	36
2.5. A-B Volcano plots and C-D VIP plots	37
2.6. Box and whisker plots.....	43
3.1. C ₁₆ -DABCO Mannose Functionalized Dendrimer (DABCOMD) Structure.....	60
3.2. Overview of the protocol.	63
3.3. Hierarchical Clustering.	68
3.4. A-E 2D sPLS-DA plots F 2D ortho PLS-DA plots.....	70
3.5. PCA biplot for all sample types.....	72
3.6. PCA biplot A Mid log phase B Stationary phase	73
3.7. PCA biplot C Unchallenged D Challenged	75
3.8. Box and whisker plots.....	96
5.1. Structure of C ₁₆ -DABCO Mannose Functionalized Dendrimer (DABCOMD)	126

LIST OF FIGURES CONTINUED

Figure	Page
A1. Overview of procedures	139
A2. Growth Plot of Wild Type and C ₁₆ -DABCO Mannose Functionalized Dendrimer Mutated <i>E. coli</i>	145
A3. pH Plot of Wild Type and C ₁₆ -DABCO Mannose Functionalized Dendrimer Mutated <i>E. coli</i>	145
A4. Control Experiment of Sterile Techniques.....	146
A5. Top: Profiling Fit of NMR Data Bottom: Annotated NMR Spectra	147
A6. a Hierarchical Clustering b Resulting classification of all input data.....	148
A7. 3D sPSL-DA plots	148
A8. Top Mid Log Phase Compounds Significantly Correlated with N-acetylglucosamine	150
A9. Top Mid Log Phase Compounds Significantly Correlated with Homocysteine	150
A10. Top Mid Log Phase Compounds Significantly Correlated with Lysine.....	151
A11. Mid Log Phase Top Impacted Pathways.....	151
A12. Stationary Phase Top Impacted Pathways	152
A13. Box and whisker plots for the metabolites shown in Table 2.1 data.....	153
B1. Overview of procedures	160
B2. Growth DABCOMD Mutated <i>B. cereus</i> , DABCOMD challenged Wild Type and DABCOMD challenged DABCOMD Mutated <i>B. cereus</i>	164

LIST OF FIGURES CONTINUED

Figure	Page
B3. NMR spectra for each of the 8 sample types	164
B4. a, d-g Hierarchical Clustering b Sample abbreviation key c Resulting classification of all input data	166
B5. 2D ortho PLS-DA plots.....	167
B6. PCA plot showing the distribution of all sample types.....	168
B7. 3D sPLS-DA plots.....	169
B8. Volcano Plots for the mid log phase	170
B9. Volcano Plots for the stationary phase	171
B10. Very Important Features (VIP) for the paired mid log phase samples.....	172
B11. Very Important Features (VIP) for the paired stationary phase samples.....	173
B12. Very Important Features (VIP) scores obtained from the PLS-DA which shows important metabolites in a all samples types b mid log samples c stationary phase samples d unchallenged samples e DABCOMD challenged samples	174
B13. Pattern Hunter Correlations between Metabolites Observed in the Mid Log Phase Comparison of Unchallenged Mutant and Unchallenged Wild Type Samples	178
B14. Pattern Hunter Correlations between Metabolites Observed in the Mid Log Phase Comparison of Challenged Mutant and Challenged Wild Type Samples	180

LIST OF FIGURES CONTINUED

Figure	Page
B15. Pattern Hunter Correlations between Metabolites Observed in the Mid Log Phase Comparison of Challenged Wild Type and Unchallenged Wild Type Samples	182
B16. Pattern Hunter Correlations between Metabolites Observed in the Mid Log Phase Comparison of Challenged Mutant and Unchallenged Mutant Samples	183
B17. Pattern Hunter Correlations between Metabolites Observed in the Mid Log Phase Comparison of Challenged Mutant and Challenged Wild Type Samples	185
B18. Pattern Hunter Correlations between Metabolites Observed in the Mid Log Phase Comparison of Unchallenged Mutant and Challenged Wild Type Samples	187
B19. Pattern Hunter Correlations between Metabolites Observed in the Stationary Phase Comparison of Unchallenged Mutant and Unchallenged Wild Type Samples	189
B20. Pattern Hunter Correlations between Metabolites Observed in the Stationary Phase Comparison of Challenged Mutant and Challenged Wild Type Samples	190
B21. Pattern Hunter Correlations between Metabolites Observed in the Stationary Phase Comparison of Challenged and Unchallenged Wild Type Samples.....	191
B22. Pattern Hunter Correlations between Metabolites Observed in the Stationary Phase Comparison of Challenged and Unchallenged Mutant Samples	192

LIST OF FIGURES CONTINUED

Figure	Page
B23. Pattern Hunter Correlations between Metabolites Observed in the Stationary Phase Comparison of Challenged Mutant and Unchallenged Wild Type Samples	193
B24. Pattern Hunter Correlations between Metabolites Observed in the Stationary Phase Comparison of Challenged Wild Type and Unchallenged Mutant Samples	194
B25. Top Impacted Pathways for Mid Log Phase Comparison of Unchallenged Mutant and Unchallenged Wild Type Samples.....	195
B26. Top Impacted Pathways for Mid Log Phase Comparison of Challenged Mutant and Challenged Wild Type Samples.....	196
B27. Top Impacted Pathways for Mid Log Phase Comparison of Challenged and Unchallenged Wild Type Samples.....	196
B28. Top Impacted Pathways for Mid Log Phase Comparison of Challenged and Unchallenged Mutant Samples	197
B29. Top Impacted Pathways for Mid Log Phase Comparison of Challenged Mutant and Unchallenged Wild Type Samples.....	197
B30. Top Impacted Pathways for Mid Log Phase Comparison of Challenged Wild Type and Unchallenged Mutant Samples	198
B31. Top Impacted Pathways for Stationary Phase Comparison of Unchallenged Mutant and Unchallenged Wild Type Samples.....	198

LIST OF FIGURES CONTINUED

Figure	Page
B32. Top Impacted Pathways for Stationary Phase Comparison of Challenged Mutant and Challenged Wild Type Samples.....	199
B33. Top Impacted Pathways for Stationary Phase Comparison of Challenged and Unchallenged Wild Type Samples.....	199
B34. Top Impacted Pathways for Stationary Phase Comparison of Challenged and Unchallenged Mutant Samples	200
B35. Top Impacted Pathways for Stationary Phase Comparison of Challenged Mutant and Unchallenged Wild Type Samples.....	200
B36. Top Impacted Pathways for Stationary Phase Comparison of Challenged Wild Type and Unchallenged Mutant Samples	201
B37. Mid Log Phase Metabolite Box and Whisker Plots	201
B38. Stationary Phase Metabolite Box and Whisker Plots.....	206
B39. Challenged Sample Types Metabolite Box and Whisker Plots	210
B40. Unchallenged Sample Types Metabolite Box and Whisker Plots	215
B41. All Sample Types Metabolite Box and Whisker Plots.....	219
C1. Procedures for the determination of RNA purity and results	227
C2. Shows the RNA samples ruined by freezer failure	228
C3. Nonviable RNA sample plot determined by the NanoDrop.....	231

LIST OF FIGURES CONTINUED

Figure	Page
C4. Bioanalyzer results showing degraded RNA	235
C5. Bioanalyzer results showing viable RNA with a large quantity of small RNA	238
C6. Shows the spectra of multiple viable RNA	243
C7. Displays the NanoDrop® screen showing the absorbance readings and ratios along with the concentration and spectrum of a viable sample.....	244
C8. Bioanalyzer results showing viable RNA	244

GLOSSARY

<i>E. coli</i>	<i>Escherichia coli</i>
<i>B. cereus</i>	<i>Bacillus cereus</i>
PAMAM	Poly(amidoamine)
DABCO	1,4-diazabicyclo-2,2,2,-octane
C ₁₆ -DABCO	DABCO with a 16-carbon chain
DABCOMD	C ₁₆ -DABCO and Mannose Functionalized G(4)-PAMAM Dendrimer
Unchallenged	No DABCOMD added to the growth media
Challenged	DABCOMD in the growth media at a nonlethal concentration
D	Challenged
WT	Wild Type
Mut	33-day Mutants
ML	Mid Log Phase
S	Stationary Phase
MIC	Minimum Inhibitory Concentration
QAC	Quaternary Ammonium Compounds
BMHII	Brodo Mueller Hinton II media
OD ₆₀₀	Optical Density at 600 nm
CFU	Colony Forming Unit
CSV	Comma Delineated Form

GLOSSARY CONTINUED

^1H	Proton
NMR	Nuclear Magnetic Resonance
PCA	Principal Component Analysis
PLS-DA	Partial Least Squares Discriminate Analysis
sPLS-DA	Sparse Partial Least Squares Discriminate Analysis
ortho PLS-DA	Orthogonal Partial Least Squares Discriminate Analysis
VIP	Very important features from the PLS-DA

ABSTRACT

Novel antibiotics developed using a new scaffold are needed to combat the rising tide of antibiotic resistant bacteria. Multivalent antibiotics are a relatively new approach that have the potential to greatly increase the efficacy of antibiotics while making it difficult for bacteria to develop resistance. Dendrimers are an attractive framework for the multivalent presentation of antibacterial moieties. Quaternary ammonium compounds (QAC) are a positively charged class of membrane disruptors that are attracted to the large negative charge on phospholipid membranes. Nuclear magnetic resonance (NMR) metabolomics is a quantitative method used for comparison of metabolic profiles of wild type and mutated bacterial samples, enabling the study of bacterial response to antimicrobials. Proton (^1H) NMR hydrophilic metabolomics was used to study gram-negative and gram-positive bacteria upon exposure to 1,4-diazabicyclo-2,2,2-octane (DABCO) with a 16-carbon chain tethered onto a mannose functionalized poly(amidoamine) (PAMAM) dendrimer (denoted as DABCOMD), a membrane disrupting multivalent QAC. Stock *Escherichia coli* (*E. coli*) (denoted as wild type) and DABCOMD mutated *E. coli* (denoted as mutants) were collected in the mid log and stationary phases. The same procedures were used for *Bacillus cereus* (*B. cereus*) as for *E. coli* samples (denoted as unchallenged), except that a DABCOMD challenged sample set was added (denoted as challenged). The challenged sample set procedures were identical to the unchallenged, except DABCOMD was included at 33 % of the MIC value in the growth media for growth curve acquisition and sample collection. The greatest differences observed between the metabolic profiles of the wild type and mutated *E. coli* samples and between the challenged and unchallenged *B. cereus* samples were in energy-associated metabolites and membrane-related pathways. The mutants in all sample types were associated with higher levels of spent energy molecules (including AMP and NAD^+) and peptidoglycan related compounds (including N-acetylglucosamine). Overall, more changes were observed for *B. cereus* (gram-positive), especially in challenged mutant *B. cereus* samples, than for *E. coli* (gram-negative) samples. Since DABCOMD is a positively charged multivalent membrane disruptor, both *B. cereus* and *E. coli* mutated to garner protection by altering their peptidoglycan layer composition, which is energetically costly.

CHAPTER ONE

INTRODUCTION

Antibiotic resistant bacteria are an ever-increasing global health concern as the number of new antibiotics produced decreases every year and the quantity of bacteria gaining resistance to common antibiotics increases (Mintzer et al. 2011; Alanis 2005; Hoerr et al. 2016; González-Bello 2017; Todar 2012). As more and more bacteria are becoming resistant to antimicrobials, a need to develop antimicrobials that are more difficult for bacterial resistance acquisition is becoming more urgent. Synthesizing and studying an antimicrobial that functions on both gram-negative and gram-positive bacteria is preferred, since most bacteria are resistant to at least one classification of antibiotic already (Hoerr et al. 2016). Multivalent scaffolds are of particular interest, since a multivalent scaffold bombards target pathways/membranes by presenting multiple active units bound in close proximity, overwhelming defenses. Antimicrobial functionalized glycodendrimers are being studied as a way to reduce the development of bacterial resistance (Cloninger 2002; Andre et al. 2001; Roy 2003). The readily changeable size (generation number) and density of functional endgroups of poly(amidoamine) (PAMAM) dendrimers make these scaffolds attractive for development of new antimicrobial agents (Mintzer et al. 2011; Paleos et al. 2010; Lu and Pieters 2019; Cloninger 2002). Functionalization of PAMAM dendrimers with carbohydrates, creating glycodendrimers, increases the dendrimer solubility, and antimicrobial compounds can be appended to the carbohydrate endgroups (Cloninger 2002; Andre et al. 2001; Roy 2003). Certain cationic antimicrobials such as quaternary

ammonium compounds (QAC) are able to disrupt and destroy the membranes of bacteria (McDonnell et al. 1999). Multivalent membrane disruptors are an especially intriguing class of compounds since they are able to obliterate bacterial defenses while simultaneously being very difficult for resistance acquisition (Lu and Pieters 2019; Pieters et al. 2009). It is very challenging for the bacteria to make enough changes to their membranes to prevent the multivalent barrage of membrane disrupting positively charged compounds (Chamorro et al. 2012; Hurdle et al. 2011; Pieters et al. 2009).

There are generally four important features of a cationic biocide (Timofeeva and Kleshcheva 2011; Chen et al. 2017). First, the molecule must hold its structure (it cannot fold in on itself, therefore hiding its' positive charge). Next, a cationic antimicrobial must be highly positively charged. Third, the compound should have an alkyl chain of at least three carbons (longer than three carbons is generally preferred). Finally, for gram-positive bacteria, the antimicrobial agent should have a high molar mass (Timofeeva and Kleshcheva 2011; Chen et al. 2017). The multivalent QAC used in this study can function on both gram-negative and gram-positive bacteria and is a mannose functionalized PAMAM dendrimer appended with 1,4-diazabicyclo-2,2,2-octane (DABCO) (Pokhrel et al. 2004) with a 16-carbon chain (denoted as DABCOMD). DABCOMD has a molar mass of about 30 kDa and a diameter of about 8 nm with a 16-carbon chain that is approximately 1.9 nm long in its extended state. DABCOMD, shown in Figure 1.1, was synthesized by Harrison VanKoten and co-workers (VanKoten et al. 2016). DABCOMD is a highly promising candidate as a cationic biocide because this compound meets the four criteria described above. The dendrimer provides a stable,

easily functionalizable multivalent structure, mannose increases the solubility, and C₁₆-DABCO has a 16-carbon chain and two positive charges, thus giving each DABCOMD an average positive charge of sixteen.

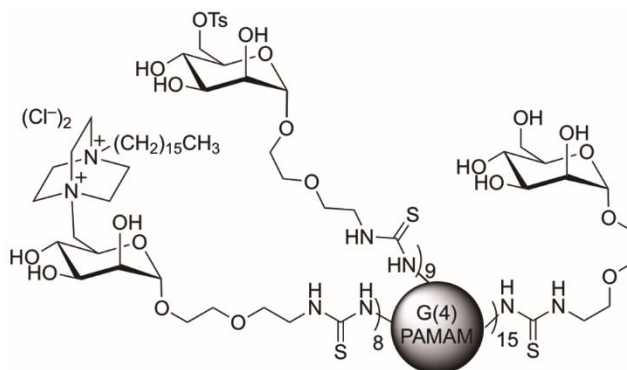


Figure 1.1 Structure of C₁₆-DABCO Mannose Functionalized Dendrimer (DABCOMD)

A significant portion of antimicrobials being utilized are designed to interfere with metabolism, whereas QACs and other cationic biocides use electrostatic attraction and their highly positively charged bulky structures to interfere with and cause damage to cell membranes (Kügler et al. 2005; Timofeeva and Kleshcheva 2011; Gerba 2015; Tiller et al. 2001). Outer cellular structure is different between gram-positive and gram-negative bacteria. Gram-positive bacteria have an outer cell wall composed of a thick peptidoglycan layer and an inner cell phospholipid membrane, while gram-negative bacteria have both an outer and inner phospholipid membrane with a thin peptidoglycan layer in between. Phospholipid membranes have a thickness of about 4 nm (Milo and Phillips 2015). The peptidoglycan layer in gram-positive bacteria is about 20 nm to 80 nm wide, while it is less than 10 nm wide in gram-negative bacteria (Kim et al. 2015; Mai-Prochnow et al. 2016). Due to their natural membrane disruption properties,

multivalent cationic antimicrobials such as DABCOMD should be effective even against antibiotic resistant bacteria due to their high charge density and large bulk (Kügler et al. 2005; Gerba 2015).

An electrostatic attraction draws the cationic biocides to the negatively charged lipopolysaccharide and phospholipid membrane in gram-negative bacteria (Timofeeva and Kleshcheva 2011; Tiller et al. 2001; Sabnis et al. 2021). The lipopolysaccharide is composed of O-antigen bound to the core oligosaccharides bound to lipid A within the membrane (Bertani and Ruiz 2018). The large negative charge on the lipopolysaccharide can be decreased by binding phosphatidylethanolamine to the oligosaccharides (Bertani and Ruiz 2018; Sabnis et al. 2021). The phospholipid membrane of *E. coli* is mostly composed of phosphatidylglycerol (net negative charge), phosphatidylethanolamine (net neutral charge) and diphosphatidylglycerol also known as cardiolipin (net negative charge) (Rowlett et al. 2017; Malanovic and Lohner 2016). Cardiolipin has a more conically shaped head group due to a glycerol binding two phosphatidylglycerols. It is thought that the negative charge and unique structure aid in facilitating bilayer phase transition (Malanovic and Lohner 2016). Cardiolipin could be one of the regions where cationic biocides electrostatically bind and breach the membrane. Phospholipids can be modified with alanine or lysine to decrease the negative charge on the phospholipid membrane (Cox et al. 2014; Hebecker et al. 2015). It is likely that the interaction of the cation biocides with the negative charges on the membrane results in the loss of the cationic counterions normally present (Ca^{2+} and Mg^{2+}) (Kügler et al. 2005; Timofeeva and Kleshcheva 2011; Chen et al. 2017; Tiller et al. 2001; Sabnis et al. 2021). The

counterions provide stability and bridge the phosphate groups. The release of these counterions likely leads to the destabilization of the membrane due to repulsions between phosphate groups (Kügler et al. 2005; Timofeeva and Kleshcheva 2011; Chen et al. 2017; Tiller et al. 2001; Sabnis et al. 2021). After the outer membrane is breached, the biocide can move inside and disrupt the thin peptidoglycan layer, then the inner membrane (Timofeeva and Kleshcheva 2011; Nguyen et al. 2011; Chen et al. 2017; Richards et al. 2018; Tiller et al. 2001; Sabnis et al. 2021). Once the inner membrane has been breached, leakage and lysis occur (Timofeeva and Kleshcheva 2011; Nguyen et al. 2011; Chen et al. 2017; Richards et al. 2018; Tiller et al. 2001; Sabnis et al. 2021).

The positive charge on the biocide is attracted to the highly negatively charged teichoic and lipoteichoic acids in gram-positive bacteria (Timofeeva and Kleshcheva 2011). Teichoic acid and lipoteichoic acid in *bacillus cereus* generally are composed of glycerol phosphate polymers, with teichoic acid attached to the peptidoglycan layer and lipoteichoic acid attached to the phospholipid membrane and protruding out through the peptidoglycan layer (Brown et al. 2013; Percy and Gründling 2014; Wu et al. 2021). Teichoic acid is attached to the peptidoglycan layer in *bacillus cereus* by binding to N-acetylmuramic acid via a linker composed of N-acetylglucosamine bound to N-acetylmannosamine (Brown et al. 2013; Percy and Gründling 2014; Wu et al. 2021). The glycerol phosphate polymer is attached to N-acetylmannosamine. Teichoic acid/lipoteichoic acid can be modified to decrease their overall negative charge by attaching alanine to a glycerol (Schneewind and Missiakas 2014; Brown et al. 2013; Percy and Gründling 2014). The phospholipid membrane in *bacillus cereus* is mainly

composed of phosphatidylglycerol, phosphatidylethanolamine and cardiolipin (diphosphatidylglycerol) (Lang and Lundgren 1970). Phosphatidylglycerol has a net charge of negative one, phosphatidylethanolamine has a net neutral charge and cardiolipin has a net charge of negative one (due to hydrogen bonding) (Malanovic and Lohner 2016). Lysine and alanine esters of these phospholipid components can also be utilized to decrease the overall negative charge (Cox et al. 2014; Schneewind and Missiakas 2014; Hebecker et al. 2015). The general mechanism that has been proposed for QAC action on gram-positive bacteria is the negatively charged teichoic acid and lipoteichoic acid attract the positively charged cationic biocide (Timofeeva and Kleshcheva 2011). The electrostatic interaction between the cationic biocide and teichoic acid/lipoteichoic acid results in disruption of the peptidoglycan layer, especially with a bulky cation disrupting the packing structure of peptidoglycan (Timofeeva and Kleshcheva 2011). Once the cationic biocide makes it through the peptidoglycan layer, it is attracted to negative charges on the phospholipid membrane, resulting in the disruption of the phospholipid membrane until leakage occurs. Lysis and death follow (Timofeeva and Kleshcheva 2011; Gerba 2015).

Another important step in understanding bacterial resistance is determining which metabolomic pathways are involved in the bacteria strain's ability to resist the antimicrobial agent. Metabolomics is the study of the small molecules (metabolites) produced in cellular metabolism. Metabolites are easily affected by the environment of the organism and can be used to distinguish between phenotypes (Barding et al. 2012; Dettmer et al. 2007; Wishart 2008; Lindon et al. 2007). Therefore, metabolites are ideal

for studying the complex relationship that exists between an organism's metabolic pathways and its' environment (Dettmer et al. 2007; Shulaev 2006). Bacterial environments are easily manipulated, they have short generation times and a nasty habit of taking up nearby genetic material, leading to a high number of mutants per generation (Denamur and Matic 2006; Martinez and Baquero 2000; Ceragioli et al. 2010; Bundy et al. 2005). The diversity of bacterial mutations unfortunately means bacteria readily become more resistant to common antimicrobials. Since QACs do not enter the cell and bind a specific target within a cell (Hurdle et al. 2011), internal defense mechanisms such as efflux pumps (which would pump the antimicrobial out) and internal degradation enzymes (which would bind and cleave the antimicrobial within the cell) (Humann and Lenz 2009; Martinez and Baquero 2000; Shepherd and Ibbra 2013; Xu et al. 2006; Todar 2020; Denamur and Matic 2006; Anderson et al. 2012) cannot be used to defend bacteria from the QACs. Bacteria can, however, attempt to lessen the effects of the QAC by strengthening their cell membranes to decrease the likelihood of a breach (for example, by increasing the degree of crosslinking), by making their membranes less attractive by increasing their overall positive charge (for example, by incorporating a higher concentration of a positively charged compound like lysine), and by thickening their peptidoglycan layers (Nikolaidis et al. 2014; Shepherd and Ibbra 2013; Zhao et al. 2018; Xu et al. 2006; Anderson et al. 2012). These modifications are not only energetically costly, but they also can interfere with nutrient uptake by making it more difficult for nutrients to pass through the cell membrane (Chamorro et al. 2012; Pieters et al. 2009). If the nutrient disruption is bad enough, the overall growth of the bacteria could be

stunted, and higher concentrations of spent energy compounds would be found in a metabolite study, since the mutated bacteria would need to use up more energy.

Proton (^1H) nuclear magnetic resonance (NMR) metabolomics is a quantitative method that has been reliably used for decades to study the biochemical end byproducts of bacterial response to environmental stressors, such as being grown in the presence of a multivalent antimicrobial (Barding et al. 2012; Dettmer et al. 2007; Wishart 2008; Turkoglu et al. 2019; Lämmerhofer and Weckwerth 2013; Lindon et al. 2007). After the NMR data is collected, Chenomx Suite Software contains a chemical compound database that allows profiling of NMR spectra (Chenomx 2020). The identity and concentration of the metabolites are determined by clicking on a peak, which brings up a list of possible compounds. Clicking on the compound will bring up its spectrum, which can be fitted to the sample spectrum to determine if it matches and sizing it to fit the sample spectrum, thus identifying the compound and determining its concentration. Not all peaks are able to be identified, as identification is limited by the database of NMR compound spectra available. The identified and quantified metabolite lists are standardized. The concentration and corresponding metabolite identities for each individual sample are input into several mathematical analyses to eliminate outliers, determine similarities and differences between sample types and determine which metabolites are the most indicative of which sample type.

Hierarchical clustering is used to show the relationships between individual samples, sample types and whether the different sample types group separately or cluster together based on the similarity of the metabolites and concentrations in each individual sample

(Addinsoft 2021). Principal component analysis (PCA) is a multivariate statistical analysis that uses an unsupervised approach to cluster observations based on a set of variables, including individual samples and metabolites with their associated concentrations on a PCA biplot (Lindon et al. 2007; Ammons et al. 2014). Therefore, quantified data can be used to cluster phenotypes. Since PCA uses an unsupervised statistical approach, the patterns observed are more likely to be true. Generally, only the first two factors are needed (x-axis and y-axis) to observe the data. Factors are mathematical manipulations that cluster phenotypes together. If the two factors add up to about 50 % of the variance, then only the first two factors are needed. If there are no outliers and the sample types are indeed unique, then the individual samples will cluster with their phenotype (Lindon et al. 2007; Lämmerhofer and Weckwerth 2013). Partial least squares discriminate analysis (PLS-DA) is a multivariate linear regression model for large and complicated data sets (Chung and Keles 2010). PLS-DA forms linear combinations of predictors in a supervised manner and was originally designed for continuous response data. Sparse PLS-DA (sPLS-DA) can achieve variable selection and dimension reduction simultaneously (Chung and Keles 2010). With orthogonal PLS-DA (ortho PLS-DA), the first component is used as a predictor for class, and the second component is the variation orthogonal (perpendicular) to the first component, which can result in greater separation of sample types (Westerhuis et al. 2010). The various PLS-DA analyses can be used to determine the importance of metabolites to different phenotypes and to demonstrate similarity clustering. MetaboAnalyst 5.0 Pattern Hunter shows positive and negative correlations between variables in different sample types

(Pang et al. 2021 and references therein). The correlations in Pattern Hunter show whether or not metabolites are possibly changing together in the same pathways, as metabolites with a high correlation are likely changing related to the same pathway or stressor. In this study, pattern hunter shows which (if any) metabolites positively or negatively correlate to other metabolites and how strong that correlation is, when observing the differences between two different sample types. A volcano plot contains fold change and p-value data (Pang et al. 2021 and references therein). On a volcano plot, the statistically significant fold change and p-value lines are visible. None of the metabolites that fall below the horizontal line and/or fall between the two vertical lines have a significant p-value and/or fold change. These statistical analyses in conjunction with NMR metabolomics were used to study pathways and processes by which *E. coli* and *B. cereus* attempted to garner protection from DABCOMD in their attempts to develop resistance.

The goals of this project were to elucidate resistance mutations that accompany *E. coli* and *B. cereus* exposure to DABCOMD and compare them to determine how gram-negative and gram-positive bacteria are responding to DABCOMD. Elucidation of how bacteria respond and mutate in the presence of multivalent antimicrobials could guide future antimicrobial research. NMR hydrophilic metabolomics was used to study the resistance pathways involved in garnering protection from DABCOMD, a positively charged multivalent membrane disruptor, in *Escherichia coli* and *Bacillus cereus*.

The specific aims of this project were as follows:

- NMR Hydrophilic Metabolomic Analysis of Wild Type and DABCOMD Mutant *E. coli*
- NMR Hydrophilic Metabolomic Analysis of DABCOMD Challenged and Unchallenged Wild Type and DABCOMD Mutant *B. cereus*
- Comparison of Metabolic changes between Gram-Negative (*E. coli*) and Gram-Positive (*B. cereus*) Bacteria

Organization and Summary

There are five chapters presented in this dissertation. Following this introductory chapter, the results and conclusions of the NMR hydrophilic studies of *E. coli* are found in chapter 2, with additional data being found in Appendix A. The research and results for the *B. cereus* project are found in chapter 3, with additional data available in Appendix B. Chapter 4 discusses and compares the overall trends in both projects and chapter 5 contains future work and the significance of this research. A discussion of the RNA study can be found in Appendix C.

Chapter 2 contains the published manuscript for *E. coli* hydrophilic NMR metabolomic research (Aries and Cloninger 2020). The metabolic pathways of *E. coli* mutated in the presence of DABCOMD was compared to wild type *E. coli* in order to better understand how they are attempting to garner protection from the multivalent QAC. The altered energy and membrane related pathways observed with the mutated *E. coli* in comparison to the wild type is discussed. Appendix A contains additional data and information not found in the manuscript.

Chapter 3 contains the submitted manuscript for *B. cereus* hydrophilic NMR metabolomic research. The procedures for the *B. cereus* samples were the same as with the *E. coli* samples (denoted as unchallenged), except a DABCOMD challenged sample set was added for both the mutant and wild type samples (denoted as challenged). The challenged sample set contained 33 % of the MIC value for DABCOMD in the growth media and the unchallenged samples did not have DABCOMD added to their growth media. The metabolism of challenged and unchallenged *B. cereus* mutated in the presence of DABCOMD was compared to the challenged and unchallenged wild type *B. cereus* samples in order to better understand how they are attempting to gain resist to the multivalent QAC. The largest differences observed were an association of higher concentrations of spent energy molecules and membrane related pathways in the mutant *B. cereus* samples, especially the challenged mutant *B. cereus* samples. Appendix B contains additional data and information not found in the manuscript.

Chapter 4 contains a summary of the results for the hydrophilic NMR metabolomics studies on *E. coli* and *B. cereus*. A comparison of the results of exposing gram-negative (*E. coli*) and gram-positive (*B. cereus*) bacteria to DABCOMD is discussed. More changes in metabolite concentrations were observed in the gram-positive bacteria. Moreover, a change in the slope of the growth curve and final stationary phase concentration was only observed in the gram-positive bacteria.

Chapter 5 contains the overall impact and final conclusions of this research. Future work with DABCOMD, *E. coli* and *B. cereus* metabolomic research that should be investigated is discussed. Studying common methods of bacterial mutations in response

to multivalent membrane disruptors can further research into the development of additional antimicrobial that are difficult for resistance acquisition. Both *E. coli* (gram-negative) and *B. cereus* (gram-positive) were unable to overcome the multivalent membrane disrupting properties of DABCOMD, therefore resistance was attempted, and mutations were garnered, but resistance was not acquired. Thus, the antimicrobial properties of DABCOMD should be further evaluated on other bacteria and organisms.

Figure 1.2 is an illustration of DABCOMD attacking bacteria.

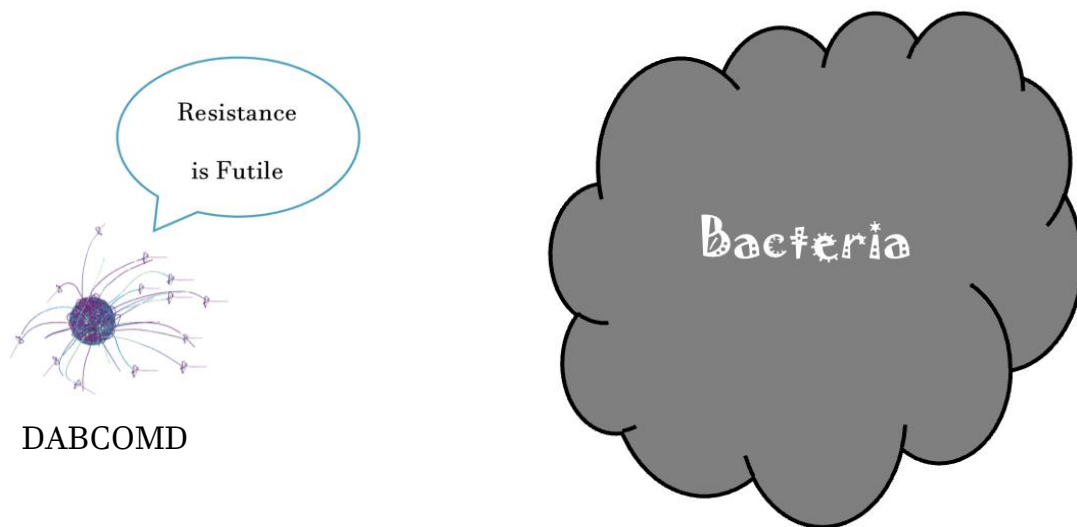


Figure 1.2. Illustration of DABCOMD attacking bacteria.

Appendix C contains RNA research information. The RNA samples were lost due to a freezer failure. Since all critical RNA samples were lost, no RNA information was obtained. The procedures for RNA extraction are provided along with data demonstrating viable and nonviable RNA samples on both the NanoDrop® and Bioanalyzer. The modifications to the procedures, why they were changed, and the results of the alterations are discussed.

References

- Addinsoft (2021). XLSTAT Statistical and Data Analysis Solution. New York, USA.
<https://www.xlstat.com>.
- Alanis, A. J. (2005) Review Article: Resistance to Antibiotics: Are we in the post-antibiotic era? *Archives of Medical Research*, 36, 697-705.
- Ammons, MC. B., Tripet, B. P., Carlson, R. P., Kirker, K. R., Gross, M. A., Stanisich, J. J., Copié, V. (2014) Quantitative NMR Metabolite Profiling of Methicillin-Resistant and Methicillin-Susceptible *Staphylococcus aureus* Discriminates between Biofilm and Planktonic Phenotypes. *Journal of Proteome Research*, 13, 2973-2985.
- Aries, M.L., Cloninger, M.J. (2020) NMR Metabolomic Analysis of Bacterial Resistance Pathways Using Multivalent Quaternary Ammonium Functionalized Macromolecules. *Metabolomics*, 16(82), 1-11. doi.org/10.1007/s11306-020-01702-1
- Anderson, R. J., Groundwater, P. W., Todd, A., Worsley, A. J. (2012). *Microorganisms: In Antibacterial Agents: Chemistry, Mode of Action, Mechanisms of Resistance and Clinical Applications*. (pp. 3-32). West Sussex, UK: Wiley.
- Anderson, R. J., Groundwater, P. W., Todd, A., Worsley, A. J. (2012). *Glycopeptide Antibiotics: In Antibacterial Agents: Chemistry, Mode of Action, Mechanisms of Resistance and Clinical Applications*. (pp. 305-318). West Sussex, UK: Wiley.
- Andre, S., Pieters R. J., Vrsaidas, I., Kaltner, H., Kuwabara, I., Liu, F-T., Liskamp, R. M. J., Gabius, H-J. (2001) Wedgelike Glycodendrimers as Inhibitors of Binding of Mammalian Galectins to Glycoproteins, Lactose Maxiclusters, and Cell Surface Glyconjugates. *ChemBioChem*, 2, 822-830.
- Barding, G. A., Salditos, R., Larive, C.K. (2002) Quantitative NMR for Bioanalysis and Metabolomics. *Analytical Bioanalytical Chemistry*, 404, 1165-1179.
- Bertani, B., Ruiz, N. (2018) Function and Biogenesis of Lipopolysaccharides. *EcoSal Plus*, 8(1), 1-33. doi:10.1128/ecosalplus.ESP-0001-2018
- Brown, S., Santa Maria, J.P. Jr., Walker, S. (2013) Wall Teichoic Acids of Gram-Positive Bacteria. *Annual Review of Microbiology*, 67, 1-28. doi:10.1146/annurev-micro-092412-155620.

- Bundy, J.G., Willey, T.L., Castell, R.S., Ellar, D.J., Brindle, K.M. (2005) Discrimination of Pathogenic Clinical Isolates and Laboratory Strains of *Bacillus cereus* by NMR-Based Metabolomic Profiling. *FEMS Microbiology Letters*, 242, 127-136.
- Ceragiolo, M., Mols, M., Moezelaar, R., Ghelardi, E., Senesi, S., Abee, T. (2010) Comparative Transcriptomic and Phenotypic Analysis of the Responses of *Bacillus cereus* to Various Disinfectant Treatments. *Applied and Environmental Microbiology*, 76(10), 3352-3360.
- Chamorro, C., Boerman, M.A., Arnusch, C.J., Breukink, E., Pieters, R.J. (2012) Enhancing Membrane Disruption by Targeting and Multivalent Presentation of Antimicrobial Peptides. *Biochimica et Biophysica Acta*, 1818, 2171-2174.
- Chen, A., Peng, H., Blakey, I., Whittaker, A.K. (2017) Biocidal Polymers: A Mechanistic Overview. *Polymer reviews*, 57(2), 276-310.
- Chenomx (2020) N.M.R. Suite 8.4. Edmonton: Chenomx Inc.
- Chung, D., Keles S. (2010) Sparse Partial Least Squares Classification for High Dimensional Data. *Statistical Applications in Genetics and Molecular Biology*, 9(1), article 17.
- Cloninger, M. J. (2002) Biological Applications of Dendrimers. *Current Opinions in Chemical Biology*, 6, 742-748.
- Cox, E., Michalak, A., Pagentine, S., Seaton, P., Pokorny, A. (2014) Lysylated Phospholipids Stabilize Models of Bacterial Lipid Bilayers and Protect Against Antimicrobial Peptides. *Biochimica et Biophysica Acta*, 1838(9), 2198-2204.
- Denamur, E., Matic, I. (2006) Evolution of Mutation Rates in Bacteria. *Molecular Microbiology*, 60 (4), 820-827.
- Dettmer, K., Aronov, P. A., Hammock, B. D. (2007) Mass Spectrometry-Based Metabolomics. *Mass Spectrometry Review*, 26, 51-78.
- Gerba, C.P. (2015) Quaternary Ammonium Biocides: Efficacy in Application. *Applied and Environmental Microbiology*, 81(2), 464-469.
- González-Bello, C. (2017) Antibiotic Adjuvants- A Strategy to Unlock Bacterial Resistance to Antibiotics. *Bioorganic and Medicinal Chemistry Letters*, 27, 4221-4228.

- Hebecker, S., Krausze, J., Hasenkampf, T., Schneider, J., Groenewold, M., Reichelt, J., Jahn, D., Heinz, D.W., Moser, J. (2015) Structures of Two Bacterial Resistance Factors Mediating tRNA-Dependent Aminoacylation of Phosphatidylglycerol with Lysine or Alanine. *PNAS*, 112(34), 10691-10696.
- Hoerr, V., Duggan, G. E., Zbytniuk, L., Poon, K. K. H., Große, C., Neugebauer, U., Methling, K., Löffler, B., Vogel, H. J. (2016) Characterization and Prediction of the Mechanism of action of antibiotics through NMR Metabolomics. *BMC Microbiology*, 16(82), 1-14. doi:10.1186/s12866-016-0696-5
- Hurdle J.G., O'Neill, A.J., Chopra, I., Lee, R.E. (2011) Targeting Bacterial Membrane Function: an Underexploited Mechanism of Treating Persistent Infections. *Nature Reviews Microbiology*, 9, 62-75.
- Humann, J., Lenz, L. L. (2009) Bacterial Peptidoglycan Degrading Enzymes and their Impact on Host Muropeptide Detection. *Journal of Innate Immunity*, 1, 88-97.
- Kim, S.J., Chang, J., Singh, M. (2015) Peptidoglycan Architecture of Gram-Positive Bacteria by Solid-State NMR. *Biochimica et Biophysica Acta*, 1848, 350–362.
- Kügler, R., Bouloussa, O., Rondelez, F. (2005) Evidence of Charge-Density Threshold for Optimum Efficiency of Biocidal Cationic Surfaces. *Microbiology*, 151, 1341-1349.
- Lämmerhofer, M., Weckwerth, W., Eds, (2013) NMR-Based Metabolomic Analysis: In Metabolomics in Practice: Successful Strategies to Generate and Analyze Metabolic Data. (pp. 209-233). Weinheim, Germany: Wiley-VCH.
- Lang, D.R., Lundgren, D.G. (1970) Lipid Composition of *Bacillus cereus* During Growth and Sporulation. *Journal of Bacteriology*, 101(2), 483-489.
- Lindon, J. C., Nicholson, J. K., Holmes, E. (2007). NMR Spectroscopic Techniques for Application to Metabonomics: In the Handbook of Metabolomics and Metabonomics. (pp. 55-112). Oxford, UK: Elsevier.
- Lu, W., Pieters, R. J. (2019) Carbohydrate-Protein Interactions and Multivalency: Implications for the Inhibition of Influenza A Virus Infections. *Expert Opinion on Drug Discovery*, 14(4), 387-395.
- Mai-Prochnow, A., Clauson, M., Hong, J., Murphy, A.B. (2016) Gram-Positive and Gram-Negative Bacteria Differ in their Sensitivity to Cold Plasma. *Scientific Reports*, 6(38610), 1-11. doi:0.1038/srep38610

- Malanovic, N., Lohner K. (2016) Antimicrobial Peptides Targeting Gram-Positive Bacteria. *Pharmaceuticals*, 9(59), 1-33.
- Martinez, J. L., Baquero, F. (2000) Minireview: Mutation Frequency and Antibiotic Resistance. *Antimicrobial Agents and Chemotherapy*, 44(7), 1771-1777.
- McDonnell, G., Russell, A. D. (1999) Antiseptics and Disinfectants: Activity, Action and Resistance. *Clinical Microbiology Review*, 12(1), 147-226.
- Mintzer, M. A., Dane, E. L., O'Toole, G. A., Grinstaff, M. W. (2011) Exploiting Dendrimer Multivalency to Combat Emerging and Reemerging Infectious Diseases. *Molecular Pharmaceutics*, 9, 342-354.
- Nguyen, L.T., Haney, E.F., Vogel, H.J. (2011) The Expanding Scope of Antimicrobial Peptide Structures and their Modes of Action. *Trend in Biotechnology*, 29(9), 464-472.
- Nikolaidis, I., Favini-Stabile, S., Dessen, A. (2014) Resistance to antibiotics targeted to the bacterial cell wall. *Protein Science*. 23, 243-259.
- Paleos, C. M., Tsiourvas, D., Sideratou Z., Tziveleka, L-A. (2010) Drug Delivery using Multifunctional Dendrimers and Hyperbranched Polymers. *Expert Opinion on Drug Delivery*, 7, 1387-1398.
- Pang, Z., Chong, J., Zhou, G., Morais D., Chang, L., Barrette, M., Gauthier, C., Jacques, PE., Li, S., and Xia, J. (2021) MetaboAnalyst 5.0: narrowing the gap between raw spectra and functional insights *Nucleic Acids Research* 49. doi: 10.1093/nar/gkab382
- Percy, M.G., Gründling, A. (2014) Lipoteichoic Acid Synthesis and Function in Gram-Positive Bacteria. *Annual Review of Microbiology*, 68, 81-100.
- Milo R., Phillips, R. (2015) Cell Biology by the Numbers. (pp. 88-91). Garland Science. <http://book.bionumbers.org/what-is-the-thickness-of-the-cell-membrane/> Accessed December 13, 2021.
- Pieters, R.J., Arnusch, C.J., Breukink, E. (2009) Membrane Permeabilization by Multivalent Anti-Microbial Peptides. *Protein & Peptide Letters*, 16 (7), 1-7.

- Pokhrel, S., Nagaraja, K. S., Varghese, B. (2004) Preparation, Characterization and X-ray Structure Analysis of 1,4-diazabicyclo-2,2,2-octane (DABCO) and Ammonium Cation with Tetrathiomolybdate Anion. *Journal of Structural Chemistry*, 45(5), 900-905.
- Richards, S-J., Isufi, K., Wilkins, L.E., Lipecki, J., Fullam, E., Gibson, M.I. (2018) Multivalent Antimicrobial Polymer Nanoparticles Target Mycobacteria and Gram-Negative Bacteria by Distinct Mechanisms. *Biomacromolecules*, 19, 256-264.
- Rowlett V.W., Mallampalli, V.K.P.S., Karlstaedt, A., Dowhan, W., Taegtmeier, H., Margolin, W., Vitrac, H. (2017) Impact of Membrane Phospholipid Alterations in *Escherichia coli* on Cellular Function and Bacterial Stress Adaptation. *Journal of Bacteriology*, 199(13), 1-22.
- Roy, R. (2003) A Decade of Glycodendrimer Chemistry. *Trends in Glycoscience and Glycotechnology*, 15(85), 291-310.
- Sabnis, A., Hagart, K.L.H., Klockner, A., Becce, M., Evan, L.E., Furniss, R.C.D., Despoina, A.I., Mavridou, D.A., Murphy, R., Stevens, M.M., Davies, J.C., Larrouy-Maumus, G.J., Clarke, T.B., Edwards, A.M., (2021) Colistin kills bacteria by targeting lipopolysaccharide in the cytoplasmic membrane. *eLife* 2021;10:e65836 DOI: 10.7554/eLife.65836
- Schneewind, O., Missiakas, D. (2014) Lipoteichoic Acids, Phosphate-containing Polymers in the Envelope of Gram-positive Bacteria. *Journal of Bacteriology*, 196(6), 1133-1142.
- Shepherd, J., Ibba, M. (2013) Direction of Aminoacylated transfer RNAs into Antibiotic Synthesis and Peptidoglycan-Mediated Antibiotic Resistance. *FEBS Letters*, 587(18), 2895-2904.
- Shulaev, V. (2006) Metabolomics technology and bioinformatics. *Briefings in Bioinformatics*, 7(2), 128-139.
- Tiller, J.C., Liao, C-J., Lewis, K., Klivanov, A.M. (2001) Designing Surfaces that Kill Bacteria on Contact. *PNAS*, 98(11), 5981-5985.
- Timofeeva, L., Kleshcheva, N. (2011) Antimicrobial Polymers: Mechanism of Action, Factors of Activity, and Applications. *Applications in Microbiology and Biotechnology*, 89, 475-492.
- Todar, K., (2020). Textbook of Bacteriology (Online). University of Wisconsin, <http://textbookofbacteriology.net>. Accessed October 2021

- Turkoglu, O., Cital, A., Katar, C., Mert, I., Kumar, p., Yilmaz, A., Uygur, D.S., Erkata, S., Graham, S.F., Bahado-Singh, R.O. (2019) Metabolomic Identification of Novel Diagnostic Biomarkers in Ectopic Pregnancy. *Metabolomics*, 15(143), 1-11.
- VanKoten, H.W., Dlakic, W.M., Engel, R., Cloninger, M.J. (2016) Synthesis and Biological Activity of Highly Cationic Dendrimer Antibiotics. *Molecular Pharmaceutics* 13, 3827-3834. doi.org/10.1021/acs.molpharmaceut.6b00628
- Westerhuis, J.A., Van Velzen, E. J. J., Hoefsloot, H. C. J., Smilde, A. K. (2010) Multivariate Paired Data Analysis: Multilevel PLSDA versus OPLSDA. *Metabolomics*, 6, 119-128.
- Wishart, D.S. (2008) Quantitative Metabolomics using NMR. *Trends in Analytical Chemistry*, 27(3), 228-237.
- Wu, X., Han, J., Gong, G., Koffas, M.A.G., Zha, J. (2021) Wall Teichoic Acids: Physiology and Applications. *FEMS Microbiology Reviews*, 45(4), 1-23.
- Xu, C., Lin, L., Ren, H., Zhang, Y., Wang, S., Peng, X. (2006) Analysis of Outer Membrane Proteome of *Escherichia coli* Related to Resistance to Ampicillin and Tetracycline. *Proteomics*, 6, 462-473.
- Zhao, H., Roistacher, D.M., Helmann J.D. (2018) Aspartate Deficiency Limits Peptidoglycan Synthesis and Sensitizes Cells to Antibiotics Targeting Cell Wall Synthesis in *Bacillus subtilis*. *Molecular Microbiology*, 109(6), 826-844.

CHAPTER TWO

NMR METABOLOMIC ANALYSIS OF BACTERIAL RESISTANCE PATHWAYS
USING MULTIVALENT QUARternARY AMMONIUM FUNCTIONALIZED
MACROMOLECULES

Contribution of Authors and Co-Authors

Manuscript in Chapter 2 and Supplementary Information in Appendix A

Author: Michelle Lynne Aries

Contributions: Grew and collected bacterial culture samples, extracted the metabolites, prepared the samples for NMR spectral acquisition, processed the NMR data, performed data analysis and interpretation, wrote the first manuscript and revised drafts.

Co-Author: Dr. Mary Jane Cloninger

Contributions: Supervised all aspects of the research project, oversaw experimental design, edited, and revised the manuscript.

Manuscript Information

Michelle L. Aries and Mary J. Cloninger

Metabolomics

Status of Manuscript:

Prepared for submission to a peer-reviewed journal

Officially submitted to a peer-reviewed journal

Accepted by a peer-reviewed journal

Published in a peer-reviewed journal

Published by Springer Science + Business Media, LLC part of Springer Nature 2020
July 23rd, 2020

Metabolomics 16, Article number: 82

doi.org/10.1007/s11306-020-01702-1

CHAPTER TWO

NMR METABOLOMIC ANALYSIS OF BACTERIAL RESISTANCE PATHWAYS
USING MULTIVALENT QUARTERNARY AMMONIUM FUNCTIONALIZED
MACROMOLECULES

Michelle L. Aries and Mary J. Cloninger

*Department of Chemistry and Biochemistry, Montana State University, Bozeman, MT,
59717 USA*

Abstract

Multivalent antimicrobial dendrimers are an exciting new system that is being developed to address the growing problem of drug resistant bacteria. Nuclear Magnetic Resonance (NMR) metabolomics is a quantitative and reproducible method for the determination of bacterial response to environmental stressors and for visualization of perturbations to biochemical pathways. NMR metabolomics is used to elucidate metabolite differences between wild type and antimicrobially mutated *Escherichia coli* (*E. coli*) samples. Proton (^1H) NMR hydrophilic metabolite analysis was conducted on samples of *E. coli* after 33 growth cycles of a minimum inhibitory challenge to *E. coli* by poly(amidoamine) dendrimers functionalized with mannose and with C₁₆-DABCO quaternary ammonium endgroups and compared to the metabolic profile of wild type *E. coli*. The wild type and mutated *E. coli* samples were separated into distinct sample sets by hierarchical clustering, principal component analysis (PCA) and sparse partial least squares discriminate analysis (sPLS-DA). Metabolite components of membrane

fortification and energy related pathways had a significant p-value and fold change between the wild type and mutated *E. coli*. Amino acids commonly associated with membrane fortification from cationic antimicrobials, such as lysine, were found to have a higher concentration in the mutated *E. coli* than in the wild type *E. coli*.

N-acetylglucosamine, a major component of peptidoglycan synthesis, was found to have a 25-fold higher concentration in the mid log phase of the mutated *E. coli* than in the mid log phase of the wild type. The metabolic profile suggests that *E. coli* change their peptidoglycan composition in order to garner protection from the highly positively charged and multivalent C₁₆-DABCO and mannose functionalized dendrimer.

Keywords Metabolomics · Quaternary ammonium compounds · Nuclear magnetic resonance · Dendrimers · DABCO · Antibiotic Resistance

Introduction

New infectious diseases with novel drug targets emerge every year, and the occurrence of bacterial resistance to existing antibiotics is increasing at the same time that the number of new antibiotics produced per year is decreasing. This, in conjunction with a large quantity of bacteria in hospitals having at least one antibiotic that is ineffectual, is a critical global health concern (Mintzer et al. 2011; Alanis 2005; Martinez and Baquero 2000; Xue et al. 2013; Gonzáles-Bello 2017). Many of these multidrug resistant bacteria are gram negative (Hoerr et al. 2016; Gonzáles-Bello 2017), including strains of *Escherichia coli* (*E. coli*) (Gonzáles-Bello 2017).

E. coli is an appropriate microbial on which to study resistance pathways for new antimicrobial agents due to the extensive genetic and metabolic studies that have been previously reported (González-Bello 2017, Hoerr et al. 2016). In addition, *E. coli* has a short generation time, is easily mutable, is a commonly occurring infection and has a thin cell wall. The most common processes used by *E. coli* for antibiotic resistance include random beneficial genetic mutations, horizontal gene transfer, and strengthening of the cell wall and basic defense systems (Denamur and Matic 2006; Todar 2012; González-Bello 2017; Anderson et al. 2012; Hoerr et al. 2016). *E. coli* have a beneficial mutation rate of 2×10^{-9} per genome per replication due to random genetic mutations (Denamur and Matic 2006; Martinez and Baquero 2000; González-Bello 2017). Horizontal gene transfers occur due to bacterial DNA uptake from the environment, swapping plasmids with other bacteria, and virus phage DNA injection. Bacterial communities that are antibiotic resistant can even shield antibiotic susceptible bacteria of different species from certain types of antibiotics (Perlin et al. 2009). Bacteria can also become antibiotic resistant by using efflux pumps, antibiotic degrading or altering enzymes, and alterations to their peptidoglycan layer composition (Martinez and Baquero 2000, Humann and Lenz 2009, Shepherd and Ibba 2013, Todar 2012; Anderson et al. 2012).

Peptidoglycan, which is the main component in bacterial membranes, is composed of an alternating chain of *N*-acetylglucosamine and *N*-acetylmuramic acid interlinked with pentapeptide side chains. Changes to the peptidoglycan layer are known to change the permeability of the membrane and to alter the pattern of noncovalent interactions that are achieved by antibiotics interacting with the cell surface (Anderson et

al. 2012; Shepherd and Ibba 2013). For example, glycine is a common amino acid used to crosslink the peptidoglycan (Shepherd and Ibba 2013; Hammes et al. 1973), and decreased amounts of crosslinking have been correlated with a decrease in bacterial survival rates (Loskill et al. 2014). Aminoacyl-tRNAs are redirected from protein synthesis to peptidoglycan synthesis in order to change the pentapeptide side chains, thereby protecting the bacteria against binding by environmental stressors such as antibiotics (Shepherd and Ibba 2013). Generally, the pentapeptide side chain amino acids are switched out in order to change membrane fluidity, permeability, crosslinking, charge, and hydrophobicity to improve survivability (Loskill et al. 2014; Shepherd and Ibba 2013; Humann and Lenz 2009; Anderson et al. 2012). Like genetic mutation, these defense mechanisms greatly increase the rate of antibiotic resistance in bacteria and decrease the number of currently effective antibiotics (Martinez and Baquero 2000; Gonzáles-Bello 2017; Anderson et al. 2012).

Antibiotics designed using new scaffolds and directed at previously unassessed bacterial metabolic pathways are needed because bacteria may be less likely to develop resistance to them. In addition, new antibiotics that allow for administration of a therapeutic cocktail that simultaneously targets multiple bacterial pathways could increase efficacy and decrease resistance. In particular, scaffolds that allow antibiotics to function multivalently are attractive because they can take advantage of multiple individual active units attached to a central core, thus concentrating several of the antibiotic moieties in close proximity. Dendrimers are an appealing multivalent scaffold because they are highly modular; the size of the dendrimer can be easily changed by

changing dendrimer generation, and a variety of antibiotics in varying densities can be used (Mintzer et al. 2011; Paleos et al. 2010; Vembu et al. 2015; Chen et al. 2000; Lu and Pieters 2019). Poly(amidoamine) (PAMAM) dendrimers can be functionalized with carbohydrates, amino acids, antibiotics and other bioactive groups (Cloninger 2002; Andre et al. 2001; Roy 2003). Carbohydrate functionalized PAMAM dendrimers, i.e. glycodendrimers, have been shown to have higher activity than their carbohydrate monomer counterparts (Wolfenden et al 2015; VanKoten et al. 2016; Andre et al. 2001) and have been shown to disrupt bacterial activity (Roy 2003; Andre et al. 2001; Chabre and Roy 2008; Mintzer et al. 2011; VanKoten et al. 2016). Functionalization of the carbohydrate endgroups with an antibiotic has provided significantly higher activity and a greater challenge for bacterial resistance than their monomer counterparts (García-Gallego et al. 2017; Wrońska et al. 2019; Mintzer et al. 2011; Chen et al 2000).

Quaternary ammonium compounds (QAC) are used as disinfectants and surface surfactants because of their antimicrobial properties (Engel et al. 2011; McDonnell and Russell 1999; Mintzer et al. 2011; Sreepereumbuduru et al. 2016; Jiao et al. 2017). QACs have a hydrophobic portion and a positively charged hydrophilic ammonium group. The large positive charge of the QACs disrupts and/or lyses the bacterial phospholipid membrane (McDonnell and Russell 1999; Mintzer et al. 2011; Sreepereumbuduru et al. 2016; Jiao et al. 2017). The QAC studied in this report is a 1,4-diazabicyclo-2,2,2-octane (DABCO) (Pokhrel et al. 2004) with a 16-carbon chain (C₁₆-DABCO). DABCO has been shown to be effective against both gram positive and negative microbes (Sreepereumbuduru et al. 2016). C₁₆-DABCO is attached to a mannose functionalized

PAMAM dendrimer (Figure 2.1). The C₁₆-DABCO and mannose functionalized dendrimer (DABCOMD) multivalently presents the positively charged ammonium units, and VanKoten et al. (2016) conducted a minimum inhibition study using DABCOMD to determine the minimum inhibitory concentration (MIC) against both positive and negative strains of bacteria. After challenging *E. coli* with DABCOMD for 33 growth cycles, DABCOMD showed 100-fold increased antimicrobial potency relative to the monomeric C₁₆-DABCO on a per active unit basis (VanKoten et al. 2016). The *E. coli* in the MIC study became very resistant to small molecule inhibitors including Ampicillin and monomeric DABCO, while the MIC remained almost unchanged for DABCOMD. Because of the effectiveness of DABCOMD in MIC assays coupled with a lack of development of resistance over many growth cycles, a comparison of the *E. coli* before and after exposure to DABCOMD for 33 growth cycles was performed using metabolomics.

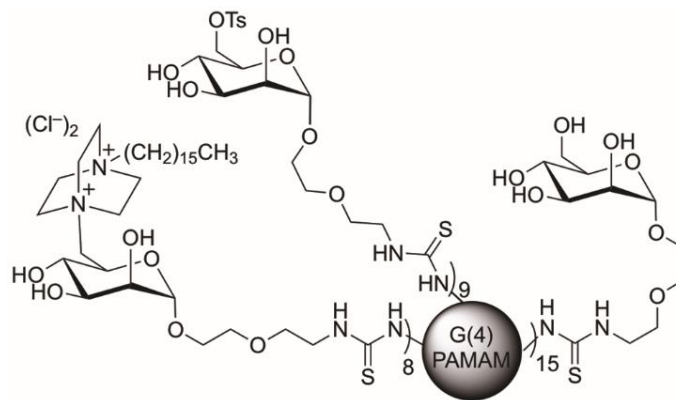


Figure 2.1. Structure of the C₁₆-DABCO Mannose Functionalized Dendrimer (DABCOMD)

Metabolomics is the study of the small molecules (metabolites) produced in cellular metabolism. Metabolites are easily affected by the environment of the organism and can be used to distinguish phenotypes (Shulaev 2006; Barding et al. 2012; Hoerr et al. 2016). Metabolomics is a quantitative and/or qualitative analysis which can be used to assess metabolite changes between wild type and mutants, making metabolomic profiling an ideal technique for studying the complex relationship that exists between an organism's metabolic pathways and its environment (Shulaev 2006; Barding et al. 2012; Dettmer et al. 2007; Hoerr et al. 2016; Lämmerhofer and Weckwerth 2013; Lindon et al. 2007). Since nuclear magnetic resonance (NMR) metabolomics is a reliable and quantitative method, this technique is an important method for comparing the biochemical byproducts of mutated and wild type metabolism (Hoerr et al. 2016; Dettmer et al. 2005; Ammons et al. 2014). Thus, the goal for this research project was to determine likely pathway changes involved in the development by *E. coli* of resistance to multivalent DABCOMD using proton (^1H) NMR hydrophilic metabolomics. The quantitative results reported herein were obtained using DABCOMD with *E. coli* in order to improve our understanding of the main resistance pathways and key mutations expected for bacterial systems upon exposure to multivalent antimicrobial compounds.

Methods

Samples

The FDA Strain Seattle 1946 *E. coli* (ATCC 25922) was used as the wild type, and the mutated samples were prepared as described in VanKoten et al. 2016. Four

sample types were used: wild type mid log phase (WT ML), wild type stationary phase (WT S), mutant mid log phase (Mut ML) and mutant stationary phase (Mut S). Samples were grown, collected, and standardized as described in Appendix A the Supplementary Material. A brief overview of procedures is show in Figure 2.2.

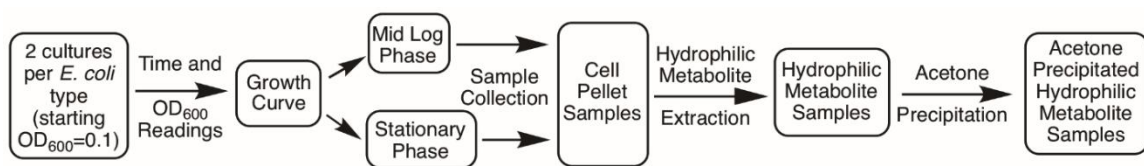


Figure 2.2. Overview of procedures from culture to extracted hydrophilic metabolites ready for NMR buffer

Metabolite Extraction Procedures

Hydrophilic Extraction The cell pellets were thawed on ice. Cold methanol (MeOH) (800 μ L) and 170 μ L of Millipore H₂O were added to each sample test tube and vortexed. The cells were sonicated for 5 minutes then vortexed. Cold chloroform (800 μ L) and 400 μ L of cold H₂O were added to each test tube. The samples were vortexed and incubated on ice for 15 minutes. The test tubes were centrifuged at 3,500 rpms for 15 minutes. The aqueous layer was transferred to a sterile Eppendorf tube and concentrated on a speed vacuum until dry. The samples were frozen at - 80 °C (Ammons et al. 2014 and 2015 and references therein).

Acetone Precipitation The samples were thawed on ice. The pellets were suspended in 250 μ L D₂O and 1,250 μ L Acetone. The samples were frozen at - 80 °C overnight. The samples were thawed on ice. They were cloudy with precipitated proteins once thawed. The samples were centrifuged at 2,000 rpms for 30 min. The

protein pellet was discarded. The speed vacuum was used to dry the metabolite samples. The metabolite pellet was frozen at - 80 °C (Ammons et al. 2014 and 2015 and references therein).

NMR Sample Preparation

Note: All D₂O used was NMR grade.

NMR Buffer Preparation An imidazole stock solution was made by adding 27.230 g of imidazole to 4.0 mL of D₂O. 3-(Trimethylsilyl)propane-1-sulfonate sodium salt (DSS) (21.23 mg) was added to 4.0 mL of D₂O to make a DSS stock solution. In 5.0 mL of D₂O, 0.345 g NaH₂PO₄·H₂O, 0.355 g Na₂HPO₄ (anhydrous) and 0.040 g NaN₃ were dissolved to create a NaPO₄ buffer stock solution. A 30 mL D₂O buffer solution was made by combining 300 µL of the DSS stock solution, 60 µL of the imidazole stock solution, 1,500 µL of the NaPO₄ buffer stock solution, and 28,140 µL of D₂O (Ammons et al. 2014 and 2015 and references therein).

Sample Preparation A culture was started from each of three overnight growths, providing three technical replicates. This process was repeated six separate times: three cultures were taken six times to provide six biological replicates and eighteen samples overall for each of the four sample types (wild type mid log, mutant mid log, wild type stationary, mutant stationary; 72 samples in total). Of the eighteen samples obtained, fifteen NMR samples were used for wild type mid log and for mutant mid log phases. Twelve NMR samples were analyzed for the wild type stationary phases, and thirteen NMR samples were analyzed for the mutant stationary phase. The metabolite samples

were placed on ice, and 700 μ L of the NMR buffer was added. The samples were gently vortexed then transferred to a capped NMR Tube. Additional information regarding sample preparation is provided in Appendix A the Supporting Information.

Data Acquisition

The samples were acquired at 298 K using a Bruker Avance III 600 MHz NMR equipped with a SampleJetTM automatic sample loading system and a 5 mm triple resonance (¹H, ¹⁵N, ¹³C) liquid-helium cooled TCI NMR CryoProbe and Topspin software (Bruker version 3.6). 1D ¹H NMR spectra were acquired using the Bruker-supplied excitation sculpting (ES)-based ‘zgesgp’ pulse sequence, and NMR spectra were recorded using 256 scans, a ¹H spectral window of 7211.538 Hz, 64K data points and a dwell time interval of 69.33 μ sec between points, amounting to a spectrum acquisition time of 4.54 s. The recovery delay (D1) time between acquisitions was set to 2 s, resulting in a total relaxation recovery time of 6.5 s between scans. The spectra were Fourier transformed and phased using the H₂O and DSS resonances.

Data Analysis

The spectra were processed and profiled using Chenomx NMR Suite 8.2 software (Chenomx 2016). The Chenomx profiler’s list of metabolites was used to identify metabolites and generate a fitted metabolite spectrum for all samples. Not all peaks were able to be identified with the program. An example fit and the complete list of metabolites identified using the Chenomx profiling software are listed in Appendix A the Supporting Information. Later, the same data was chosen at random to profile again to check for errors. The concentrations of the identified metabolites in each sample were

standardized by the concentration of the starting sample and also with the total sum of profiled metabolites. Each metabolite concentration was divided by the total concentration and multiplied by 100 to give the standardized metabolite concentration that was used (details are provided in Appendix A the Supporting Information).

XLSTAT (Addinsoft 2019) was used for hierarchical clustering and for principal component analysis (PCA) for each sample type and corresponding standardized metabolite concentrations. The metabolites and their concentration data were transformed into comma delineated form (CSV). The CSV data were uploaded to the MetaboAnalyst website version 4.0 for statistical analysis (Chong et al 2019 and references therein). A volcano plot of p-value versus fold change and sparse partial least squares discriminant analysis (sPLS-DA), Pattern Hunter and the very important features (VIP) data from the partial least squares discriminate analysis (PSL-DA) were used to determine relationships among statistically significant metabolite changes. The list of metabolites generated for each sample type was used in the MetaboAnalyst Pathway Analysis tool and using KEGG pathways (Kanehisa and Goto 2000 and references therein) in order to identify altered metabolomic pathways in the mutants in response to the DABCOMD. PCA was used to identify metabolite correlation with sample type, to demonstrate sample separation without overlap, to eliminate metabolites that were not indicative of the sample types, and to identify outlier samples. PLS-DA provided a VIP list of metabolites that are highly correlated with each other. sPLS-DA was used to identify outlier samples and to demonstrate sample separation without overlapping data sets. The volcano plot was used to highlight metabolites with both a significant p-value

(0.05 or less) and a fold change of 1.5 or higher. These statistical analyses were used in conjunction with each other to investigate the data from different statistical perspectives, and the results were combined to create a better understanding of the data.

Results

E. coli (ATCC 25922, denoted WT for wild type) were mutated in the presence of C₁₆-DABCO and mannose functionalized dendrimers (DABCOMD) for 33-growth cycles (denoted Mut for mutant) as previously described by VanKoten *et al.* 2016. The hydrophilic metabolites were extracted from the mid log and stationary phases for both the wild type and mutant samples as summarized in Figure 2.2 (Ammons *et al.* 2014 and 2015 and references therein). ¹H NMR spectra of the hydrophilic metabolites for the mid log and stationary phases of both the wild type and mutant samples were obtained. Figure 2.3a displays an example spectrum for each sample type. Chenomx NMR Suite 8.2 software was used to identify and quantify the hydrophilic metabolites present in each sample. These metabolite identities and their concentrations for each sample type were entered into MetaboAnalyst 4.0 for sPLS-DA analysis. MetaboAnalyst was used to eliminate outliers in each sample type using sPLS-DA and PCA. The outliers distinguished themselves by being located away from their sample group cluster. Wild type stationary phase contained seven nonoutlier and five outlier samples, whereas the mutant stationary phase contained eight nonoutlier and four outlier samples. Wild type mid log phase contained eleven nonoutlier and four outlier samples, whereas the mutant mid log phase contained nine nonoutlier and six outlier samples. The metabolite identities and concentrations were analyzed using XLSTAT Hierarchical Clustering, from

which the number of unique sample types was determined, and the data were classified accordingly. XLSTAT Hierarchical Clustering grouped the four sample types into their own classes as shown in Figure 2.3b. None of the samples from the mid log or stationary phases had overlapping data sets, and the mutant and wild type sample sets were also separated into their own nonoverlapping classes. This demonstrates that the wild type mid log samples, the wild type stationary samples, the DABCOMD mutated mid log samples, and the DABCOMD mutated stationary samples all form unique sample sets.

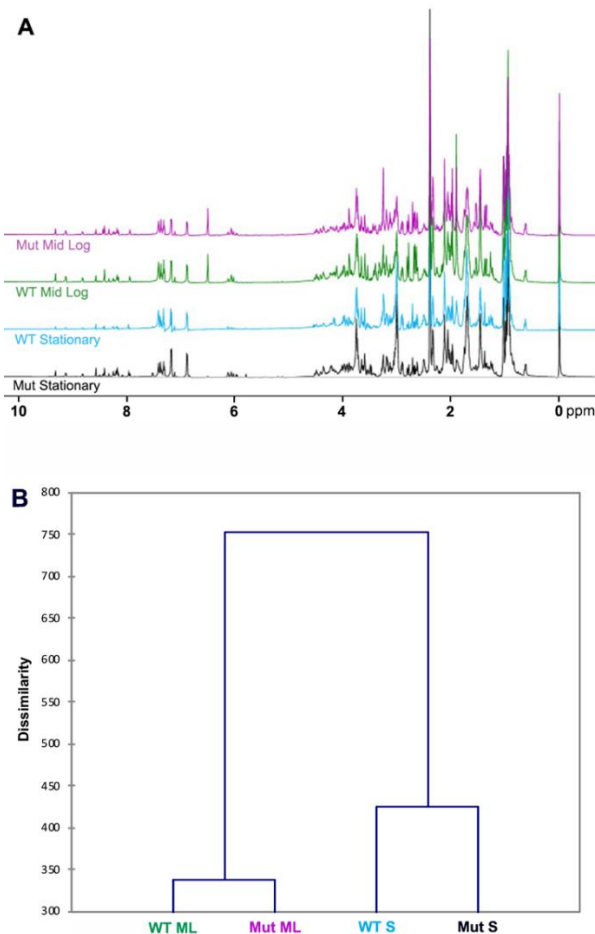


Figure 2.3. **A** An example ^1H NMR spectrum for each sample type. **B** Hierarchical Clustering indicating that there are 4 unique sample types. No overlap between sample types was observed

The name of the metabolite and its concentration for each sample were entered into XLSTAT and MetaboAnalyst 4.0 to determine sample separation, metabolite-to-sample correlation, and the statistical significance for each metabolite. To determine the separation of sample types and the metabolite indicators for each sample type, multivariate statistical analyses were performed using sPLS-DA 2D and 3D plots and a PCA biplot (Figure 2.4). Figure 2.4a shows that each sample type has significant separation on each axis, accounting for 54.2% and 67.4% of the variation. This indicated that only the first two components needed to be considered for separation and analysis. The PCA biplot where 56.0% of the variation was accounted for in the first two factors as shown in Figure 2.4b also indicated that consideration of the first two components was sufficient. Factor 1 separated the wild type from the mutant and factor 2 separated the mid log from the stationary phase. Figure 2.4b shows which metabolites are indicative of each sample type. *N*-acetylglucosamine, for example, was indicative of the DABCOMD mutated samples due to its significantly higher concentration in the samples from mutated *E. coli* than in the samples from wild type *E. coli*.

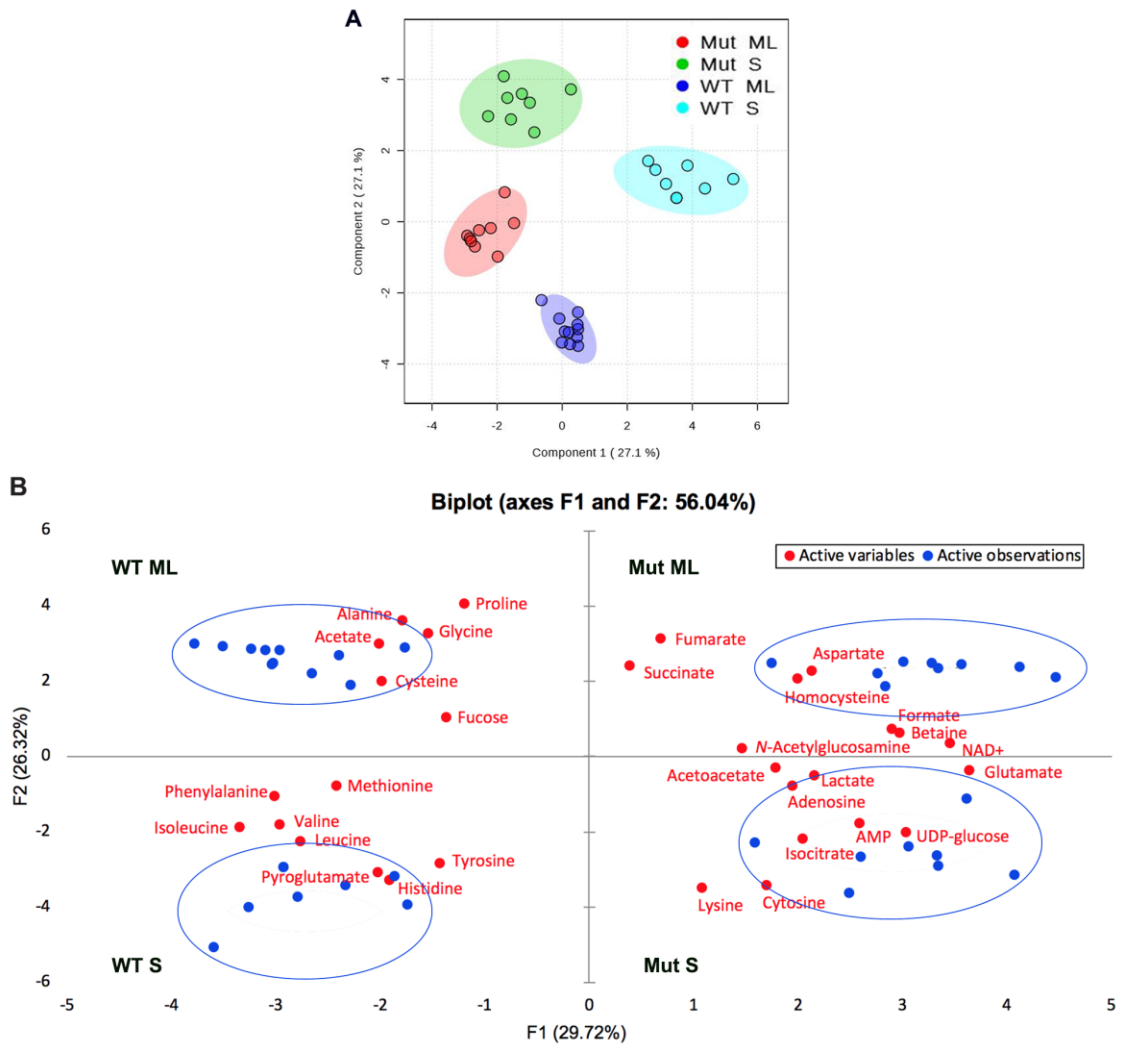


Figure 2.4. **A** 2D sPLS-DA demonstrate that each sample type can be separated into a distinct group without overlap. **B** PCA biplot shows the sample type separation (blue) and which metabolites are the most indicative of each sample type (red)

The data from each phase was entered into MetaboAnalyst 4.0 to generate a volcano plot as shown in Figure 2.5. Figure 2.5a and 2.5b show the volcano plots of both the mid log and stationary phases. Each metabolite highlighted in the volcano plot has a significant p-value (0.05 or less) and a fold change of 1.5 or higher. Figure 2.5c and 2.5d display the very important features plot (VIP scores) determined by the PSL-DA.

Metabolites with high VIP scores are highly correlated to other metabolites. By using the

VIP scores in conjunction with the other statistical analyzes, important metabolites that have been shown in previous work with antimicrobials were revealed. Interestingly, lysine appeared in the VIP scores but not in the volcano plot because the volcano plot had a cut off fold change of 1.5, whereas lysine only had a 1.3-fold change. Any metabolites with a significant VIP score were investigated.

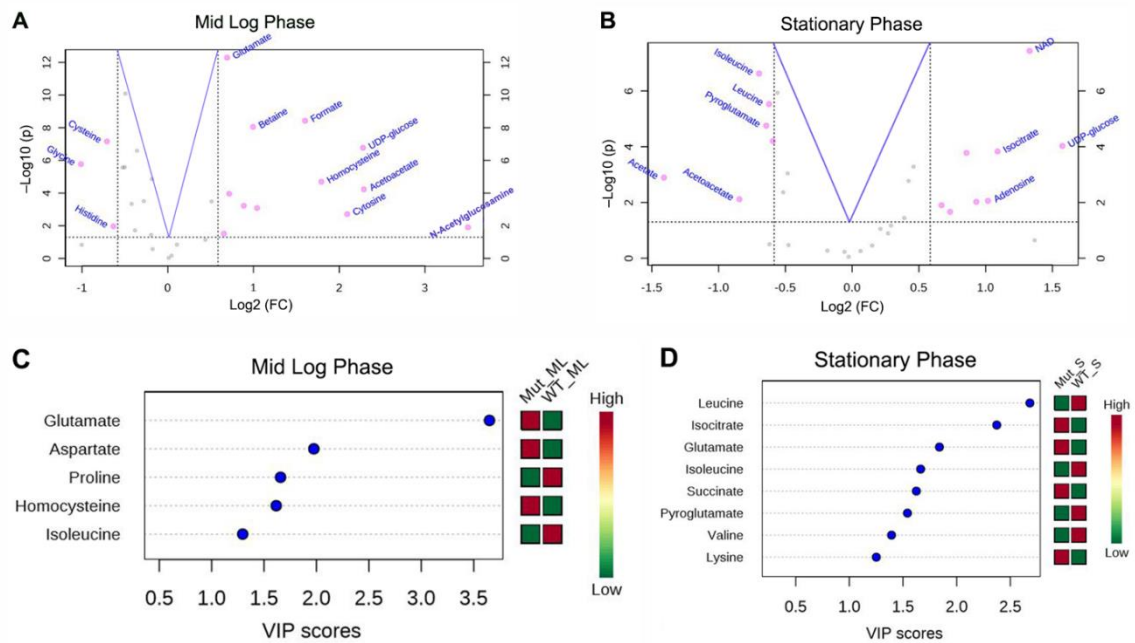


Figure 2.5. Volcano plots displaying metabolites with a significant p-values and fold changes for **A** the mid log phase and **B** the stationary phase. Important features (VIP) scores from the PLS-DA for important metabolites and their corresponding concentrations in **C** the mid log phase and **D** the stationary phase

The pathways that are likely involved with the statistically significant metabolites during their mid log and stationary phases are listed in Table 2.1. Pattern Hunter and Pathway Analysis on MetaboAnalyst 4.0 aided in determining the most likely pathways involved with several of the statistically significant metabolites. Pattern Hunter was used

to ensure significance and correct correlation among the metabolites in a given pathway. For example, histidine was found to be a statistically significant metabolite in our studies. Histidine has an important role in aminoacyl-tRNA biosynthesis, yet it did not correlate to the other metabolites in that pathway and was therefore omitted from Table 2.1. Further studies are needed to determine the pathways involved in histidine's fold change. Lysine, on the other hand, showed only a 1.3-fold increase in the mutant stationary phase relative to the wild type stationary phase, and Pattern Hunter showed a positive correlation with aspartate, glutamate, and AMP and a negative correlation with Cysteine, glycine, isoleucine and proline. Thus, the direction of fold change and corresponding metabolites for lysine correctly correlated with additional metabolite data provided in Table 2.1.

Table 2.1. Fold change of statistically significant metabolites in their corresponding metabolic pathway for the mid log and the stationary phase.

Indicated Pathway	Mid Log Phase		Stationary Phase	
	Metabolite	Fold Change ^{a,b}	Metabolite	Fold Change
Citric Acid Cycle	Fumarate	+1.5	Succinate	+1.9
	NAD ⁺	+1.6	NAD ⁺	+2.4
			Isocitrate	+2.1
Pyruvate Metabolism	Acetate	-1.4	Acetate	-2.7
Aminoacyl-tRNA Biosynthesis	Aspartate	+1.3 (VIP)	Lysine	+1.3 (VIP)
	Glutamate	+1.6 (VIP)	Glutamate	+1.3 (VIP)
	Glycine	-2.0	Glycine	+1.8
	AMP	+1.8	AMP	+1.6
	Cysteine	-1.5	Leucine	-1.6 (VIP)
	Isoleucine	-1.4 (VIP)	Isoleucine	-1.6 (VIP)
	Proline	-1.5 (VIP)	Valine	-1.4 (VIP)
Peptidoglycan Synthesis	<i>N</i> -acetylglucosamine	+25	<i>N</i> -acetylglucosamine	-1.5
	Lactate	+2.4	Lactate	+1.1
	Glutamate	+1.6 (VIP)	Glutamate	+1.3

^aA positive fold change is indicative of a higher concentration in the mutant. ^bThe metabolites with VIP next to them were determined to be very important features by the PSL-DA.

Discussion

Multiple metabolites that are likely to be involved in energy related pathways and cell membrane composition had both a significant p-value and fold change. The most significant concentration changes between the wild type and the mutant were common components of peptidoglycan synthesis, which is a critical component of the cell membrane. *N*-acetylglucosamine had the largest observed fold change, which was a 25-fold increase in concentration in samples from the mutant compared to those from the wild type during the mid log phase. Many likely components of aminoacyl-tRNA biosynthesis significantly changed in concentration when comparing mutant to wild type in both the mid log and the stationary phases. One likely explanation for the observed concentration changes is a diversion from aminoacyl-tRNA biosynthesis to peptidoglycan synthesis. Common amino acid substitutes found in the peptidoglycan pentapeptide side chain, such as lactate, glutamate and lysine had significantly higher concentrations in the mutant than the wild type. Lysine has been shown to lower the permeability of the cell membrane to cationic molecules (Shepherd and Ibba 2013) because this amino acid inserts positive charge on the membrane to reduce the attraction of the cationic antimicrobial to the membrane. Since the polyalanine tail of the peptidoglycan pentapeptide side chain is a common target for antibiotics, bacterial mutants commonly switch the last alanine amino acid of the pentapeptide side chain for a different amino acid such as lactate (Mengin-Lecreulx et al. 1994; Humann and Lenz 2009; Anderson et al. 2012). In anaerobic conditions, it would be expected that pyruvate would be converted to lactate to undergo anaerobic metabolism which would result in higher

concentrations of lactate, formate, acetate and succinate and a decreasing pH (Soini et al. 2008). The pH and growth curves for both the wild type and mutants were statistically the same (Appendix Figures A2 and A3). The mutant had a higher concentration of formate and lactate and a lower concentration of acetate and succinate in the mid log phase than the wild type. The mutant had a higher concentration of formate and succinate, a lower concentration of acetate and about the same concentration of lactate in the stationary phase than the wild type. These results add support to our theory that the increase in lactate concentration in the mutants was a result of an increased rate of peptidoglycan synthesis and peptidoglycan alterations during the mid log phase.

The mutant samples revealed a 2-fold decrease in glycine for the mid log phase and a 1.8-fold increase in glycine in the stationary phase when compared to wild type. Glycine is involved in crosslinking of the peptidoglycan, and crosslinking increases the rigidity of the membrane structure (Loskill et al. 2014). A possible explanation for the significant fold change reversal for glycine is due to cells rapidly dividing in the mid log phase and peptidoglycan crosslinking occurring to a lesser extent. When bacteria are in the stationary phase, they are expected to settle into a configuration that provides higher survivability, and the extra rigidity of the cell membrane could be less of a hindrance to normal functioning (Humann and Lenz 2009; Mengin-Lecreulx et al. 1994).

Homocysteine levels were 4-fold higher and cysteine levels were 1.5-fold lower in the mutant than in the wild type for the mid log phase. Homocysteine levels were 2.5-fold higher and cysteine levels were about the same when comparing the mutant to the wild type during the stationary phase. Thus, the excess homocysteine being produced is

not likely being used for cysteine production, but the pathway could be stopping at another intermediate such as cystathionine. Methionine's concentration was about the same in the mutant and the wild type, suggesting that methionine is not a primary product arising from the excess homocysteine. The intermediate cystathionine can be utilized in peptidoglycan synthesis (Mengin-Lecreux et al. 1994). Other metabolites such as N-acetylglucosamine, lactate and glutamate are involved in peptidoglycan synthesis and were also found to be in excess in the mutant during the mid log phase (and have about the same concentration as the wild type in the stationary phase), adding credence to the theory that cystathionine is at least part of the homocysteine sink in these studies. When cystathionine is added to media, bacteria uptake and incorporate it into their peptidoglycan layer (Mengin-Lecreux et al. 1994). This truncates the pentapeptide side chain by excluding the D-ala-D-ala tail. Lacking a polyalanine tail can provide protection against some antimicrobials (Loskill et al. 2014; Shepherd and Ibba 2013; Anderson et al. 2012). Thus, the *E. coli* grown in the presence of DABCOMD most likely changed their peptidoglycan composition to aid in repelling and protecting against this cationic antimicrobial, and this explains the shifting levels of cysteine and homocysteine. Box plots for four of the key identified metabolites that play a role in strengthening the bacterial membrane against DABCOMD are shown in Figure 2.6 a-d. Note that the widest ranges of fold changes were generally observed for mutant mid log data, which is as expected if multiple mutations are occurring.

The synthesis of extra components for the peptidoglycan layer in the mutant would be expected to be energetically costly for the mutant bacteria. Acetate, an energy

related metabolite associated with pyruvate and the citric acid cycle, had a lower concentration in the mutant than the wild type. Spent energy-related metabolites such as NAD⁺ and AMP, on the other hand, were present in higher concentrations in the mutant than in the wild type. Likely components of both the citric acid cycle and aminoacyl-tRNA biosynthesis showed statistically significant changes in the concentrations of metabolites in both the mid log and stationary phases. The mutant *E. coli* most likely required more energy-related metabolites, yet they were still able to compensate for their mutations and obtain the same growth density and comparable growth curves as the wild type. Box plots showing fold changes and fold change range comparisons for example metabolites wild type and mutant *E. coli* are shown in Figure 2.6 e-g. The increased energetic costs incurred by the mutant is evident in the figure.

Quaternary ammonium antimicrobial compounds induce the formation of a hole in the bacterial membrane (Sreepereumbuduru et al. 2016; McDonnell and Russell 1999; Jiao et al. 2017). The DABCOMD studied here, which bears multiple quaternary ammonium groups per macromolecule, is a particularly effective quaternary ammonium antibacterial agent because the dendrimer framework brings multiple cationic groups into close proximity and thereby enforces multiple simultaneous cation/membrane interactions at the cell surface. The results of this ¹H NMR metabolomics study reveal that *E. coli* grown in the presence of DABCOMD show a significant increase in metabolites most likely associated with peptidoglycan component synthesis, which is critically important for strengthening the bacterial membrane. Changes in energy related

pathways were also observed, indicating that the mutated bacteria were required to work harder in order to maintain the same level of function as wild type *E. coli*.

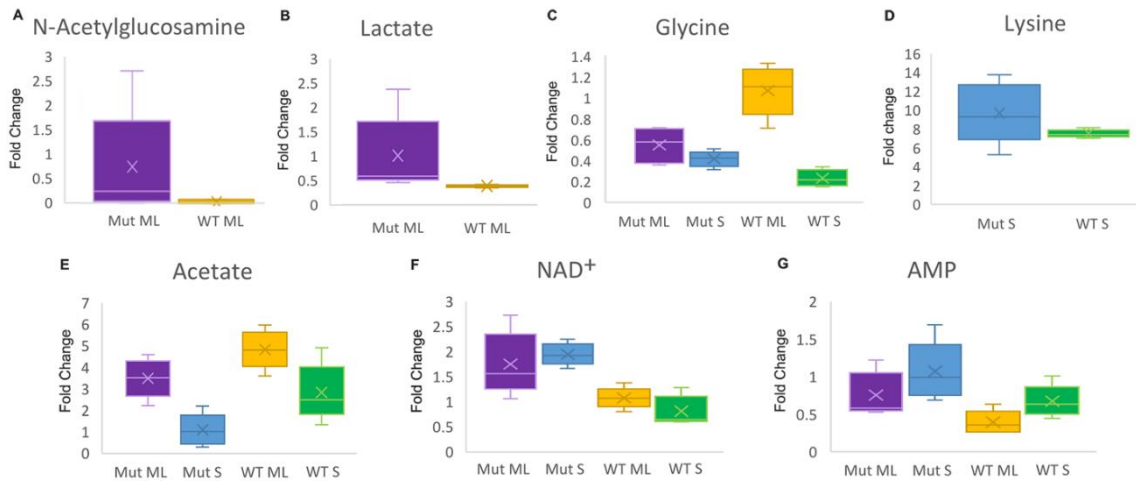


Figure 2.6. **A-D** Box and whisker plots to show the differences in fold changes and the fold change ranges for example metabolites involved in peptidoglycan synthesis and membrane permeability. **A** N-acetylglucosamine in the mid log phase, **B** lactate in the mid log phase, **C** glycine in both the mid log and the stationary phases, and **D** lysine in the stationary phase. **E-G** Box plots to show the differences in fold changes and the fold change ranges for example metabolites involved in energy processes. **E** Acetate, **F** NAD⁺, and **G** AMP fold changes in both mid log and stationary phases. The ends of the whiskers are the minimum and maximum values, the center line is the median, the x is the mean, and the colored middle “box” encompasses the middle 50% of scores for the group.

Conclusion

Novel antimicrobials are needed to combat the increasing occurrence of antibiotic resistant bacteria, and multivalency has been shown to improve the effectiveness of antimicrobial compounds. NMR metabolomics is a reliable and quantitative method to study the effect of antimicrobials on bacterial biochemical pathways. Here, NMR hydrophilic metabolomics was used to study the metabolic changes associated with mutation of *E. coli* by DABCOMD, a multivalent quaternary ammonium compound.

Mutated and wild type samples were easily separated by hierarchical clustering, PCA and sPLS-DA analyses. Common components of energy pathways and peptidoglycan synthesis were found to have significant p-values and fold changes when comparing the wild type *E. coli* to the mutated *E. coli* in both the mid log and the stationary phases. Lysine, an amino acid commonly associated with decreasing the effectiveness of cationic antimicrobials, was found to have a higher concentration in the mutant than in the wild type. The mutated *E. coli* also had a 25-fold increase in *N*-acetylglucosamine (a major component of the peptidoglycan) during the mid log phase. Overall, the NMR hydrophilic metabolite data indicates that *E. coli* are most likely altering their peptidoglycan composition to protect their membranes from the large positive charge found on the multivalent C₁₆-DABCO and mannose functionalized PAMAM dendrimers.

Data Availability Statement

The data presented in this study are openly available in NIH Common Fund's National Metabolomics Data Repository (NMDR) website, the Metabolomics Workbench, where it has been assigned Study ID ST001351 (Metabolomics Workbench 2020).

Acknowledgements

Funding from NIGMS 62444 is gratefully acknowledged. Dr. Harrison VanKoten provided the bacterial stocks. Dr. Brian Tripet and Dr. Mary Cloud Ammons helped to develop the procedures for metabolite extraction and analysis, and Dr. Brian Tripet helped with acquisition of NMR spectra.

Compliance with Ethical Standards

Conflict of interest Both authors declare that they have no conflicts of interest.

Research involving human and/or animal participants This article does not contain any studies with human and/or animal participants performed by either of the authors.

References

- Addinsoft (2019) XLSTAT 2019: Data Analysis and Statistical Solution for Microsoft Excel. Paris, France.
- Alanis, A. J. (2005) Review Article: Resistance to Antibiotics: Are we in the post-antibiotic era? *Archives of Medical Research*, 36, 697-705.
- Ammons, MC. B., Tripet, B. P., Carlson, R. P., Kirker, K. R., Gross, M. A., Stanisich, J. J., Copié, V. (2014) Quantitative NMR Metabolite Profiling of Methicillin-Resistant and Methicillin-Susceptible *Staphylococcus aureus* Discriminates between Biofilm and Planktonic Phenotypes. *Journal of Proteome Research*, 13, 2973-2985.
- Ammons, MC. B., Morrissey, K., Tripet, B. P., Van Leuven, J. T., Han, A., Lazarus, G. S., Zenilman, J. M., Stewart, P. S., James, G. A., Copié, V. (2015) Biochemical Association of Metabolic Profile and Microbiome in Chronic Pressure Ulcer Wounds. *PLOS one*, 10(5), 1-22. doi:10.1371/journal.pone.0126735.
- Anderson, R. J., Groundwater, P. W., Todd, A., Worsley, A. J. (2012). Microorganisms: In Antibacterial Agents: Chemistry, Mode of Action, Mechanisms of Resistance and Clinical Applications. (pp. 3-32). West Sussex, UK: Wiley.
- Anderson, R. J., Groundwater, P. W., Todd, A., Worsley, A. J. (2012). Glycopeptide Antibiotics: In Antibacterial Agents: Chemistry, Mode of Action, Mechanisms of Resistance and Clinical Applications. (pp. 305-318). West Sussex, UK: Wiley.
- Andre, S., Pieters R. J., Vrsaidas, I., Kaltner, H., Kuwabara, I., Liu, F-T., Liskamp, R. M. J., Gabius, H-J. (2001) Wedgelike Glycodendrimers as Inhibitors of Binding of Mammalian Galectins to Glycoproteins, Lactose Maxiclusters, and Cell Surface Glyconjugates. *ChemBioChem*, 2, 822-830.
- Barding, G. A., Salditos, R., Larive, C.K. (2002) Quantitative NMR for Bioanalysis and Metabolomics. *Analytical Bioanalytical Chemistry*, 404, 1165-1179.
- Chabre, Y., Roy, R. (2008) Recent Trends in Glycodendrimer Syntheses and Applications. *Current Topics in Medicinal Chemistry*, 8(14), 1237-1285.
- Chen, C. Z., Beck-Tan, N. C., Dhurjati, P., Van Dyk, T. K., LaRossa, R. A., Cooper, S. L. (2000) Quaternary Ammonium Functionalized Poly(propylene imine) Dendrimers as Effective Antimicrobials: Structure-Activity Studies, *Biomacromolecules*, 1, 473-480.
- Chenomx (2016) N.M.R. Suite 8.2. Edmonton: Chenomx Inc.

- Chong, J., Wishart, D. S., Xia, J. (2019) Using MetaboAnalyst 4.0 for Comprehensive and Integrative Metabolomics Data Analysis. *Current Protocols in Bioinformatics*, 68, e86.
- Cloninger, M. J. (2002) Biological Applications of Dendrimers. *Current Opinions in Chemical Biology*, 6, 742-748.
- Denamur, E., Matic, I. (2006) Evolution of Mutation Rates in Bacteria. *Molecular Microbiology*, 60 (4), 820-827.
- Dettmer, K., Aronov, P. A., Hammock, B. D. (2007) Mass Spectrometry-Based Metabolomics. *Mass Spectrometry Review*, 26, 51-78.
- Engel, R., Ghani, I., Montenegro, D., Thomas, M., Klaritch-Vrana, B., Castaño, A., Friedman, L., Leb, J., Rothman, L., Lee, H., Capodiferro, C., Ambinder, D., Cere, E., Awad, C., Sheikh, F., Rizzo, J.L., Nisbett, L-M., Testani, E., Melkonian, K. (2011) Polycationic Glycosides. *Molecules*, 16, 1508-1518.
- García-Gallego, S., Franci, G., Falanga, A., Gómez, R., Folliero, V., Galdiero, S., Javier de la Mata, F., Galdiero, M. (2017) Function Oriented Molecular Design: Dendrimers as Novel Antimicrobials. *Molecules*, 22, 1581-1610.
- González-Bello, C. (2017) Antibiotic Adjuvants- A Strategy to Unlock Bacterial Resistance to Antibiotics. *Bioorganic and Medicinal Chemistry Letters*, 27, 4221-4228.
- Hammes, W., Schleifer, K. H., Kandler, O. (1973) Mode of Action of Glycine on the Biosynthesis of Peptidoglycan. *Journal of Bacteriology*, 116(2), 1029-1053.
- Hoerr, V., Duggan, G. E., Zbytniuk, L., Poon, K. K. H., Große, C., Neugebauer, U., Methling, K., Löffler, B., Vogel, H. J. (2016) Characterization and Prediction of the Mechanism of action of antibiotics through NMR Metabolomics. *BMC Microbiology*, 16(82), 1-14. doi:10.1186/s12866-016-0696-5
- Humann, J., Lenz, L. L. (2009) Bacterial Peptidoglycan Degrading Enzymes and their Impact on Host Muropeptide Detection. *Journal of Innate Immunity*, 1, 88-97.
- Jiao, Y., Niu, L-n., Ma, S., Li, J., Tay, F. R., Chen, J-h. (2017) Quaternary Ammonium-Based Biomedical Materials: State-of-the-Art, Toxicological Aspects and Antimicrobial Resistance. *Progress in Polymer Science*, 71, 53-90.
- Kanehisa, M., Goto, S. (2000) KEGG: Kyoto Encyclopedia of Genes and Genomes. *Nucleic Acid Research*, 28, 27-30.

- Lämmerhofer, M., Weckwerth, W., Eds, (2013) NMR-Based Metabolomic Analysis: In Metabolomics in Practice: Successful Strategies to Generate and Analyze Metabolic Data. (pp. 209-233). Weinheim, Germany: Wiley-VCH.
- Lindon, J. C., Nicholson, J. K., Holmes, E. (2007). NMR Spectroscopic Techniques for Application to Metabonomics: In the Handbook of Metabolomics and Metabonomics. (pp. 55-112). Oxford, UK: Elsevier.
- Loskill et al. (2014) Reduction of the Peptidoglycan Crosslinking Causes a Decrease in the Stiffness of the *Staphylococcus aureus* Cell Envelope. *Biophysical Journal*, 107, 1082-1089.
- Lu, W., Pieters, R. J. (2019) Carbohydrate-Protein Interactions and Multivalency: Implications for the Inhibition of Influenza A Virus Infections. *Expert Opinion on Drug Discovery*, 14(4), 387-395.
- Martinez, J. L., Baquero, F. (2000) Minireview: Mutation Frequency and Antibiotic Resistance. *Antimicrobial Agents and Chemotherapy*, 44(7), 1771-1777.
- McDonnell, G., Russell, A. D. (1999) Antiseptics and Disinfectants: Activity, Action and Resistance. *Clinical Microbiology Review*, 12(1), 147-226.
- Mengin-Lecreux, D., Blanot, D., VanHeijenoort, J. (1994) Replacement of Diaminopimelic acid by Cystathionine or Lanthionine in the Peptidoglycan of *Escherichia coli*. *Journal of Bacteriology*, 176(14), 434-437.
- Metabolomics Workbench. (2020) https://www.metabolomicsworkbench.org/Study_ID/ST001351. Accessed November 13, 2021.
- Mintzer, M. A., Dane, E. L., O'Toole, G. A., Grinstaff, M. W. (2011) Exploiting Dendrimer Multivalency to Combat Emerging and Reemerging Infectious Diseases. *Molecular Pharmaceutics*, 9, 342-354.
- Paleos, C. M., Tsiourvas, D., Sideratou Z., Tziveleka, L-A. (2010) Drug Delivery using Multifunctional Dendrimers and Hyperbranched Polymers. *Expert Opinion on Drug Delivery*, 7, 1387-1398.
- Perlin, M. H., Clark, D. R., McKenzie, C., Patel, H., Jackson, N., Kormanik, C., Powell, C., Bajorek, A., Myers, D. A., Dugatkin, L.A., Atlas, M. R. (2009) Protection of Salmonella by Ampicillin-Resistant *Escherichia coli* in the presence of otherwise Lethal Drug Concentrations. *Proceedings of the Royal Society B*, 276, 3759-3768.

- Pokhrel, S., Nagaraja, K. S., Varghese, B. (2004) Preparation, Characterization and X-ray Structure Analysis of 1,4-diazabicyclo-2,2,2-octane (DABCO) and Ammonium Cation with Tetrathiomolybdate Anion. *Journal of Structural Chemistry*, 45(5), 900-905.
- Roy, R. (2003) A Decade of Glycodendrimer Chemistry. *Trends in Glycoscience and Glycotechnology*, 15(85), 291-310.
- Shepherd, J., Ibba, M. (2013) Direction of Aminoacylated transfer RNAs into Antibiotic Synthesis and Peptidoglycan-Mediated Antibiotic Resistance. *FEBS Letters*, 587(18), 2895-2904.
- Shulaev, V. (2006) Metabolomics technology and bioinformatics. *Briefings in Bioinformatics*, 7(2), 128-139.
- Soini, J., Ukkonen, K., Neubauer, P. (2008) High Cell Density Media for *Escherichia coli* are Generally Designed for Aerobic Cultivations – Consequences for Large-Scale bioprocesses and Shake Flask Cultures. *Microbial Cell Factors* 7, 26-36.
- Sreeperumbuduru, R. S., Abid, Z. M., Claunch, K. M., Chen, H. H., McGillivray, S. M., Simanek, E. E. (2016) Synthesis and Antimicrobial Activity of Triazine Dendrimers with DABCO Groups. *Royal Society of Chemistry Advances*, 6, 8806-8810.
- Todar, K., (2012). Textbook of Bacteriology (Online). University of Wisconsin, <http://textbookofbacteriology.net>. Accessed 9 April 2015
- VanKoten, H.W., Dlakic, W. M., Engel, R., Cloninger, M. J. (2016) Synthesis and Biological Activity of Highly Cationic Dendrimer Antibiotics. *Molecular Pharmaceutics* 13, 3827-3834.
- Vembu, S., Pazhamalai, S., Gopalakrishnan, M. (2015) Potential Antibacterial Activity of Triazine Dendrimer: Synthesis and Controllable Drug Release Properties. *Bioorganic and Medicinal Chemistry*, 23, 4561-4566.
- Wolfenden, M., Cousin, J., Nangia-Makker, P., Raz, A., Cloninger, M. (2015) Glycodendrimers and Modified ELISAs: Tools to Elucidate Multivalent Interactions of Galectins 1 and 3. *Molecules*, 20, 7059-7096.
- Wrońska, N., Majoral, J. P., Appelhans, D., Bryszewska, M., Lisowska, K. (2019) Synergistic Effects of Anionic/Cationic Dendrimers and Levofloxacin on Antibacterial Activities. *Molecules*, 24, 2894-2905.

Xue, X., Chen, X., Mao, X., Hou, Z., Zhou, Y., Bai, H., Meng, J., Da, F., Sang, G., Wang, Y., Lou, X. (2013) Amino-Terminated Generation 2 Poly(amidoamine) Dendrimer as a Potential Broad-Spectrum, Nonresistance-Inducing Antibacterial Agent. *AAPS Journal*, 15, 132-142.

CHAPTER THREE

NMR HYDROPHILIC METABOLOMIC ANALYSIS OF BACTERIAL RESISTANCE
PATHWAYS USING MULTIVALENT ANTIMICROBIALS WITH CHALLENGED
AND UNCHALLENGED WILD TYPE AND MUTATED GRAM-POSITIVE
BACTERIA

Contribution of Authors and Co-Authors

Manuscript in Chapter 3 and Supplementary Information in Appendix B

Author: Michelle Lynne Aries

Contributions: Grew and collected bacterial culture samples, extracted the metabolites, prepared the samples for NMR spectral acquisition, processed the NMR data, performed data analysis and interpretation, wrote the first manuscript and revised drafts.

Co-Author: Dr. Mary Jane Cloninger

Contributions: Supervised all aspects of the research project, oversaw experimental design, edited, and revised the manuscript.

Manuscript Information

Michelle L. Aries and Mary J. Cloninger

Status of Manuscript:

Prepared for submission to a peer-reviewed journal

Officially submitted to a peer-reviewed journal

Accepted by a peer-reviewed journal

Published in a peer-reviewed journal

International Journal of Molecular Sciences

Accepted for publication on December 9th, 2021

CHAPTER THREE

NMR HYDROPHILIC METABOLOMIC ANALYSIS OF BACTERIAL RESISTANCE
PATHWAYS USING MULTIVALENT ANTIMICROBIALS WITH CHALLENGED
AND UNCHALLENGED WILD TYPE AND MUTATED GRAM-POSITIVE
BACTERIA

Michelle L. Aries and Mary J. Cloninger

*Department of Chemistry and Biochemistry, Montana State University, Bozeman,
MT, 59717 USA*

Abstract

Multivalent membrane disruptors are a relatively new antimicrobial scaffold that are difficult for bacteria to develop resistance to and can act on both gram-positive and gram-negative bacteria. Proton Nuclear Magnetic Resonance (^1H NMR) metabolomics is an important method for studying resistance development in bacteria, since this is both a quantitative and qualitative method to study and identify phenotypes by changes in metabolic pathways. In this project, the metabolic differences between wild type *Bacillus cereus* (*B. cereus*) samples and *B. cereus* that was mutated through 33 growth cycles in a non-lethal dose of a multivalent antimicrobial agent were identified. For additional comparison, samples for analysis of the wild type and mutated strains of *B. cereus* were prepared in both challenged and unchallenged conditions. A C_{16} -DABCO (1,4-diazabicyclo-2,2,2-octane) and mannose functionalized poly(amidoamine) dendrimer (DABCOMD) was used as the multivalent quaternary ammonium

antimicrobial for this hydrophilic metabolic analysis. Overall, the study reported here indicates that *B. cereus* are likely changing their peptidoglycan layer to protect themselves from the highly positively charged DABCOMD. This membrane fortification most likely led to the slow growth curve of the mutated and especially the challenged mutant samples. The association of these sample types with metabolites associated with energy expenditure is attributed to the increased energy required for the membrane fortifications to occur as well as to the decreased diffusion of nutrients across the mutated membrane.

Keywords Metabolomics; Quaternary ammonium compounds; Nuclear magnetic resonance; Dendrimers; DABCO; Antibiotic Resistance; Gram-Positive Bacteria; *Bacillus cereus*; *B. cereus*; Membrane Disruption

Introduction

The number of bacteria that develop resistance to known antibiotics is rapidly increasing. Antibiotic resistant bacteria are a universal health concern, especially since the majority of bacteria in hospitals are already resistant to at least one class of antimicrobial (Mintzer et al. 2011; Alanis 2005; Hoerr et al. 2016; González-Bello 2017; Todar 2012). The number of new antibiotics being developed every year decreases due to the challenges of effectively dispatching both antibiotic resistant bacteria and novel infectious bacteria. Both gram-negative and gram-positive bacteria have become drug resistant (Hoerr et al. 2016). Therefore, synthesizing an antimicrobial that works on both gram negative and gram-positive infectious bacteria would be preferred.

Bacillus cereus (*B. cereus*) is a gram-positive bacterium that infects humans and is an appropriate bacterium on which to conduct antimicrobial studies (Bundy et al. 2005; Kilcullen et al. 2016). Humans encounter *B. cereus* throughout the environment, and this strain of bacteria has been shown to produce a variety of compounds toxic to humans (Kilcullen et al. 2016; Todar 2020; Bottone 2010; Ceragioli et al. 2010). *B. cereus* can lead to a variety of infectious outcomes ranging from food poisoning to fatal meningitis, with food poisoning comprising the majority of infections (Bundy et al. 2005; Todar 2020; Bottone 2010; Ceragioli et al. 2010). It also has a short generation time, is easily mutable, has high mutation rates, and has a wide body of prior research reports (Ceragioli et al. 2010; Bundy et al. 2005; Kilcullen et al. 2016; Bottone 2010). Mutations in *B. cereus* that result in antibiotic resistance occur in the usual ways; randomly occurring genetic mutations, horizontal gene transfer, fortification of the cell wall (alterations in composition of the peptidoglycan layer), changes to the efflux pumps, and antibiotic degrading or altering enzymes (Humann and Lenz 2009; Martinez and Baquero 2000; Shepherd and Ibba 2013; Xu et al. 2006; Todar 2020; Denamur and Matic 2006; Anderson et al. 2012). Bacteria are proficient at DNA uptake from the environment, viral phage DNA injection, and bacterial plasmid swapping resulting in horizontal gene transfer. Antibiotic resistant bacterial communities can protect even distantly related antibiotic susceptible bacteria from antibiotics (Perlin et al. 2009).

Fortification of the bacterial cell walls is a common mutation which results in changes to the composition of the peptidoglycan layer since a significant quantity of antibiotics must pass through the cell wall for the antibiotic to be effective (Nikolaidis et

al. 2014; Shepherd and Ibba 2013; Zhao et al. 2018; Xu et al. 2006; Anderson et al. 2012). The pentapeptide side chains linked to N-acetylglucosamine and N-acetylmuramic acid in the peptidoglycan are responsible for crosslinking (Anderson et al. 2012; Shepherd and Ibba 2013; Schleifer and Kandler 1972; Nikolaidis et al. 2014; Vollmer et al. 2008). Changing the composition of the pentapeptide side chains is a relatively easy way for bacteria to attempt to repel environmental stressors, such as being grown in the presence of an antimicrobial agent, since these changes alter the cell wall's permeability, charge ratios, and patterns of noncovalent interactions (Anderson et al. 2012; Shepherd and Ibba 2013; Nikolaidis et al. 2014). Products from aminoacyl-tRNA biosynthesis can be diverted away from protein synthesis and toward peptidoglycan synthesis when alterations to the pentapeptide side chain would offer additional protection against antimicrobials (Shepherd and Ibba 2013). Glycine, for example, is involved in the crosslinking of the pentapeptide side chains of the peptidoglycan (Shepherd and Ibba 2013; Hammes et al. 1973), and a decrease in crosslinking has been shown to decrease overall bacterial survivability (Loskill et al. 2014). In addition, when alanine is converted to lactate in the pentapeptide side chain that truncates the D-ala-D-ala tail, and resistance to vancomycin occurs (Anderson et al. 2012). Lysine is a positively charged amino acid that is incorporated into the pentapeptide side chain to create a greater overall positive charge, which can aid in repelling positively charged antimicrobials (Shepherd and Ibba 2013). Thus, changing hydrophobicity, charge, permeability, rigidity and crosslinking by switching components of the pentapeptide side chain have been shown to increase bacterial survival (Loskill et al. 2014; Shepherd and

Ibba 2013; Humann and Lenz 2009; Anderson et al. 2012). These mutations have been shown to increase bacterial resistance to antimicrobial agents, thus decreasing the availability of effective antibiotics to treat infections (Martinez and Baquero 2000; Gonzáles-Bello 2017; Anderson et al. 2012).

It is of the utmost importance to develop innovative antibiotics based upon new scaffolds such that resistant and novel bacteria are less likely to have automatic resistance, or develop resistance upon exposure, in comparison to conventional antibiotics. One way to increase the potency of an antibiotic is by using a multivalent framework such as a dendrimer, which can serve as a multivalent delivery agent by presenting a concentrated dose of the antibiotic. Dendrimers can moreover interact with multiple cellular receptors simultaneously since multiple antibiotic units are bound to each dendrimer (Paleos et al. 2010; Lu and Pieters 2019; Cloninger 2002; Mintzer et al. 2011). The multivalent presentation can lower the total requisite concentration of antibiotic since dendrimers have increased local concentrations of the antimicrobial endgroups relative to the monomeric antimicrobials (Wolfenden et al 2015; VanKoten et al. 2016; Andre et al. 2001). Dendrimers are attractive scaffolds to use for multivalent antimicrobials because a plethora of antibiotic types can be readily attached to the scaffold in a variety of densities, and the size of the dendrimer can be systematically altered by varying the dendrimer generation (Mintzer et al. 2011; Paleos et al. 2010; Vembu et al. 2015; Chen et al. 2000; Lu and Pieters 2019). The poly(amidoamine) (PAMAM) dendrimers used in this report can be functionalized with multiple units of amino acids, antibiotics,

carbohydrates, and other bioactive assemblages (Cloninger 2002; Andre et al. 2001; Roy 2003).

Carbohydrate functionalized PAMAM dendrimers have been previously shown to act as antimicrobial agents (Roy 2003; Andre et al. 2001; Chabre and Roy 2008; Mintzer et al. 2011). Further functionalization of glycodendrimers with antibiotic moieties has been shown to increase the effectiveness of the antibiotics relative to their monomeric counterparts by increasing activity and/or making it more difficult for the bacteria to develop resistance. In addition, the carbohydrates can increase the system's solubility (García-Gallego et al. 2017; Wrońska et al. 2019; Mintzer et al. 2011; Chen et al 2000).

Quite a few of the conventional small molecule inhibitors target one pathway and require specific substrate binding affinity. Therefore, if the bacteria can alter that specific binding interaction, they develop (or start to develop) resistance (Mintzer et al. 2011; Hurdle et al. 2011). An advantage of some membrane disruptors is that the antibiotic does not have to be taken into the cell (Hurdle et al. 2011) where it could be degraded, pumped out, or sequestered. Causing membrane disruption while presenting a multivalent barrage makes it unlikely that the bacteria can quickly and effectively develop resistance, since they would have to change their membrane to such a degree that it would entail numerous mutations (Chamorro et al. 2012; Hurdle et al. 2011; Pieters et al. 2009). An added benefit of membrane disruptors is that they also cause energy and nutrient disruption since they damage the membrane and induce membrane rigidity (Hurdle et al. 2011).

Quaternary ammonium compounds (QACs) are common membrane disruptors. QACs have a positively charged ammonium group that is attracted to the bacterial phospholipid membrane, enabling membrane disruption and/or lysis (McDonnell and Russell 1999; Mintzer et al. 2011; Sreperumbuduru et al. 2016; Jiao et al. 2017). QACs are used as common surfactants and disinfectants (Engel et al. 2011; McDonnell and Russell 1999; Mintzer et al. 2011; Sreperumbuduru et al. 2016; Jiao et al. 2017); the QAC of interest in this study is 1,4-diazabicyclo-2,2,2-octane (DABCO) (Pokhrel et al. 2004) with an attached 16-carbon alkyl chain (C₁₆-DABCO). DABCO kills both gram positive and negative bacteria (Sreperumbuduru et al. 2016). A multivalent display of C₁₆-DABCO was appended to the mannosides on a mannose functionalized PAMAM dendrimer (DABCOMD) to create a multivalent antimicrobial (Figure 3.1) (VanKoten et al. 2016). DABCOMD presents multiple positively charged units and was used against both gram positive and gram-negative bacteria to ascertain the minimum inhibitory concentration (MIC) by VanKoten et al. in his 2016 study. After the MIC study was completed for 33 growth cycles, DABCOMD was 100-fold more potent against *B. cereus* than its monomeric C₁₆-DABCO counterpart. After the MIC study, *B. cereus* became very resistant to monomeric antimicrobials such as ampicillin and monomeric DABCO, but MIC values for multivalent DABCOMD remained relatively unchanged (VanKoten et al. 2016). The *B. cereus* sample arising after 33 growth cycles was collected and labeled as mutant (Mut) for metabolomic resistance pathway analysis. The mutant was compared to the wild type (WT, commercially available bacterial stock that was used to start the MIC study) using nuclear magnetic resonance (NMR) hydrophilic metabolomics

to better understand why *B. cereus* was unable to develop protective resistance against DABCOMD over the 33 growth cycles of the MIC study. A DABCOMD challenged (denoted Mut D or WT D) sample set of all sample types was also conducted by including a small amount of DABCOMD in the growth media while the samples were grown for sample collection. The unchallenged sample sets did not have anything added to the growth media (Figure 3.2). With the challenged and unchallenged sample comparisons, we could compare how the mutant and wild type samples respond to being grown in an annoying but unlethal amount of DABCOMD. A summary of the sample sets that were used for this study, and the abbreviations that are used throughout the manuscript, are provided in Table 1.

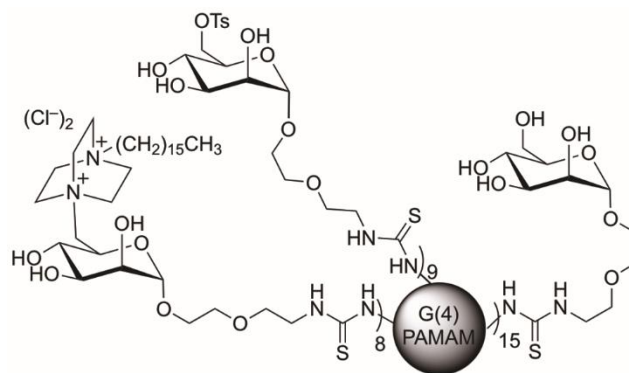


Figure 3.1. C₁₆-DABCO Mannose Functionalized Dendrimer (DABCOMD) Structure

Metabolomics, or the study of the small molecule biochemical byproducts of cellular metabolism (metabolites), is both a quantitative and qualitative method that can be used to compare two or more sample types by analyzing differences in their metabolite composition and concentration (Barding et al. 2012; Dettmer et al. 2007; Wishart 2008;

Turkoglu et al. 2019; Lämmerhofer and Weckwerth 2013; Lindon et al. 2007).

Metabolomic profiling enables the study of the interrelationship between an organism and its environment by measuring the mutations that occur as well as the changes to the organism's metabolic pathways that are incurred upon mutation (Shulaev 2006; Barding et al. 2012; Dettmer et al. 2007; Hoerr et al. 2016; Lämmerhofer and Weckwerth 2013; Lindon et al. 2007). Metabolomics studies have been used in applications including to determine phenotypes, distinguish biomarkers for diseases, and study biofilms and other environmental factors effecting organisms, because they change rapidly with response environmental changes. (Shulaev 2006; Barding et al. 2012; Hoerr et al. 2016; Tautenhahn et al. 2012; Turkoglu et al. 2019). Untargeted metabolomics can give a more complete picture of the mutated pathways involved in an altered metabolism than a targeted approach, since unexpected changes frequently occur in nature (Tautenhahn et al. 2012). NMR is a quantitative and reliable technique that has been used to study the differences between a wild type and mutated metabolism for over 40 years, because it is a nondestructive method that does not require separation of metabolites and is capable of observing certain molecules (sugars, amines, nonreactive species, etc.) more readily than mass spectrometry (Wishart 2008; Hoerr et al. 2016; Dettmer et al. 2005; Tautenhahn et al. 2012; Turkoglu et al. 2019; Ammons et al. 2014). Here, we report an untargeted proton (^1H) NMR hydrophilic metabolomics study that was used to observe metabolomic pathway alterations that occurred upon exposure of *B. cereus* to the multivalent antimicrobial agent DABCOMD. The goal of this study was to obtain an increased

comprehension of important mutations and major resistance strategies of gram-positive bacteria upon exposure to multivalent cationic antimicrobial compounds.

Table 3.1. Sample sets used in this study.

Sample Group¹	Abbreviation
Wild Type Mid Log	WT ML
Wild Type Stationary	WT S
Wild Type DABCOMD Mid Log	WT D ML
Wild Type DABCOMD Stationary	WT D S
Mutant Mid Log	Mut ML
Mutant Stationary	Mut S
Mutant DABCOMD Mid Log	Mut D ML
Mutant DABCOMD Stationary	Mut D S

¹ The color-coding of the sample sets shown here is used throughout this manuscript.

Materials and Methods

Samples

FDA strain PC1 213 *B. cereus* (ATCC 11778) was used for all the wild type (WT) samples and was mutated in the presence of DABCOMD as previously described in VanKoten et al. 2016 to create the mutant (Mut) samples. Unchallenged samples of both WT and Mut bacteria were grown in Brodo Mueller Hinton II Media (BMHII), the challenged samples (WT D and Mut D) were grown in BMHII with 0.37 μ M/L of DABCOMD added to the media (this is 33 % of the MIC value (VanKoten et al. 2016)). All other procedures were the same between the two groups. There were eight different sample types: unchallenged wild type mid log phase samples (WT ML), challenged wild type mid log phase samples (WT D ML), unchallenged wild type stationary phase (WT S), challenged wild type stationary phase (WT D S), unchallenged mutant mid log

phase (Mut ML), challenged mutant mid log phase (Mut D ML), unchallenged mutant stationary phase (Mut S), and challenged mutant stationary phase (Mut D S). A detailed description of how the samples were grown, collected, and standardized is provided in Appendix B the Supplementary Materials. A visual overview for the procedures is shown in Figure 3.2.

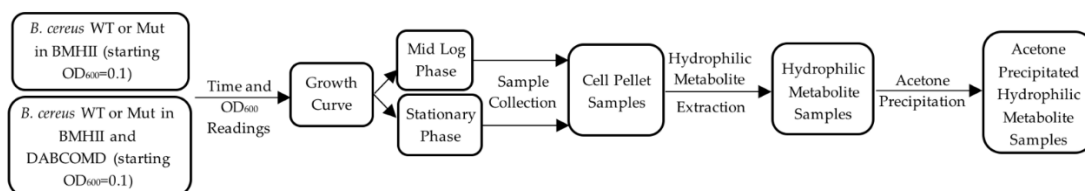


Figure 3.2. Overview of the protocol from the start of the cultures to the hydrophilic metabolite samples ready to be pelleted, frozen at -80°C , and put in NMR buffer. The processes for unchallenged and challenged samples are the same except for the inclusion of DABCOMD in the challenged sample media.

Metabolite Extraction Procedures

Note: All H₂O used was Millipore and all reagents used were cold (kept in the refrigerator).

Hydrophilic Extraction Sample cell pellets were thawed on ice and in glass test tubes. Methanol (800 μL) and Millipore water (170 μL) were pipetted into each test tube, and the samples were vortexed. The sonicator was used on each test tube for 5 minutes followed by vortexing. After chloroform (800 μL) and Millipore water (400 μL) were added to each test tube, they were vortexed and incubated for 15 minutes on ice. The samples were centrifuged for 15 minutes at 3,500 rpms. After the aqueous layer was pipetted into a sterile Eppendorf tube, the samples were dried on a speed vacuum. The

hydrophilic pellets were frozen at $-80\text{ }^{\circ}\text{C}$ (Aries and Cloninger 2020; Ammons et al. 2014 and 2015 and references therein).

Acetone Precipitation The frozen metabolite pellets were thawed on ice. D_2O (250 μL) and 1,250 μL acetone were added to the pellets, then they were frozen overnight at $-80\text{ }^{\circ}\text{C}$. The pellets were thawed on ice, causing them to become cloudy with precipitated proteins. After the samples were thawed, they were centrifuged for 30 minutes at 2,000 rpms. The liquid was pipetted into capped Eppendorf tubes, and the protein pellet was discarded. A speed vacuum dried the samples, and the resulting hydrophilic pellets were frozen at $-80\text{ }^{\circ}\text{C}$ (Aries and Cloninger 2020; Ammons et al. 2014 and 2015 and references therein).

NMR Sample Preparation

Note: NMR grade D_2O was always used.

NMR Buffer Preparation Imidazole (27.230 g) was added to 4.0 mL of D_2O to make an imidazole stock solution. A DSS stock solution was created by adding 21.23 mg of 3-(Trimethylsilyl)propane-1-sulfonate sodium salt (DSS) to 4.0 mL of D_2O . A sodium phosphate buffer stock solution was made by adding 0.345 g $\text{NaH}_2\text{PO}_4\cdot\text{H}_2\text{O}$, 0.355 g Na_2HPO_4 (anhydrous) and 0.040 g NaN_3 to 5.0 mL of D_2O . The stock solutions of imidazole (60 μL), sodium phosphate (1,500 μL), and DSS (300 μL) were added to 28,140 μL of D_2O to create a 30 mL D_2O buffer solution (Aries and Cloninger 2020; Ammons et al. 2014 and 2015 and references therein).

Sample Preparation Metabolite samples were prepared by taking the cell pellets obtained after acetone precipitation, placing them on ice, and adding 700 μL of the NMR buffer. The mixture was vortexed and transferred to capped glass NMR tube.

Appendix B the Supplementary Materials contain additional details regarding sample preparation.

Data Acquisition

Spectra were collected for each hydrophilic metabolite sample by using Topspin software (Bruker version 3.6) with a SampleJetTM automatic sample loading system on a Bruker Avance III 600 MHz NMR equipped with a 5 mm triple resonance (^1H , ^{15}N , ^{13}C) liquid-helium cooled TCI NMR CryoProbe at 298 K. A Bruker-supplied excitation sculpting (ES)-based ‘zgesgp’ pulse sequence was used to acquire 1D ^1H NMR spectra for all samples. All the NMR spectra were recorded using a ^1H spectral window of 7211.538 Hz, 256 scans, 64K data points and a dwell time interval of 69.33 μsec between points, resulting in a spectrum acquisition time of 4.54 s. A recovery delay (D1) time between acquisitions of 2 s was used, amounting to a total relaxation recovery time of 6.5 s between scans. A Fourier transformation was used on the spectra. H_2O and DSS resonances were used to phase the spectra.

Data Analysis

Chenomx NMR Suite 8.4 software (Chenomx 2020) was used to profile the spectra. The identity and concentration of the metabolites in each sample were obtained by using Chenomx profiler’s list of metabolites to generate a fitted metabolite spectrum. Chenomx is unable at this point to identify all peaks observed in the NMR spectra. The

constant sum method was used to standardize the concentrations of the metabolites identified in each sample (Emwas et al. 2018). The concentration of each individual metabolite was divided by the total concentration of all metabolites measured. This method works on the premise that the concentration of each individual metabolite changes relative to the concentration of the total sample (Emwas et al. 2018). XLSTAT hierarchical clustering, principal component analysis (PCA) and PCA biplot were used to analyze the standardized metabolite concentrations for each sample (Addinsoft 2021). A comma delineated form (CSV) of the standardized metabolite data were uploaded to MetaboAnalyst 5.0 for statistical analysis (Pang et al. 2021 and references therein). MetaboAnalyst 5.0 was used to generate volcano plots, 2D and 3D sparse partial least squares discriminate analysis (sPLS-DA), orthogonal partial least squares discriminate analysis (ortho PLS-DA), Pattern Hunter and PLS-DA very important features (VIP) data to determine correlations, and statistical significance of observed metabolite changes in each sample type. PCA, 2D and 3D sPLS-DA, ortho PLS-DA were used to identify outlier samples, demonstrate sample separation, and identify metabolite correlations to sample types. Volcano plots were used to determine which metabolites had significant fold changes and p-values (0.5 or less)), while pattern hunter was used to ascertain correlations between the metabolites in each paired sample type. The metabolites that were determined to be statistically significant were uploaded into the MetaboAnalyst Pathway Analysis tool and KEGG pathways (Kanehisa and Goto 2000 and references therein). All these statistical analyses were used in conjunction to ascertain the most

probable metabolomic pathway changes that occurred in the mutant samples and with the DABCOMD challenged sample types.

Results

^1H NMR spectra were obtained for the eight sample types listed in Table 3.1. Chenomx NMR Suite 8.4 software was used to profile each ^1H NMR spectrum to obtain the identity and concentration of the metabolites found in each sample. MetaboAnalyst 5.0 was used for 2D and 3D sPLS-DA, ortho PLS-DA, and PCA to eliminate outliers in each sample type. Outliers were apparent as they did not cluster with the rest of their group. The unchallenged wild type mid log and stationary phases had five nonoutlier samples; the DABCOMD challenged wild type mid log phase had six nonoutlier samples; the DABCOMD challenged wild type stationary phase had five nonoutlier samples; the unchallenged mutant mid log phase had seven nonoutliers; the unchallenged mutant stationary phase had five nonoutlier samples; the DABCOMD challenged mutant mid log phase had six nonoutlier samples; and the DABCOMD challenged mutant stationary phase had seven nonoutlier samples.

The metabolite identities and concentrations obtained from Chenomx NMR Suite 8.4 Software were input into XLSTAT Hierarchical Clustering with all sample types or with the following smaller groups of sample sets: mid log phase, stationary phase, challenged samples, and unchallenged samples. XLSTAT Hierarchical Clustering of all the sample types showed that WT ML and WT D ML were clustered together, Mut D S and WT D S were clustered together, and all other sample types were separated (Figure 3.3). Clustering of WT ML and WT D ML, and clustering of Mut D S and WT D

S, was also observed in smaller groupings as shown in Appendix Figure B4 of the Supplementary Materials. Hierarchical Clustering of the unchallenged samples showed complete separation of all sample types (Appendix Figure B4 of the Supplementary Materials).

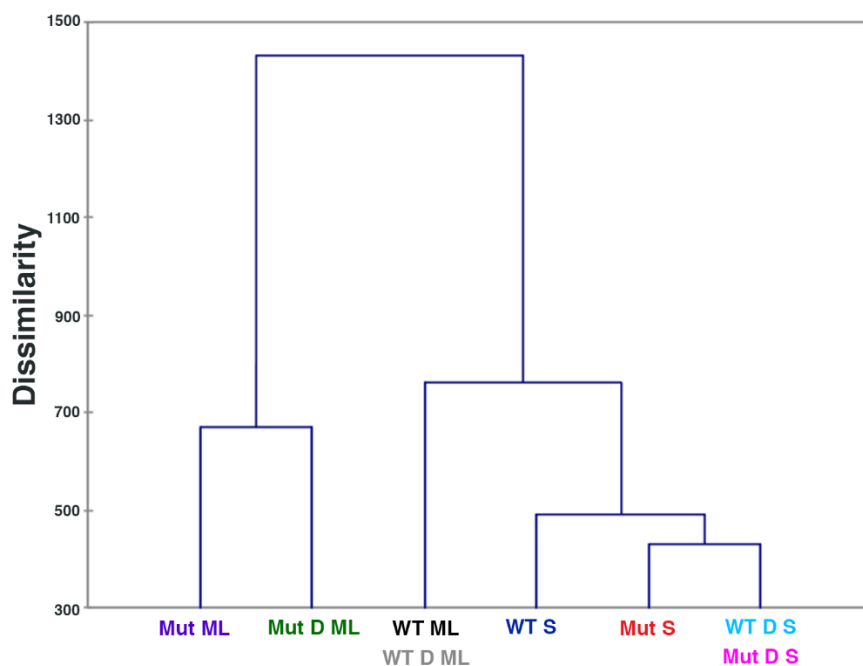


Figure 3.3. Hierarchical Clustering showing that WT ML and WT D ML cluster together, WT D S and Mut D S cluster together, and all other sample types are separate. Full names of sample groups are given in Table 3.1.

XLSTAT and MetaboAnalyst 5.0 multivariate statistical analyses, PCA biplots, 2D and 3D sPLS-DA, and ortho PLS-DA were used to determine the statistical significance for each metabolite, the metabolite to sample correlation, and sample clustering. Figure 3.4 shows the 2D sPLS-DA for all the samples together (a), only the mid log phase samples (b), only the stationary phase samples (c), only unchallenged samples (d), only the DABCOMD challenged samples (e), and ortho PLS-DA for all the

samples together (f). 3D sPLS-DA plots are provided in Appendix B the Supplementary Materials. Figure 3.4a shows the overlap of samples when all samples are plotted together. The observed overlap is likely due to the greater difference between mid log phase samples; because the stationary phase samples are more similar, they cluster together in plots that include the mid log phase. Therefore, the data was also observed using the smaller groups shown in Figures 3.4b-e containing the comparison sets listed above to render the differences between sample types more readily observable.

When only the mid log phase samples are plotted, the wild type samples (WT ML and WT D ML) had a small overlap while the mutant samples had a large separation (Figure 3.4b). This is due to the challenged and control wild type samples being more similar to each other, while the mutant samples were more different in the presence of DABCOMD than when they were unchallenged. As expected, WT D S clusters between WT S and Mut D S, whereas Mut S clusters farther away (Figure 3.4c). Figure 3.4d indicates that the wild type samples (WT ML and WT S) are similar to each other, whereas the mutant sample types (Mut ML and Mut S) are significantly different from each other, causing the wild type samples to cluster. Figure 3.4e shows that WT D S and Mut D S cluster closer together than the mid log phase samples, but sample overlaps were not observed. Ortho PLS-DA uses component one as a predictor of class, and component two is the variation perpendicular to the first component. The observable separation is improved when all of the sample types are plotted together using ortho PLS-DA relative to 2D sPLS-DA (Figure 3.4f). In addition, complete separation of the smaller sample

groups shown in Figures 3.4b-e was observable when ortho PLS-DA was used (graphs are available in Appendix B the Supplementary Materials).

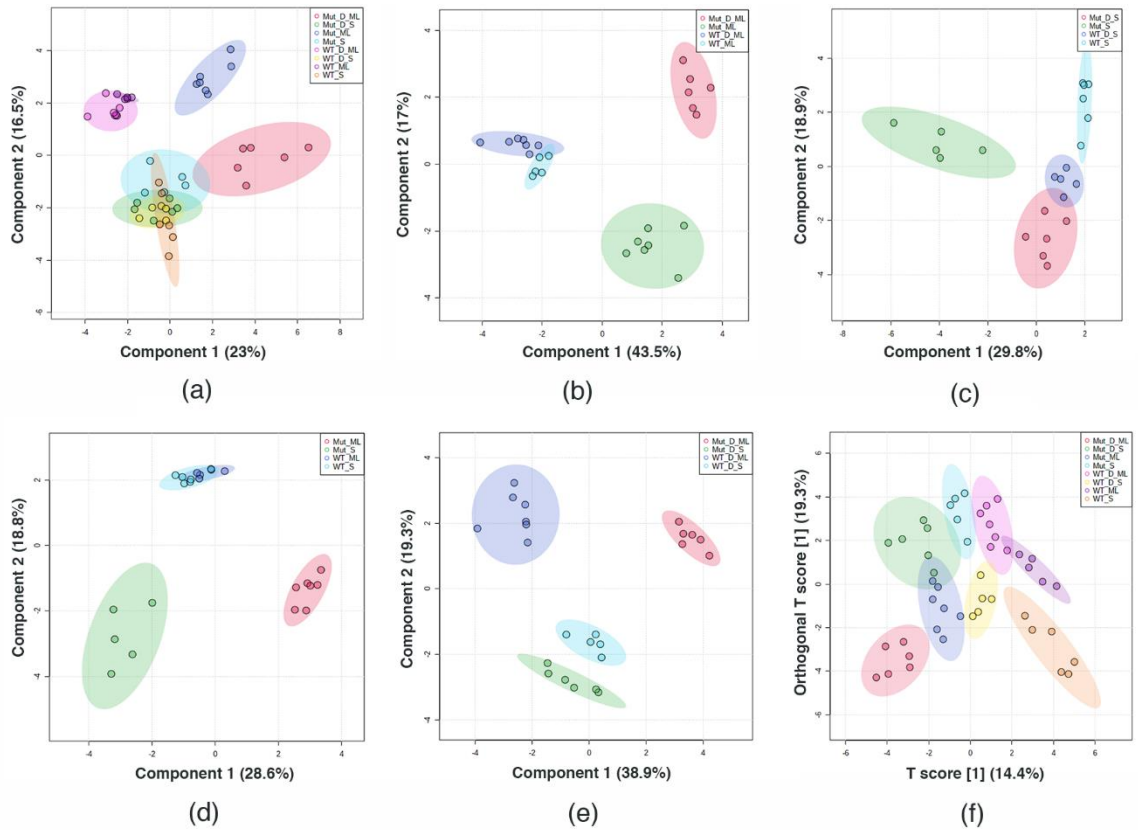


Figure 3.4. 2D sPLS-DA **(a)** Contains all sample types: showing overlap of WT ML with WT D ML, the overlap of all stationary phases, Mut ML is separate, and Mut D ML is separate. **(b)** Contains only mid log samples: showing slight overlap of WT ML with WT D ML and complete separation of Mut ML and Mut D ML. **(c)** Contains only stationary phase samples: showing slight overlap of WT D S and Mut D S, and complete separation of WT S and Mut S. **(d)** Contains unchallenged samples: showing a complete separation of Mut ML and Mut S samples and a 2D overlap of the WT ML with WT S (overlap not present in the 3D plot (Fig. S7d)). **(e)** Contains only DABCOMD challenged samples: showing complete separation of all sample types. **(f)** 2D ortho PLS-DA containing all sample types: demonstrates the greatest degree of separation with all sample types together, with only an overlap of the oval of WT ML with the oval of WT D ML, and a overlap of the oval of Mut D S with the ovals of WT S and Mut ML.

Figure 3.5 shows the PCA plot of sample separation when all the samples are plotted together, accounting for 43.22 % of variation. The percent variation indicates that only the first two components are needed for analysis. As expected from the hierarchical clustering (Figure 3.3), WT ML and WT D ML cluster together in the PCA plot, as do WT D S and Mut D S. In addition, the PCA plot shows overlap of all stationary phase clusters. The observed overlap of stationary phase clusters is due to the greater difference in the sample sets from the mid log phase. In particular, the two mutant sample types Mut ML and Mut D ML are sufficiently separated to cause the stationary phases to cluster closer together by comparison. The corresponding metabolites are also plotted in Figure 3.5. For example, N-acetylglucosamine, a peptidoglycan component, can be seen to have the strongest correlation to the DABCOMD challenged mutant mid log phase sample type due to its significantly higher concentration in that sample type.

PCA biplots showing only the mid log phase (Figure 3.6a) or the stationary phase (Figure 3.6b) were quite useful to show sample type and metabolite clustering. Since the first two components account for 63.23 % and 51.56 % of the variance for mid log and stationary phase data comparisons, respectively, only the first two components are needed for analysis. Figure 3.6a shows a slight separation between the challenged and unchallenged wild type samples (WT D ML and WT ML, respectively) and a large separation between the mutant sample types Mut D ML and Mut ML. When considering metabolites, N-acetylglucosamine, for example, is indicative of the mutants because it can be seen between Mut ML and Mut D ML and is the most indicative of the DABCOMD challenged mutant mid log phase sample type because it is closest to this

sample cluster (Figure 3.6a). Figure 3.6b shows complete separation of all stationary phase sample types, with WT D S and Mut D S being clustered the closest.

N-acetylglucosamine is closest to the mutant stationary phase cluster, indicating that this compound is most indicative of this sample type in the stationary phase.

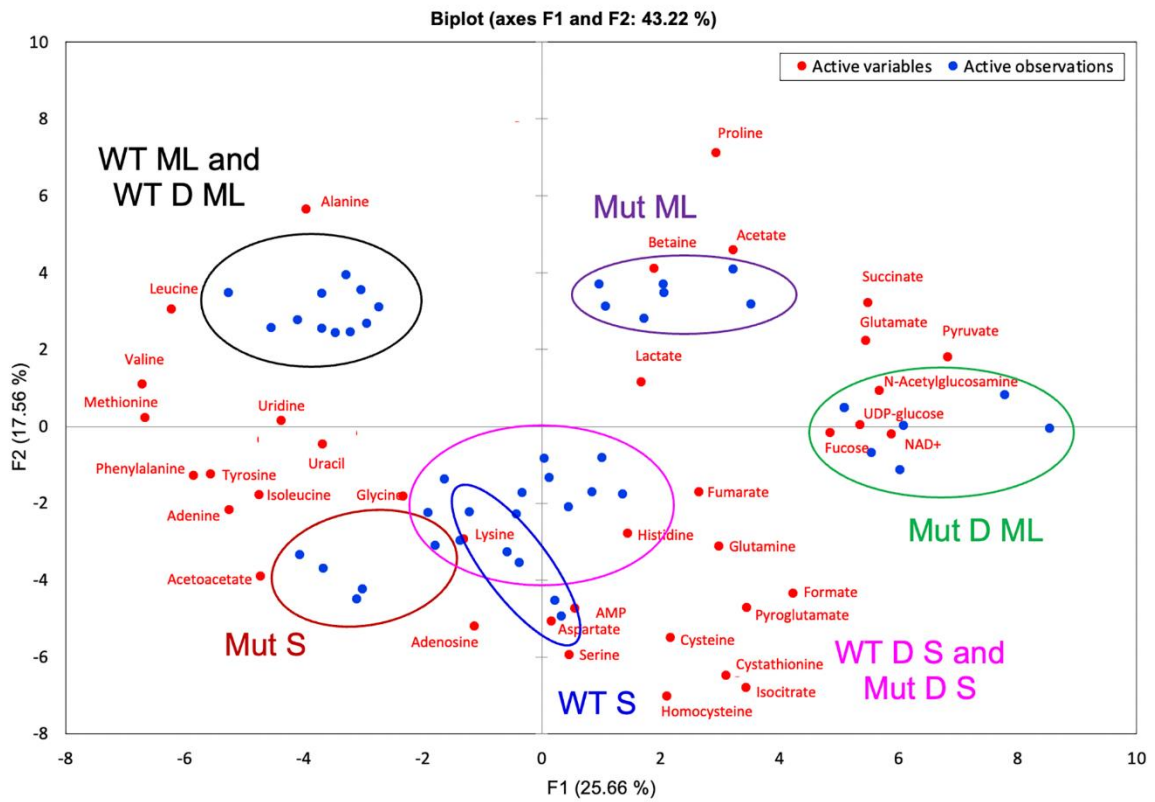


Figure 3.5. PCA biplot showing the distribution samples (blue dots) with color coordinated sample labels and circles and the distribution of metabolites (red dots).

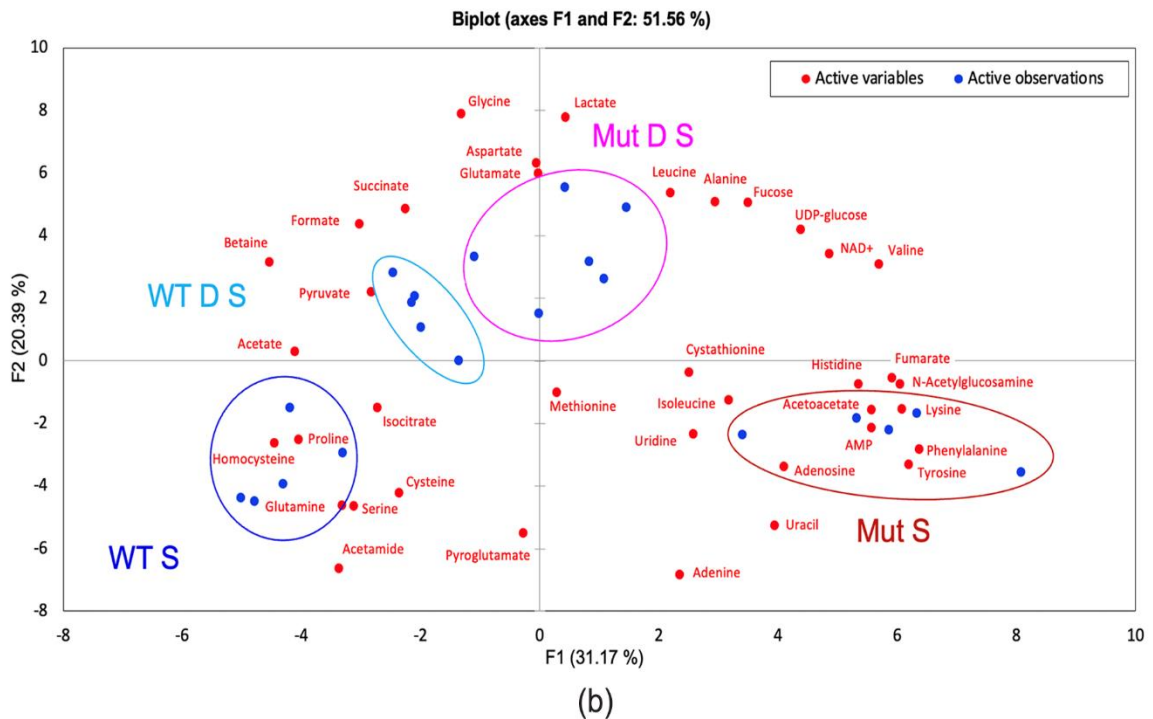
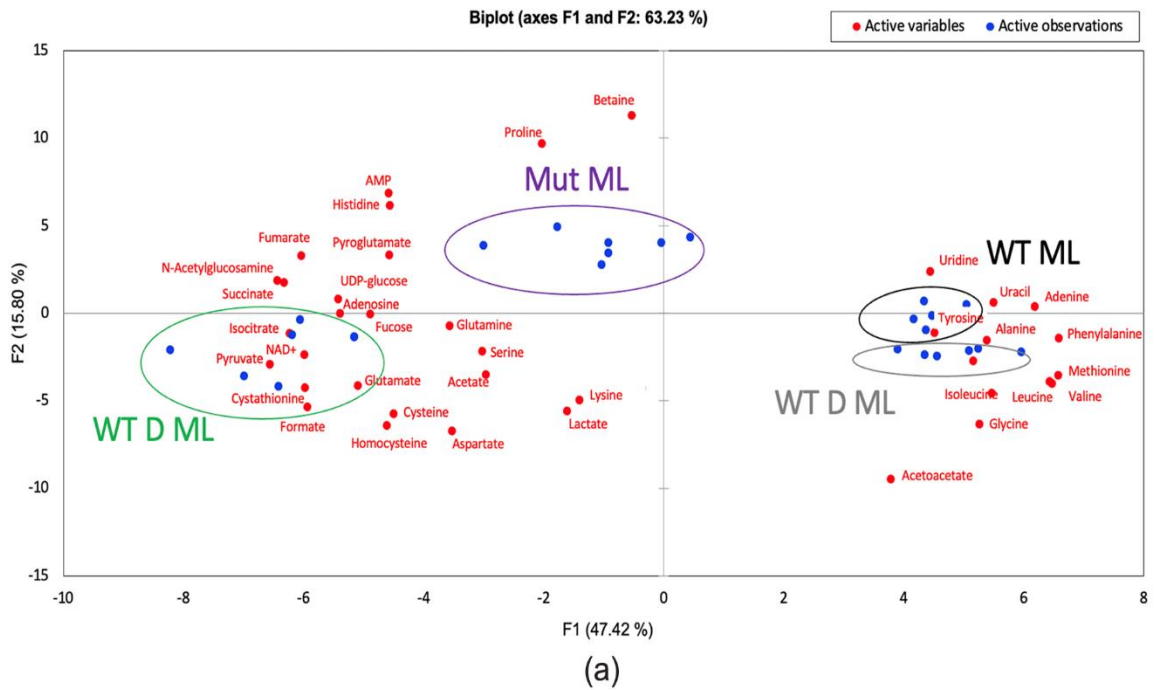


Figure 3.6. PCA biplots showing the distribution samples (blue dots) with color coordinated sample labels and circles and the distribution of metabolites (red dots). (a) Mid log phase samples showing WT ML and WT D ML very close together, Mut ML separated, and Mut D ML separated. (b) Stationary phase samples showing complete separation.

Figure 3.7 shows the PCA biplot for (a) only unchallenged sample types and (b) only DABCOMD challenged sample types, accounting for 50.73 % and 60.77 % of the variance, respectively. Again, only the first two components are needed for analysis. Figure 3.7a shows complete separation of sample types (WT ML, WT S, Mut ML and Mut S) and reveals the metabolites that are most closely associated with each sample type.

For example, N-acetylglucosamine is located between the mutant sample types but is located closer to the Mut ML sample type than the Mut S sample type. This indicates that N-acetylglucosamine is important and in higher concentrations in both mutant samples in comparison to the wild type sample types, but this metabolite is the most indicative of the Mut ML sample type. Figure 3.7b shows the overlap of the two stationary phase DABCOMD challenged sample types, indicating that the mutant and wild type samples are more different in the mid log phase and more similar in the stationary phase. One reasonable explanation for this observation is that the organisms have settled into similar stationary phases as they have adjusted to the low levels of DABCOMD present in the media.

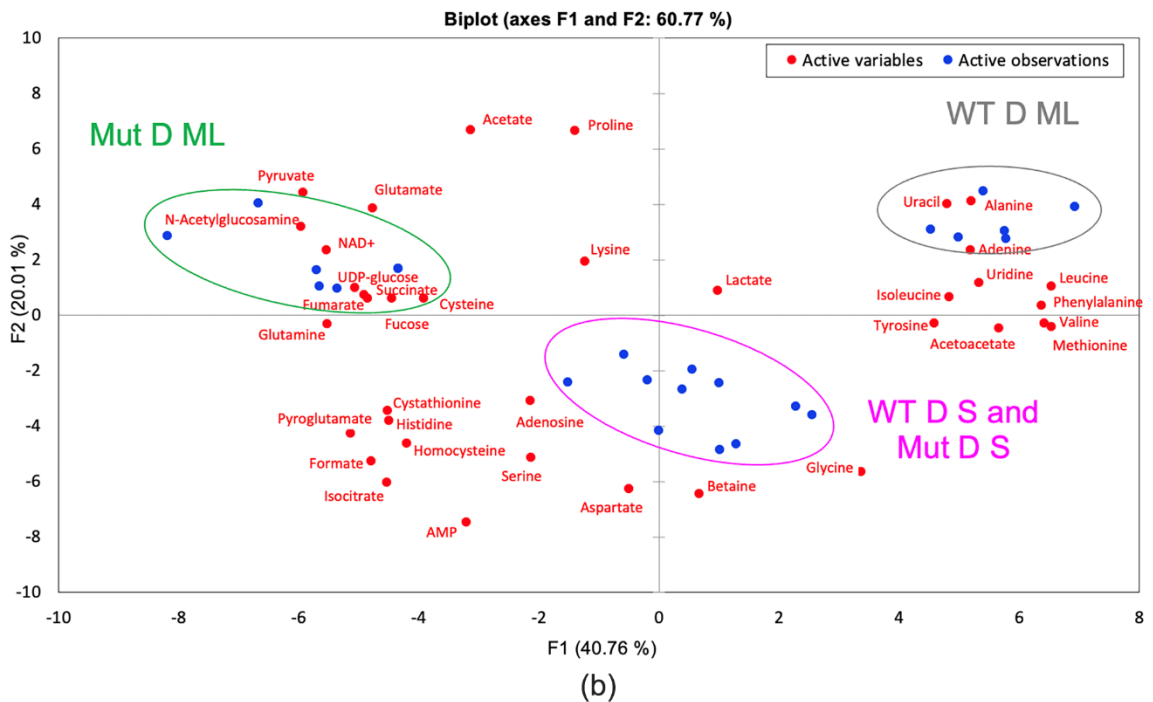
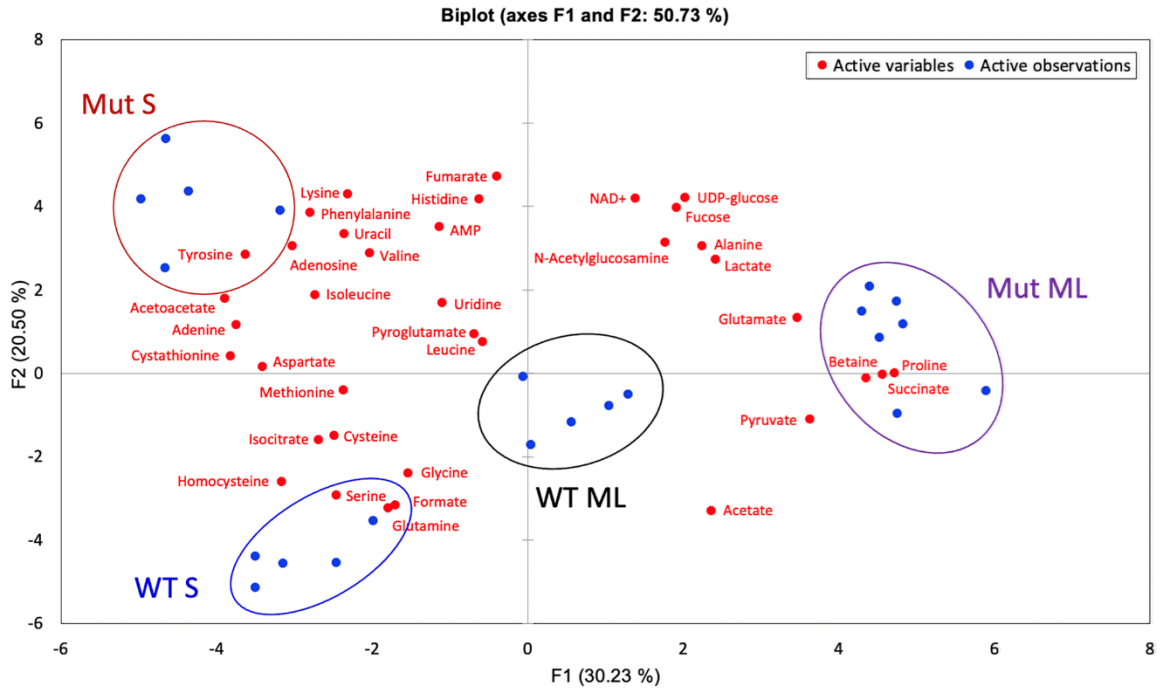


Figure 3.7. PCA biplots showing the distribution samples (blue dots) with color coordinated sample labels and circles and the distribution of metabolites (red dots). (a) Mut ML, Mut S, WT ML, and WT S samples showing complete separation. (b) DABCOMD challenged samples showing complete separation of WT D ML and Mut D ML, and the overlap of WT D S and Mut D S.

The metabolite identities and concentrations were entered into MetaboAnalyst 5.0 to create volcano plots of all the metabolites for pairs of sample types (Shown in Appendix Figures B8 and B9 of the Supplementary Materials). The volcano plots reveal metabolites with a p-value of 0.05 or less and a fold change of 1.25 or more. The volcano plots when comparing sample sets in the mid log phase, showed that the WT ML and WT D ML sample types are the most similar, whereas Mut ML and Mut D ML sample types show significantly more differences from each other. One possible rationale for this is that the mutants are reacting more to the low concentrations of DABCOMD in the media than the wild type, which are experiencing DABCOMD for the first time. The volcano plots using stationary phase samples overall showed less differences between sample sets. This is as expected since the samples should logically show more of a difference in the growth phase, where the bacteria need to accomplish more tasks to survive.

Very important features scores, or variable importance projections (VIP) in conjunction with other statistical analyses such as PCA biplots, volcano plots, pattern hunter and pathway hunter were used to generate Tables 3.2-3.11 showing important and statistically significant metabolites between paired sample types for easier analysis of the significant differences and to display the most likely pathways where the metabolite changes occurred. Pattern Hunter was used to check the correlation of a metabolite with the other metabolites found in the same pathway. If a metabolite did not correlate, it was not listed in that pathway. Uracil and aspartate were listed in the alanine pathway only if pattern hunter showed a correlation between alanine and these amino acids (shown in

Appendix B the Supplementary Materials). Betaine is shown in the glycine pathway only if pattern hunter showed a correlation between betaine and glycine (shown in Appendix B the Supplementary Materials). Metabolites found to be in and correlating to more than one pathway are shown in multiple pathways, since those metabolites are probably being used in multiple pathways.

Tables 3.2-3.11 show pairs of sample groups for mid log and stationary phase data. Pathways involving both energy and peptidoglycan synthesis are present. An in-depth discussion of the results shown in Tables 3.2-3.11 is provided in the following sections. Additional tables are provided in the Supplementary Materials, and a discussion of the implications arising from the broad trends observed when all sample sets are considered is provided in the discussion section.

Unchallenged Mutant versus Unchallenged Wild Types and Challenged Mutant versus Challenged Wild Types Comparisons

Tables 3.2–3.5 provide the comparisons between the mutant and wild type and also between the DABCOMD-challenged and unchallenged sample types. Statistically significant p-values and fold changes in metabolites commonly found in cell membrane composition and energy production pathways were observed when comparing these sample types. Components of peptidoglycan synthesis had very large fold change differences. When comparing Mut ML to WT ML, N-acetylglucosamine had a 61.5-fold increase in concentration in the Mut ML sample type. Comparing Mut D ML to WT D ML, there was a 94.2-fold higher concentration in the Mut D ML sample type. In the stationary phase, the fold change difference of N-acetylglucosamine was lower but was still very high between the mutants and wild types, with Mut D S having a 19.4-fold

increase and Mut S having a 48.7-fold increase in concentration when compared to their wild type counterparts. Mut ML displayed a 1.7-fold increase in lactate and a 3.0-fold increase in betaine when compared to WT ML and correlated with glycine, methionine, cysteine, and N acetylglucosamine. When comparing Mut D ML to WT D ML, there was not a significant change in betaine, but significant changes in the concentrations of aspartate, cysteine, homocysteine, methionine (VIP), and serine were observed and correlated with each other, cystathionine and N-acetylglucosamine. Mut S had a 2.4-fold decrease in betaine (VIP) and a 2.9-fold increase in lysine concentrations when compared to WT S. Glycine (VIP) and cystathionine were in higher concentrations, whereas glutamine and alanine were found in lower concentrations in Mut D S, when compared to WT D S. Nucleotide metabolism components in the mid log phase, such as adenine, uracil and uridine had a decreased concentration, while adenosine had a higher concentration in the challenged mutant sample in comparison with the challenged wild type sample. The same was true of the unchallenged mutant samples in comparison to the unchallenged wild type samples, except changes in uridine were not observed. In the stationary phase, adenine and uracil were in higher concentrations in WT D in comparison to Mut D, whereas adenosine and uracil were in a higher concentration in WT in comparison to Mut samples. The aminoacyl-tRNA biosynthesis pathway in both the challenged and unchallenged groups contained the largest number of metabolites with different concentrations when comparing the mutant samples with the wild type samples. A likely explanation is that aminoacyl-tRNA biosynthesis products were being diverted to peptidoglycan synthesis, since DABCOMD is a cationic quaternary ammonium

compound that causes a hole to form in the membrane. It is interesting to note that, when comparing the differences between WT and Mut to WT D and Mut D, the same pathways undergo mutations, except that betaine (involved in glycine and methionine metabolism) did not change significantly in the DABCOMD challenged samples. However, betaine can be used to make a variety of metabolites in methionine metabolism that did show significant changes such as serine, cystathionine, cysteine, homocysteine, and methionine, as well as glycine and pyruvate. The challenged sample type comparisons (Mut D and WT D) had a greater number of changes in concentration of more metabolites than the unchallenged sample types (Mut and WT). This is reasonable since betaine would be expected to be converted and consumed to make more of the metabolite differences observed in the challenged mutant samples. Challenged mutant samples had many significant increases in the concentrations of metabolites closely correlated with betaine, in comparison to the unchallenged mutant samples. More research is needed to determine what additional pathway changes may be causing the betaine concentration changes.

The DABCOMD challenged samples (Mut D vs WT D) showed changes in a greater number of metabolites per pathway, when compared to the unchallenged samples (Mut vs WT). When comparing Mut ML to WT ML and Mut D ML to WT ML, energy related metabolites found in the citric acid cycle and pyruvate metabolism, such as fumarate, isocitrate, succinate, formate and pyruvate, were found to be in excess in the mutant sample types. Acetoacetate, the exception, was in excess in the wild type samples. Energy metabolites such as AMP and NAD⁺ were in higher concentrations in both the

challenged and unchallenged mutant sample types relative to their wild type counterparts (6.8-fold and 37-fold increases for AMP and NAD⁺, respectively, for Mut D ML relative to wild type WT D ML). In the unchallenged samples, the mutant samples (Mut ML) had a 12.3-fold increase in NAD⁺ and a 9.1-fold increase in AMP concentrations when compared the unchallenged wild type samples (WT ML). This increase in the concentration of NAD⁺ in the challenged samples was observed in the stationary phase as well.

Table 3.2. Fold change of statistically significant metabolites in their corresponding metabolic pathways for the mid log phase of mutant versus wild type.

Mut ML versus WT ML					
Indicated Pathway	Metabolite	Fold Change^{1,2}	Indicated Pathway	Metabolite	Fold Change^{1,2}
Citric Acid Cycle	Acetoacetate	-2.8	Alanine Metabolism	Uracil ⁴	-1.2
	Fumarate ³	+4.9		Nucleotide Metabolism	Adenine
	Isocitrate	+1.7	Adenosine		+2.9
	NAD ⁺ ³	+12.3	Uracil ⁴		-1.2
	Succinate	+1.4			
Pyruvate Metabolism	Formate	+1.7	Aminoacyl-tRNA Biosynthesis	AMP ³	+9.1
	Pyruvate	+1.4		Glutamine ⁴	-1.6
Peptidoglycan Synthesis	Glutamine ⁴	-1.6		Histidine	+6.2
	Glycine ⁴	-2.2		Isoleucine	-4.6
	Lactate	+1.7		Leucine	-3.4 (VIP)
	N-Acetylglucosamine ³	+61.5		Phenylalanine	-2.0 (VIP)
Methionine Metabolism	Betaine ⁴	+3.0 (VIP)		Proline	+1.8 (VIP)
	Cysteine	+1.4		Tyrosine	-1.5
	Methionine	-2.6		Valine	-3.8 (VIP)
Glycine Metabolism	Betaine ⁴	+3.0 (VIP)			

¹A positive fold change is indicative of a higher concentration in the mutant. ²The metabolites with VIP next to them were determined to be very important features by the PSL-DA. ³These metabolites had concentrations lower than 0.01 for the sample with the lowest concentration. ⁴These metabolites are shown in multiple pathways where a correlation was shown by Pattern Hunter.

Table 3.3. Fold change of statistically significant metabolites in their corresponding metabolic pathways for the mid log phase of DABCOMD challenged mutant versus DABCOMD challenged wild type.

Mut D ML versus WT D ML					
Indicated Pathway	Metabolite	Fold Change^{1,2}	Indicated Pathway	Metabolite	Fold Change^{1,2}
Citric Acid Cycle	Acetoacetate	-1.6	Alanine Metabolism	Aspartate ⁴	+1.8
	Fumarate ³	+5.8		Uracil ⁴	-7.7 (VIP)
	Isocitrate	+6.1 (VIP)	Nucleotide Metabolism	Adenine	-2.1
	NAD ⁺ ³	+37.0		Adenosine	+3.0
	Succinate	+2.2 (VIP)		Uracil ⁴	-7.7 (VIP)
Pyruvate Metabolism	Acetate	+1.3 (VIP)	Aminoacyl-tRNA Biosynthesis	Uridine	-4.4
	Formate	+16.3 (VIP)		Alanine ⁴	-2.1 (VIP)
	Pyruvate	+2.9		AMP ³	+6.8
Peptidoglycan Synthesis	Alanine ⁴	-2.1 (VIP)		Aspartate ⁴	+1.8
	Glutamate ⁴	+1.7 (VIP)		Glutamate ⁴	+1.7 (VIP)
	Glutamine ⁴	+4.1 (VIP)		Glutamine ⁴	+4.1 (VIP)
	Glycine ⁴	-1.6		Glycine ⁴	-1.6
	N-Acetylglucosamine ³	+94.2		Histidine ³	+8.7
Methionine Metabolism	Aspartate ⁴	+1.8		Isoleucine	-5.5
	Cysteine	+1.8		Leucine	-11.3 (VIP)
	Homocysteine	+2.7		Phenylalanine	-4.0 (VIP)
	Methionine	-5.1 (VIP)		Tyrosine	-3.4
	Serine	+1.7	Valine	-11.2 (VIP)	

¹A positive fold change is indicative of a higher concentration in the mutant. ²The metabolites with VIP next to them were determined to be very important features by the PSL-DA. ³These metabolites had concentrations lower than 0.01 for the sample with the lowest concentration. ⁴These metabolites are shown in multiple pathways where a correlation was shown by Pattern Hunter.

Table 3.4. Fold change of statistically significant metabolites in their corresponding metabolic pathways for the stationary phase of mutant versus wild type.

Mut S versus WT S					
Indicated Pathway	Metabolite	Fold Change^{1,2}	Indicated Pathway	Metabolite	Fold Change^{1,2}
Citric Acid Cycle	Acetoacetate	+1.8	Nucleotide Metabolism	Adenosine	+3.2
	Fumarate ³	+8.9		Uracil ⁴	+2.2 (VIP)
	NAD+ ³	+11.1	Alanine ⁴	+1.4 (VIP)	
Pyruvate Metabolism	Acetate	-3.9 (VIP)	Aminoacyl-tRNA Biosynthesis	AMP	+3.3
	Formate	-7.3 (VIP)		Histidine ³	+21.6
Peptidoglycan Synthesis	Alanine ⁴	+1.4 (VIP)		Leucine	+1.8
	Lysine	+2.9 (VIP)		Phenylalanine	+3.1 (VIP)
	N-Acetylglucosamine ³	+48.7		Proline	-1.7 (VIP)
Glycine Metabolism	Betaine	-2.4 (VIP)		Tyrosine	+1.7
				Valine	+3.1 (VIP)

¹A positive fold change is indicative of a higher concentration in the mutant. ²The metabolites with VIP next to them were determined to be very important features by the PSL-DA. ³These metabolites had concentrations lower than 0.01 for the sample with the lowest concentration. ⁴These metabolites are shown in multiple pathways where a correlation was shown by Pattern Hunter.

Table 3.5. Fold change of statistically significant metabolites in their corresponding metabolic pathways for the stationary phase of DABCOMD challenged mutant versus DABCOMD challenged wild type.

Mut D S versus WT D S					
Indicated Pathway	Metabolite	Fold Change ^{1,2}	Indicated Pathway	Metabolite	Fold Change ^{1,2}
Citric Acid Cycle	NAD+ ³	+13.5	Alanine Metabolism	Aspartate ^{4,5}	+1.5 (VIP)
	Isocitrate ⁵	-1.3 (VIP)	Metabolism	Uracil ⁴	-3.0 (VIP)
	Succinate	-1.9 (VIP)	Nucleotide Metabolism	Adenine	-1.4 (VIP)
Pyruvate Metabolism	Acetate	+1.3 (VIP)	Metabolism	Uracil ⁴	-3.0 (VIP)
	Formate ⁵	+1.3 (VIP)		Alanine ^{4,5}	-1.2 (VIP)
Peptidoglycan Synthesis	Alanine ^{4,5}	-1.2 (VIP)	Aminoacyl-tRNA Biosynthesis	Aspartate ^{4,5}	+1.5 (VIP)
	Cystathionine	+1.7		Glutamine	-2.1 (VIP)
	Glutamine ^{4,5}	-2.1 (VIP)		Glycine ⁴	+1.5 (VIP)
	Glycine ^{4,5}	+1.5 (VIP)		Leucine ⁵	+1.4 (VIP)
	N-Acetylglucosamine ³	+19.4		Phenylalanine	+1.5 (VIP)
Methionine Metabolism	Aspartate ^{4,5}	+1.5 (VIP)	Valine	+1.7 (VIP)	
	Cysteine	-1.6			

¹A positive fold change is indicative of a higher concentration in the mutant. ²The metabolites with VIP next to them were determined to be very important features by the PSL-DA. ³These metabolites had concentrations lower than 0.01 for the sample with the lowest concentration. ⁴These metabolites are shown in multiple pathways where a correlation was shown by Pattern Hunter. ⁵These metabolites do not have significant p-values, but they are VIPs.

Challenged Wild Type versus Unchallenged Wild Type Comparisons

The sample comparison set that included the fewest observable changes was the comparison between the wild type samples grown in the presence and absence of DABCOMD, which is shown in Tables 3.6 and 3.7. The main differences were an increase in alanine, glutamate, and lactate concentrations, and a decrease in cystathionine and glutamine. These metabolites are commonly found components of peptidoglycan synthesis. Adding a small amount of the DABCOMD to the wild type (which had never been exposed to DABCOMD before) likely caused enhanced mutations for protection of their peptidoglycan layer through common substitutions to the pentapeptide

side chains. The growth curves were comparable for these two sample types (shown in Appendix B the Supplementary Information), again suggesting that although changes to the peptidoglycan composition in response exposure to low levels of DABCOMD by the wild type samples did cost some energy and cause some membrane disruption, dramatic metabolic changes did not occur. The only component of nucleotide metabolism that had a significant observable change was the decreased concentration of uridine in the challenged wild type samples in comparison with the unchallenged wild types in the stationary phase. In the stationary phase, the greatest number of observable changes were in amino acids involved in aminoacyl-tRNA biosynthesis, and changes in the concentrations of metabolites involved in the same types of pathways (energy production and peptidoglycan synthesis) as were observed in the mid log phase.

Table 3.6. Fold change of statistically significant metabolites in their corresponding metabolic pathways for the mid log phase of DABCOMD challenged wild type versus unchallenged wild type.

WT D ML versus WT ML		
Indicated Pathway	Metabolite	Fold Change ^{1,2}
Citric Acid Cycle	Isocitrate	- 1.6
Pyruvate Metabolism	Acetate	- 1.2 (VIP)
Aminoacyl-tRNA Biosynthesis	Alanine ³	+ 1.3 (VIP)
	Glutamate ³	+ 1.2 (VIP)
	Glutamine ³	- 3.5 (VIP)
	Valine	+ 1.2
Peptidoglycan Synthesis	Alanine ³	+ 1.3 (VIP)
	Cystathionine	- 1.6
	Glutamate ³	+ 1.2 (VIP)
	Glutamine ³	- 3.5 (VIP)
	Lactate	+ 2.8

¹A positive fold change is indicative of a higher concentration in the mutant. ²The metabolites with VIP next to them were determined to be very important features by the PSL-DA. ³These metabolites are shown in multiple pathways where a correlation was shown by Pattern Hunter.

Table 3.7. Fold change of statistically significant metabolites in their corresponding metabolic pathways for the stationary phase of DABCOMD challenged wild type versus unchallenged wild type.

WT D S versus WT S					
Indicated Pathway	Metabolite	Fold Change ^{1,2}	Indicated Pathway	Metabolite	Fold Change ^{1,2}
Citric Acid Cycle	Succinate	+3.0 (VIP)	Peptidoglycan Synthesis	Alanine ⁴	+1.6 (VIP)
	Pyruvate Metabolism	Acetate		-1.9 (VIP)	Glutamate ⁴
Aminoacyl-tRNA Biosynthesis	Alanine ⁴	+1.6 (VIP)	Glycine Metabolism	Glutamine ⁴	-1.2
	Glutamate ⁴	+1.6 (VIP)		Betaine	+1.4 (VIP)
	Glutamine ⁴	-1.2	Nucleotide Metabolism	Uridine	-1.6
	Histidine ³	+9.3			
Biosynthesis	Leucine	+1.9 (VIP)			
	Proline	-1.4 (VIP)			
	Valine	+1.9			

¹A positive fold change is indicative of a higher concentration in the mutant. ²The metabolites with VIP next to them were determined to be very important features by the PSL-DA. ³These metabolites had concentrations lower than 0.01 for the sample with the lowest concentration. ⁴These metabolites are shown in multiple pathways where a correlation was shown by Pattern Hunter.

Challenged Mutant versus Unchallenged Mutant Comparisons

Adding low levels of DABCOMD to the mutant samples created a significant difference in metabolite concentrations in multiple pathways associated with peptidoglycan synthesis, and energy related pathways, as shown in Tables 3.8 and 3.9. In addition, the growth curve of the challenged samples was significantly slower than their unchallenged mutant counterparts (Appendix Figure B2). Since the mutants had been previously exposed to DABCOMD, when DABCOMD was added to their media again, even in low levels, it caused them to fortify their defenses against the cationic antimicrobial agent to such an extent that their rate of growth was slow. The slower growth rate and the identification of spent energy molecules in the metabolite analysis can both be attributed to increased membrane disruption and fortification. The import of

essential nutrients is reduced while extra energy is also needed to induce membrane fortifications. In the mid log phase, the challenged samples had higher concentrations of the following energy metabolites: NAD⁺, succinate, isocitrate, acetate, formate and pyruvate. Multiple metabolites that can be used in peptidoglycan synthesis also had higher concentrations in the challenged mutant samples, including cystathionine, glycine, glutamate, and glutamine. Alanine, on the other hand, had higher a concentration in the unchallenged mutant samples. Betaine had a negative correlation with glycine, aspartate, cystathionine, cysteine, homocysteine and pyruvate in the mid log phase while exhibiting a positive correlation to glycine and aspartate and a negative correlation to N-acetylglucosamine levels in the stationary phase. Alanine had a positive correlation with uracil and methionine, and a negative correlation with N-acetylglucosamine, cysteine and cystathionine levels; aspartate, cysteine and homocysteine concentrations had a positive correlation with cystathionine levels. Nucleotide metabolism components in the mid log phase, such as adenine and uracil had a decreased concentration in the challenged mutants in comparison with the unchallenged mutant sample types. The same is true of the stationary phase, except adenosine was also observed to be in lower concentrations in the challenged mutant samples, in comparison to the unchallenged mutant samples. In the stationary phase, glycine (VIP), glutamate (VIP) and lactate were found in higher concentrations in the challenged samples, whereas lysine and N-acetylglucosamine were observed in higher concentrations in the unchallenged samples. Energy pathway related metabolites such as succinate, acetate and formate were VIPs and were found in higher concentrations in the challenged samples. Changes in the

concentrations of components of aminoacyl-tRNA biosynthesis were observed in both the mid log and stationary phases as well.

Table 3.8. Fold change of statistically significant metabolites in their corresponding metabolic pathways for the mid log phase of DABCOMD challenged mutant versus unchallenged mutant.

Mut D ML versus Mut ML						
Indicated Pathway	Metabolite	Fold Change ^{1,2}	Indicated Pathway	Metabolite	Fold Change ^{1,2}	
Citric Acid Cycle	Acetoacetate	+2.2	Alanine Metabolism	Uracil ⁴	-4.7 (VIP)	
	Isocitrate	+2.2		Nucleotide Metabolism	Adenine	-1.5
	NAD ⁺ ³	+3.0			Uracil ⁴	-4.7 (VIP)
	Succinate	+1.3			Alanine ⁴	-1.4 (VIP)
Pyruvate Metabolism	Acetate	+1.3 (VIP)	Aspartate ⁴	Aspartate ⁴	+2.1	
	Formate	+12.1 (VIP)		Glutamate ⁴	+1.6 (VIP)	
	Pyruvate	+1.9		Glutamine ⁴	+1.8 (VIP)	
Peptidoglycan Synthesis	Alanine ⁴	-1.4 (VIP)	Aminoacyl-tRNA Biosynthesis	Glycine ⁴	+1.2	
	Cystathionine	+4.7		Leucine	-2.7	
	Glutamate ⁴	+1.6 (VIP)		Phenylalanine	-2.0	
	Glutamine ⁴	+1.8 (VIP)		Proline	-1.5 (VIP)	
	Glycine ⁴	+1.2		Tyrosine	-1.8	
Methionine Metabolism	Aspartate ⁴	+2.1				
	Betaine ⁴	-4.0 (VIP)				
	Cysteine	+2.2				
Glycine Metabolism	Homocysteine	+5.4				
	Betaine ⁴	-4.0 (VIP)				

¹A positive fold change is indicative of a higher concentration in the mutant. ²The metabolites with VIP next to them were determined to be very important features by the PSL-DA. ³These metabolites had concentrations lower than 0.01 for the sample with the lowest concentration. ⁴These metabolites are shown in multiple pathways where a correlation was shown by Pattern Hunter.

Table 3.9. Fold change of statistically significant metabolites in their corresponding metabolic pathways for the stationary phase of DABCOMD challenged mutant versus unchallenged mutant.

Mut D S versus Mut S					
Indicated Pathway	Metabolite	Fold Change^{1,2}	Indicated Pathway	Metabolite	Fold Change^{1,2}
Citric Acid Cycle	Succinate	+2.3 (VIP)	Nucleotide Metabolism	Adenine	-2.7 (VIP)
Pyruvate Metabolism	Acetate	+2.6 (VIP)		Adenosine	-4.4
	Formate	+10.1 (VIP)		Uracil	-8.6 (VIP)
	Glutamate ^{3,4}	+1.3 (VIP)		AMP	-2.1
	Glutamine ³	-1.7		Glutamate ^{3,4}	+1.3 (VIP)
Peptidoglycan Synthesis	Glycine ³	+2.9 (VIP)		Glutamine ³	-1.7
	Lactate	+1.9	Aminoacyl-tRNA	Glycine ³	+2.9 (VIP)
	Lysine	-2.0		Histidine	-3.4
	N-Acetylglucosamine	-2.5	Biosynthesis	Isoleucine	-2.7 (VIP)
Glycine Metabolism	Betaine	+2.8 (VIP)		Leucine	+1.5
				Phenylalanine	-2.2 (VIP)
				Tyrosine	-1.5

¹A positive fold change is indicative of a higher concentration in the mutant. ²The metabolites with VIP next to them were determined to be very important features by the PSL-DA. ³These metabolites are shown in multiple pathways where a correlation was shown by Pattern Hunter. ⁴These metabolites do not have significant p-values, but they are VIPs.

Challenged Wild Type versus Unchallenged Mutants Comparisons

The comparison of the DABCOMD challenged wild type (never been exposed to DABCOMD before) to the unchallenged mutant samples (mutated in the presence of DAB-COMD) is shown in Tables 10 and 11. These samples always cluster separately in the mid log phase (Figures 3.3a, 3.4a,b, B4a,d, 3.6, B5a,b, 3.6a, B6, B7a,b) and almost cluster separately in the stationary phase (Figures 3.3a, 3.4c, B4a,e, B5a,c, 3.6b, B7a,c). The only instances where these sample groups cluster together is in the stationary phase was when all 8 sample types are plotted together (Figures 3.4a, 3.5, B6). The differences between the stationary phases are smaller than those in the mid log phase, thus causing the stationary phases to cluster closer together when they are all plotted on the same

graph. The unchallenged mutant samples and the challenged wild type samples clustering into unique sample types with many metabolite concentration differences (24 and 23) and large fold change differences (61.5, 12.4 and 9.1-fold in the mid log and 48.7, 11.1 and 8.9-fold in the stationary in the mutant samples), strongly suggests that the mutant samples truly are mutated variants of the original bacterial strain. Challenged wild type samples and unchallenged mutant samples, or the challenged wild type samples and challenged mutant samples, would likely cluster together if the DABCOMD only temporarily activated different pathways. Unchallenged mutant mid log samples had higher concentrations of NAD⁺, AMP, fumarate, succinate, and pyruvate than the mid log challenged wild type samples. The unchallenged mutant samples in the mid log phase also had higher concentrations in N-acetylglucosamine and cystathionine when compared to challenged wild type samples in the mid log phase. Nucleotide metabolism components in the mid log phase had a decreased concentration of adenosine and higher concentrations of adenine and uracil in the challenged wild type samples, in comparison with the unchallenged mutant samples. In the stationary phase, the unchallenged mutant samples had a higher concentration of these metabolites relative to the metabolite concentrations found in the challenged wild type samples. These changes were also observed in the stationary phase as well, with the unchallenged mutant samples having a fold increase of 11.1 in NAD⁺, 8.9 in fumarate, 2.3 in AMP and 48.7 in N-acetylglucosamine relative to the challenged wild type samples. Lysine, N-acetylglucosamine and cystathionine were in excess in Mut S. Betaine had a 3.6-fold change decrease in WT D ML in comparison to Mut ML and negatively correlated to

glycine, aspartate, cystathionine, cysteine, homocysteine, and pyruvate. While betaine had a 3.2-fold increase in WT D S when compared to Mut S and negatively correlated to cystathionine and N-acetylglucosamine. A positive correlation to homocysteine, glycine and pyruvate was also observed for betaine in WT D S compared to Mut S. In both the mid log and the stationary phases, both WT D and Mut had significant changes in the metabolites for energy pathways, aminoacyl-tRNA biosynthesis, peptidoglycan synthesis and associated pathways.

Table 3.10. Fold change of statistically significant metabolites in their corresponding metabolic pathways for the mid log phase of DABCOMD challenged wild type versus unchallenged mutant.

WT D ML versus Mut ML					
Indicated Pathway	Metabolite	Fold Change ^{1,2}	Indicated Pathway	Metabolite	Fold Change ^{1,2}
Citric Acid Cycle	Acetoacetate	+3.5	Alanine Metabolism	Uracil ⁴	+1.6 (VIP)
	Fumarate ³	-5.0		Nucleotide Metabolism	Adenine
	Isocitrate	-2.8	Adenosine		-2.0
	NAD ⁺ ³	-12.4	Uracil ⁴		+1.6 (VIP)
	Succinate	-1.7 (VIP)	Aminoacyl-tRNA Biosynthesis	Alanine ⁴	+1.5 (VIP)
Pyruvate Metabolism	Pyruvate	-1.5		AMP ³	-9.1
Peptidoglycan Synthesis	Alanine ⁴	+1.5 (VIP)		Glutamine ⁴	-2.3
	Cystathionine	-2.3		Glycine ⁴	+2.0
	Glutamine ⁴	-2.3		Histidine ³	-11.3
	Glycine ⁴	+2.0		Isoleucine	+5.7 (VIP)
	Lactate	+1.4		Leucine	+4.3 (VIP)
N-Acetylglucosamine ³	-61.5	Phenylalanine		+2.0 (VIP)	
Methionine Metabolism	Betaine ⁴	-3.6 (VIP)		Tyrosine	+1.9 (VIP)
Glycine Metabolism	Methionine	+2.9 (VIP)		Valine	+4.6 (VIP)
	Betaine ⁴	-3.6 (VIP)			

¹A positive fold change is indicative of a higher concentration in the mutant. ²The metabolites with VIP next to them were determined to be very important features by the PSL-DA. ³These metabolites had concentrations lower than 0.01 for the sample with the lowest concentration. ⁴These metabolites are shown in multiple pathways where a correlation was shown by Pattern Hunter.

Table 3.11. Fold change of statistically significant metabolites in their corresponding metabolic pathways for the stationary phase of DABCOMD challenged wild type versus unchallenged mutant.

WT D S versus Mut S					
Indicated Pathway	Metabolite	Fold Change ^{1,2}	Indicated Pathway	Metabolite	Fold Change ^{1,2}
Citric Acid Cycle	Acetoacetate	-1.6	Glycine Metabolism	Betaine ⁴	+3.2 (VIP)
	Fumarate ³	-8.9		Alanine Metabolism	Uracil ⁴
	NAD ⁺ ³	-11.1	Pyruvate Metabolism		Adenine
	Succinate	+4.4 (VIP)		Adenosine	-4.3
Acetate	+2.1 (VIP)	Uracil ⁴		-2.9 (VIP)	
Formate	Formate	+7.9 (VIP)	Aminoacyl-tRNA Biosynthesis	AMP	-2.3
	Pyruvate	+1.5		Glutamate ^{4,5}	+1.4 (VIP)
	Cystathionine	-1.7		Glycine ⁴	+2.0 (VIP)
Peptidoglycan Synthesis	Glutamate ^{4,5}	+1.4 (VIP)		Histidine	-2.3
	Glycine ⁴	+2.0 (VIP)		Phenylalanine	-3.2 (VIP)
	Lactate	+1.5		Tyrosine	-1.7
	Lysine	-2.4 (VIP)		Valine	-1.7 (VIP)
N-Acetylglucosamine ³	-48.7				
Methionine Metabolism	Betaine ⁴	+3.2 (VIP)			
	Homocysteine	+1.5			

¹A positive fold change is indicative of a higher concentration in the mutant. ²The metabolites with VIP next to them were determined to be very important features by the PSL-DA. ³These metabolites had concentrations lower than 0.01 for the sample with the lowest concentration. ⁴These metabolites are shown in multiple pathways. ⁵These metabolites do not have significant p-values, but they are VIPs.

Discussion

When *B. cereus* was grown in the presence of DABCOMD and compared to wild type *B. cereus* to obtain the eight sample sets described above (Table 3.1), statistically significant concentration changes in metabolites likely involved in energy related and cell wall composition related pathways were observed. The largest fold changes occurred in metabolites found in peptidoglycan synthesis and energy related pathways. The most compelling outcomes from this metabolomics study and the most likely implications of the observed trends are described below.

Comparisons between Metabolite Levels

Since in the stationary phase the cells are not rapidly dividing any more, the bacteria are likely settled into a fortified membrane structure and have a decreased metabolism. For this reason, smaller differences between all the sample type metabolite concentrations were observed in the stationary phase than in the mid log phase (Vollmer and Bertsche 2008).

In the mid log phase, glycine levels were significantly different between all sample type comparisons, except between the DABCOMD challenged and unchallenged wild type samples. In the stationary phase, glycine levels were different between all sample type comparisons, except between the challenged and unchallenged wild type samples and between the unchallenged mutant and unchallenged wild type samples. Betaine concentrations differed in the mid log phase between the challenged and unchallenged mutant samples, between unchallenged mutant and wild type, and between the challenged wild type and unchallenged mutant samples. In the stationary phase, betaine concentration levels differed between the WT D and WT samples, the WT D and Mut samples, and between the Mut D and Mut samples. Betaine was correlated not only to pyruvate (energy related molecule), glycine and cystathionine (peptidoglycan related molecules), but was also correlated to many components of methionine metabolism. When comparing any of the mutant samples to the wild type samples in the mid log phase, a significant change in the lactate concentration was observable. In the stationary phase, the concentration of lactate changed when comparing Mut D to Mut, Mut D to WT, and WT D to Mut. In the mid log phase, cystathionine was in higher concentrations in the mutant sample types in comparison to the wild type samples. Interestingly, the

highest concentration of cystathionine was detected in the challenged mutant samples, and the lowest was found in the challenged wild type. In the stationary phase, there was a difference between the challenged wild type samples and both types of mutant samples (challenged and unchallenged), with the mutant samples having the higher concentration of cystathionine. Cysteine followed the same pattern as cystathionine, with the mutant samples having a higher concentration than the wild type, and the challenged mutant samples having the highest concentration in the mid log phase. In the stationary phase, the challenged mutant samples had a lower concentration of cysteine than the challenged wild type samples, and significant changes in cysteine levels between other paired sample types were not observed. In the mid log phase, methionine had a higher concentration in mutant samples in comparison to their wild type counterparts, except challenged wild type samples were higher in concentration in comparison to the unchallenged mutant samples. There was not an observed difference in the concentration of methionine in the stationary phase. For homocysteine in the mid log phase, the only sample type comparisons that showed a significant difference in concentration was between the challenged mutant samples and all other sample types they were compared against, with the challenged mutant samples having the highest concentration of homocysteine. In the stationary phase, the only difference in homocysteine levels was between the challenged wild type samples and the unchallenged mutant samples, with the unchallenged mutant samples having a lower concentration of homocysteine in comparison to the challenged wild type samples. In the mid log phase, aspartate had a higher concentration when comparing the challenged mutant samples to all sample types they were compared

against. In the stationary phase, aspartate had a significantly higher concentration in the challenged mutant samples than in their challenged and unchallenged wild type sample counterparts. In the mid log phase, the glutamate concentration was higher in all the mutant samples than their wild type counterparts, with all challenged samples having higher concentrations of glutamate than their unchallenged counterparts. This differed from the stationary phase, where a difference in glutamate levels was only observed when comparing the challenged sample types to the unchallenged samples, with the challenged sample types having the higher glutamate concentration. With glutamine in the mid log phase, the challenged mutant samples had the highest concentration while the challenged wild type samples had the lowest concentration. The mutant samples had a higher concentration of glutamine than the wild type samples. In the stationary phase, however, the wild type samples had a higher concentration of glutamine than the challenged mutant samples did, and the unchallenged wild type samples had a higher concentration of glutamine than was present in the challenged wild type samples. Significant increases in lysine concentration were observed in the stationary phase in the unchallenged mutants in comparison to the unchallenged wild type samples. There was not an observable difference between the wild type sample types (WT D to WT) or between the DABCOMD challenged sample types (Mut D to WT D).

Pyruvate concentrations displayed a significant change during the mid log phase for all sample type comparisons, except when the challenged and unchallenged wild type samples were compared. When comparing low energy metabolites such as NAD⁺ and AMP in the mid log phase, the mutant samples had a significantly higher concentration of

these metabolites than the wild type samples, and the challenged mutant samples had a higher concentration than their unchallenged mutant counterparts. In the mid log phase, the mutant samples had higher concentrations of isocitrate than their wild type counterparts. In the unchallenged wild type samples, isocitrate had a higher concentration than was found in the challenged wild type samples, whereas unchallenged mutant samples had a lower concentration of isocitrate than the challenged mutant samples. In the stationary phase, the unchallenged wild type samples had a higher concentration of isocitrate than the unchallenged mutant samples and challenged wild type samples had higher concentrations than the challenged mutant samples. Formate in the mid log phase had higher concentrations in all the mutant sample types in comparison to the wild type samples. The largest difference in formate concentrations was seen when comparing the challenged mutant samples to the challenged wild type samples. This is because there was not a significant difference between the wild type samples (challenged and unchallenged), but the challenged mutant samples had a higher concentration than the unchallenged mutant samples. There was less of a difference between the formate levels in the stationary phase sample types than in the mid log phase sample types. Figure 3.8 displays the average and range of fold changes in key energy metabolites in comparisons between the wild type, the mutants, the unchallenged and the challenged *B. cereus* samples.

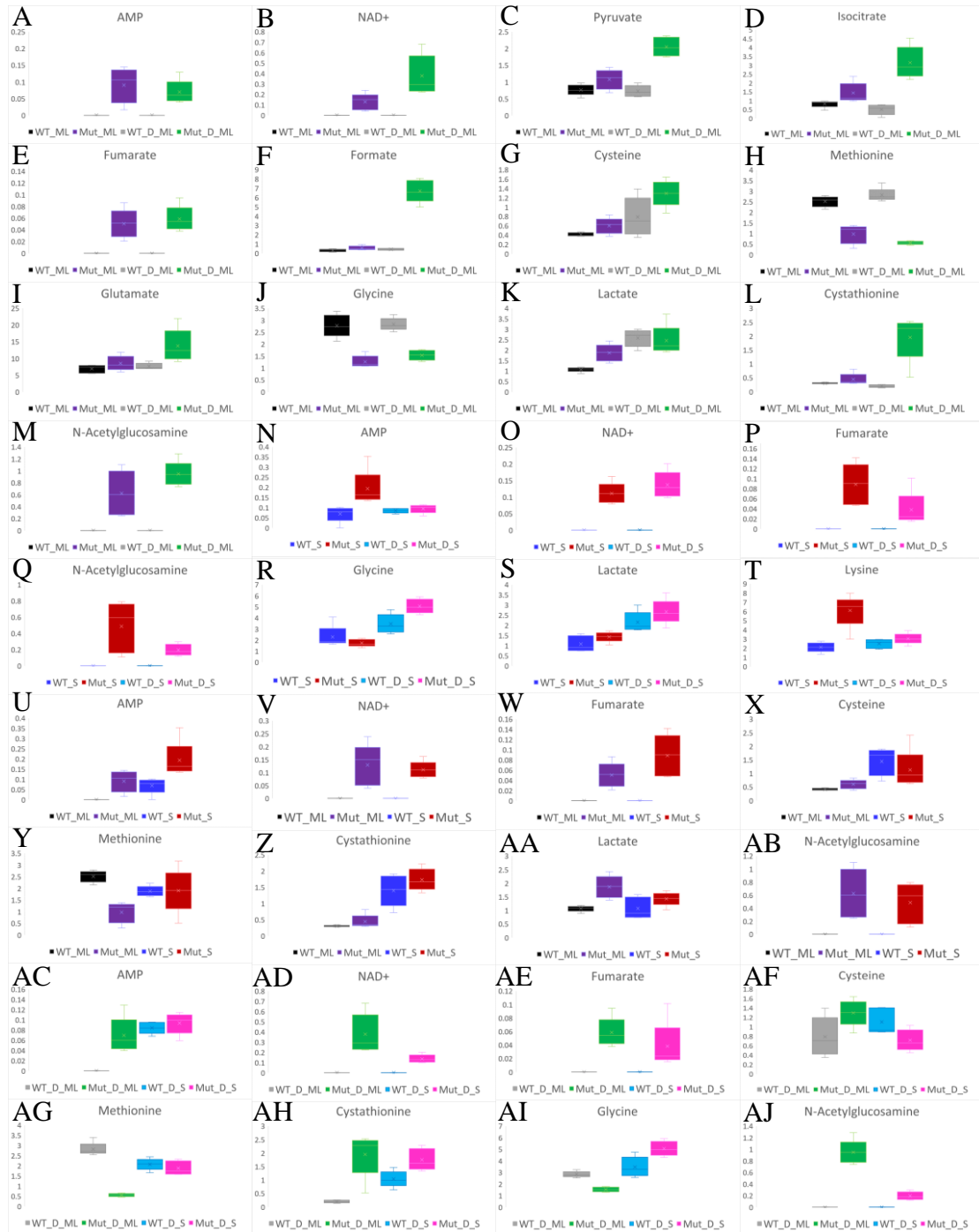


Figure 3.8. Box and whisker plots to show the differences in fold changes and the fold change ranges for example metabolites involved in peptidoglycan synthesis, membrane permeability and energy associated pathways. (a-m) Mid Log Phase Sample Comparisons. (n-t) Stationary Phase Sample Comparisons. (u-ab) Unchallenged Sample Comparisons. (ac-aj) Challenged Sample Comparisons

Significance of Metabolite Changes

Energy pathway related metabolites such as succinate, acetate and formate were VIPs found in higher concentrations in the challenged samples. Low energy metabolites, such as NAD⁺ and AMP were found in higher concentrations between the mutant samples than their wild type counterparts, and higher between the challenged mutant samples than the unchallenged mutant samples, while there was not a significant difference between the challenged and unchallenged wild type samples. The mutant samples, especially the DABCOMD challenged mutant samples, produce more metabolites to adapt to being grown in low levels of the antimicrobial compound. Growth of the mutants in DABCOMD results in increased energy requirements and a slower growth curve since the level of nutrients imported into the cell is reduced because of membrane fortification and disruption (Hurdle et al. 2011).

Significant changes in metabolites likely involved in aminoacyl-tRNA biosynthesis were observed when comparing the wild type and mutant samples, DABCOMD challenged and unchallenged in both the mid log and stationary phases. These changes were most likely due to diversion of components of aminoacyl-tRNA biosynthesis to peptidoglycan synthesis and antibiotic resistance (Shepherd and Ibba 2013). The mutant sample types generally had a lower concentration of nucleotide metabolites than their wild type counterparts. Some of these components were likely used in aminoacyl-tRNA biosynthesis. Changes were observed in the concentrations of many components of peptidoglycan synthesis that are involved in cell wall composition and frequently change in response to environmental stressors (like an antimicrobial being added to their growth media), such as lactate, glutamate, lysine, glycine, and

cystathionine. Changing the composition of the pentapeptide side chain of peptidoglycan is a common method for increasing bacterial resistance to antimicrobials (Mengin-Lecreulx et al. 1994; Humann and Lenz 2009; Vollmer et al. 2008; Nikolaidis et al. 2014; Anderson et al. 2012). Lysine, a positively charged amino acid, is commonly associated with incorporation into the peptidoglycan layer to increase the overall positive charge. Lysine substituted into the pentapeptide side chain of peptidoglycan has been shown to decrease the permeability and effectiveness of cationic antimicrobials (Shepherd and Ibba 2013). Incorporation of glycine into peptidoglycan causes crosslinking and increases rigidity (Shepherd and Ibba 2013; Hammes et al. 1973). It has been shown that increased crosslinking (glycine incorporation into peptidoglycan) is directly related to an increase in bacterial survival rates (Loskill et al. 2014). Mengin-Lecreulx et al. have previously shown that bacteria incorporate the cystathionine that was added to their media into their peptidoglycan layer. When cystathionine is incorporated into peptidoglycan, this truncates the pentapeptide side chain by binding in the number three spot and the D-ala-D-ala tail is not attached (Mengin-Lecreulx et al. 1994; Richard et al. 1993). Another metabolite that truncates the polyalanine tail is lactate (Anderson et al. 2012; Nikolaidis et al. 2014), which forms a D-ala-D-lac bond to change the terminal residue from alanine to lactate. If more lactate is needed, pyruvate can be reduced to D-lactate (Anderson et al. 2012; Nikolaidis et al. 2014). Lacking the polyalanine tail of the peptidoglycan by incorporating different metabolites is a common method used by bacteria to develop antimicrobial resistance (Loskill et al. 2014; Sheppard and Ibba 2013; Nikolaidis et al. 2014; Anderson et al. 2012). The largest change observed in this study occurred in the

levels of N-acetylglucosamine, with the mutant samples having the highest concentration. These changes were observed in the mid log phase when comparing any of the mutant samples to any of the wild type samples (DABCOMD challenged and unchallenged), but not when comparing the wild type samples to each other (DABCOMD challenged and unchallenged) or the mutant samples with each other (DABCOMD challenged and unchallenged). In the stationary phase, there was less of a difference in the concentration of N-acetylglucosamine when comparing any of the mutant sample types to any of the wild type samples and comparing Mut D S to Mut S than there was in the mid log phase. Figure 3.7 displays the fold change average and range for key observed metabolites involved in protecting *B. cereus* from DABCOMD. The significant changes in N-acetylglucosamine and other metabolites involved in peptidoglycan synthesis adds support to the theory that the mutants are changing the composition of their peptidoglycan layer to protect themselves from the positive charge on DABCOMD, thus reducing their likelihood that catastrophic membrane hole formation can occur.

Metabolomic Comparison of Gram-Positive and Negative Bacterial Exposure to DABCOMD

DABCOMD, a multivalent membrane disruptor, has been shown to work on both gram-positive and gram-negative bacteria without acquisition of resistance (VanKoten et al. 2016). Membrane disruptors, especially multivalent structures are especially intriguing because they also inadvertently cause energy and nutrient import disruption (Hurdle et al. 2011). Bacteria cannot easily change their membranes to such an extent that they become resistant to multivalent membrane disruptors, since membrane disruptors are generally attracted to the large negative charge of the membrane

(Chamorro et al. 2012; Pieters et al. 2009). The effects of DABCOMD on the gram-negative bacteria, *Escherichia coli* (*E. coli*), were previously reported (Aries and Cloninger 2020). No differences in growth curves were observed when comparing the wild type and mutated *E. coli*, whereas the mutated *B. cereus* samples had a slower growth and did not reach as high of an optical density in the stationary phase. Not as many upstream pathways to peptidoglycan synthesis and aminoacyl-tRNA biosynthesis were observed in the *E. coli* samples in comparison to the *B. cereus* samples. The fold changes for the concentrations in observed metabolites were also larger in the *B. cereus* results in comparison to the *E. coli* results, especially for metabolites associated with peptidoglycan synthesis and energy related pathways. This makes sense because gram-negative bacteria contain about 10% peptidoglycan in their cell membranes, whereas gram-positive bacteria contain up to 70% peptidoglycan in their cell walls (Schleifer and Kandler 1972). Since gram-positive bacteria (*B. cereus*) have a thicker peptidoglycan layer, more changes can be observed in comparison to the gram-negative bacteria (*E. coli*). Larger differences in observed energy related metabolites are also reasonable for gram-positive bacteria, since changes to the higher concentration of peptidoglycan in the phospholipid membrane (gram-positive) would require more energy, more rigidity, and more membrane disruption with nutrient import. The greater observed disruption of nutrient import is as expected for *B. cereus* due to its cell wall and larger concentration of peptidoglycan, and this is likely responsible for the slower growth curve that also does not reach the regular stationary phase optical density. The membrane disruption properties of DABCOMD are especially evident when observing that the challenged

mutant *B. cereus* samples had the slowest overall growth curve, had the lowest stationary phase density, and was associated with higher N-acetylglucosamine production and spent energy molecules in comparison to the unchallenged mutant *B. cereus* samples (which did not have as slow of a growth curve or as much of a fold change for peptidoglycan synthesis and spent energy pathways) and especially in comparison to the mutated *E. coli* samples (which did not have any observable change in growth curve and did not have as many peptidoglycan synthesis and spent energy changes). Overall, DABCOMD is a multivalent membrane disruptor that is difficult for either gram-positive or gram-negative bacteria to develop resistance to, since this antimicrobial compound contains multiple attached positive charges that are attracted to the negatively charged phospholipids of bacteria. In the attempt to develop resistance to DABCOMD, both gram-positive (*B. cereus*) and gram-negative (*E. coli*) bacteria were observed to fortify their membranes by altering their peptidoglycan layers, consequently incurring more energy costs and disruption of nutrient import.

Conclusions

Novel antimicrobials with new scaffolds are needed to assuage the increasing tide of ever increasing antibiotic resistant bacteria. Multivalent antimicrobials have the potential to exhibit increased efficacy relative to their monovalent counterparts. The C₁₆-DABCO and mannose functionalized dendrimer (DABCOMD) was used to study the effects of multivalent quaternary ammonium antimicrobials. The mutant samples were previously mutated in the presence of DABCOMD. In addition, samples were challenged with a low dose of DABCOMD in their growth media to generate samples for

comparison to samples grown in unchallenged media. Metabolite profiles during both the mid log and stationary phases were undertaken using ^1H NMR hydrophilic metabolite analysis to discern metabolite identifications and concentrations. Many metabolites commonly associated with energy associated pathways, peptidoglycan synthesis and related pathways were observed. The stationary phase had significantly less changes in metabolite concentrations between paired sample types than the mid log phase. An example of a stationary phase significant change is in the concentration of lysine, with which higher concentrations were associated with the mutant sample types. Since lysine is a positively charged amino acid associated with decreasing the efficacy of positively charged antimicrobials, the observed changes in lysine concentrations are highly consistent with cell wall alternations that would be expected for these studies. The largest observed metabolite concentration change (up to 94.2-fold) was in N-acetylglucosamine. Higher N-acetylglucosamine levels were associated with the mutant sample type, especially the challenged mutant sample type in comparison to their wild type counterparts. N-acetylglucosamine is a major component of peptidoglycan synthesis and is involved in cell membrane fortification and survivability. The mutant sample type, especially the challenged mutant samples, were associated with significantly more spent energy molecules (up to 37-fold increase in NAD^+), and a slower growth curve. The slower growth and association with spent energy molecules of the mutants, especially the challenged mutants, was most likely due to membrane fortification slowing the rate of nutrient entry into the cell. Moreover, making these fortifications would be energetically costly. The differences in energy requirements between the mutant and

wild type samples and DABCOMD challenged and unchallenged sample types were likely less significant in the stationary phase than the mid log phase, because the bacteria were no longer rapidly dividing, were changing their peptidoglycan layers less frequently, and were decreasing their metabolism.

Overall, there was a larger difference between the challenged wild type/mutant sample pairing than the unchallenged wild type/mutant sample pairing. The smallest difference was between the challenged and unchallenged wild type samples, while there was a large difference between the challenged and unchallenged mutant samples. The data from analyzing NMR hydrophilic metabolite concentrations from challenged versus unchallenged sample types demonstrated that the challenged mutant samples grew more slowly, had more spent energy related metabolites and had more and larger concentration changes in metabolites associated with peptidoglycan synthesis and related pathways than their unchallenged counterparts. The mutant *B. cereus* samples, especially those re-exposed to the antimicrobial, are likely changing their peptidoglycan composition to protect their cell walls from the large positive charge on DABCOMD. This change in the peptidoglycan caused them to require more energy, have a greater extent of membrane disruption of nutrient import, and grow more slowly than the wild type samples.

Data Availability Statement

The data presented in this study are openly available in NIH Common Fund's National Metabolomics Data Repository (NMDR) website, the Metabolomics Workbench, where it has been assigned Study ID ST001966 (Metabolomics Workbench 2021).

Acknowledgments

Funded by NIGMS, grant number 62444, is gratefully acknowledged. The bacterial stocks of wild type and mutants were provided by Dr. Harrison VanKoten. Dr. Brian Tripet aided in the procurement of NMR spectra.

Conflicts of Interest

The authors declare no conflict of interest. The funders had no role in the design of the study; in the collection, analyses, or interpretation of data; in the writing of the manuscript, or in the decision to publish the results.

References

- Addinsoft (2021). XLSTAT Statistical and Data Analysis Solution. New York, USA.
<https://www.xlstat.com>.
- Alanis, A. J. (2005) Review Article: Resistance to Antibiotics: Are we in the post-antibiotic era? *Archives of Medical Research*, 36, 697-705.
- Ammons, MC. B., Tripet, B. P., Carlson, R. P., Kirker, K. R., Gross, M. A., Stanisich, J. J., Copié, V. (2014) Quantitative NMR Metabolite Profiling of Methicillin-Resistant and Methicillin-Susceptible *Staphylococcus aureus* Discriminates between Biofilm and Planktonic Phenotypes. *Journal of Proteome Research*, 13, 2973-2985.
- Ammons, MC. B., Morrissey, K., Tripet, B. P., Van Leuven, J. T., Han, A., Lazarus, G. S., Zenilman, J. M., Stewart, P. S., James, G. A., Copié, V. (2015) Biochemical Association of Metabolic Profile and Microbiome in Chronic Pressure Ulcer Wounds. *PLOS one*, 10(5), 1-22. doi:10.1371/journal.pone.0126735.
- Anderson, R. J., Groundwater, P. W., Todd, A., Worsley, A. J. (2012). Microorganisms: In Antibacterial Agents: Chemistry, Mode of Action, Mechanisms of Resistance and Clinical Applications. (pp. 3-32). West Sussex, UK: Wiley.
- Anderson, R. J., Groundwater, P. W., Todd, A., Worsley, A. J. (2012). Glycopeptide Antibiotics: In Antibacterial Agents: Chemistry, Mode of Action, Mechanisms of Resistance and Clinical Applications. (pp. 305-318). West Sussex, UK: Wiley.
- Andre, S., Pieters R. J., Vrsaidas, I., Kaltner, H., Kuwabara, I., Liu, F-T., Liskamp, R. M. J., Gabius, H-J. (2001) Wedgelike Glycodendrimers as Inhibitors of Binding of Mammalian Galectins to Glycoproteins, Lactose Maxiclusters, and Cell Surface Glyconjugates. *ChemBioChem*, 2, 822-830.
- Aries, M.L., Cloninger, M.J. (2020) NMR Metabolomic Analysis of Bacterial Resistance Pathways Using Multivalent Quaternary Ammonium Functionalized Macromolecules. *Metabolomics*, 16(82), 1-11. doi.org/10.1007/s11306-020-01702-1
- Barding, G. A., Salditos, R., Larive, C.K. (2002) Quantitative NMR for Bioanalysis and Metabolomics. *Analytical Bioanalytical Chemistry*, 404, 1165-1179.
- Bottone, E.J. (2010) *Bacillus cereus*, a Volatile Human Pathogen. *Clinical Microbiology Reviews*, 23(2), 382-398.

- Bundy, J.G., Willey, T.L., Castell, R.S., Ellar, D.J., Brindle, K.M. (2005) Discrimination of Pathogenic Clinical Isolates and Laboratory Strains of *Bacillus cereus* by NMR-Based Metabolomic Profiling. *FEMS Microbiology Letters*, 242, 127-136.
- Ceragiolo, M., Mols, M., Moezelaar, R., Ghelardi, E., Senesi, S., Abee, T. (2010) Comparative Transcriptomic and Phenotypic Analysis of the Responses of *Bacillus cereus* to Various Disinfectant Treatments. *Applied and Environmental Microbiology*, 76(10), 3352-3360.
- Chamorro, C., Boerman, M.A., Arnusch, C.J., Breukink, E., Pieters, R.J. (2012) Enhancing Membrane Disruption by Targeting and Multivalent Presentation of Antimicrobial Peptides. *Biochimica et Biophysica Acta*, 1818, 2171-2174.
- Chenomx (2020) N.M.R. Suite 8.4. Edmonton: Chenomx Inc.
- Chen, C. Z., Beck-Tan, N. C., Dhurjati, P., Van Dyk, T. K., LaRossa, R. A., Cooper, S. L. (2000) Quaternary Ammonium Functionalized Poly(propylene imine) Dendrimers as Effective Antimicrobials: Structure-Activity Studies, *Biomacromolecules*, 1, 473-480.
- Cloninger, M. J. (2002) Biological Applications of Dendrimers. *Current Opinions in Chemical Biology*, 6, 742-748.
- Denamur, E., Matic, I. (2006) Evolution of Mutation Rates in Bacteria. *Molecular Microbiology*, 60 (4), 820-827.
- Dettmer, K., Aronov, P. A., Hammock, B. D. (2007) Mass Spectrometry-Based Metabolomics. *Mass Spectrometry Review*, 26, 51-78.
- Emwas A-H., Saccenti, E., Gao, X., McKay, R.T., Martins dos Santos, V.A.P., Roy, R., Wishart, D.S. (2018) Recommend Strategies for Spectral Processing and Post-Processing of 1D ¹H-NMR Data of Biofluids with a Particular Focus on Urine. *Metabolomics*, 14(31), 1-23.
- García-Gallego, S., Franci, G., Falanga, A., Gómez, R., Folliero, V., Galdiero, S., Javier de la Mata, F., Galdiero, M. (2017) Function Oriented Molecular Design: Dendrimers as Novel Antimicrobials. *Molecules*, 22, 1581-1610.
- González-Bello, C. (2017) Antibiotic Adjuvants- A Strategy to Unlock Bacterial Resistance to Antibiotics. *Bioorganic and Medicinal Chemistry Letters*, 27, 4221-4228.

- Hammes, W., Schleifer, K. H., Kandler, O. (1973) Mode of Action of Glycine on the Biosynthesis of Peptidoglycan. *Journal of Bacteriology*, 116(2), 1029-1053.
- Hoerr, V., Duggan, G. E., Zbytnuik, L., Poon, K. K. H., Große, C., Neugebauer, U., Methling, K., Löffler, B., Vogel, H. J. (2016) Characterization and Prediction of the Mechanism of action of antibiotics through NMR Metabolomics. *BMC Microbiology*, 16(82), 1-14. doi:10.1186/s12866-016-0696-5
- Humann, J., Lenz, L. L. (2009) Bacterial Peptidoglycan Degrading Enzymes and their Impact on Host Muropeptide Detection. *Journal of Innate Immunity*, 1, 88-97.
- Hurdle J.G., O'Neill, A.J., Chopra, I., Lee, R.E. (2011) Targeting Bacterial Membrane Function: an Underexploited Mechanism of Treating Persistent Infections. *Nature Reviews Microbiology*, 9, 62-75.
- Kanehisa, M., Goto, S. (2000) KEGG: Kyoto Encyclopedia of Genes and Genomes. *Nucleic Acid Research*, 28, 27-30.
- Kilcullen, K., Teunis, A., Popova, T.G., Popov, S.G. (2016) Cytotoxic Potential of *Bacillus cereus* Strains ATCC 11778 and 14579 against Human Lung Epithelial Cells under Microaerobic Growth Conditions. *Frontiers in Microbiology*, 7(69), 1-12.
- Lämmerhofer, M., Weckwerth, W., Eds, (2013) NMR-Based Metabolomic Analysis: In Metabolomics in Practice: Successful Strategies to Generate and Analyze Metabolic Data. (pp. 209-233). Weinheim, Germany: Wiley-VCH.
- Lindon, J. C., Nicholson, J. K., Holmes, E. (2007). NMR Spectroscopic Techniques for Application to Metabonomics: In the Handbook of Metabolomics and Metabonomics. (pp. 55-112). Oxford, UK: Elsevier.
- Loskill, P., Pereira, P.M., Jung, P., Bischoff, M., Herrmann, M., Pinho, M.G., Jacobs, K. (2014) Reduction of the Peptidoglycan Crosslinking Causes a Decrease in the Stiffness of the *Staphylococcus aureus* Cell Envelope. *Biophysical Journal*, 107, 1082-1089.
- Lu, W., Pieters, R. J. (2019) Carbohydrate-Protein Interactions and Multivalency: Implications for the Inhibition of Influenza A Virus Infections. *Expert Opinion on Drug Discovery*, 14(4), 387-395.

- Martinez, J. L., Baquero, F. (2000) Minireview: Mutation Frequency and Antibiotic Resistance. *Antimicrobial Agents and Chemotherapy*, 44(7), 1771-1777.
- Mengin-Lecreulx, D., Blanot, D., VanHeijenoort, J. (1994) Replacement of Diaminopimelic acid by Cystathionine or Lanthionine in the Peptidoglycan of *Escherichia coli*. *Journal of Bacteriology*, 176(14), 434-437.
- Metabolomics Workbench. (2021) [https://www.metabolomicsworkbench.org/Study ID ST001966](https://www.metabolomicsworkbench.org/Study_ID/ST001966). Accessed November 13, 2021.
- Mintzer, M. A., Dane, E. L., O'Toole, G. A., Grinstaff, M. W. (2011) Exploiting Dendrimer Multivalency to Combat Emerging and Reemerging Infectious Diseases. *Molecular Pharmaceutics*, 9, 342-354.
- Nikolaidis, I., Favini-Stabile, S., Dessen, A. (2014) Resistance to antibiotics targeted to the bacterial cell wall. *Protein Science*. 23, 243-259.
- Paleos, C. M., Tsiourvas, D., Sideratou Z., Tziveleka, L-A. (2010) Drug Delivery using Multifunctional Dendrimers and Hyperbranched Polymers. *Expert Opinion on Drug Delivery*, 7, 1387-1398.
- Pang, Z., Chong, J., Zhou, G., Morais D., Chang, L., Barrette, M., Gauthier, C., Jacques, PE., Li, S., and Xia, J. (2021) MetaboAnalyst 5.0: narrowing the gap between raw spectra and functional insights *Nucleic Acids Research* 49. doi: 10.1093/nar/gkab382
- Perlin, M. H., Clark, D. R., McKenzie, C., Patel, H., Jackson, N., Kormanik, C., Powell, C., Bajorek, A., Myers, D. A., Dugatkin, L.A., Atlas, M. R. (2009) Protection of Salmonella by Ampicillin-Resistant *Escherichia coli* in the presence of otherwise Lethal Drug Concentrations. *Proceedings of the Royal Society B*, 276, 3759-3768.
- Pokhrel, S., Nagaraja, K. S., Varghese, B. (2004) Preparation, Characterization and X-ray Structure Analysis of 1,4-diazabicyclo-2,2,2-octane (DABCO) and Ammonium Cation with Tetrathiomolybdate Anion. *Journal of Structural Chemistry*, 45(5), 900-905.
- Pieters, R.J., Arnusch, C.J., Breukink, E. (2009) Membrane Permeabilization by Multivalent Anti-Microbial Peptides. *Protein & Peptide Letters*, 16 (7), 1-7.
- Richard, C., Mengin-Lecreulx, D., Pochet, S., Johnson, E.J., Cogen, G.N., Marlière, P. Directed Evolution of Biosynthetic Pathways. *The Journal of Biological Chemistry*, 268(36) 26827-26835.

- Roy, R. (2003) A Decade of Glycodendrimer Chemistry. *Trends in Glycoscience and Glycotechnology*, 15(85), 291-310.
- Schleifer, K.H., Kandler, O. (1972) Peptidoglycan Types of Bacterial Cell Walls and their Taxonomic Implications. *Bacteriological Reviews*, 36(4), 407-477.
- Shepherd, J., Ibba, M. (2013) Direction of Aminoacylated transfer RNAs into Antibiotic Synthesis and Peptidoglycan-Mediated Antibiotic Resistance. *FEBS Letters*, 587(18), 2895-2904.
- Shulaev, V. (2006) Metabolomics technology and bioinformatics. *Briefings in Bioinformatics*, 7(2), 128-139.
- Tautenhahn, R., Cho, K., Uritboonthai, W., Zhu, Z., Patti, G.J., Siuzdak, G. (2012) An Accelerated Workflow for Untargeted Metabolomics using the METLIN Database. *Nature Biotechnology Correspondence*, 30(9), 826-828.
- Todar, K., (2020). Textbook of Bacteriology (Online). University of Wisconsin, <http://textbookofbacteriology.net>. Accessed October 2021
- Turkoglu, O., Cital, A., Katar, C., Mert, I., Kumar, p., Yilmaz, A., Uygur, D.S., Erkata, S., Graham, S.F., Bahado-Singh, R.O. (2019) Metabolomic Identification of Novel Diagnostic Biomarkers in Ectopic Pregnancy. *Metabolomics*, 15(143), 1-11.
- VanKoten, H.W., Dlakic, W.M., Engel, R., Cloninger, M.J. (2016) Synthesis and Biological Activity of Highly Cationic Dendrimer Antibiotics. *Molecular Pharmaceutics* 13, 3827-3834. doi.org/10.1021/acs.molpharmaceut.6b00628
- Vembu, S., Pazhamalai, S., Gopalakrishnan, M. (2015) Potential Antibacterial Activity of Triazine Dendrimer: Synthesis and Controllable Drug Release Properties. *Bioorganic and Medicinal Chemistry*, 23, 4561-4566.
- Vollmer, W., Bertsche, U. (2008) Murein (peptidoglycan) Structure, Architecture and Biosynthesis in *Escherichia coli*. *Biochimica et Biophysica Acta*, 1778, 1714-1734.
- Vollmer, W., Blanot, D., de Pedro, M.A. (2008) Peptidoglycan Structure and Architecture. *FEMS Microbiology Review*. 32, 149-167.
- Wishart, D.S. (2008) Quantitative Metabolomics using NMR. *Trends in Analytical Chemistry*, 27(3), 228-237.

- Wolfenden, M., Cousin, J., Nangia-Makker, P., Raz, A., Cloninger, M. (2015) Glycodendrimers and Modified ELISAs: Tools to Elucidate Multivalent Interactions of Galectins 1 and 3. *Molecules*, 20, 7059-7096.
- Wrońska, N., Majoral, J. P., Appelhans, D., Bryszewska, M., Lisowska, K. (2019) Synergistic Effects of Anionic/Cationic Dendrimers and Levofloxacin on Antibacterial Activities. *Molecules*, 24, 2894-2905.
- Xu, C., Lin, L., Ren, H., Zhang, Y., Wang, S., Peng, X. (2006) Analysis of Outer Membrane Proteome of *Escherichia coli* Related to Resistance to Ampicillin and Tetracycline. *Proteomics*, 6, 462-473.
- Zhao, H., Roistacher, D.M., Helmann J.D. (2018) Aspartate Deficiency Limits Peptidoglycan Synthesis and Sensitizes Cells to Antibiotics Targeting Cell Wall Synthesis in *Bacillus subtilis*. *Molecular Microbiology*, 109(6), 826-844.

CHAPTER FOUR

DISCUSSION AND COMPARISON OF BOTH THE *ESCHERICHIA COLI* AND THE
BACILLUS CEREUS RESULTS

The purpose of this research was to study how both gram-negative and gram-positive bacteria, which was grown in the presence of a multivalently presented, membrane disrupting antimicrobial compound, are able to mutate in an attempt to develop antimicrobial resistance. Proton (^1H) nuclear magnetic resonance (NMR) hydrophilic metabolomics methods were used for this study. The multivalent quaternary ammonium compound (QAC) that is known to cause membrane disruption incorporates 1,4-diazabicyclo-2,2,2-octane (DABCO) (Pokhrel et al. 2004) with a 16-carbon chain onto a mannose functionalized dendrimer (DABCOMD). Previous studies reported minimum inhibitory concentration (MIC) values for DABCOMD and produced mutants of *Escherichia coli* (gram-negative) and *Bacillus cereus* (gram-positive) bacteria at the culmination of the 33-cycle study (VanKoten et al. 2016). These samples obtained after the 33-cycle MIC study were referred to throughout the experiments reported as the *Escherichia coli* (*E. coli*) mutants and the *Bacillus cereus* (*B. cereus*) mutants, respectively. VanKoten et al. in their 2016 study previously showed that both bacteria became very resistant to small molecule inhibitors such as ampicillin and monomeric DABCO, while the MIC values for DABCOMD (multivalent) remained relatively constant. Little to no resistance acquisition to DABCOMD was expected or observed, because the bacteria are unable to undergo enough changes to their membranes to deter a multivalently presented membrane disruptor (Chamorro et al. 2012; Hurdle et al. 2011;

Pieters et al. 2009). In this research, the mutants generated by the original MIC study (VanKoten et al. 2016) were compared to their respective wild types (taken from the bacterial stocks that were used to start the MIC study) using ^1H NMR hydrophilic metabolomics.

Escherichia coli

Samples were collected in both the mid log phase (ML) and stationary phase (S) from both the wild type (WT) and mutant (Mut) *E. coli*. The growth curves of the wild type and mutant samples were indistinguishable. The hydrophilic metabolites were extracted and studied using ^1H NMR. The concentration data and identity of the metabolites observed using Chenomx NMR Suite 8.2 software (Chenomx 2016) in each sample were compared using XLSTAT (Addinsoft 2019) hierarchical clustering and principal component analysis (PCA) biplots, MetaboAnalyst 4.0 (Chong et al 2019 and references therein) 2D and 3D sparse partial least squares discriminate analysis (sPLS-DA), very important features (VIP), volcano plots, pattern hunter and pathway analysis tool and KEGG pathways (Kanehisa and Goto 2000 and references therein). Hierarchical Clustering, PCA and sPLS-DA showed complete separation of all sample types (WT ML, WT S, Mut ML and Mut S), demonstrating that all sample types are unique.

Statistically significant (fold change and p-value of 0.5 or less) concentration changes in energy pathways, aminoacyl-tRNA biosynthesis, peptidoglycan synthesis and related pathways were observed. The largest change observed was a 25-fold increase in the concentration of N-acetylglucosamine in the mutant mid log phase samples, in

comparison to the wild type samples. N-acetylglucosamine is a major component of peptidoglycan synthesis, which is required for survival especially due to environmental stressors (Nikolaidis et al. 2014; Shepherd and Ibba 2013; Zhao et al. 2018; Xu et al. 2006; Anderson et al. 2012). The mutant sample type had higher concentrations of glutamate (VIP) in both the mid log and stationary phases and a higher concentration of aspartate (VIP) in the mid log phase, in comparison to the wild type samples. Glycine was observed to have a 2-fold decrease in the mutant samples, in comparison to the wild type samples. One likely explanation for the drop in glycine levels is that the mutant samples are consuming glycine in an attempt to increase the crosslinking of the pentapeptide side chain of peptidoglycan, which has been shown to increase survivability (Shepherd and Ibba 2013; Hammes et al. 1973). An increase in lactate concentration in the mutant samples was observed in both phases, while an increase in lysine concentration was observed in the stationary phase in comparison to the wild type samples. Both lactate and lysine have been shown to be components of the pentapeptide side chain of peptidoglycan (Shepherd and Ibba 2013; Anderson et al. 2012). Incorporation of lactate has been shown to truncate the D-ala-D-ala tail of the pentapeptide (Shepherd and Ibba 2013). Incorporation of lysine (positively charged) into the number three spot of the pentapeptide side chain has been shown to be a strategy for garnering protection from positively charged antimicrobials (Anderson et al. 2012). Since DABCOMD is a multivalent positively charged membrane disruptor, the bacteria are most likely mutating to increase their membrane strength and overall positive charge by altering their peptidoglycan layer. The mutant sample type was also associated with

higher concentrations of spent energy related molecules such as NAD⁺ and AMP in both the mid log and stationary phases, in comparison to the wild type samples. The increase in spent energy metabolites is thought to be the result of the increased energy expenditure required for altering peptidoglycan layers to garner additional protection against DABCOMD. The membrane disrupting properties of DABCOMD could also be slowing the rate of nutrient uptake from the growth media, resulting in the increase in spent energy metabolites (Hurdle et al. 2011). There was a larger difference in the concentrations of the mid log phase metabolites than was observed in the stationary phase metabolites. However, a smaller difference was expected for the stationary phase samples, in comparison to the mid log phase samples, because the cells in stationary phase are not rapidly dividing anymore. Thus, they do not require as much energy and have settled into their fortified membrane composition (Vollmer and Bertsche 2008).

Analysis of *E. coli* NMR hydrophilic metabolomic data of the wild type and mutant samples demonstrated that multiple components of peptidoglycan that are known to increase survivability were observed. An increase in spent energy metabolites in the mutant samples in comparison with the wild type samples was also observed. The mutant *E. coli* samples are almost certainly mutating in an attempt to garner protection from the large positive charge found on the multivalent DABCOMD antimicrobial agent by strengthening their membranes via alterations in the composition of their peptidoglycan pentapeptide side chains.

Bacillus cereus

The same procedures were used for the *B. cereus* samples as were used for the *E. coli* samples, except a DABCOMD challenged sample set was added. The DABCOMD challenged sample set used 0.37 $\mu\text{M/L}$, or 33 % of the reported MIC value (VanKoten et al. 2016) of DABCOMD added to the media. The samples labeled as the unchallenged samples did not have DABCOMD added to the media. Except for the addition of a small amount of DABCOMD added to the growth media of the challenged samples, the procedures were the same for both challenged and unchallenged sample types. The wild type (WT) and mutant (Mut) *B. cereus* samples, DABCOMD challenged (denoted D) and unchallenged sample types were collected in the mid log phase (ML) and stationary phase (S) yielding eight sample types: WT ML, WT S, WT D ML, WT D S, Mut ML, Mut S, Mut D ML and Mut D S. The growth curves of both the challenged and unchallenged wild type samples were indistinguishable. The growth curve of the unchallenged mutant samples (Mut) was slower and did not reach the same optical density as both wild type samples (WT D and WT). The challenged mutant samples (Mut D) had the slowest growth and had the lowest optical density overall. The hydrophilic metabolites obtained from all eight sample types were studied using ^1H NMR. Chenomx NMR Suite 8.4 software (Chenomx 2020) was used to determine the identity and concentration of the metabolites found in each sample. The data was analyzed using XLSTAT (Addinsoft 2021) hierarchical clustering and principal component analysis (PCA) biplot, MetaboAnalyst 5.0 (Pang et al. 2021 and references therein) 2D and 3D sparse partial least squares discriminate analysis (sPLS-DA),

orthogonal partial least squares discriminate analysis (ortho PLS-DA), very important features (VIP), volcano plots, pattern hunter and pathway analysis tool and KEGG pathways (Kanehisa and Goto 2000 and references therein). WT ML and WT D ML samples clustered together, Mut D S and WT D S samples clustered together, and all other sample types separated. When only the unchallenged samples were compared, all four sample types separated, while when only the challenged samples were compared, both the stationary phase samples (Mut D and WT D) clustered together. Fold changes and p-values (0.5 or less) were used to determine the statistical significance of metabolite concentration changes between sample types.

The mutant and challenged sample types were associated with higher levels of spent energy molecules such as NAD^+ and AMP than their wild type and unchallenged sample counterparts. It is likely that the slower growth associated with the higher concentrations of spent energy molecules in the mutants, and especially in the challenged mutants, is due to the increase in membrane fortification. The strengthened membrane that is formed upon exposure to a membrane disruptor decreases the rate of nutrient uptake into the cell, thus costing the cell more energy to survive (Hurdle et al. 2011). The stationary phase comparisons showed a smaller number of differences between all sample types and metabolite concentration fold changes differences in comparison to the mid log phase. This smaller difference is most likely due to the lack of rapid cell division, decreased metabolism (slower nutrient uptake not as important) and overall settling into a beneficial membrane composition during the stationary phase (Vollmer and Bertsche 2008).

The greatest number of metabolite changes were involved in aminoacyl-tRNA biosynthesis in both the mid log and stationary phases. The challenged mutant samples were associated with the greatest number of changed metabolites. The changes in many components of aminoacyl-tRNA biosynthesis are likely to be causing upstream changes as well. Both mutant sample types were associated with an overall lower concentration in nucleotide metabolites than their wild type and unchallenged counterparts, most likely due to an increase in aminoacyl-tRNA biosynthesis components. Byproducts of aminoacyl-tRNA biosynthesis are likely being diverted to peptidoglycan synthesis and garnering antibiotic resistance (Shepherd and Ibba 2013).

The largest observed concentration changes were associated with cell membrane composition and energy production pathways. N-acetylglucosamine, which had the largest concentration changes when comparing mutated to wild type samples, is a major component of peptidoglycan synthesis. Peptidoglycan is important for protection against antimicrobials since it is a component of the cell wall (Nikolaidis et al. 2014; Shepherd and Ibba 2013; Zhao et al. 2018; Xu et al. 2006; Anderson et al. 2012). DABCOMD challenged mutants were associated with the highest concentration of N-acetylglucosamine, while unchallenged wild type samples were associated with the lowest concentration of N-acetylglucosamine. Other important components of the peptidoglycan such as glycine, lysine, lactate, cystathionine, glutamate, and glutamine were also observed, adding additional evidence that the peptidoglycan layer is altered in response to DABCOMD. Peptidoglycan pentapeptide composition frequently changes in response to environmental stressors and is known to increase bacterial resistance to

antimicrobials (Mengin-Lecreulx et al. 1994; Humann and Lenz 2009; Vollmer et al. 2008; Nikolaidis et al. 2014; Anderson et al. 2012). In the stationary phase, the mutant samples, especially the challenged mutant samples, were associated with higher concentrations of lysine, in comparison to their wild type counterparts. Since lysine is positively charged, incorporation of this amino acid into the pentapeptide side chain of peptidoglycan increases the overall positive charge on the membrane, thereby decreasing the efficacy of cationic antimicrobials (Shepherd and Ibba 2013). An increase in lysine concentration may have only been observed in the stationary phase because the *B. cereus* bacteria had settled into a more fortified peptidoglycan composition since they were not rapidly dividing anymore (Vollmer and Bertsche 2008). Changes in glycine concentrations were observed likely because glycine induces crosslinking and increases rigidity of the peptidoglycan layer, which has been shown to increase bacterial survival rates (Shepherd and Ibba 2013; Hammes et al. 1973; Loskill et al. 2014). Lactate is a common pentapeptide truncator (Anderson et al. 2012; Nikolaidis et al. 2014) and was found to be associated with the mutant sample type, especially the challenged mutant samples. Truncation of the D-ala-D-ala tail in the peptide side chain of peptidoglycan is a common method to develop antimicrobial resistance (Loskill et al. 2014; Sheppard and Ibba 2013; Nikolaidis et al. 2014; Anderson et al. 2012). Higher cystathionine levels were generally associated with the mutant samples, especially the challenged mutant samples. Previous research shows that cystathionine can be incorporated into and truncate the pentapeptide side chain of peptidoglycan (Mengin-Lecreulx et al. 1994; Richard et al. 1993). The numerous changes in peptidoglycan synthesis and related

pathways associated with the mutant samples add support to the theory that the mutants, and to a larger extent, the challenged mutant samples are altering the composition of their peptidoglycan layer to garner more protection from the multivalently presented positive charge on DABCOMD.

Overall, more metabolites and concentration changes were observed between the challenged samples (Mut D vs WT D) than between their unchallenged counterparts (Mut vs WT). The smallest change was observed between the challenged and unchallenged wild type samples. The metabolite data revealed that the mutant samples, especially the challenged mutant samples, had a slower growth curve, decreased ending optical density, were associated with more spent energy metabolites and larger concentration changes in metabolites commonly found in peptidoglycan synthesis, than their wild type and/or unchallenged counterparts. The mutated *B. cereus* samples, especially the DABCOMD challenged mutant samples, are most likely altering their peptidoglycan layer. This results in higher energy costs and slower nutrient import for these sample sets, since they have garnered protection from the highly positively charged DABCOMD.

Comparison of Gram-Negative and Gram-Positive Bacteria Metabolomics Data

Bacteria do not readily acquire resistance to multivalent membrane disruptors because large changes to their membranes would be required (Chamorro et al. 2012; Pieters et al. 2009). Multivalent membrane disruptors can cause mutations that impede nutrient import in addition to strengthening the cell Membrane overall (Hurdle et al. 2011). DABCOMD is a membrane disruptor that multivalently presents QACs that have efficacy against both gram-positive and gram-negative bacteria. Even after a 33-cycle

MIC study (VanKoten et al. 2016), resistance to DABCOMD was not conferred. The growth curve was the same for the wild type and the DABCOMD mutated *E. coli*, while the mutated *B. cereus* samples and especially the DABCOMMD challenged mutant samples had slower growth curves and lower ending optical densities than their wild type *B. cereus* counterparts. The *E. coli* sample comparisons (WT vs Mut) did not have as many metabolite changes, especially upstream of peptidoglycan synthesis and aminoacyl-tRNA biosynthesis, in comparison to the *B. cereus* sample comparisons (WT vs Mut and challenged vs unchallenged). The *B. cereus* sample comparisons also had larger fold change differences than the *E. coli* sample comparisons, especially for the metabolites involved in peptidoglycan synthesis and energy related pathways. DABCOMD damages the bacterial membrane, and gram-positive bacteria contain up to 70 % peptidoglycan while gram-negative bacteria contain only about 10 % peptidoglycan in their membranes (Schleifer and Kandler 1972). Due to the significant differences in membrane compositions, a more significant difference was expected for the *B. cereus* samples (gram-positive) than for the *E. coli* samples. Differences in energy related metabolites were larger in the gram-positive bacteria, *B. cereus*, than in the gram-negative bacteria, *E. coli*. Since gram-positive bacteria have more peptidoglycan than gram-negative bacteria, altering the peptidoglycan of *B. cereus* should be more energetically costly while increasing the difficulty of nutrient uptake, when compared to *E. coli*. It is likely that the greater disruption to nutrient uptake and the thicker membranes of *B. cereus* in comparison to *E. coli* also explain the slower growth curve, overall decreased optical density, and association with higher concentrations of spent energy molecules and

peptidoglycan components (N-acetylglucosamine) for *B. cereus* mutant samples.

Differences between sample types were larger when the mutants are grown in DABCOMD.

DABCOMD is a multivalent membrane disruptor that has multiple positive charges (QACs) that are attracted to the negatively charged phospholipid components of the bacterial membrane. Both gram-positive (*B. cereus*) and gram-negative (*E. coli*) bacteria alter their peptidoglycan layers to garner protection from DABCOMD, consequently causing interference of nutrient uptake and increase in energy requirements. Since gram-positive bacteria have thicker membranes than gram-negative bacteria and DABCOMD is a membrane disruptor, a larger number of changes in the concentration and number of metabolite differences between wild type and mutant samples were observed for the gram-positive bacteria (*B. cereus*) than for the gram-negative bacteria (*E. coli*).

References

- Addinsoft (2019) XLSTAT 2019: Data Analysis and Statistical Solution for Microsoft Excel. Paris, France.
- Addinsoft (2021). XLSTAT Statistical and Data Analysis Solution. New York, USA. <https://www.xlstat.com>.
- Anderson, R. J., Groundwater, P. W., Todd, A., Worsley, A. J. (2012). Glycopeptide Antibiotics: In Antibacterial Agents: Chemistry, Mode of Action, Mechanisms of Resistance and Clinical Applications. (pp. 305-318). West Sussex, UK: Wiley.
- Chamorro, C., Boerman, M.A., Arnusch, C.j., Breukink, E., Pieters, R.J. (2012) Enhancing Membrane Disruption by Targeting and Multivalent Presentation of Antimicrobial Peptides. *Biochimica et Biophysica Acta*, 1818, 2171-2174.
- Chenomx (2016) N.M.R. Suite 8.2. Edmonton: Chenomx Inc.
- Chenomx (2020) N.M.R. Suite 8.4. Edmonton: Chenomx Inc.
- Chong, J., Wishart, D. S., Xia, J. (2019) Using MetaboAnalyst 4.0 for Comprehensive and Integrative Metabolomics Data Analysis. *Current Protocols in Bioinformatics*, 68, e86.
- Hammes, W., Schleifer, K. H., Kandler, O. (1973) Mode of Action of Glycine on the Biosynthesis of Peptidoglycan. *Journal of Bacteriology*, 116(2), 1029-1053.
- Humann, J., Lenz, L. L. (2009) Bacterial Peptidoglycan Degrading Enzymes and their Impact on Host Muropeptide Detection. *Journal of Innate Immunity*, 1, 88-97.
- Hurdle J.G., O'Neill, A.J., Chopra, I., Lee, R.E. (2011) Targeting Bacterial Membrane Function: an Underexploited Mechanism of Treating Persistent Infections. *Nature Reviews Microbiology*, 9, 62-75.
- Kanehisa, M., Goto, S. (2000) KEGG: Kyoto Encyclopedia of Genes and Genomes. *Nucleic Acid Research*, 28, 27-30.
- Loskill, P., Pereira, P.M., Jung, P., Bischoff, M., Herrmann, M., Pinho, M.G., Jacobs, K. (2014) Reduction of the Peptidoglycan Crosslinking Causes a Decrease in the Stiffness of the *Staphylococcus aureus* Cell Envelope. *Biophysical Journal*, 107, 1082-1089.

- Mengin-Lecreulx, D., Blanot, D., VanHeijenoort, J. (1994) Replacement of Diaminopimelic acid by Cystathionine or Lanthionine in the Peptidoglycan of *Escherichia coli*. *Journal of Bacteriology*, 176(14), 434-437.
- Nikolaidis, I., Favini-Stabile, S., Dessen, A. (2014) Resistance to antibiotics targeted to the bacterial cell wall. *Protein Science*. 23, 243-259.
- Pang, Z., Chong, J., Zhou, G., Morais D., Chang, L., Barrette, M., Gauthier, C., Jacques, PE., Li, S., and Xia, J. (2021) MetaboAnalyst 5.0: narrowing the gap between raw spectra and functional insights *Nucleic Acids Research* 49. doi: 10.1093/nar/gkab382
- Pieters, R.J., Arnusch, C.J., Breukink, E. (2009) Membrane Permeabilization by Multivalent Anti-Microbial Peptides. *Protein & Peptide Letters*, 16 (7), 1-7.
- Pokhrel, S., Nagaraja, K. S., Varghese, B. (2004) Preparation, Characterization and X-ray Structure Analysis of 1,4-diazabicyclo-2,2,2-octane (DABCO) and Ammonium Cation with Tetrathiomolybdate Anion. *Journal of Structural Chemistry*, 45(5), 900-905.
- Richard, C., Megin-Lecreulx, D., Pochet, S., Johnson, E.J., Cogen, G.N., Marlière, P. Directed Evolution of Biosynthetic Pathways. *The Journal of Biological Chemistry*, 268(36) 26827-26835.
- Schleifer, K.H., Kandler, O. (1972) Peptidoglycan Types of Bacterial Cell Walls and their Taxonomic Implications. *Bacteriological Reviews*, 36(4), 407-477.
- Shepherd, J., Ibba, M. (2013) Direction of Aminoacylated transfer RNAs into Antibiotic Synthesis and Peptidoglycan-Mediated Antibiotic Resistance. *FEBS Letters*, 587(18), 2895-2904.
- VanKoten, H.W., Dlakic, W. M., Engel, R., Cloninger, M. J. (2016) Synthesis and Biological Activity of Highly Cationic Dendrimer Antibiotics. *Molecular Pharmaceutics* 13, 3827-3834.
- Vollmer, W., Bertsche, U. (2008) Murein (peptidoglycan) Structure, Architecture and Biosynthesis in *Escherichia coli*. *Biochimica et Biophysica Acta*, 1778, 1714-1734.
- Vollmer, W., Blanot, D., de Pedro, M.A. (2008) Peptidoglycan Structure and Architecture. *FEMS Microbiology Review*. 32, 149-167.
- Xu, C., Lin, L., Ren. H., Zhang, Y., Wang, S., Peng. X. (2006) Analysis of Outer Membrane Proteome of *Escherichia coli* Related to Resistance to Ampicillin and Tetracycline. *Proteomics*, 6, 462-473.

Zhao, H., Roistacher, D.M., Helmann J.D. (2018) Aspartate Deficiency Limits Peptidoglycan Synthesis and Sensitizes Cells to Antibiotics Targeting Cell Wall Synthesis in *Bacillus subtilis*. *Molecular Microbiology*, 109(6), 826-844.

CHAPTER FIVE

CONCLUSIONS

This study used NMR hydrophilic metabolomics to determine how *Escherichia coli* (*E. coli*) and *Bacillus cereus* (*B. cereus*) mutated in the presence of DABCOMD. DABCOMD is a multivalent quaternary ammonium compound (QAC) that has 1,4-diazabicyclo-2,2,2-octane (DABCO) with a 16-carbon chain and mannose endgroups tethered to a dendrimer framework (Figure 5.1). DABCOMD is effective against both gram-positive and gram-negative bacteria. In addition to changes in growth curves, the mutant *B. cereus* samples (especially the DABCOMD challenged mutant *B. cereus* samples) in comparison to their wild type counterparts are also associated with the highest concentration of spent energy metabolites and N-acetylglucosamine production (major component of peptidoglycan synthesis). In comparison to *B. cereus*, the mutant *E. coli* samples had no growth curve change and displayed fewer changes in energy related metabolites and peptidoglycan synthesis compared to the wild type. Both gram-positive (*B. cereus*) and gram-negative (*E. coli*) bacteria attempt to garner protection from DABCOMD by altering the composition of their peptidoglycan layer for protection against positively charged membrane disruptors. These alterations in the peptidoglycan layer result in higher energy costs and interference with nutrient uptake.

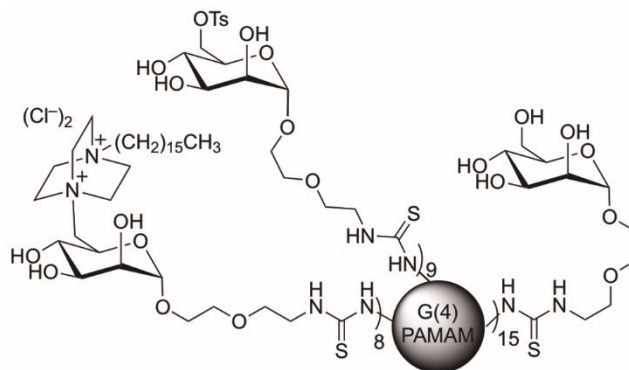


Figure 5.1. Structure of C₁₆-DABCO Mannose Functionalized Dendrimer (DABCOMD)

The study of multivalent antimicrobial materials is critically important since these compounds have the potential to function on antibiotic resistant bacteria with increased efficacy (Wolfenden et al 2015; VanKoten et al. 2016; Andre et al. 2001). Bacteria also have a reduced ability to develop resistance to multivalent antimicrobials, in comparison to monovalent antimicrobial compounds (Wolfenden et al. 2015; VanKoten et al. 2016; Andre et al. 2001). Nuclear magnetic resonance (NMR) metabolomics experiments are widely used for the quantitative elucidation of the biochemical pathways associated with development of resistance during bacterial growth in the presence of an antimicrobial agent (Barding et al. 2012; Dettmer et al. 2007; Wishart 2008; Turkoglu et al. 2019; Lämmerhofer and Weckwerth 2013; Lindon et al. 2007; Hoerr et al. 2016). A better understanding of the process by which bacteria develop resistance to multivalent antimicrobials elucidates both highly conserved and easily mutable metabolomic processes. More in depth research into pathways that were identified in these studies as being difficult for effective mutation may provide targets for future antimicrobial research. A limitation of NMR metabolomics studies is that there is not a comprehensive

compound profile list that contains all metabolites present in an NMR sample at this point in time, resulting in the inevitable omission of identifications for some metabolites. Even though the list of compounds that can be identified in NMR metabolomics samples increases every year, and most peaks can be identified, there are still peaks that do not have a match in the database.

DABCOMD Likely Mechanism of Action

DABCOMD is multivalent QAC that works on both gram-positive and gram-negative bacteria and resistance was not obtained by either *B. cereus* or *E. coli*.

DABCOMD is a promising candidate as a cationic biocide because its highly positively charged (on average plus sixteen per dendrimer) and the 16-carbon chain of C₁₆-DABCO is ideal for membrane association. The dendrimer provides a stable, easily functionalizable multivalent structure and mannose endgroups increase the solubility. The likely mechanisms of action of DABCOMD are different in gram-positive and gram-negative bacteria.

Gram-negative: *Escherichia coli*

DABCOMD is a cationic biocide that is likely using the same mechanisms of action as has been reported for other cationic biocides against *E. coli* (gram-negative) (Kügler et al. 2005; Timofeeva and Kleshcheva 2011; Chen et al. 2017; Tiller et al. 2001; Sabnis et al. 2021). The large positive charge of the DABCOMD is likely electrostatically attracted to the negatively charged lipopolysaccharides and the negatively charged phospholipids on the cell membrane of *E. coli* (Timofeeva and

Kleshcheva 2011; Tiller et al. 2001; Sabnis et al. 2021). Electrostatic interactions happening in close proximity to the membrane likely result in the release of divalent counter cations, causing the destabilization of the phospholipid membrane (Kügler et al. 2005; Timofeeva and Kleshcheva 2011; Chen et al. 2017; Tiller et al. 2001; Sabnis et al. 2021). After the destabilization of the phospholipid outer membrane occurs, further penetration of DABCOMD into the thin peptidoglycan layer and inner membrane likely results, leading to inner membrane disruption, leakage, and cell lysis (Timofeeva and Kleshcheva 2011; Nguyen et al. 2011; Chen et al. 2017; Richards et al. 2018; Tiller et al. 2001; Sabnis et al. 2021).

It is likely that the bacteria are altering their peptidoglycan layer composition to decrease the efficacy of DABCOMD. Changes were observed in the concentrations of lysine, glycine, lactate and other amino acids commonly associated with peptidoglycan synthesis. Increasing the lysine concentration has been shown to decrease the efficacy of cationic antimicrobials by decreasing the overall negative charge of the bacterial exterior (Cox et al. 2014; Hebecker et al. 2015; Shepherd and Ibba 2013). Increased crosslinking of peptidoglycan with glycine has been shown to increase survivability of bacteria in hostile environments (Loskill et al. 2014). And truncation of the D-ala-D-ala tail in the side chain of peptidoglycan by lactate has been shown as a bacteria response to antimicrobials (Anderson et al. 2012). Concentration changes in alanine were observed between the mutant and the wild type samples. Alanine is an important component of peptidoglycan synthesis, but it has also been shown to decrease the negative charge on cell membranes (Hebecker et al. 2015; Loskill et al. 2014; Shepherd and Ibba 2013;

Humann and Lenz 2009; Anderson et al. 2012). It is likely that the mutant bacteria are attempting to garner protection from the highly positively charged DABCOMD by adding alanine esters to their phosphatidyl glycerol phospholipids. Another common mechanism to decrease the overall negative charge of lipopolysaccharides that could be occurring in the mutants is adding phosphatidylethanolamine to their saccharides (Bertani and Ruiz 2018; Sabnis et al. 2021).

More research is needed to determine the mechanism of DABCOMD on gram-negative bacteria, as well as to determine the likely modifications occurring to protect themselves from DABCOMD.

Gram-positive: *Bacillus cereus*

DABCOMD likely has the same mechanism of action as that of previously reported cationic biocides (Timofeeva and Kleshcheva 2011; Gerba 2015). The large positive charge on DABCOMD is likely electrostatically attracted to the large positive charge on teichoic acid and lipoteichoic acids protruding from the surface of the cell wall (peptidoglycan layer) (Timofeeva and Kleshcheva 2011). Once the DABCOMD electrostatically binds close to the surface of the peptidoglycan layer, disruption likely occurs. DABCOMD should then be able to penetrate down to the phospholipid membrane (Timofeeva and Kleshcheva 2011). DABCOMD is likely interacting with the negatively charged phospholipid membrane, resulting in its highly positive charge displacing divalent counter cations such as calcium or magnesium, causing further disruption (Timofeeva and Kleshcheva 2011). Membrane leakage and eventually lysis are the ultimate outcome (Timofeeva and Kleshcheva 2011; Gerba 2015).

The mutant samples were likely attempting to garner protection from the highly positively charged DABCOMD by altering their peptidoglycan, teichoic acid, lipoteichoic acid and inner membrane phospholipid compositions. Alanine, lysine, glycine, lactate and other associated compound concentration changes were observed between the challenged and unchallenged and wild type and mutant samples. Glycine is an important component for crosslinking in peptidoglycan (Shepherd and Ibba 2013; Hammes et al. 1973) and has been previously shown to increase survivability in hostile environments (Loskill et al. 2014). Truncation of the D-ala-D-ala tail in peptidoglycan by lactate has been previously shown as a bacterial response to an antibiotic (Anderson et al. 2012). Lysine has been previously shown to decrease the efficacy of cationic antimicrobials and is important for peptidoglycan synthesis and important addition to phospholipids residues (Cox et al. 2014; Schneewind and Missiakas 2014; Hebecker et al. 2015; Shepherd and Ibba 2013). Alanine is an important component of peptidoglycan synthesis and phospholipid charge composition alternations (Cox et al. 2014; Schneewind and Missiakas 2014; Hebecker et al. 2015; Loskill et al. 2014; Shepherd and Ibba 2013; Humann and Lenz 2009; Anderson et al. 2012). Thus, it is likely that the mutant bacteria are attempting to garner protection from the highly positively charged DABCOMD by increasing peptidoglycan crosslinking and by altering the composition of their peptidoglycan layers, teichoic acid, lipoteichoic acid, and phospholipid residues to decrease their net negative charge. Adding lysine and alanine esters to their phosphatidyl glycerol phospholipids and adding alanine molecules to their glycerol residues in their teichoic acid and lipoteichoic acids would decrease the overall negative charge on these

molecules, thus decreasing the electrostatic attraction of cationic biocides (Cox et al. 2014; Schneewind and Missiakas 2014; Hebecker et al. 2015).

More research is needed to determine the mechanism of action of DABCOMD on gram-positive bacteria, as well as to determine the likely modifications occurring to protect the gram-positive bacteria from DABCOMD.

Future Work

Hydrophilic metabolomics data obtained using liquid chromatography–mass spectrometry (LC-MS) should be compared to the hydrophilic NMR data presented here. This would enable determination of how complementary the data sets are and would be expected to provide a more complete picture of the metabolomic pathways involved in mutations to multivalent antimicrobial agents. Hydrophobic metabolomic profiling should be performed using LC-MS and gas chromatography–mass spectrometry (GC-MS). The LC-MS data should be compared to the GC-MS data to determine if using both instruments is a way of observing a more complete picture of the altered pathways.

Comparing hydrophobic metabolomics data to hydrophilic metabolomics data should be complementary and may also show distinct pathway changes. It would be quite interesting to observe the differences in metabolite pathways that emerge from the two methods. DABCOMD is a membrane disruptor, and the largest fold changes in metabolite concentrations were in N-acetylglucosamine (an integral part of peptidoglycan synthesis). Thus, it would be expected that changes to hydrophobic phospholipid components would be observed and could potentially point to more details regarding

what is occurring at the phospholipid membrane in response to DABCOMD. These potential changes to the phospholipid membrane could further shed light on some of the metabolite concentration changes observed in the hydrophilic metabolite data. After the most efficient methods for the study of multivalent antimicrobials are determined (LC-MS vs GC-MS for hydrophobic data and NMR vs LC-MS for hydrophilic data), then efficient methods can be used to study the responses of more bacteria, and even perhaps additional organisms such as fungi and *Caenorhabditis elegans* (*C. elegans*), to a variety of multivalent antimicrobials. These studies would be expected to guide development of new antimicrobial agents.

References

- Anderson, R. J., Groundwater, P. W., Todd, A., Worsley, A. J. (2012). Glycopeptide Antibiotics: In *Antibacterial Agents: Chemistry, Mode of Action, Mechanisms of Resistance and Clinical Applications*. (pp. 305-318). West Sussex, UK: Wiley.
- Andre, S., Pieters R. J., Vrsaidas, I., Kaltner, H., Kuwabara, I., Liu, F-T., Liskamp, R. M. J., Gabius, H-J. (2001) Wedgelike Glycodendrimers as Inhibitors of Binding of Mammalian Galectins to Glycoproteins, Lactose Maxiclusters, and Cell Surface Glyconjugates. *ChemBioChem*, 2, 822-830.
- Barding, G. A., Salditos, R., Larive, C.K. (2002) Quantitative NMR for Bioanalysis and Metabolomics. *Analytical Bioanalytical Chemistry*, 404, 1165-1179.
- Bertani, B., Ruiz, N. (2018) Function and Biogenesis of Lipopolysaccharides. *EcoSal Plus*, 8(1), 1-33. doi:10.1128/ecosalplus.ESP-0001-2018
- Chen, A., Peng, H., Blakey, I., Whittaker, A.K. (2017) Biocidal Polymers: A Mechanistic Overview. *Polymer reviews*, 57(2), 276-310.
- Cox, E., Michalak, A., Pagentine, S., Seaton, P., Pokorny, A. (2014) Lysylated Phospholipids Stabilize Models of Bacterial Lipid Bilayers and Protect Against Antimicrobial Peptides. *Biochimica et Biophysica Acta*, 1838(9), 2198-2204.
- Dettmer, K., Aronov, P. A., Hammock, B. D. (2007) Mass Spectrometry-Based Metabolomics. *Mass Spectrometry Review*, 26, 51-78.
- Gerba, C.P. (2015) Quaternary Ammonium Biocides: Efficacy in Application. *Applied and Environmental Microbiology*, 81(2), 464-469.
- Hammes, W., Schleifer, K. H., Kandler, O. (1973) Mode of Action of Glycine on the Biosynthesis of Peptidoglycan. *Journal of Bacteriology*, 116(2), 1029-1053.
- Hebecker, S., Krausze, J., Hasenkampf, T., Schneider, J., Groenewold, M., Reichelt, J., Jahn, D., Heinz, D.W., Moser, J. (2015) Structures of Two Bacterial Resistance Factors Mediating tRNA-Dependent Aminoacylation of Phosphatidylglycerol with Lysine or Alanine. *PNAS*, 112(34), 10691-10696.
- Hoerr, V., Duggan, G. E., Zbytniuk, L., Poon, K. K. H., Große, C., Neugebauer, U., Methling, K., Löffler, B., Vogel, H. J. (2016) Characterization and Prediction of the Mechanism of action of antibiotics through NMR Metabolomics. *BMC Microbiology*, 16(82), 1-14. doi:10.1186/s12866-016-0696-5

- Humann, J., Lenz, L. L. (2009) Bacterial Peptidoglycan Degrading Enzymes and their Impact on Host Muropeptide Detection. *Journal of Innate Immunity*, 1, 88-97.
- Kügler, R., Bouloussa, O., Rondelez, F. (2005) Evidence of Charge-Density Threshold for Optimum Efficiency of Biocidal Cationic Surfaces. *Microbiology*, 151, 1341-1349.
- Lämmerhofer, M., Weckwerth, W., Eds, (2013) NMR-Based Metabolomic Analysis: In Metabolomics in Practice: Successful Strategies to Generate and Analyze Metabolic Data. (pp. 209-233). Weinheim, Germany: Wiley-VCH.
- Lindon, J. C., Nicholson, J. K., Holmes, E. (2007). NMR Spectroscopic Techniques for Application to Metabonomics: In the Handbook of Metabolomics and Metabonomics. (pp. 55-112). Oxford, UK: Elsevier.
- Loskill, P., Pereira, P.M., Jung, P., Bischoff, M., Herrmann, M., Pinho, M.G., Jacobs, K. (2014) Reduction of the Peptidoglycan Crosslinking Causes a Decrease in the Stiffness of the *Staphylococcus aureus* Cell Envelope. *Biophysical Journal*, 107, 1082-1089.
- Nguyen, L.T., Haney, E.F., Vogel, H.J. (2011) The Expanding Scope of Antimicrobial Peptide Structures and their Modes of Action. *Trend in Biotechnology*, 29(9), 464-472.
- Richards, S-J., Isufi, K., Wilkins, L.E., Lipecki, J., Fullam, E., Gibson, M.I. (2018) Multivalent Antimicrobial Polymer Nanoparticles Target Mycobacteria and Gram-Negative Bacteria by Distinct Mechanisms. *Biomacromolecules*, 19, 256-264.
- Rowlett V.W., Mallampalli, V.K.P.S., Karlstaedt, A., Dowhan, W., Taegtmeier, H., Margolin, W., Vitrac, H. (2017) Impact of Membrane Phospholipid Alterations in *Escherichia coli* on Cellular Function and Bacterial Stress Adaptation. *Journal of Bacteriology*, 199(13), 1-22.
- Sabnis, A., Hagart, K.L.H., Klockner, A., Becce, M., Evan, L.E., Furniss, R.C.D., Despoina, A.I., Mavridou, D.A., Murphy, R., Stevens, M.M., Davies, J.C., Larrouy-Maumus, G.J., Clarke, T.B., Edwards, A.M., (2021) Colistin kills bacteria by targeting lipopolysaccharide in the cytoplasmic membrane. *eLife* 2021;10:e65836 DOI: 10.7554/eLife.65836

- Schneewind, O., Missiakas, D. (2014) Lipoteichoic Acids, Phosphate-containing Polymers in the Envelope of Gram-positive Bacteria. *Journal of Bacteriology*, 196(6), 1133-1142.
- Shepherd, J., Ibba, M. (2013) Direction of Aminoacylated transfer RNAs into Antibiotic Synthesis and Peptidoglycan-Mediated Antibiotic Resistance. *FEBS Letters*, 587(18), 2895-2904.
- Tiller, J.C., Liao, C-J., Lewis, K., Klivanov, A.M. (2001) Designing Surfaces that Kill Bacteria on Contact. *PNAS*, 98(11), 5981-5985.
- Timofeeva, L., Kleshcheva, N. (2011) Antimicrobial Polymers: Mechanism of Action, Factors of Activity, and Applications. *Applications in Microbiology and Biotechnology*, 89, 475-492.
- Turkoglu, O., Cital, A., Katar, C., Mert, I., Kumar, p., Yilmaz, A., Uygur, D.S., Erkata, S., Graham, S.F., Bahado-Singh, R.O. (2019) Metabolomic Identification of Novel Diagnostic Biomarkers in Ectopic Pregnancy. *Metabolomics*, 15(143), 1-11.
- VanKoten, H.W., Dlakic, W.M., Engel, R., Cloninger, M.J. (2016) Synthesis and Biological Activity of Highly Cationic Dendrimer Antibiotics. *Molecular Pharmaceutics* 13, 3827-3834. doi.org/10.1021/acs.molpharmaceut.6b00628
- Wishart, D.S. (2008) Quantitative Metabolomics using NMR. *Trends in Analytical Chemistry*, 27(3), 228-237.
- Wolfenden, M., Cousin, J., Nangia-Makker, P., Raz, A., Cloninger, M. (2015) Glycodendrimers and Modified ELISAs: Tools to Elucidate Multivalent Interactions of Galectins 1 and 3. *Molecules*, 20, 7059-7096.

APPENDICES

APPENDIX A
SUPPLEMENTARY MATERIALS FOR CHAPTER 2:
E. COLI MANUSCRIPT

Table of Contents

Detailed methods description.....	139
Growth and pH curves.....	145
Sterile Technique Test.....	146
Sample NMR spectra.....	147
Hierarchical Clustering and sPLS-DA plot.....	148
Table A1 lists all metabolites identified.....	149
Metabolomic analysis charts and plots.....	150
Box plots for the metabolites.....	153
References.....	157

Methods

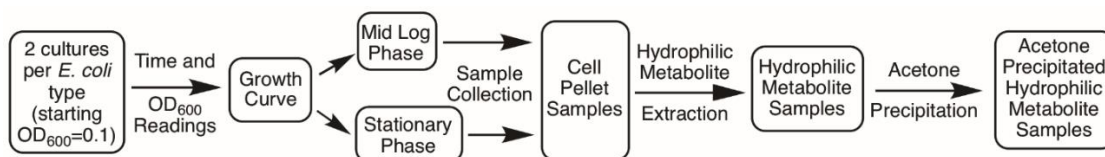


Figure A1. Overview of procedures from culture to extracted hydrophilic metabolites ready for NMR buffer

Preparation and Sterilization of Media

One liter of media was prepared in a 2 L Erlenmeyer flask by adding 22 g of Brodo Mueller Hinton II Media (BMHII) and filling to 1 L with Millipore water. The flask was capped with aluminum foil and autoclave tape. The solution was heated and stirred on a hot plate with a stir bar for 10-15 min until homogeneous. The media was autoclaved. After the media was autoclaved, sterile procedures were used every time the aluminum foil lid was removed.

Sterile Technique

The hood was sprayed with 70% ethanol while the glass door was opened 1 foot or less. Anything coming into or near the hood was sprayed with 70% ethanol. No lids were removed during this process. All equipment and supplies were sprayed with 70% ethanol and/or autoclaved before they were placed in the hood. After the ethanol had fully evaporated inside the hood, a Bunsen burner was lit. All flasks were autoclaved and

capped with aluminum foil. The rim of each flask was passed through the flame before and after pouring media. The lids on all containers were closed for as much as time as possible.

Overnight Culture Preparation

Sterile technique was used to pour 80 mL of BMHII media into four 250 mL Erlenmeyer flasks. Two 80 mL cultures were started per type of *E. coli* from stored stock samples. All equipment and supplies were sterilized before removing the stock *E. coli* from the freezer. The stock *E. coli* was kept on ice and was not allowed to thaw. The sterile pipette tip was used to scrape the frozen bacterial stock and injected into the media. The culture flasks were placed into the incubator overnight at 37 °C at 250 revolutions per minute (rpms).

Starting the Culture

After 12 hours, the overnight cultures were checked for cloudiness. Three sterile 1 L Erlenmeyer flasks were prepared by adding 500 mL of sterile BMHII media to each 1 L flask using the sterile technique. The optical density at 600 nm (OD₆₀₀) of each flask was brought up to about 0.1 by adding the overnight culture. After the OD₆₀₀ of each culture was taken, the flasks were placed back in the 37 °C incubator at 250 rpms.

A culture was started from each of the three overnight growths, providing three technical replicates. This process was repeated six separate times: three cultures were taken six times to provide six biological replicates and eighteen samples overall for each of the four sample types (wild type mid log, mutant mid log, wild type stationary, mutant

stationary; 72 samples in total). Of the eighteen samples obtained, fifteen NMR samples were used for wild type mid log and for mutant mid log phases. Twelve NMR samples were analyzed for the wild type stationary phases, and thirteen NMR samples were analyzed for the mutant stationary phase.

OD₆₀₀ Readings

A sterile capped cuvette was filled with sterile media to use as a blank. For the 1:5 dilution blank, 0.20 mL of sterile media and 0.80 mL of sterile Millipore water was used. SpectraMax plus[®] SoftMax Pro 5[®] Molecular Devices Spectrometer was used to collect the OD₆₀₀ readings. The spectrometer was set to a wavelength of 600 nm. The blank cuvette was wiped down with a Kimwipe and inserted into the spectrometer. The blank spectrum was acquired, and the cuvettes were filled with 1 mL of each culture. Each sample was individually wiped down and inserted into the spectrometer. The OD₆₀₀ was recorded. The OD₆₀₀ was plotted versus time in minutes to generate a growth plot.

Culture Growth

The cultures were kept in the incubator at 37 °C and 250 rpms except for as short of a time as possible during sample collection. The OD₆₀₀ was taken every 0.5 h with the first few cultures grown and every hour with the last set of cultures grown. The 1:5 dilution of the samples in the cuvettes was implemented to keep the OD₆₀₀ readings in the linear phase. When the cultures reached mid log phase (half of the ending OD₆₀₀) and stationary phase, samples were collected. After the cultures reached stationary phase, the

cultures were left for another 6 to 8 hours before the OD₆₀₀ readings were taken again. The new OD₆₀₀ readings were compared to the ones 6-8 h prior to ensure that the culture was in stationary phase when the samples were obtained.

Sample Collection

The mid log phase samples were collected when the OD₆₀₀ reached half of the stationary phase OD₆₀₀. One 150 mL aliquot per culture was poured into a screw-cap conical centrifuge tube. The samples were centrifuged at 2,500 rpms for 12 min and the supernatant was discarded. The pellets were washed with 15 mL of cold sterile 1x PBS. The samples were transferred to glass centrifuge tubes, and OD₆₀₀ readings of each tube were taken with a 1:10 dilution. Each tube was centrifuged at 2,500 rpms for 12 min. The supernatant was discarded, and the pellets were frozen at -80 °C. The mutated did not centrifuge down as fast as the wild type. The mutated samples had to be centrifuged for twice as long (24 min).

Dry Mass Measurements

Watch glasses were sterilized, dried and massed. The cultures were watched until they had an OD₆₀₀ of about 1. Samples (25 mL) were collected and centrifuged at 2500 rpms for 25 min. The supernatant was discarded, and the pellets were rinsed with 5 mL of sterile PBS and vortexed. The samples were centrifuged at 2500 rpms for 25 min, and the supernatant was discarded. The cell pellets were scraped onto the watch glasses and put in the oven at 100 °C for 10 h. The masses of the dry samples were obtained. (Wang)

Colony Forming Units (CFUs)

YTP Agar was made using 4 g yeast extract, 8 g tryptone, 8 g glucose, 6.4 g agar and 400 mL Millipore water. The solution was boiled and poured into petri dishes. Each culture (100 μ L) was pipetted into a glass test tube A containing 9.9 mL of sterile PBS. The pipette was used to gently mix the test tube. An aliquot of 1 mL of solution from test tube A was pipetted into test tube B, which contained 9 mL of sterile PBS. This procedure was repeated with test tubes C and D, respectively. Five 100 μ L aliquots were pipetted onto different regions of the agar plates. This procedure was repeated 9 times per culture type. The agar plates were placed into a 37 °C incubator. After 24 h, each aliquot was divided into sections and counted. The number of CFUs/mL was calculated. (Wang; Ammons et al. 2014 and references therein)

Determining the Concentration of the Sample

The samples were brought up in 5 mL of 1xPBS and vortexed. Three aliquots were pipetted into separate cuvettes. PBS (1x) was added to each cuvette to create a 1:10 dilution. The cuvette was pipetted up and down 5 times. The optical density of each cuvette was taken at 600 nm. OD₆₀₀ measurements were taken on three aliquots per sample type to check for consistency. The CFUs and dry mass of the wild type and mutant were calculated and compared. The results showed that they were statistically the same and were as expected for *E. coli*. The hydrophilic metabolites were extracted and put in an NMR buffer as described in the main paper, and ¹H NMR spectra were obtained. The spectra were profiled with Chenomx Suite 8.2 Software. The total sum of

the concentrations of the metabolites found in each profiled spectrum was compared to the total concentration found from the OD₆₀₀. The results were as expected: none of the samples had an inconsistent change in concentration. The total concentration of each sample was used as the standardization concentration. The samples were standardized as shown in Equation A1.

Standardization of Metabolite Concentration

The concentration of each metabolite, which was determined by Chenomx Suite 8.2 Software, was divided by the total concentration of the sample, which was determined by OD₆₀₀ and checked with the total sum (Chenomx). This ratio was multiplied by 100 to give the standardized concentration (Equation A1).

$$\frac{\text{Concentration of the Individual Metabolite}}{\text{Total Concentration of Sample}} * 100 = \text{Standardized Concentration} \quad (\text{A1})$$

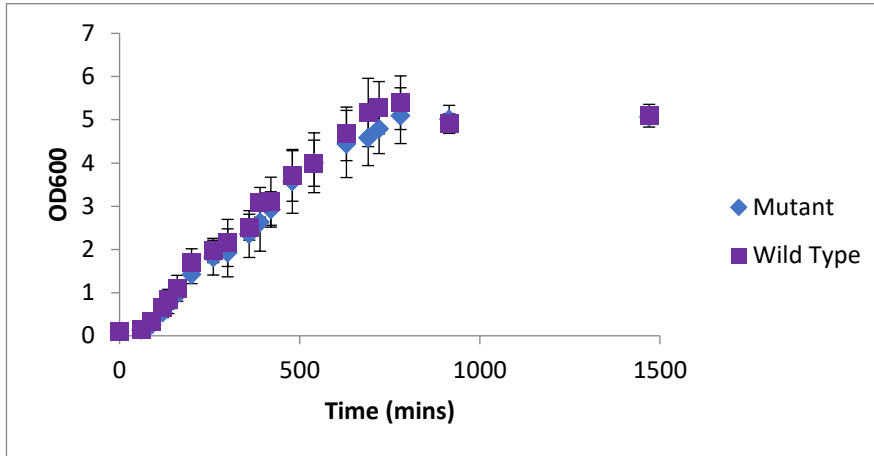
Data

Figure A2. Growth Plot of Wild Type and C₁₆-DABCO Mannose Functionalized Dendrimer Mutated *E. coli*

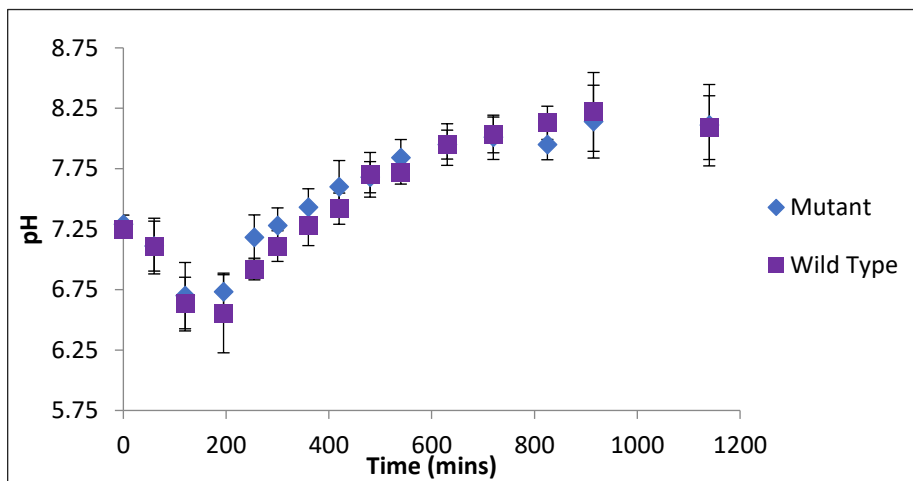


Figure A3. pH Plot of Wild Type and C₁₆-DABCO Mannose Functionalized Dendrimer Mutated *E. coli*

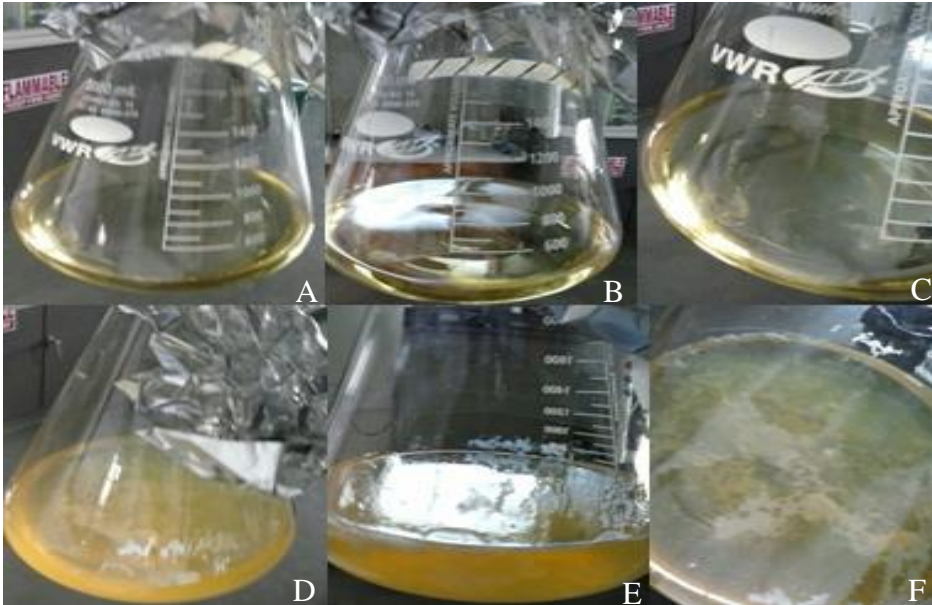


Figure A4. Control Experiment of Sterile Techniques. **a**, **b** and **c** are the results after autoclaved media was poured into sterile Erlenmeyer flasks using the sterile techniques described in the methods section and left for two weeks. **d**, **e** and **f** are the results after autoclaved media was poured into sterile Erlenmeyer flasks in the open air and left for two weeks. The control experiment was preformed three separate times with 3 flasks per group

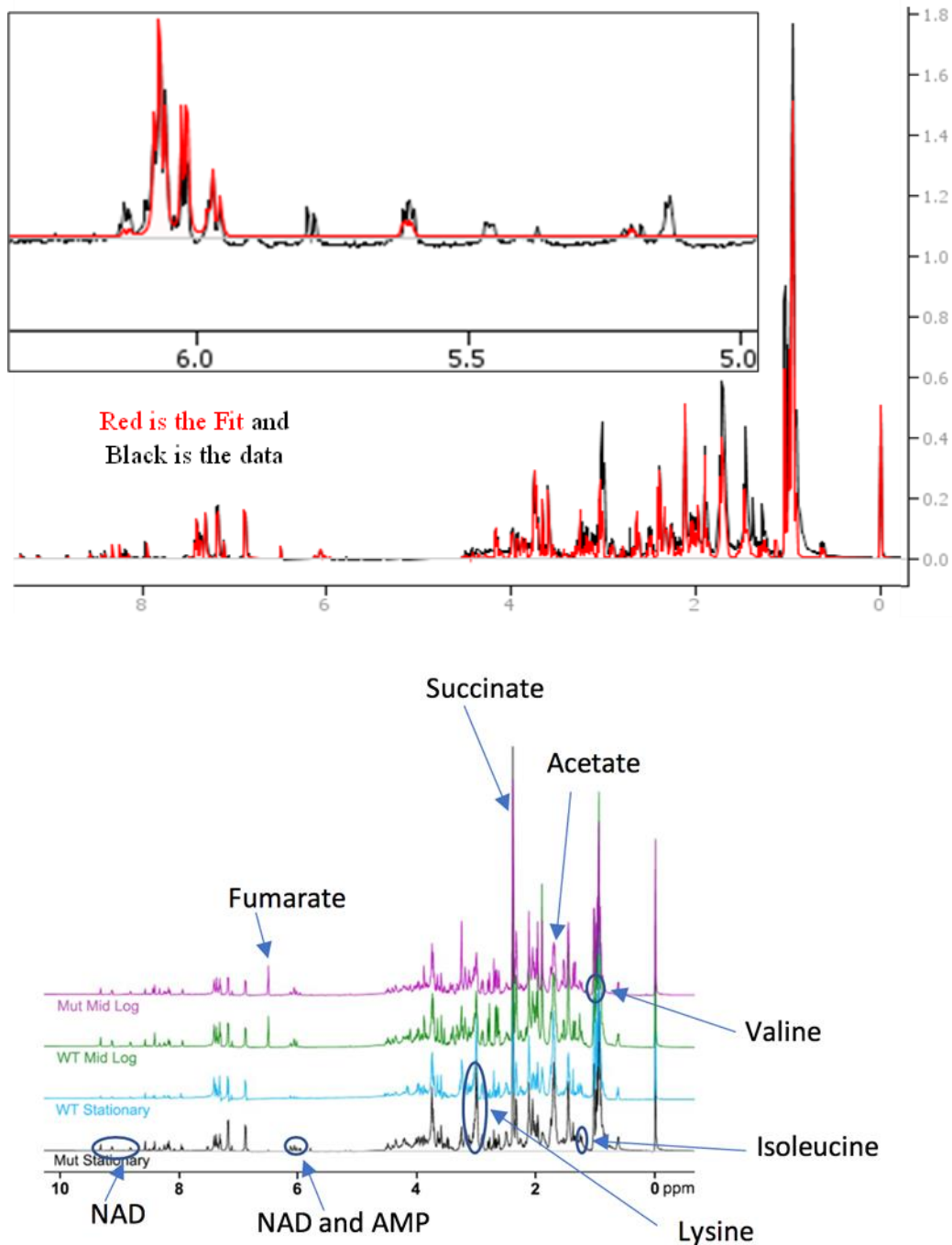
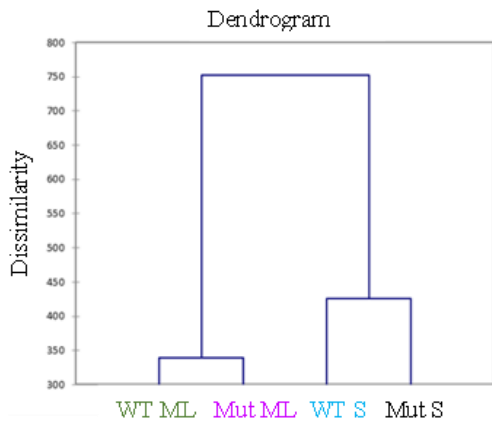


Figure A5. **Top:** Wild Type Stationary Profiling Fit of Data using Chenomx 8.2 Suite Software. Profiled compounds overall fit well. Original spectrum is shown in black. Compounds that could be identified are shown in red. There are a few unidentified metabolites that could not be identified with the software, as emphasized in the embedded expansion. **Bottom:** Spectra are annotated to show some of the obvious identifiable compound resonances so that their changes across the sample types can be seen.



(a)

Results by Class:

1	2	3	4
WT_S_1	Mut_S_1	Mut_ML_1	WT_ML_1
WT_S_2	Mut_S_2	Mut_ML_2	WT_ML_2
WT_S_3	Mut_S_3	Mut_ML_3	WT_ML_3
WT_S_5	Mut_S_7	Mut_ML_4	WT_ML_6
WT_S_6	Mut_S_8	Mut_ML_6	WT_ML_7
WT_S_7	Mut_S_9	Mut_ML_7	WT_ML_8
WT_S_9	Mut_S_10	Mut_ML_8	WT_ML_9
WT_S_10	Mut_S_12	Mut_ML_9	WT_ML_10
		Mut_ML_10	WT_ML_11
			WT_ML_12
			WT_ML_13

(b)

Figure A6. **a** Hierarchical Clustering indicating that there are 4 unique sample types. **b** Resulting classification of all input data showing that no input sample types overlapped

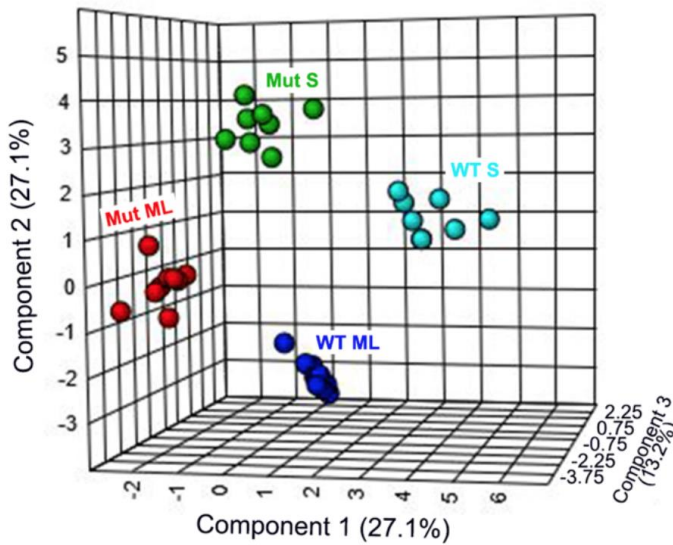


Figure A7. 3D sPSL-DA plot demonstrates that each sample type can be separated into a distinct group without overlap

Table A1. All Metabolites Identified using the Chenomx NMR Suite 8.2 Software Profiling Program and Metabolite Library.

All Identified Metabolites	CAS #
Acetate	71-50-1
Acetoacetate	541-50-4
Adenosine	58-61-7
Alanine	56-41-7
AMP	61-19-8
Aspartate	56-84-8
Betaine	107-43-7
Cysteine	54-90-4
Cytosine	71-30-7
Formate	141-53-7
Fucose	2438-80-4
Fumarate	142-42-7
Glutamate	56-86-0
Glycine	56-40-6
Histidine	71-00-1
Homocysteine	6027-13-0
Isocitrate	320-77-4
Isoleucine	73-32-5
Lactate	50-21-5
Leucine	61-90-5
Lysine	56-87-1
Methionine	59-51-8
N-Acetylglucosamine	7512-17-6
NAD+	53-84-9
Phenylalanine	63-91-2
Proline	609-36-9
Pyroglutamate	28874-51-3
Succinate	110-15-6
Tyrosine	60-18-4
UDP-glucose	133-89-1
Valine	72-18-4

Top Compounds Correlated with N-acetylglucosamine

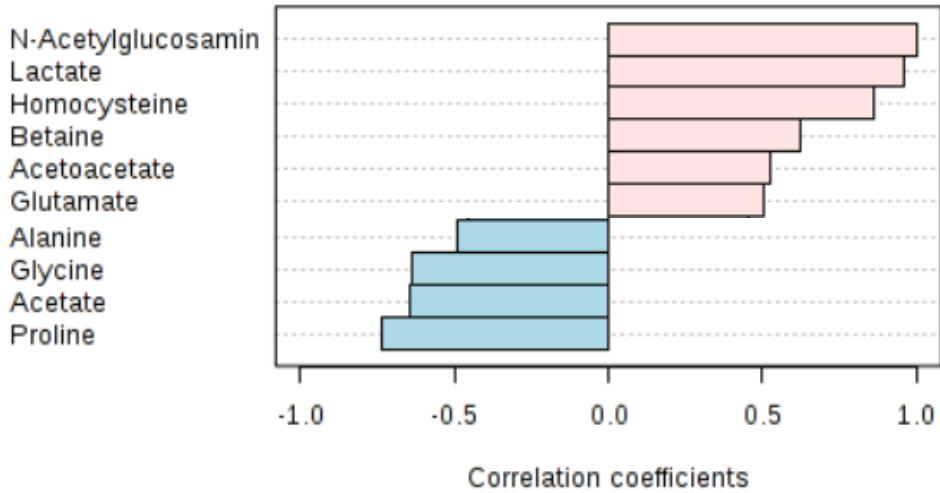


Figure A8. Top Mid Log Phase Compounds Significantly Correlated with *N*-acetylglucosamine

Top Compounds Correlated with Homocysteine

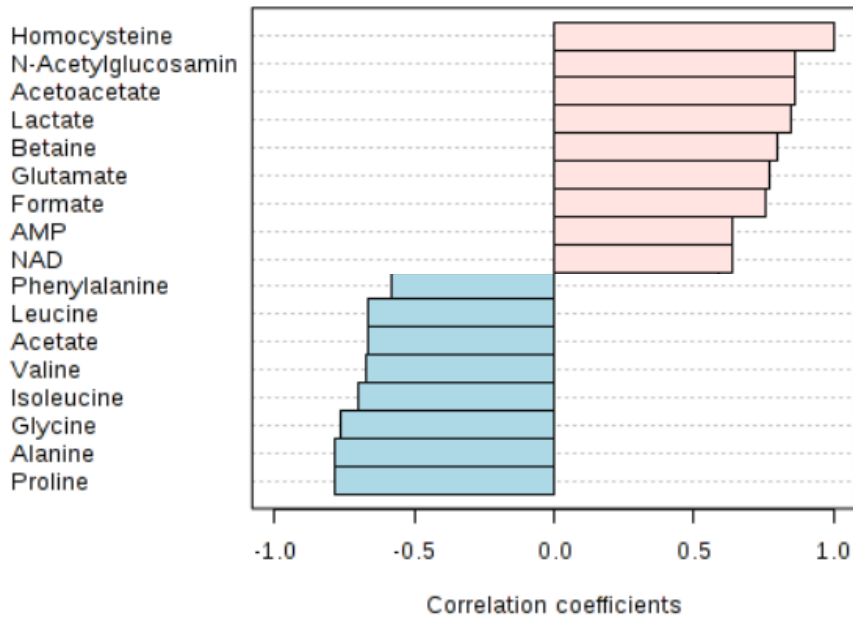


Figure A9. Top Mid Log Phase Compounds Significantly Correlated with Homocysteine

Top Compounds Correlated with Lysine

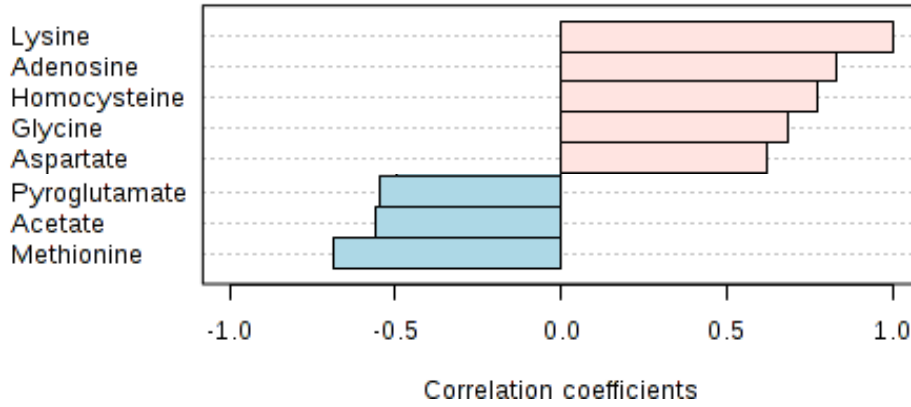


Figure A10. Top Stationary Phase Compounds Significantly Correlated with Lysine

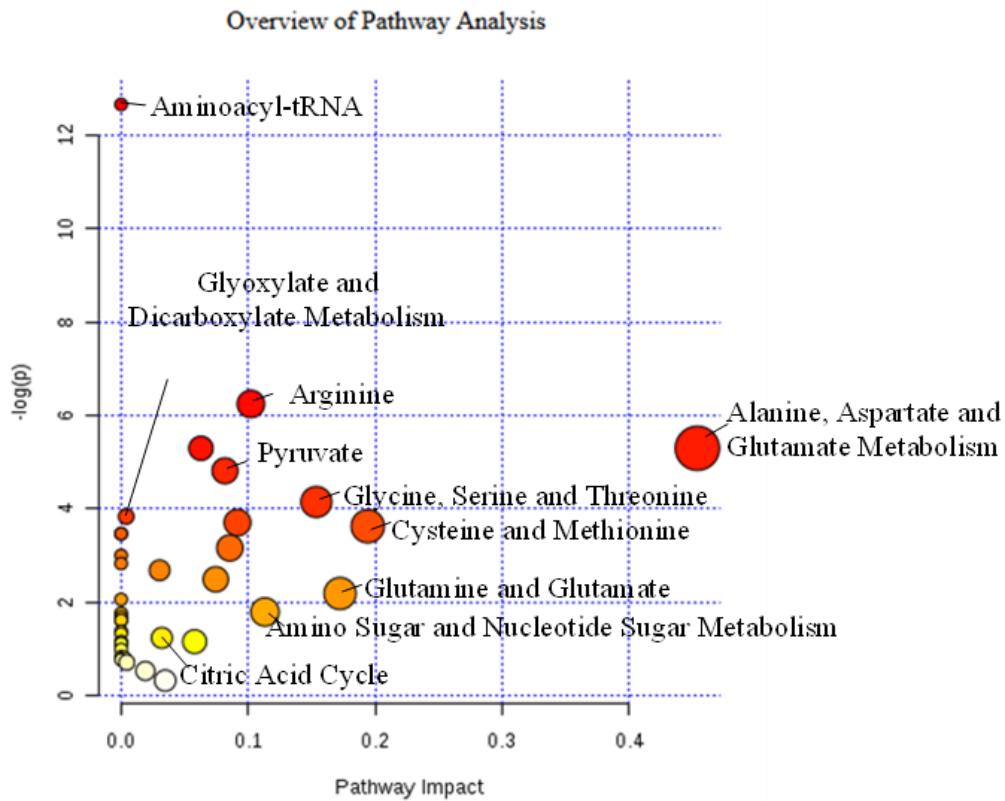


Figure A11. Mid Log Phase Top Impacted Pathways. The larger and darker the circles are, the larger the impact the significant metabolites have on the listed pathway

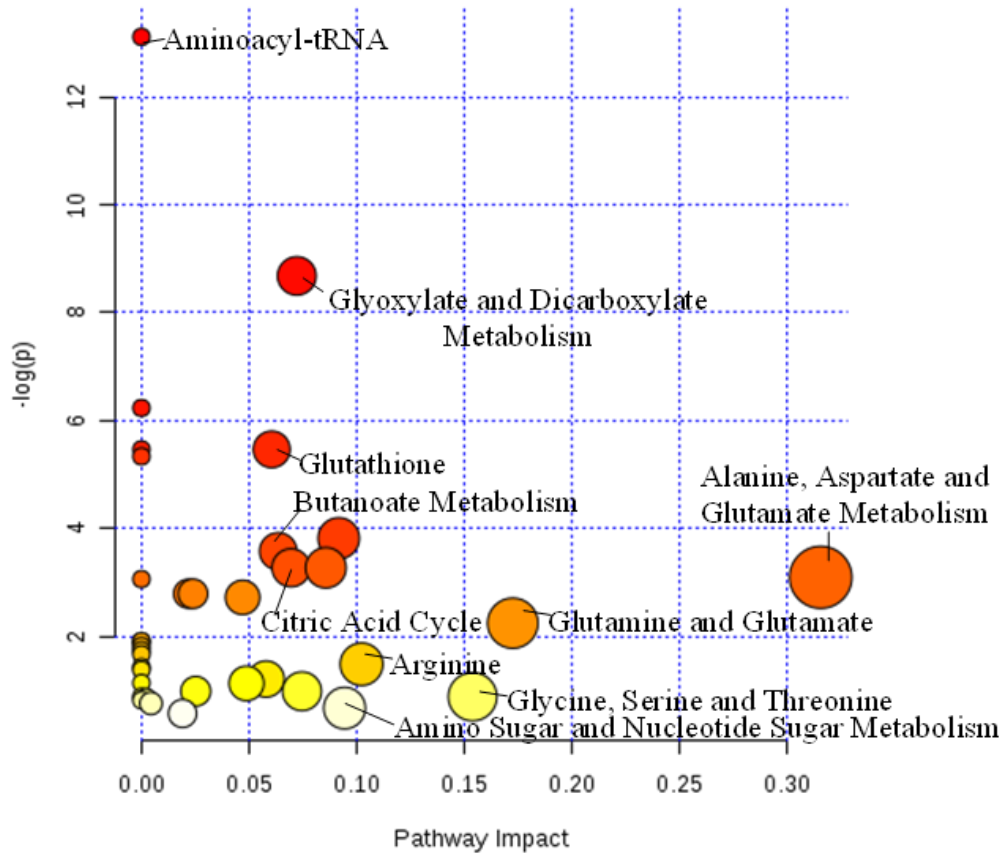
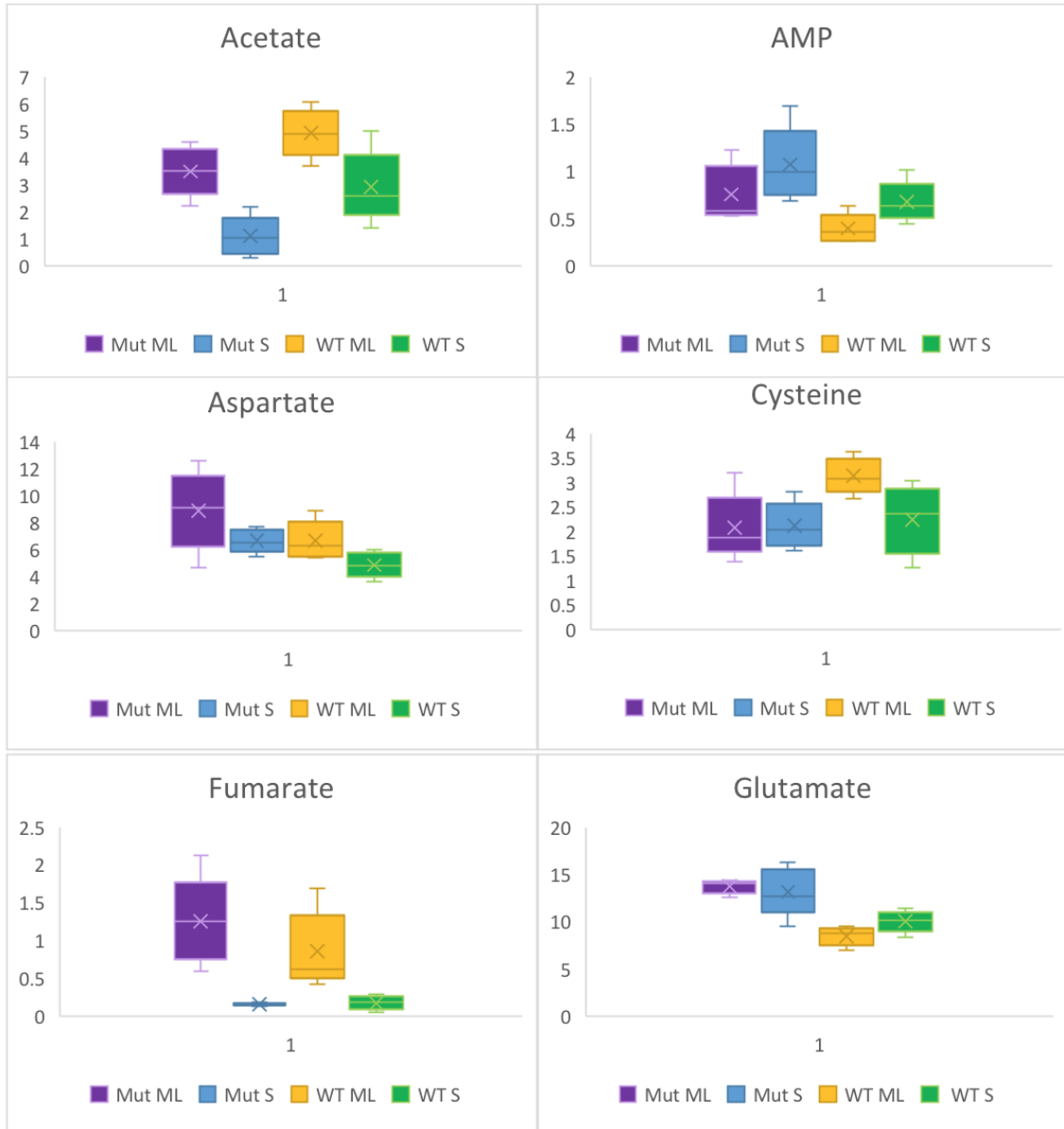
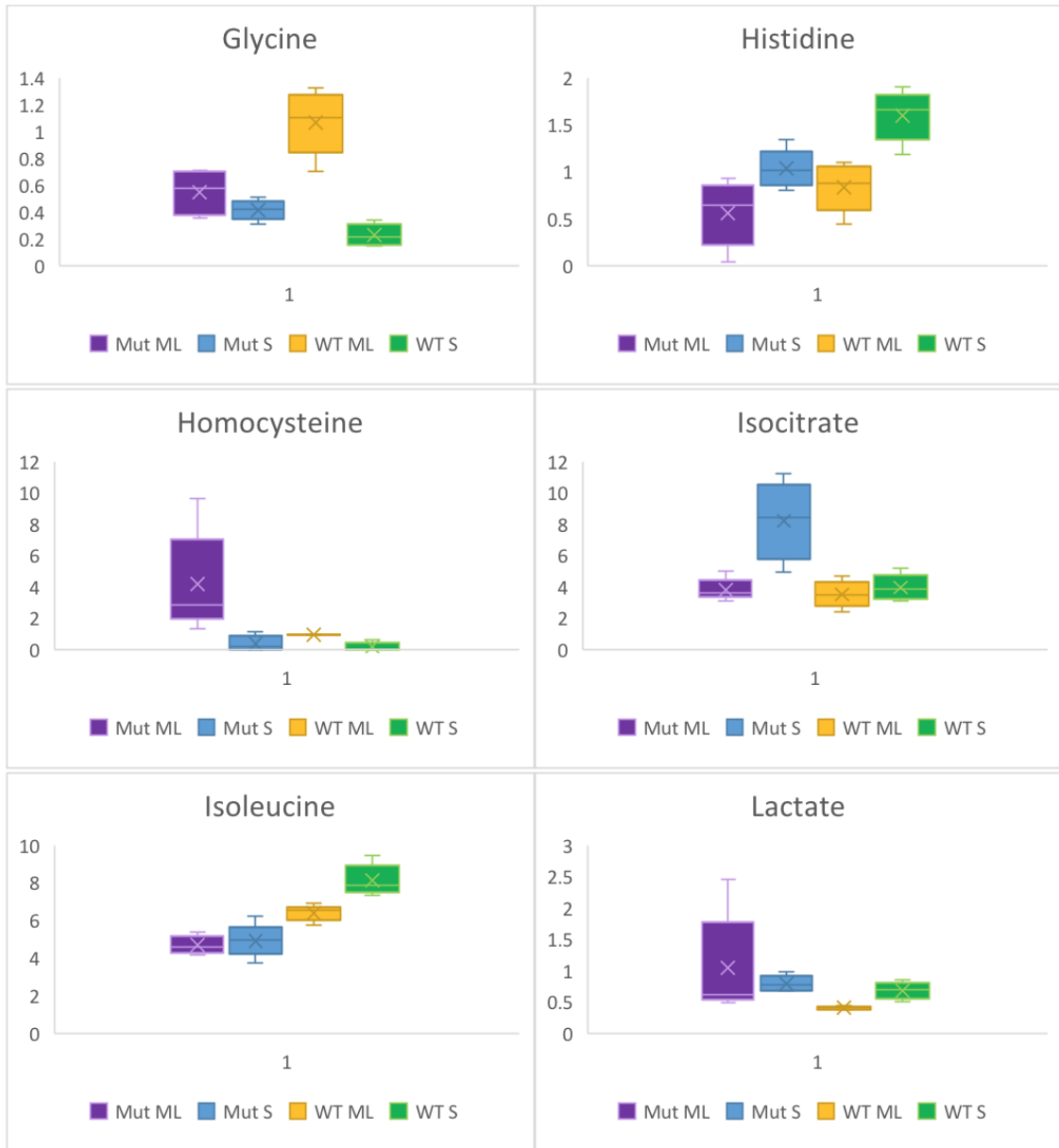
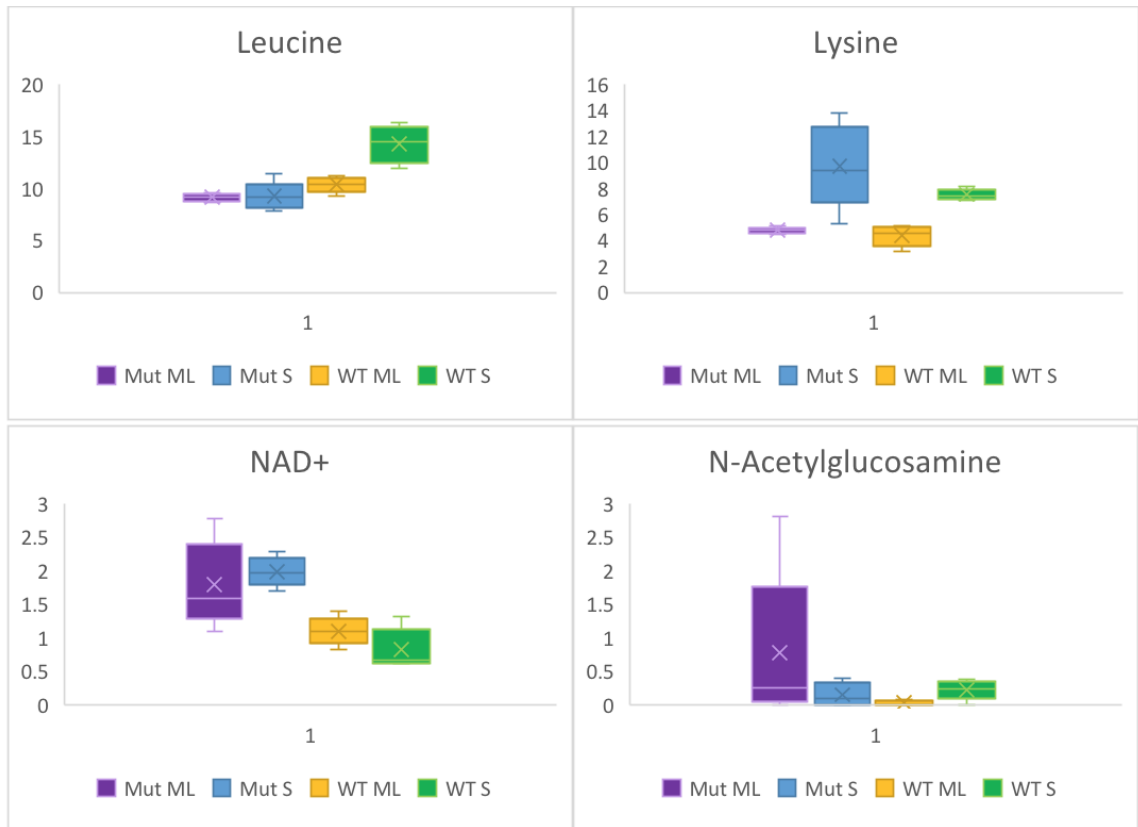


Figure A12. Stationary Phase Top Impacted Pathways. The larger and darker the circles are, the larger the impact the significant metabolites have on the listed pathway







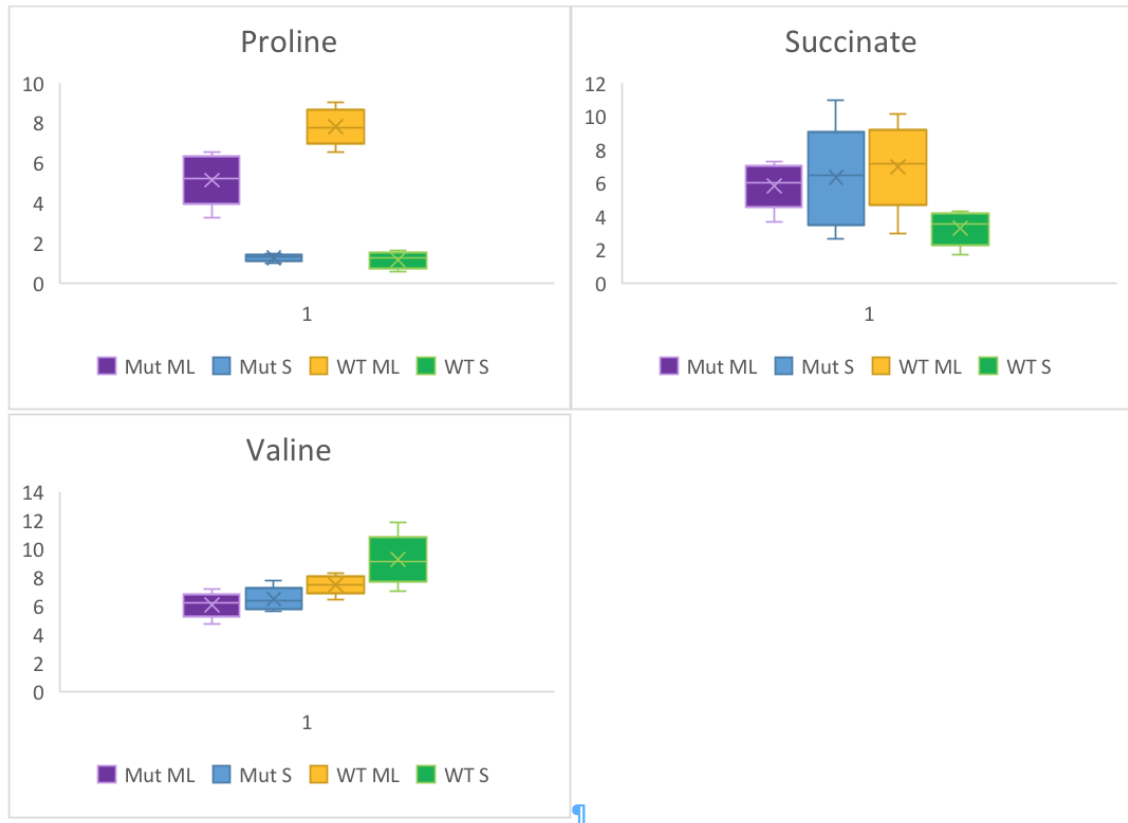


Figure A13. Box and whisker plots for the metabolites shown in Table 2.1 of the manuscript show the variation of each metabolite among each of the 4 sample types. The ends of the whiskers are the minimum and maximum values, the center line is the median, the x is the mean, and the colored middle “box” encompasses the middle 50% of scores for the group.

References

- Ammons, MC. B., Tripet, B. P., Carlson, R. P., Kirker, K. R., Gross, M. A., Stanisich, J. J., Copié, V. (2014) Quantitative NMR Metabolite Profiling of Methicillin-Resistant and Methicillin-Susceptible *Staphylococcus aureus* Discriminates between Biofilm and Planktonic Phenotypes. *J Proteome Res*, 13, 2973-2985.
- Wang, N. S. [Online] Experiment No. 9 °C Measurements of Cell Biomass Concentration. Department of Chemical and Biomolecular Engineering, University of Maryland, MD. <http://www.eng.umd.edu/~nsw/ench485/lab9c.htm>

APPENDIX B

SUPPLEMENTARY MATERIALS FOR CHAPTER 3:

B. CEREUS MANUSCRIPT

Table of Contents

Detailed Methods Description.....	160
Growth Curve.....	164
Sample NMR Spectra.....	164
Table B1 Significant Metabolites Identified.....	165
Hierarchical Clustering.....	166
Ortho PLS-DA.....	167
PCA plot.....	168
3D sPLS-DA.....	169
Volcano Plots	170
VIP Plots.....	172
Challenged Mutant versus Unchallenged Wild Type Tables S2 and S3	175
Pattern Hunter Metabolite Correlations	178
Pathway Analysis Plots	195
Box Plots.....	201
References.....	224

Procedures

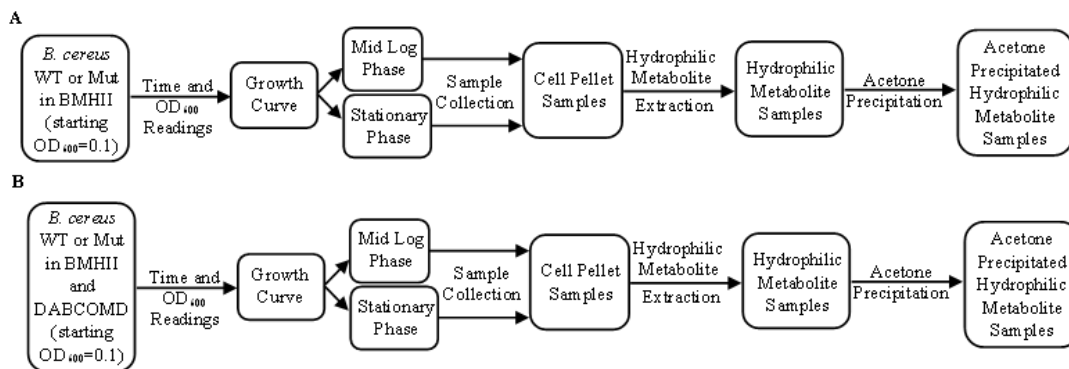


Figure B1. Procedure overview. Overview of the start of the cultures to the hydrophilic metabolite samples ready to be pelleted and frozen at -80°C then put into NMR buffer. (a) unchallenged sample procedures (b) challenged sample procedures.

Preparation and Sterilization of Media

Growth media (1 L) was prepared by adding 22 g of Brodo Mueller Hinton II Media (BMHII) and filling to 1 L with Millipore water in a 2 L Erlenmeyer flask, which was capped with aluminum foil with a strip of autoclave tape. The media was heated and stirred until homogeneous with a stir bar on a hot plate for 10-15 minutes, then autoclaved. Sterile methods were used whenever the aluminum foil lid was removed.

Sterile Technique

The autoclave was used on all supplies and solutions that needed to be sterilized and could withstand the autoclave. The door in the hood was never raised more than a foot. The hood, all equipment and supplies, my gloves and lab coat sleeves were sprayed down with 70% ethanol. No lids were removed until after the ethanol dried, only when necessary and for as short of a time as possible. A Bunsen burner was lit, and the rim of each flask was passed through the flame before and after any pouring occurred.

Overnight Culture Preparation

In a 250 mL Erlenmeyer flask, 80 mL of the already prepared and sterilized BMHII media was poured using sterile technique. Frozen stock and mutated *B. cereus* samples were kept on ice while separate sterile pipette tips were used to scrape the frozen bacterial stock. The pipette tips with frozen bacterial stock were ejected into separate media filled 250 mL Erlenmeyer flasks. These flasks were put in an incubator at 37 °C with 250 revolutions per minute (rpms) overnight.

Starting the Culture

The overnight cultures were cloudy and used to start the sample cultures. Sterile technique was used to add 500 mL of sterile BMHII media to each 1 L flask, and overnight culture was added until the optical density at 600 nm (OD₆₀₀) reached 0.1. After each flask's OD₆₀₀ was brought up 0.1, they were placed back into the 37 °C incubator at 250 rpms.

OD₆₀₀ Readings

A blank was created by filling a capped cuvette with sterile media. Sterile media (0.20 mL) and 0.80 mL of sterile Millipore water was used to create a 1:5 dilution blank. The OD₆₀₀ readings were conducted on a SpectraMax plus[®] SoftMax Pro 5[®] Molecular Devices Spectrometer set to 600 nm wavelength. Before any cuvette was placed into the spectrometer, it was wiped down with a Kimwipe. A blank spectrum was acquired prior to running a sample cuvette filled with 1 mL of culture. The OD₆₀₀ was recorded and plotted versus time (min) to generate the sample growth plots.

Culture Growth

Note: All cultures were kept in the 37 °C incubator at 250 rpms, exception during sample collection.

To generate the growth plot and track individual sample progress, the OD₆₀₀ was taken every half of an hour for the first few cultures and every hour for the last few cultures of every sample type grown. When the sample's OD₆₀₀ was going to be greater than 1, a 1:5 dilution of all samples was enacted in the OD cuvettes to keep them in the linear phase. Sample collection was conducted in the mid log (half of the ending OD₆₀₀) and stationary phases. After the stationary phase samples were collected, the cultures were left overnight and the OD₆₀₀ was taken again, to ensure that the OD₆₀₀ did not increase and that the cultures were in stationary phase the night before.

Sample Collection

Samples were collected in the mid log phase (half the ending OD₆₀₀) and the stationary phase. Two 150 mL aliquots per culture were combined to form one sample. Screw-cap conical centrifuge tubes were used to centrifuge the samples at 2,500 rpms for 12 minutes. The supernatant was discarded, and the cell pellets were washed with 15 mL of cold sterile 1x PBS. The samples were transferred to glass centrifuge tubes. A 1:10 dilution was used to obtain OD₆₀₀ readings of for each sample. They were centrifuged at 2,500 rpms for 12 minutes for the wild type samples, and for 24 minutes for the mutant samples, since it took longer for the mutant samples to centrifuge down.

Dry Mass Measurements

At an OD₆₀₀ of 1, 25 mL of sample culture was collected. They were centrifuged at 2500 rpms for 25 minutes and the supernatant was discarded. The cell pellets were rinsed with 5 mL of sterile 1x PBS and vortexed, then centrifuged at 2500 rpms for 25 minutes. The supernatant was discarded, and the cell pellet was scraped onto a sterile and pre-massed watch glass. The watch glasses were placed in the oven at 100 °C for 10 hours. The masses of the dried samples were obtained. (Aries and Cloninger 2020; Wang)

Colony Forming Units (CFUs)

An YTP Agar solution was created from 4 g yeast extract, 8 g tryptone, 8 g glucose, 6.4 g agar and 400 mL Millipore water. After the solution was boiled, it was poured into petri dishes. A glass test tube labeled A contained 9.9 mL of sterile PBS and 100 µL of culture and was gently mixed with a pipette tip. A glass test tube labeled B contained 9 mL of sterile PBS and 1 mL from test tube A and was gently mixed with a pipette tip. A glass test tube labeled C contained 9 mL of sterile PBS and 1 mL from test tube B and was gently mixed with a pipette tip. A glass test tube labeled D contained 9 mL of sterile PBS and 1 mL from test tube C and was gently mixed with a pipette tip. A 100 µL aliquot was taken from test tube D and pipetted onto an agar plate and a bacterial spreader was used. This was repeated nine times per sample type. The agar plates were incubated at 37 °C for 24 hours. Each plate was divided into sections and the CFUs were counted. The number of CFUs per milliliter was calculated. (Aries and Cloninger 2020; Wang; Ammons et al. 2014 and references therein)

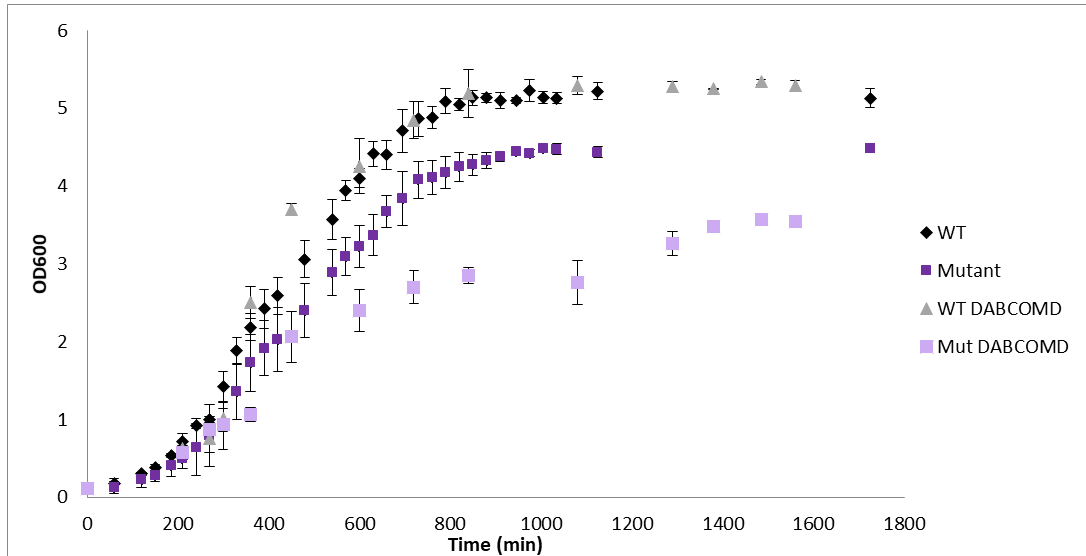
Data

Figure B2. Growth Plot of Wild Type, DABCOMD Mutated *B. cereus*, DABCOMD challenged Wild Type and DABCOMD challenged DABCOMD Mutated *B. cereus*. The challenged groups are labeled with DABCOMD after the sample type.

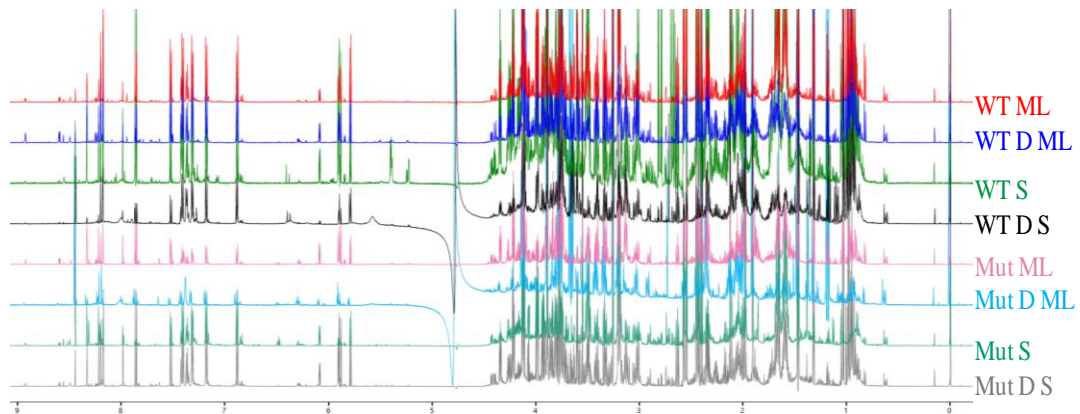


Figure B3. Spectra for each of the 8 sample types.

Table B1. All Metabolites Identified using the Chenomx NMR Suite 8.4 Software Profiling Program and Metabolite Library

All Identified Metabolites	CAS #
Acetate	71-50-1
Acetoacetate	541-50-4
Adenine	73-24-5
Adenosine	58-61-7
Alanine	56-41-7
AMP	61-19-8
Aspartate	56-84-8
Betaine	107-43-7
Cystathionine	56-88-2
Cysteine	54-90-4
Formate	141-53-7
Fucose	2438-80-4
Fumarate	142-42-7
Glutamate	56-86-0
Glutamine	56-85-9
Glycine	56-40-6
Histidine	71-00-1
Homocysteine	6027-13-0
Isocitrate	320-77-4
Isoleucine	73-32-5
Lactate	50-21-5
Leucine	61-90-5
Lysine	56-87-1
Methionine	59-51-8
N-Acetylglucosamine	7512-17-6
NAD ⁺	53-84-9
Phenylalanine	63-91-2
Proline	609-36-9
Pyroglutamate	28874-51-3
Pyruvate	127-17-3
Serine	302-84-1
Succinate	110-15-6
Tyrosine	60-18-4
UDP-glucose	133-89-1
Uracil	66-22-8
Uridine	58-96-8
Valine	72-18-4

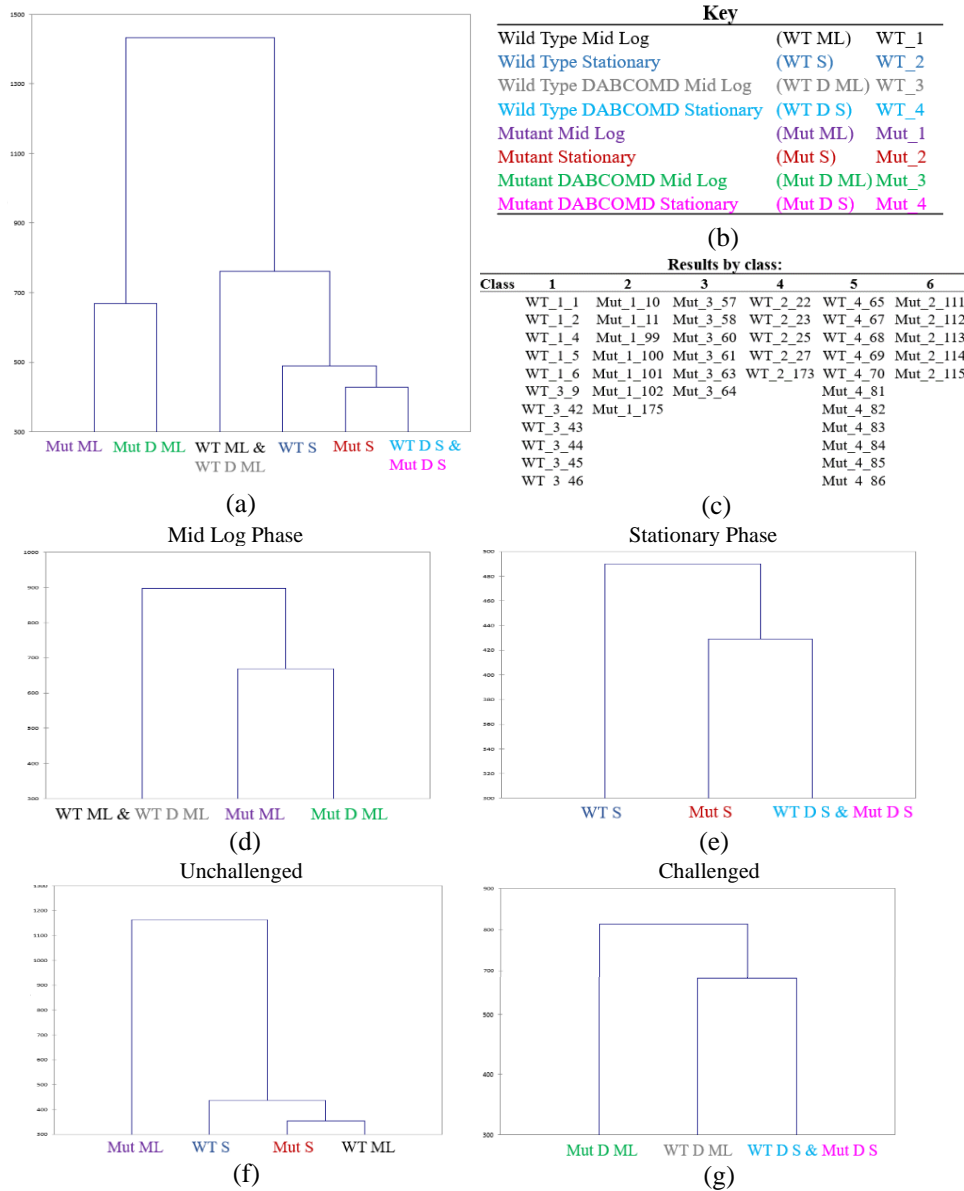


Figure B4. (a) Hierarchical Clustering of all sample types showing that WT ML and WT D ML cluster together, WT D S and Mut D S cluster together and all other sample types separate. (b) Sample abbreviation key. (c) Resulting classification of all input data showing the clustering of each individual sample. (d) Hierarchical Clustering of mid log phase samples showing that WT ML and WT D ML cluster together, and all other sample types separate. (e) Hierarchical Clustering of stationary phase samples showing that WT D S and Mut D S cluster together, and all other sample types separate. (f) Hierarchical Clustering of unchallenged sample types showing complete separation of sample types. (g) Hierarchical Clustering of DABCOMD challenged samples showing that the stationary phases cluster together, while the mid log phases separate.

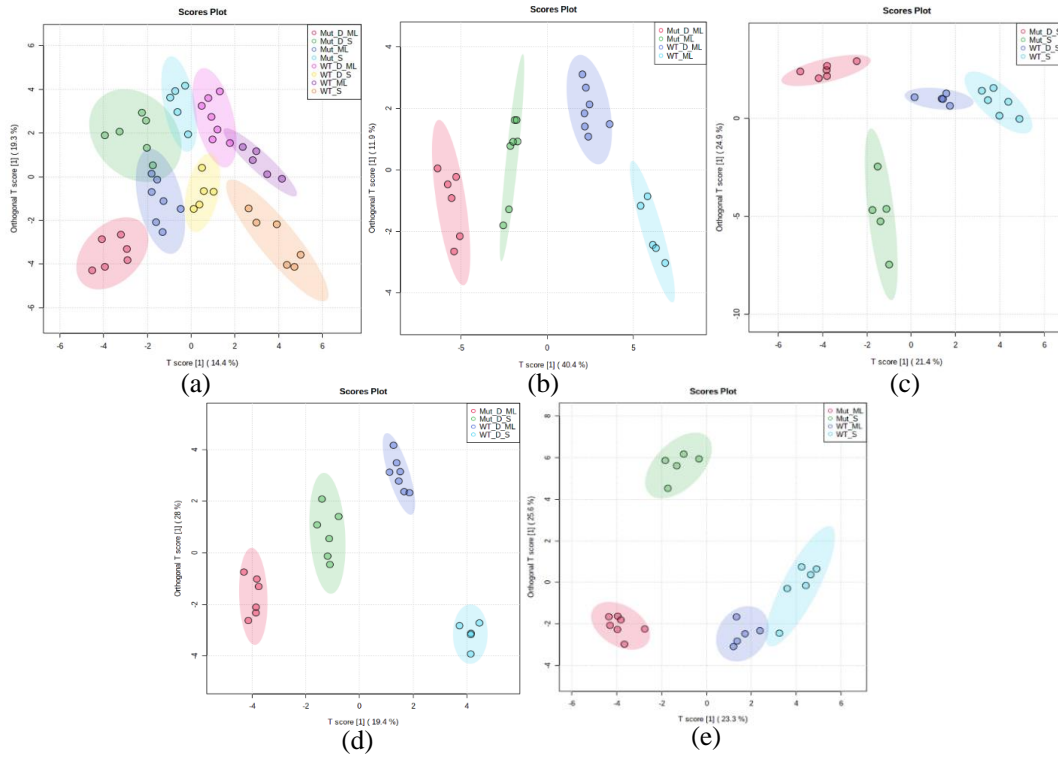


Figure B5. 2D ortho PLS-DA **(a)** Contains all sample types: demonstrates the greatest degree of separation with all sample types together, with only an overlap of the oval of WT ML with the oval of WT D ML, and a overlap of the oval of Mut D S with the ovals of WT S and Mut ML. **(b-e)** demonstrates complete separation of all sample types: **(b)** mid log phase samples. **(c)** stationary phase samples. **(d)** DABCOMD challenged samples. **(e)** unchallenged samples.

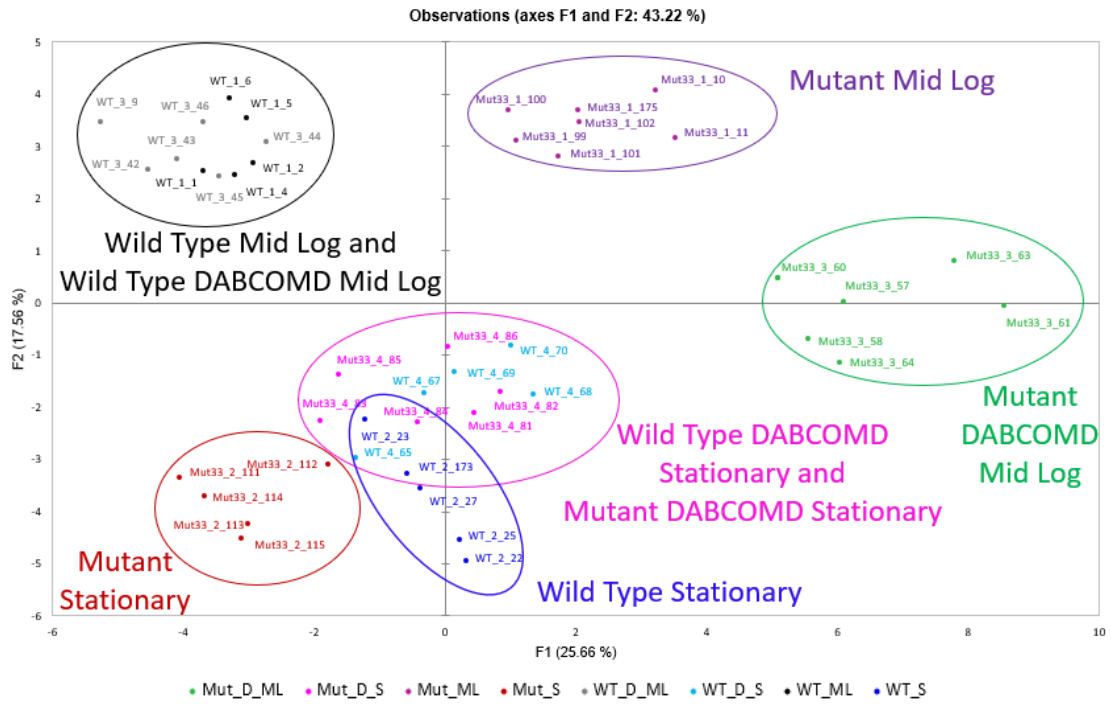


Figure B6. PCA plot showing the distribution of all sample types with sample labels corresponding to those listed in Figure B4c.

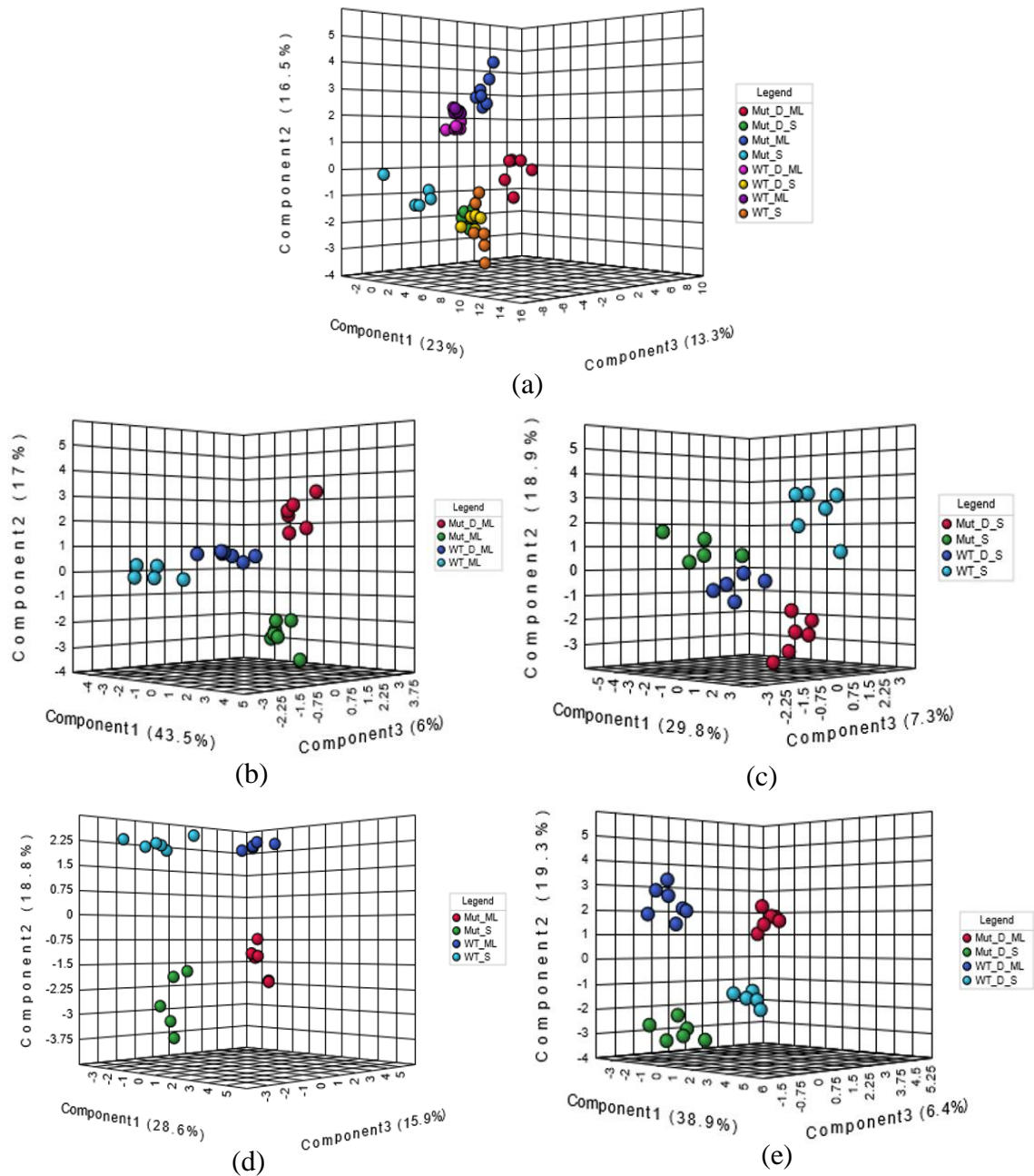


Figure B7. 3D sPLS-DA **a** Contains all sample types: showing a slight overlap of WT ML with WT D ML, Mut ML separated, Mut D ML separated, Mut S separated, while WT S, WT D S and Mut D S clustered. **b** Contains only mid log samples: showing WT ML clustering near WT D ML and complete separation of Mut ML and Mut D ML. **c** Contains only stationary phase samples: showing WT D S clustering between Mut D S and Mut S, WT S being the most distinct group. **d** Contains only unchallenged samples: showing a complete separation of sample types **e** Contains only DABCOMD challenged samples: showing complete separation of all sample types.

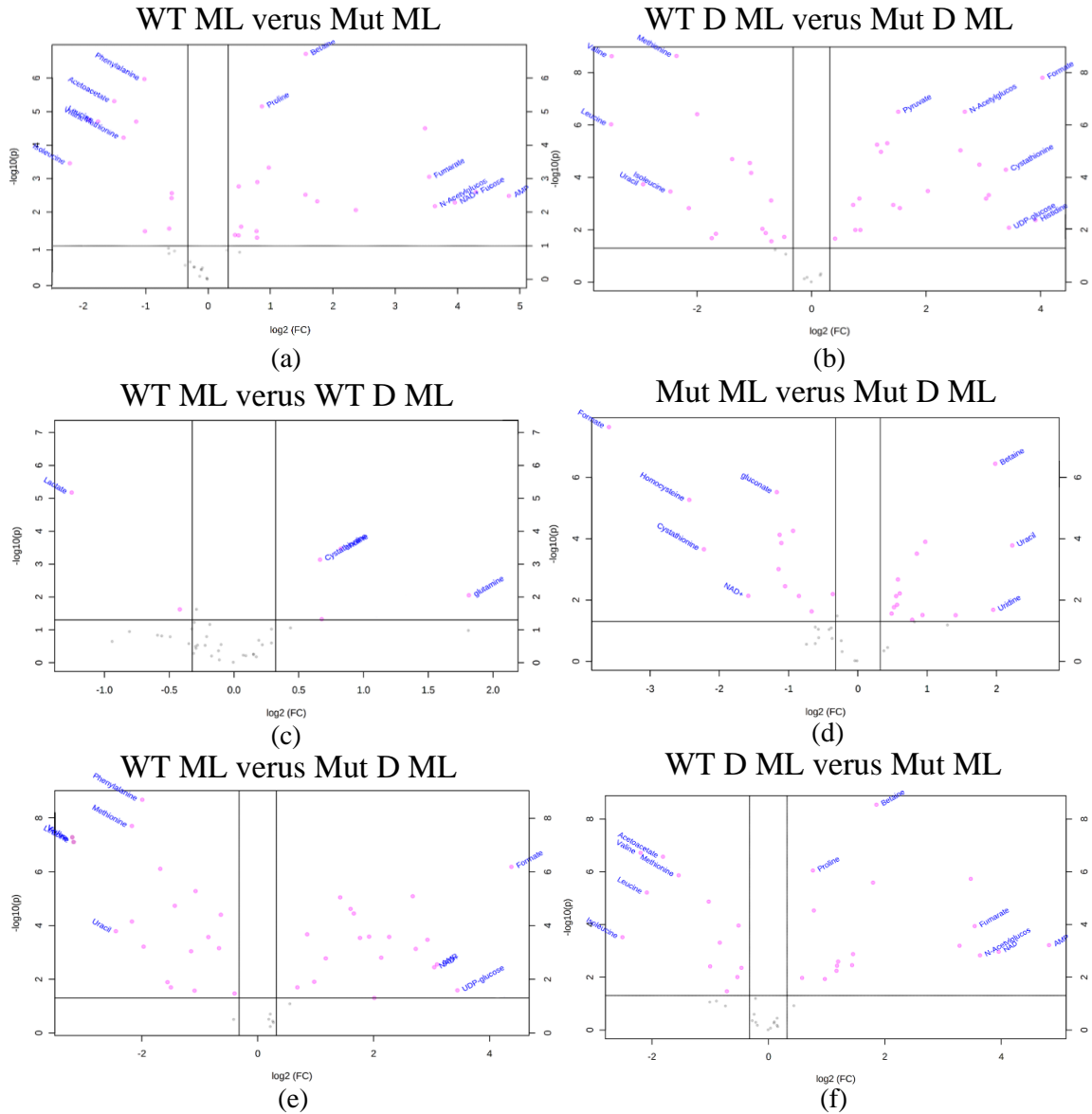


Figure B8. Volcano Plot showing significant p-values and fold changes for metabolites in the mid log phase paired up **a** WT and Mut **b** WT D and Mut D **c** WT and WT D **d** Mut and Mut D **e** WT and Mut D **f** WT D and Mut.

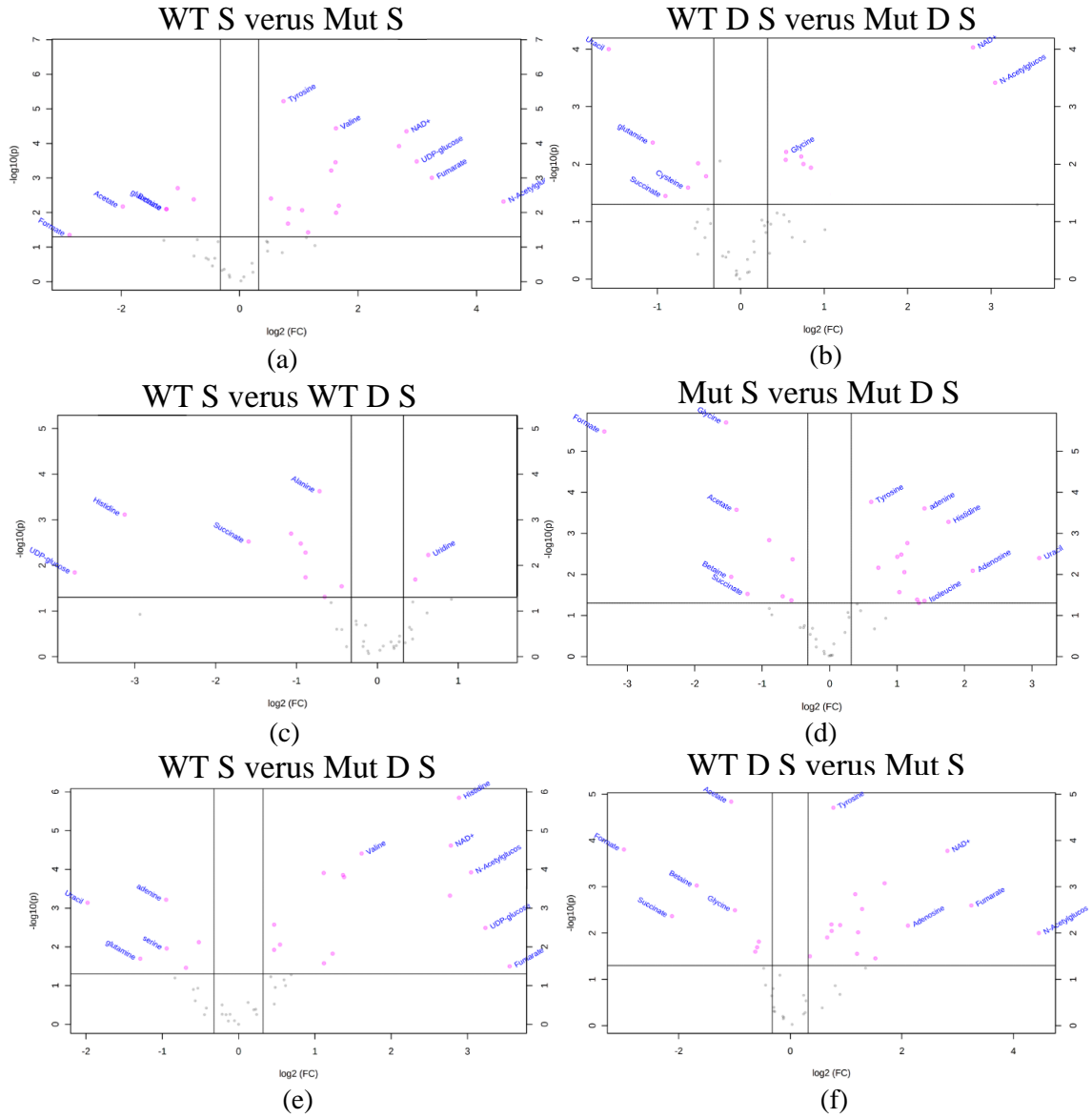


Figure B9. Volcano Plot showing significant p-values and fold changes for metabolites in the stationary phase paired up **a** WT and Mut **b** WT D and Mut D **c** WT and WT D **d** Mut and Mut D **e** WT and Mut D **f** WT D and Mut.

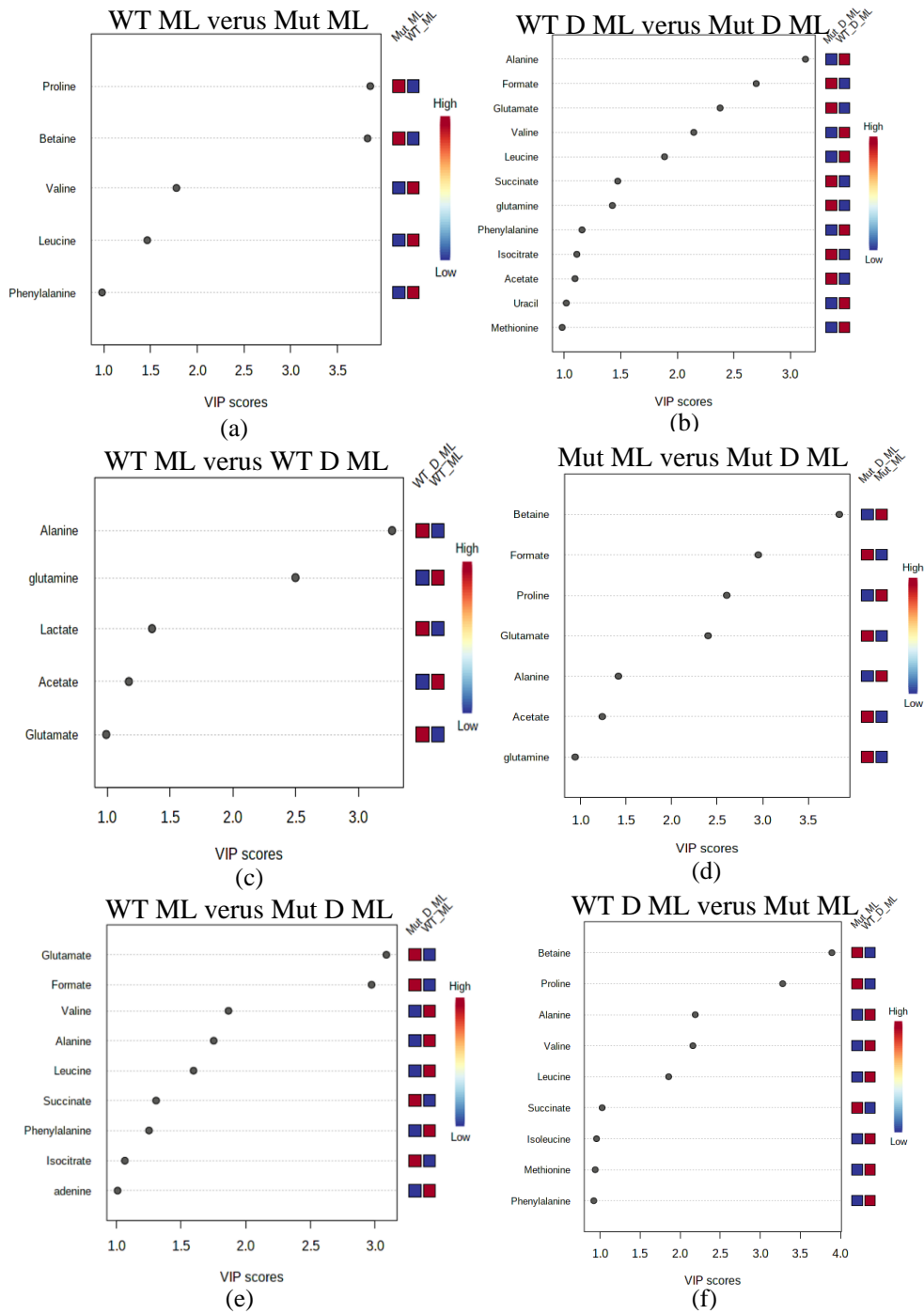


Figure B10. Very Important Features (VIP) scores obtained from the PLS-DA which shows important metabolites in paired mid log phase samples **a** WT and Mut **b** WT D and Mut D **c** WT and WT D **d** Mut and Mut D **e** WT and Mut D **f** WT D and Mut.

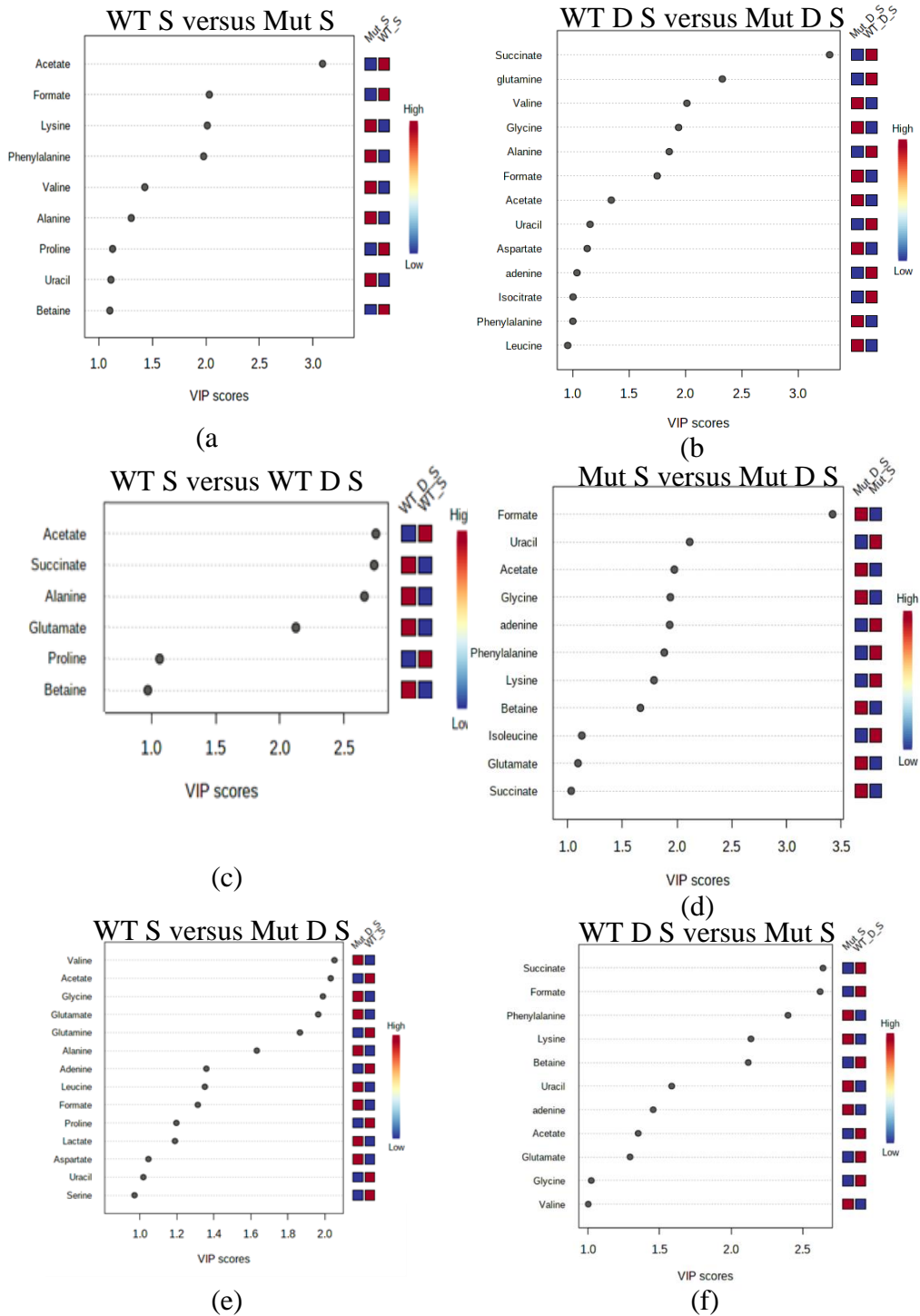


Figure B11. Very Important Features (VIP) scores obtained from the sPLS-DA which shows important metabolites in paired stationary phase samples **a** WT and Mut **b** WT D and Mut D **c** WT and WT D **d** Mut and Mut D **e** WT and Mut D **f** WT D and Mut.

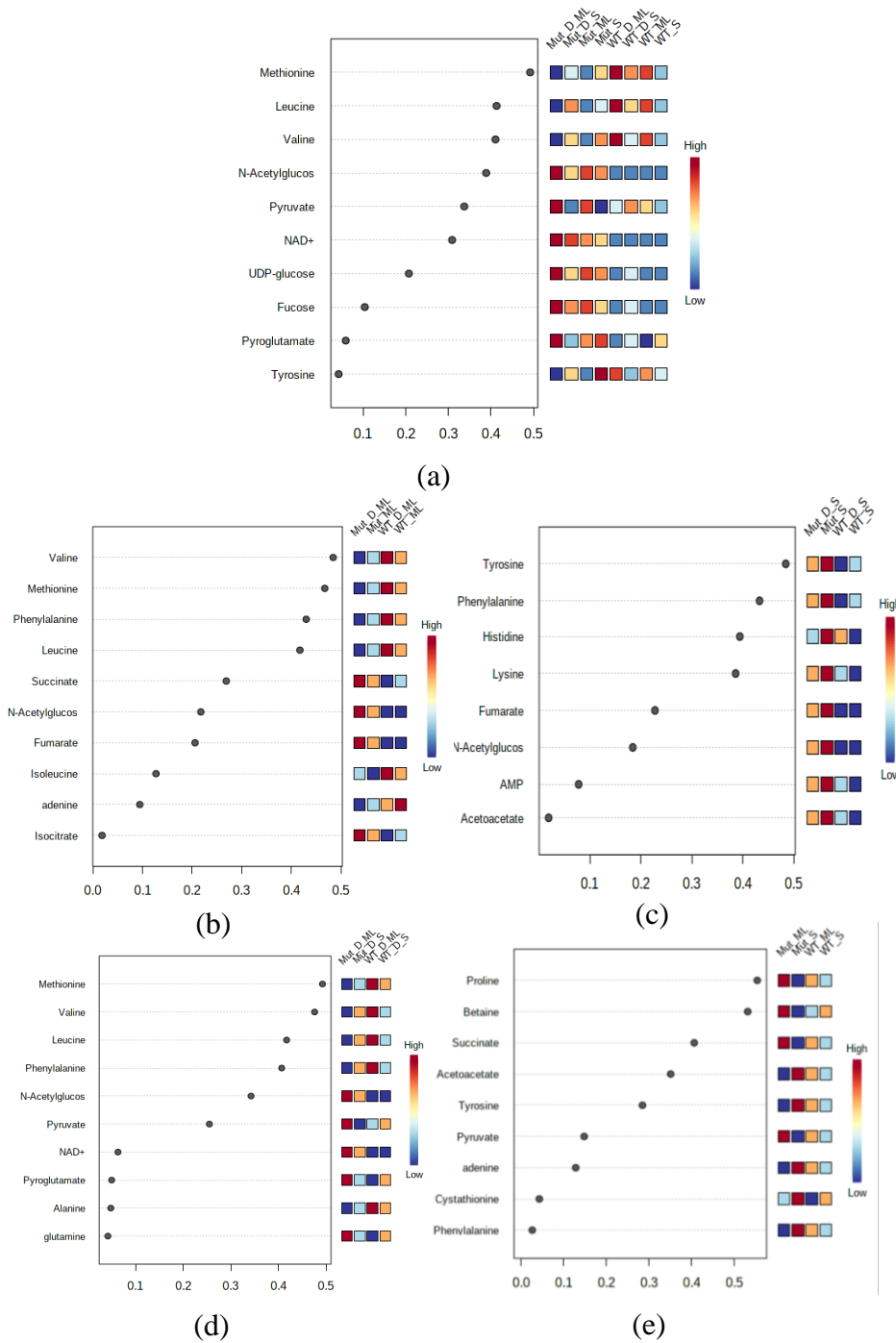


Figure B12. Very Important Features (VIP) scores obtained from the sPLS-DA which shows important metabolites in **a** all samples types **b** mid log samples **c** stationary phase samples **d** DABCOMD challenged samples **e** unchallenged samples

Table B2. Fold change of statistically significant metabolites in their corresponding metabolic pathways for the mid log phase of DABCOMD challenged mutant versus unchallenged wild type.

Mut D ML versus WT ML					
Indicated Pathway	Metabolite	Fold Change^{1,2}	Indicated Pathway	Metabolite	Fold Change^{1,2}
Citric Acid Cycle	Acetoacetate	-1.3	Alanine Metabolism	Uracil ⁴	-5.5 (VIP)
	Fumarate ³	+5.8		Nucleotide Metabolism	Adenine
	Isocitrate	+3.8	Uracil ⁴		-5.5 (VIP)
	NAD ⁺ ³	+37.0 (VIP)	Uridine		-3.9
Pyruvate Metabolism	Succinate	+1.8 (VIP)	Aminoacyl-tRNA Biosynthesis	Alanine ⁴	-1.6 (VIP)
	Formate	+20.8 (VIP)		AMP ³	+6.8
Peptidoglycan Synthesis	Pyruvate	+2.7		Aspartate ⁴	+1.6
	Alanine ⁴	-1.6 (VIP)		Glutamate ⁴	+2.0 (VIP)
	Cystathionine	+6.6		Glycine ⁴	-1.8
	Glutamate ⁴	+2.0 (VIP)		Histidine	+4.8
	Glycine ⁴	-1.8		Isoleucine	-4.5
	Lactate	+2.2		Leucine	-9.0 (VIP)
Methionine Metabolism	N-Acetylglucosamine ³	+94.2		Phenylalanine	-4.0 (VIP)
	Aspartate ⁴	+1.6		Tyrosine	-2.7
	Cysteine	+3.2	Valine	-9.2 (VIP)	
	Homocysteine	+5.1			
	Methionine	-4.5			

¹A positive fold change is indicative of a higher concentration in the mutant. ²The metabolites with VIP next to them were determined to be very important features by the PSL-DA. ³These metabolites had concentrations lower than 0.01 for the sample with the lowest concentration. ⁴These metabolites are shown in multiple pathways where a correlation was shown by Pattern Hunter.

Table B3. Fold change of statistically significant metabolites in their corresponding metabolic pathways for the stationary phase of DABCOMD challenged mutant versus unchallenged wild type.

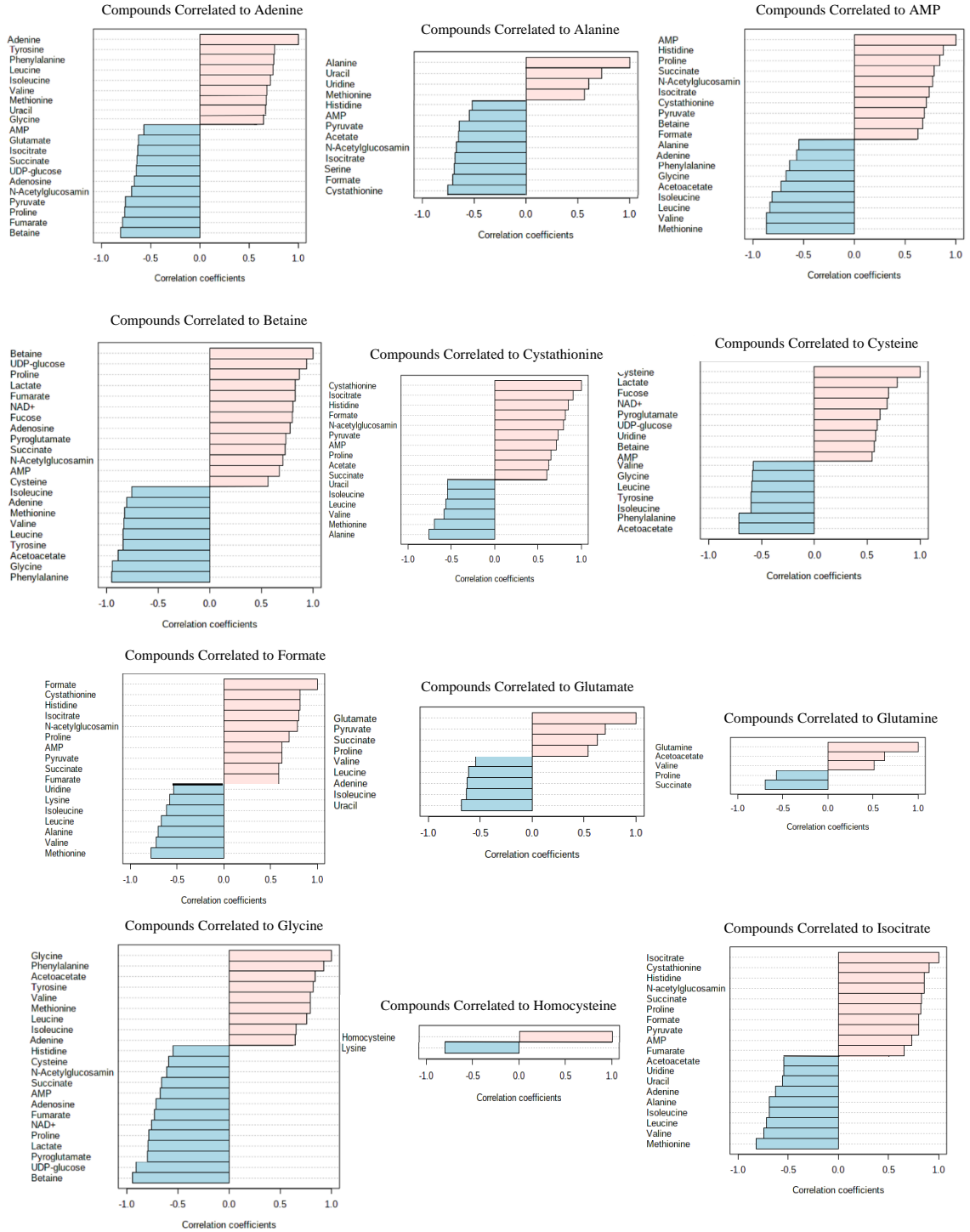
Mut D S versus WT S						
Indicated Pathway	Metabolite	Fold Change^{1,2}	Indicated Pathway	Metabolite	Fold Change^{1,2}	
Citric Acid Cycle	Fumarate ³	+ 3.6	Metabolism	Alanine	Uracil ⁴ - 3.9 (VIP)	
	NAD ⁺ ³	+ 13.5		Nucleotide Metabolism	Adenine	- 1.9 (VIP)
	Isocitrate ⁵	- 1.2			Uracil ⁴	- 3.9 (VIP)
	Succinate ⁵	+ 1.6				
Pyruvate Metabolism	Formate	+ 1.4 (VIP)	Aminoacyl-tRNA Biosynthesis	Alanine ⁴	+ 1.4 (VIP)	
				Aspartate ⁴	+ 2.2 (VIP)	
Peptidoglycan Synthesis	Alanine ⁴	+ 1.4 (VIP)		Glutamate ^{4,5}	+ 1.5 (VIP)	
	Glutamate ^{4,5}	+ 1.5 (VIP)		Glycine ⁴	+ 2.2	
	Glycine ⁴	+ 2.2 (VIP)		Histidine ³	+ 6.4	
	Lactate	+ 2.6 (VIP)		Leucine	+ 2.6 (VIP)	
	Lysine	+ 1.5		Phenylalanine	+ 1.4 (VIP)	
Methionine Metabolism	N-Acetylglucosamine ³	+ 19.4		Proline	- 1.4 (VIP)	
	Aspartate ⁴	+ 2.2 (VIP)		Valine	+ 3.1 (VIP)	
	Serine	- 1.9 (VIP)				

¹A positive fold change is indicative of a higher concentration in the mutant. ²The metabolites with VIP next to them were determined to be very important features by the PSL-DA. ³These metabolites had concentrations lower than 0.01 for the sample with the lowest concentration. ⁴These metabolites are shown in multiple pathways where a correlation was shown by Pattern Hunter. ⁵These metabolites do not have significant p-values, but they are VIPs.

Challenged Mutant versus Unchallenged Wild Types Comparisons: Tables B2 and B3

When comparing challenged mutant mid log (Mut D ML) to unchallenged wild type (WT) ML, comparisons of Mut to WT and challenged to unchallenged are effectively being concurrently evaluated. This unsurprisingly leads to many observable differences in the concentrations of metabolites in energy production, aminoacyl-tRNA biosynthesis, peptidoglycan synthesis and related pathways. For example, the challenged mutant samples had higher concentrations of energy related metabolites, except for acetoacetate which was lower. It is particularly interesting

that isocitrate was 3.8-fold higher and formate was 20.8-fold higher in the mutant samples. The challenged Mut samples had a 37-fold increase in NAD⁺ and a 6.8-fold increase in AMP when compared to the unchallenged WT. N-acetylglucosamine had a 94.2-fold increase in the challenged Mut samples when compared to the unchallenged WT samples. Aspartate correlated to cysteine, homocysteine, methionine, and cystathionine. Nucleotide metabolism components in the mid log phase had a decreased concentration in the challenged mutant samples, and multiple components of aminoacyl-tRNA biosynthesis changed. When comparing Mut D S to WT S, the same types of pathways changed as with the mid log phase, although the fold change differences were not as large. N-acetylglucosamine, lysine, lactate, glycine, glutamate (VIP) and alanine (VIP), all components of peptidoglycan synthesis, were in higher concentration in the challenged mutant stationary phase, in comparison to the unchallenged wild type stationary phase.



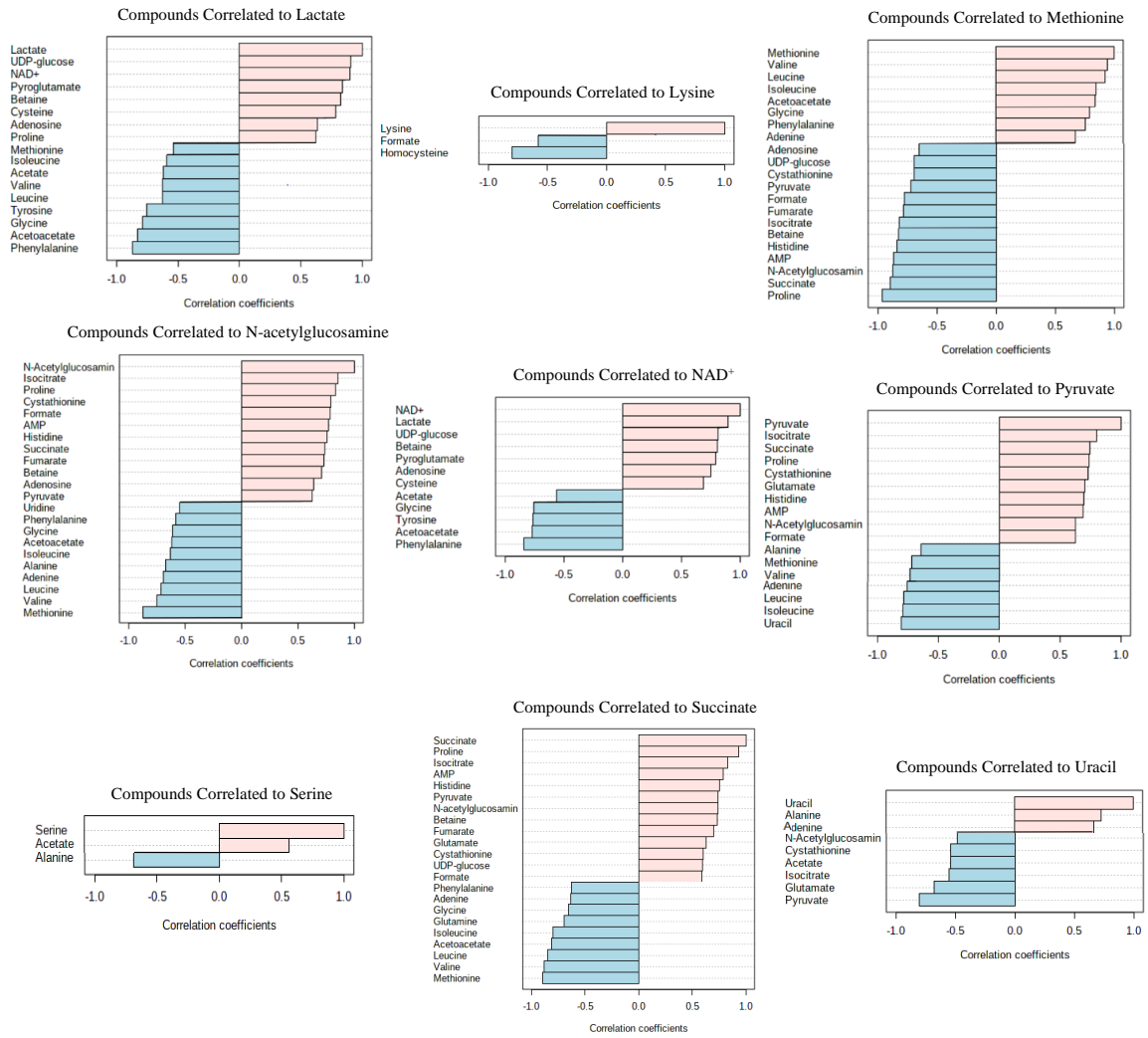
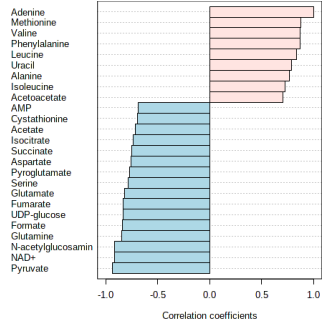
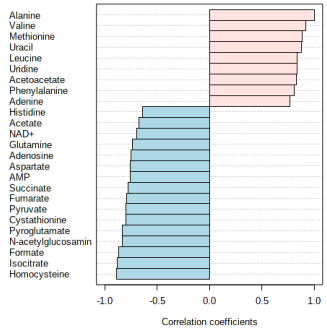


Figure B13. Pattern Hunter Correlations between Metabolites Observed in the Mid Log Phase Comparison of Unchallenged Mutant and Unchallenged Wild Type Samples.

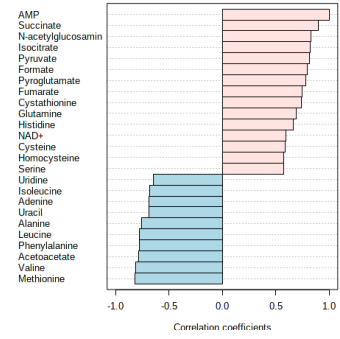
Compounds Correlated to Adenine



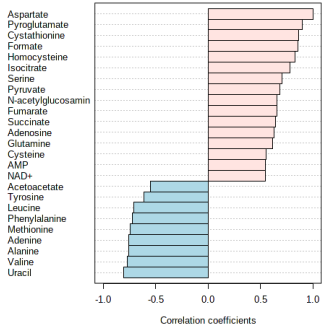
Compounds Correlated to Alanine



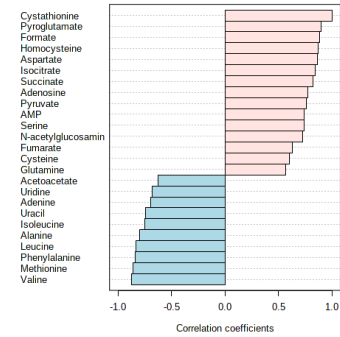
Compounds Correlated to AMP



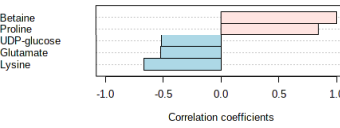
Compounds Correlated to Aspartate



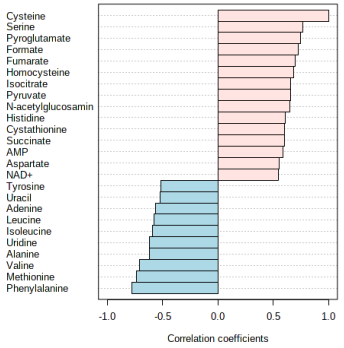
Compounds Correlated to Cystathionine



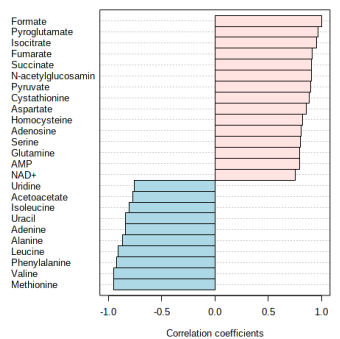
Compounds Correlated to Betaine



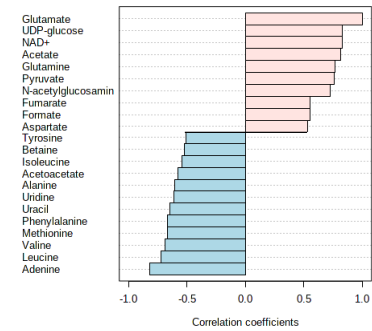
Compounds Correlated to Cysteine



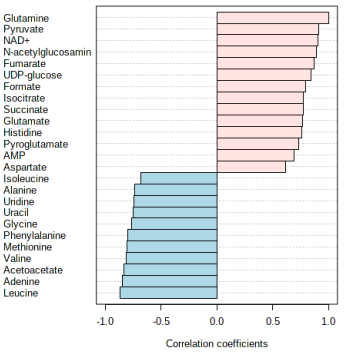
Compounds Correlated to Formate



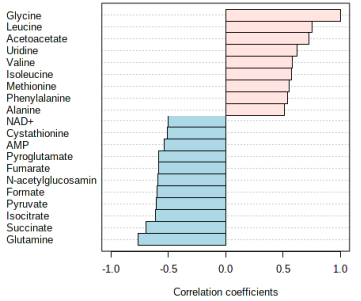
Compounds Correlated to Glutamate



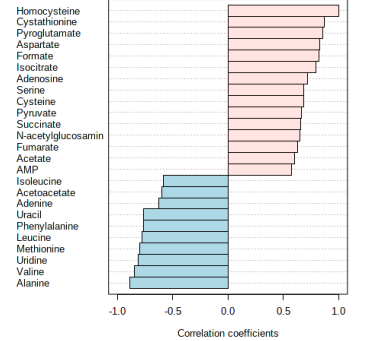
Compounds Correlated to Glutamine



Compounds Correlated to Glycine



Compounds Correlated to Homocysteine



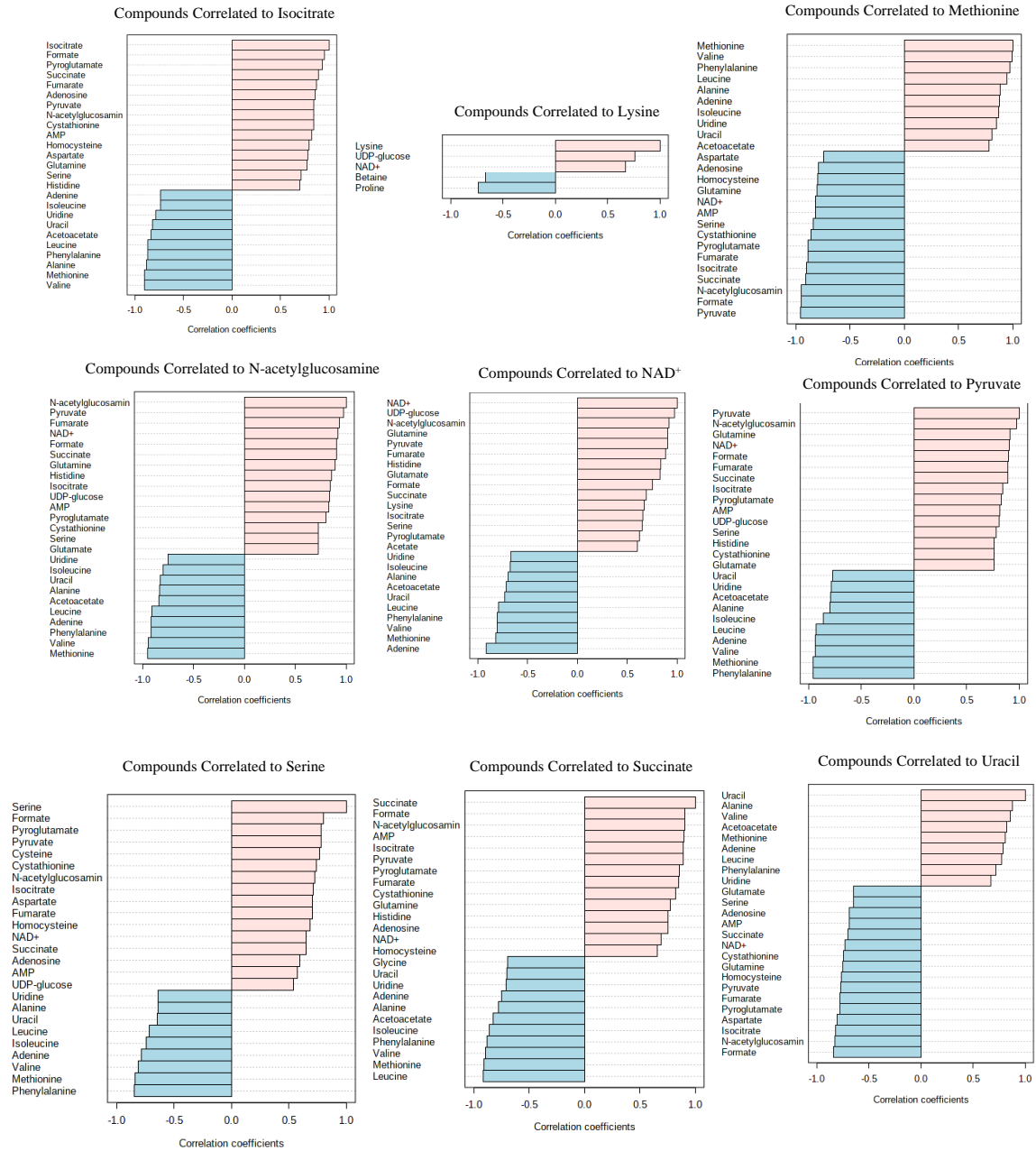


Figure B14. Pattern Hunter Correlations between Metabolites Observed in the Mid Log Phase Comparison of Challenged Mutant and Challenged Wild Type Samples.

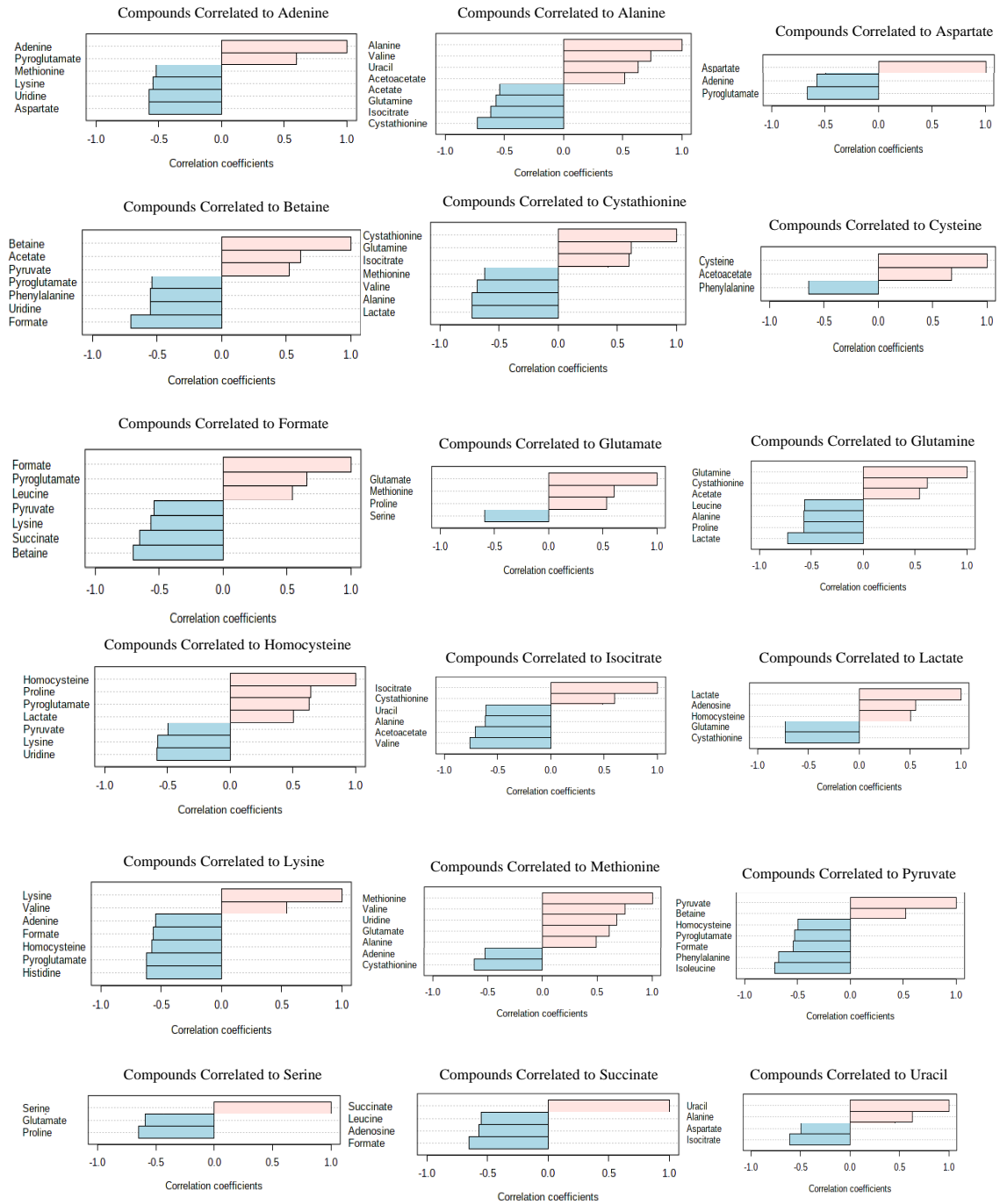
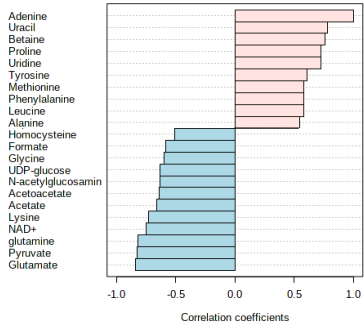
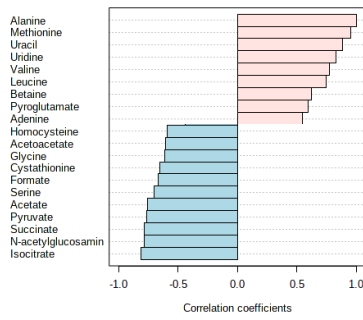


Figure B15. Pattern Hunter Correlations between Metabolites Observed in the Mid Log Phase Comparison of Challenged Wild Type and Unchallenged Wild Type Samples.

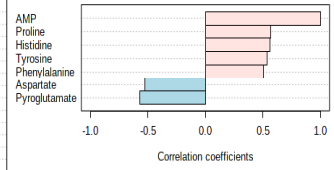
Compounds Correlated to Adenine



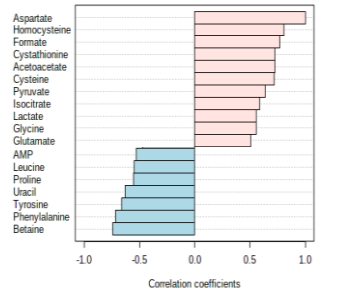
Compounds Correlated to Alanine



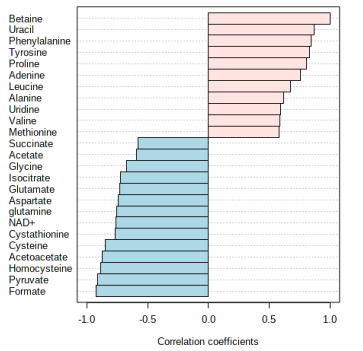
Compounds Correlated to AMP



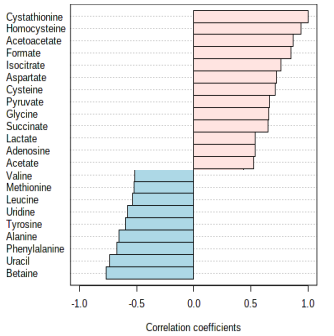
Compounds Correlated to Aspartate



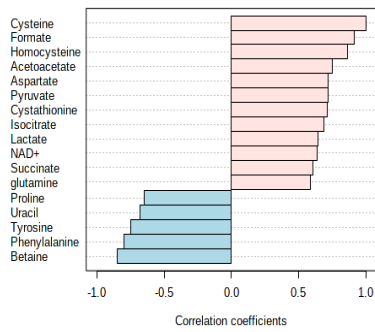
Compounds Correlated to Betaine



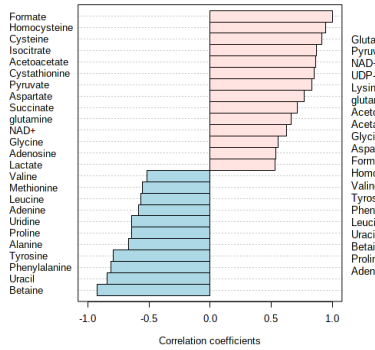
Compounds Correlated to Cystathionine



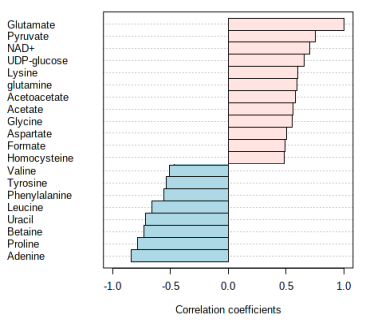
Compounds Correlated to Cysteine



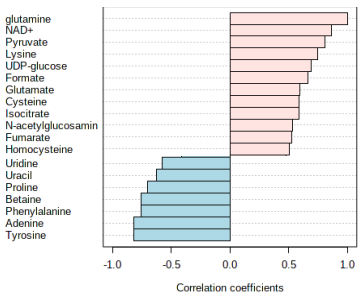
Compounds Correlated to Formate



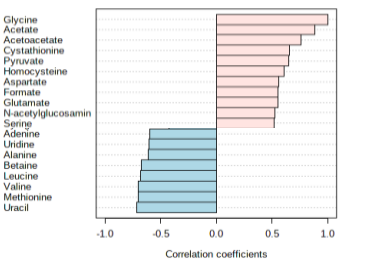
Compounds Correlated to Glutamate



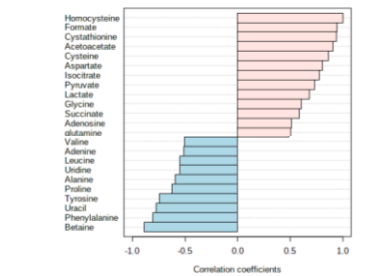
Compounds Correlated to Glutamine



Compounds Correlated to Glycine



Compounds Correlated to Homocysteine



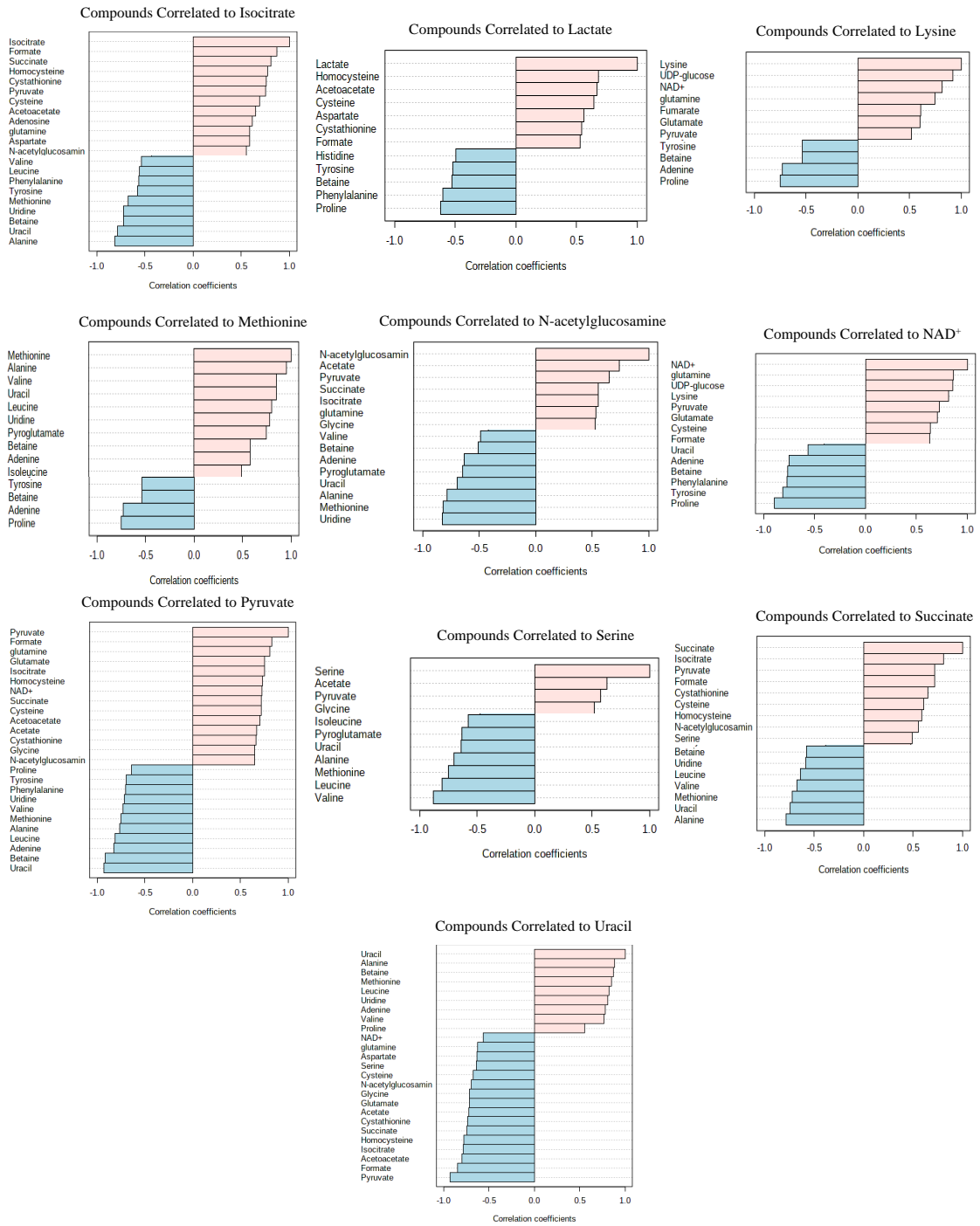
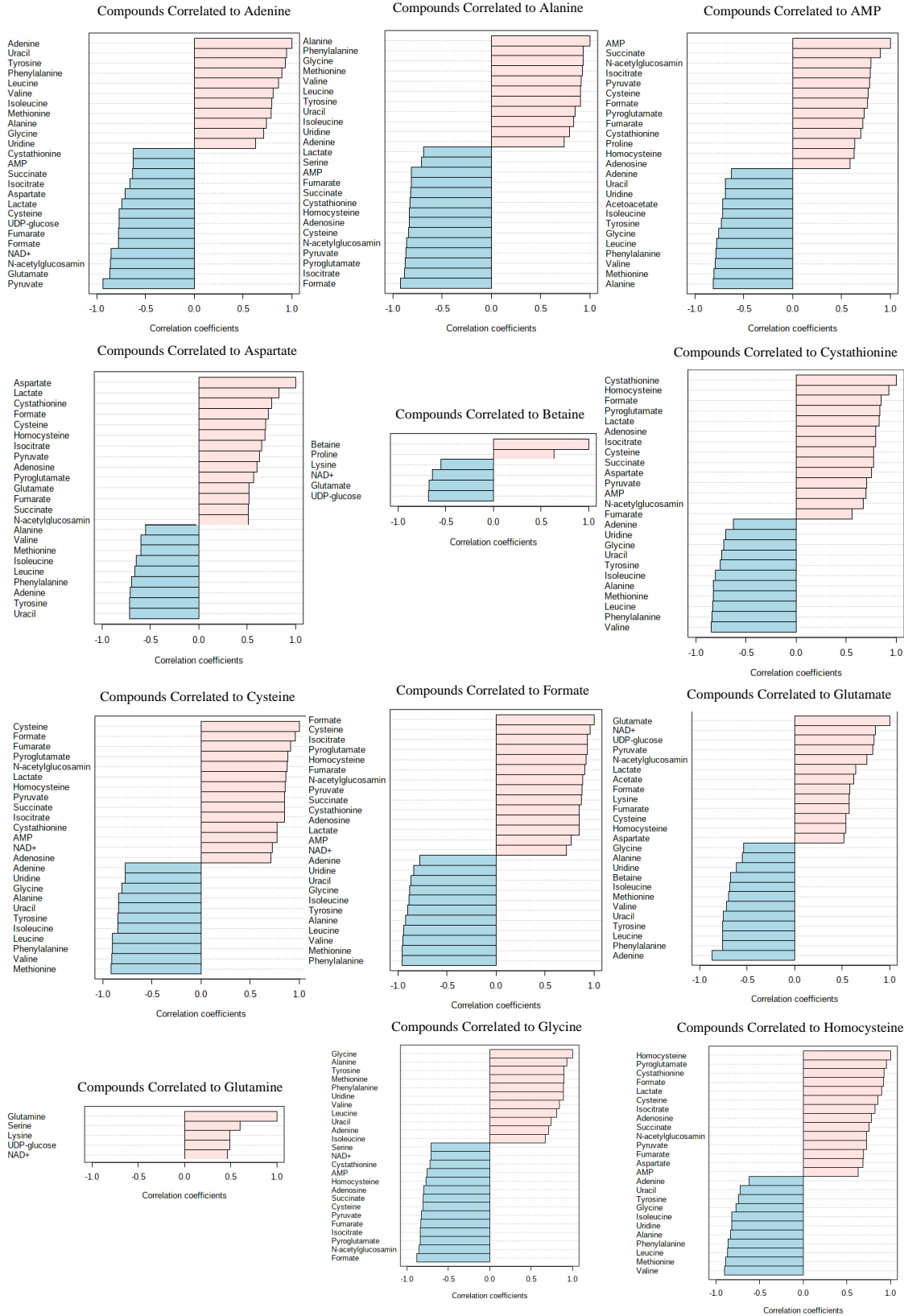


Figure B16. Pattern Hunter Correlations between Metabolites Observed in the Mid Log Phase Comparison of Challenged Mutant and Unchallenged Mutant Samples.



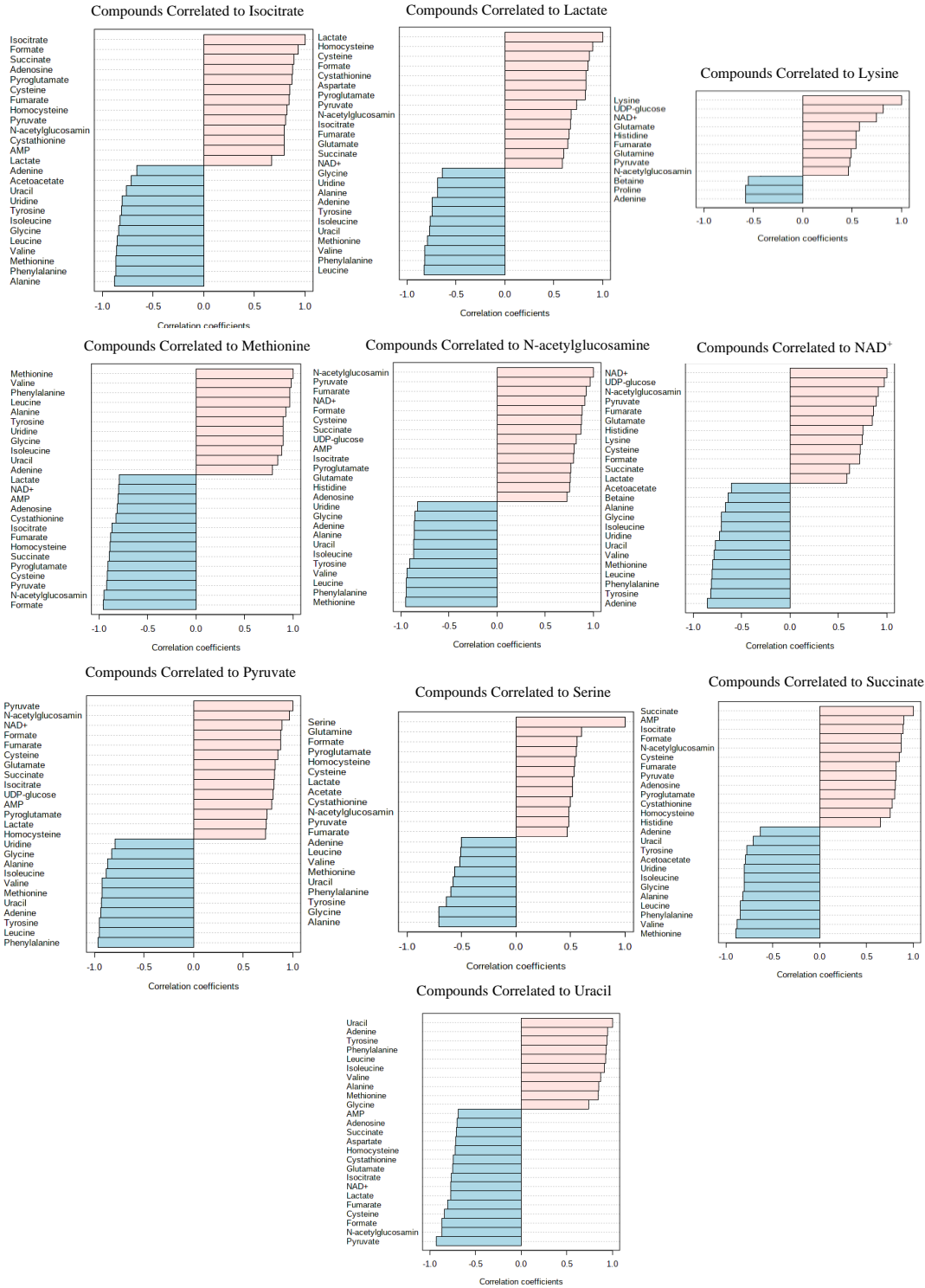
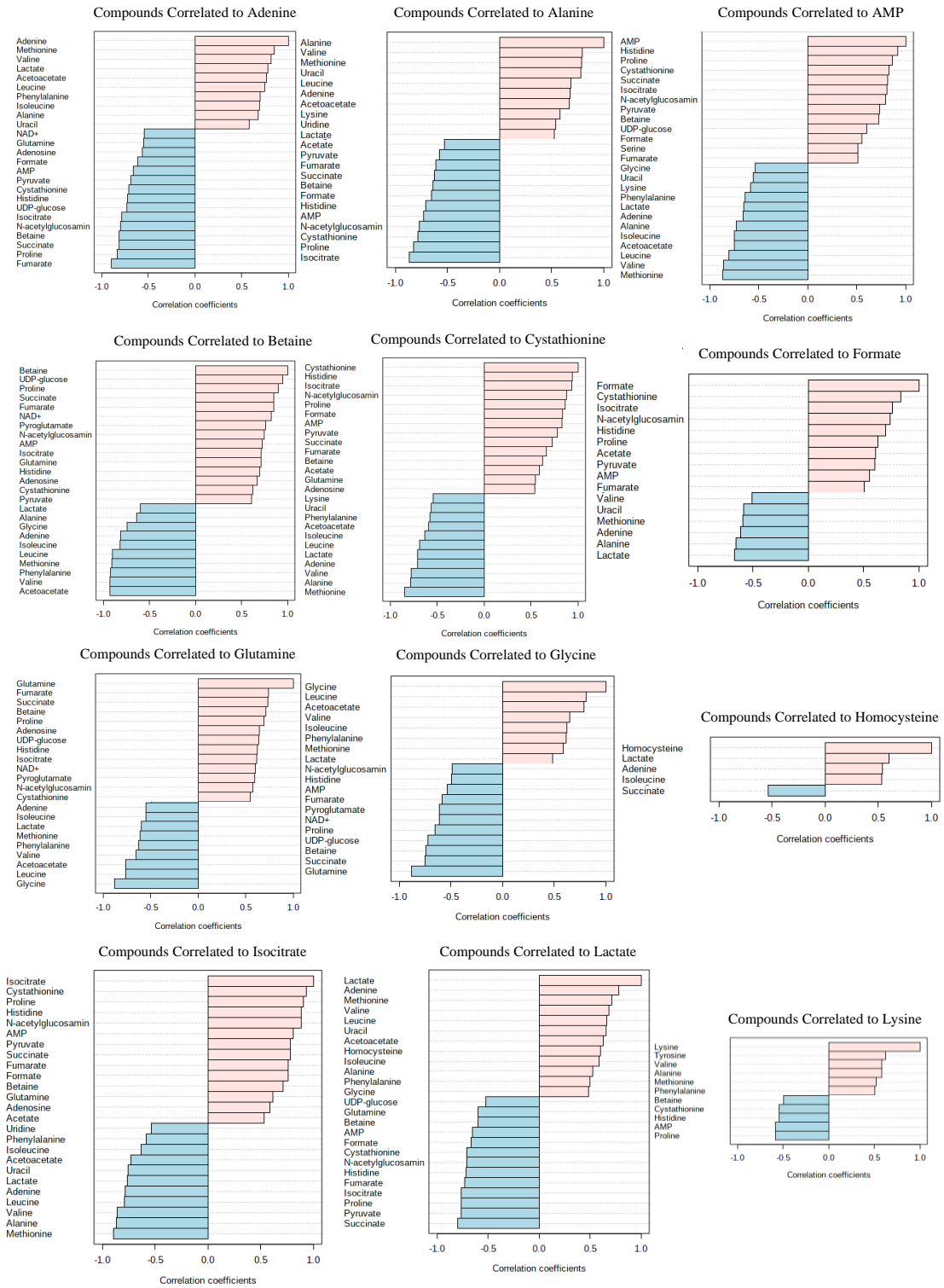


Figure B17. Pattern Hunter Correlations between Metabolites Observed in the Mid Log Phase Comparison of Challenged Mutant and Unchallenged Wild Type Samples.



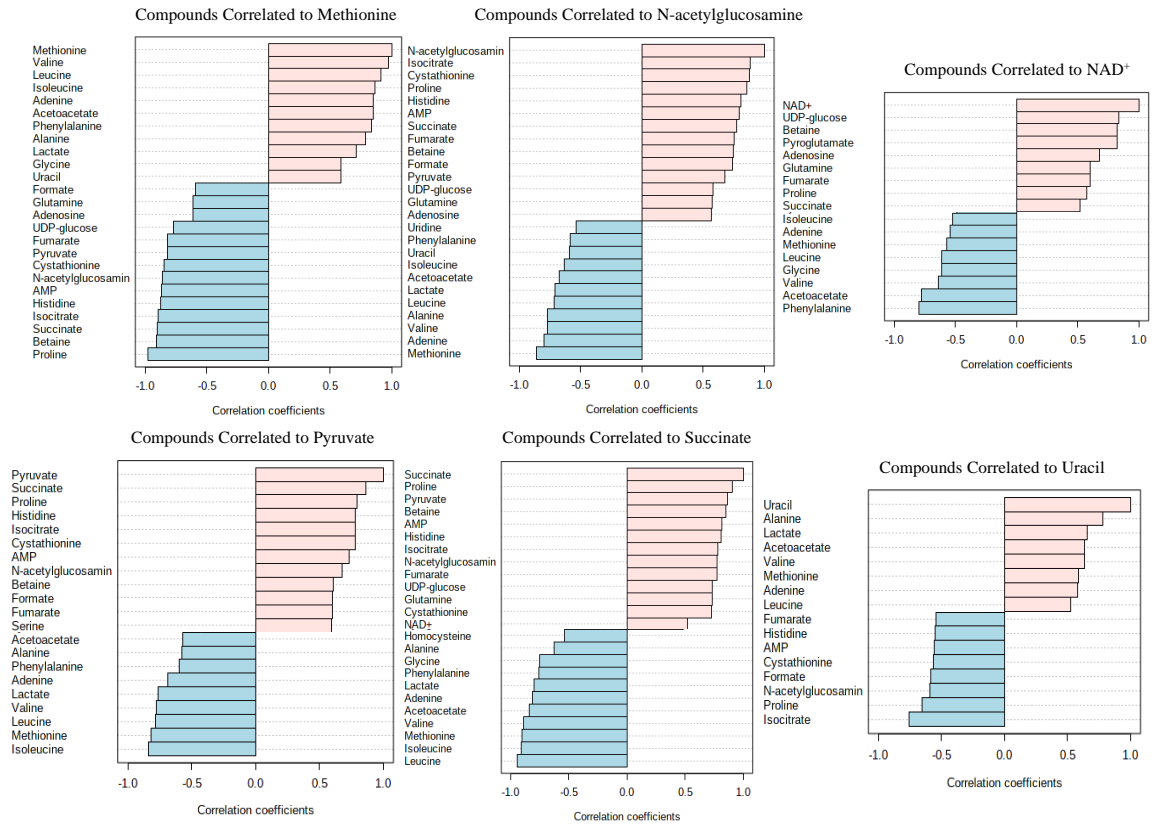


Figure B18. Pattern Hunter Correlations between Metabolites Observed in the Mid Log Phase Comparison of Unchallenged Mutant and Challenged Wild Type Samples.

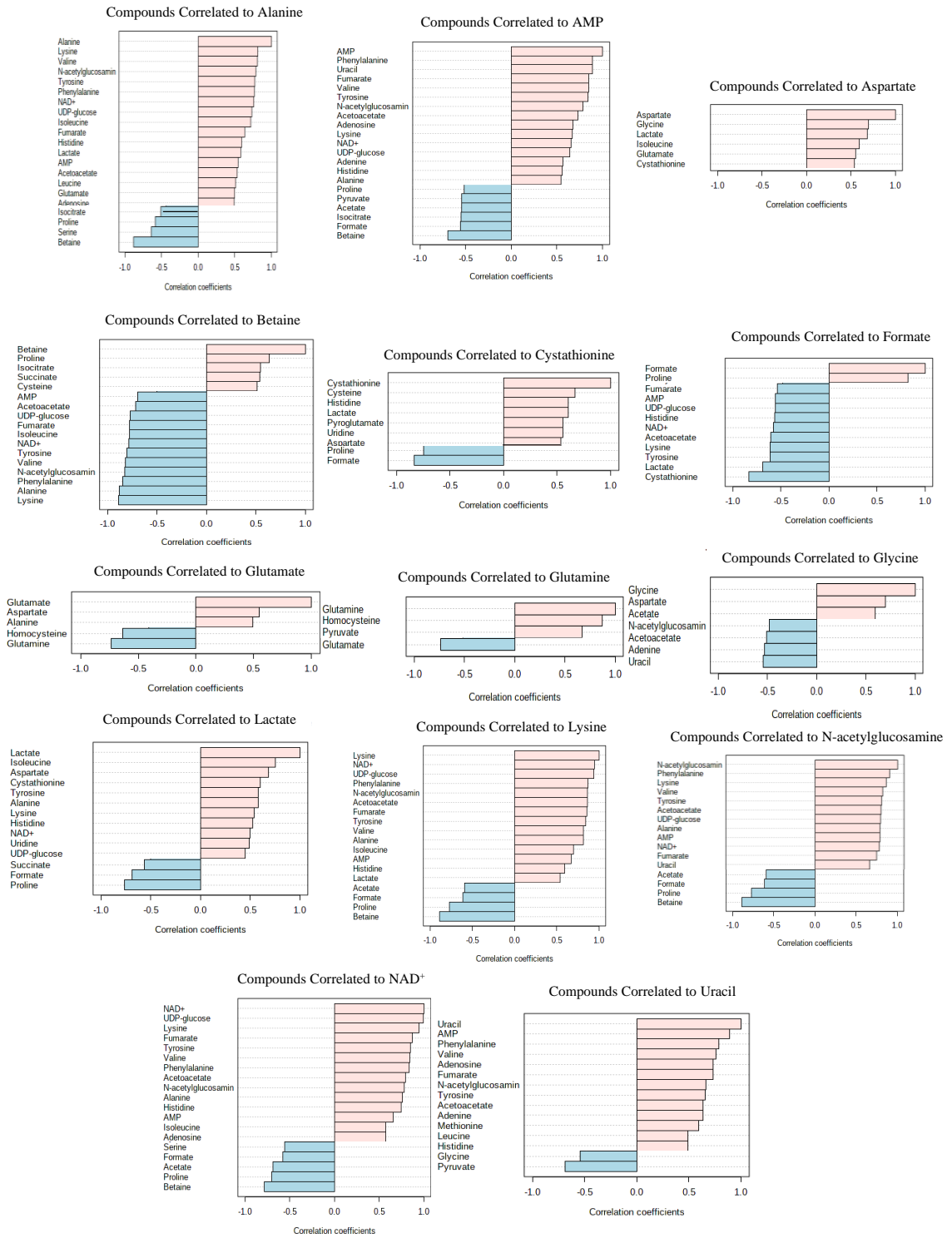


Figure B19. Pattern Hunter Correlations between Metabolites Observed in the Stationary Phase Comparison of Unchallenged Mutant and Unchallenged Wild Type Samples.

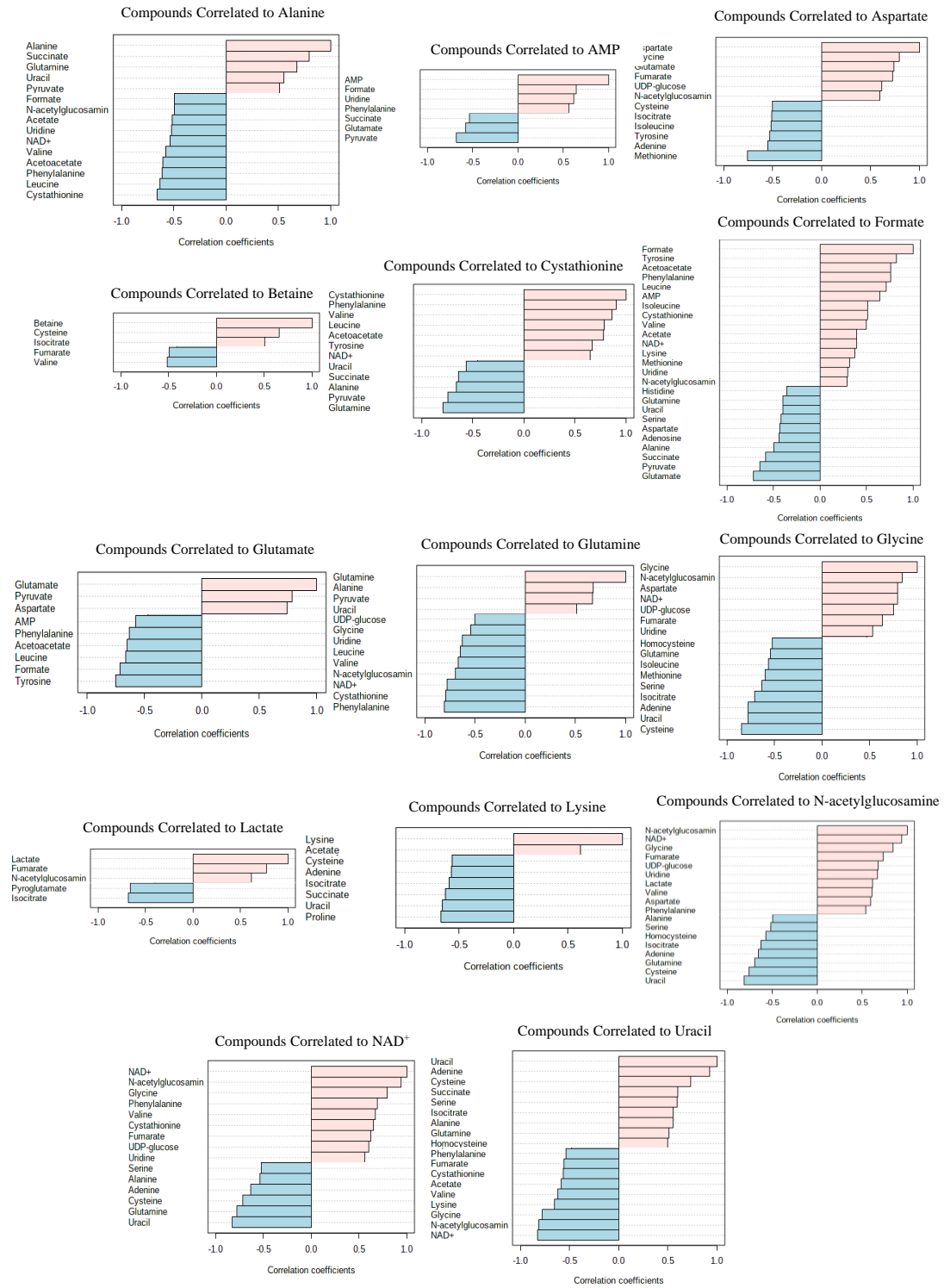


Figure B20. Pattern Hunter Correlations between Metabolites Observed in the Stationary Phase Comparison of Challenged Mutant and Challenged Wild Type Samples.

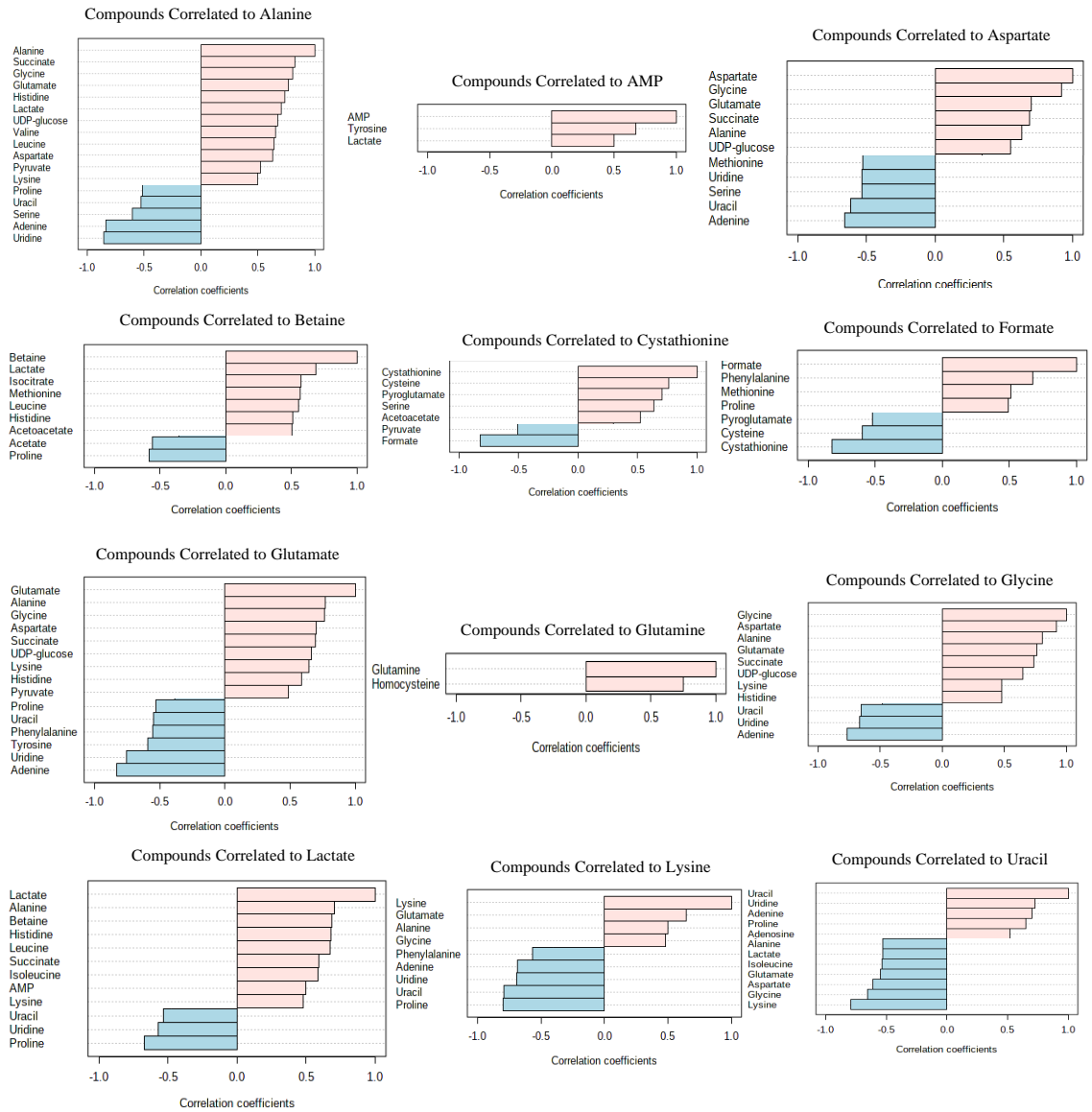


Figure B21. Pattern Hunter Correlations between Metabolites Observed in the Stationary Phase Comparison of Challenged and Unchallenged Wild Type Samples.

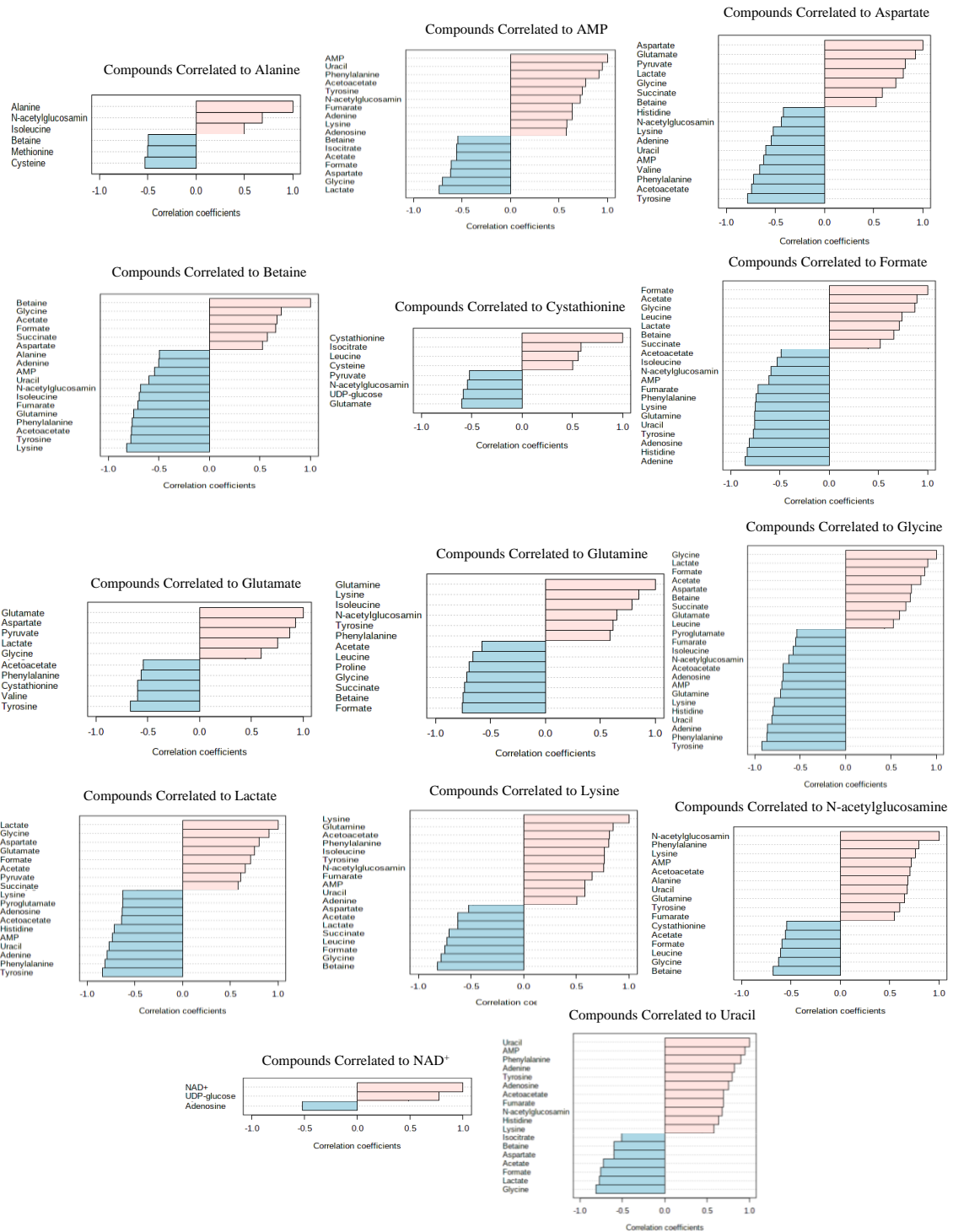


Figure B22. Pattern Hunter Correlations between Metabolites Observed in the Stationary Phase Comparison of Challenged and Unchallenged Mutant Samples.

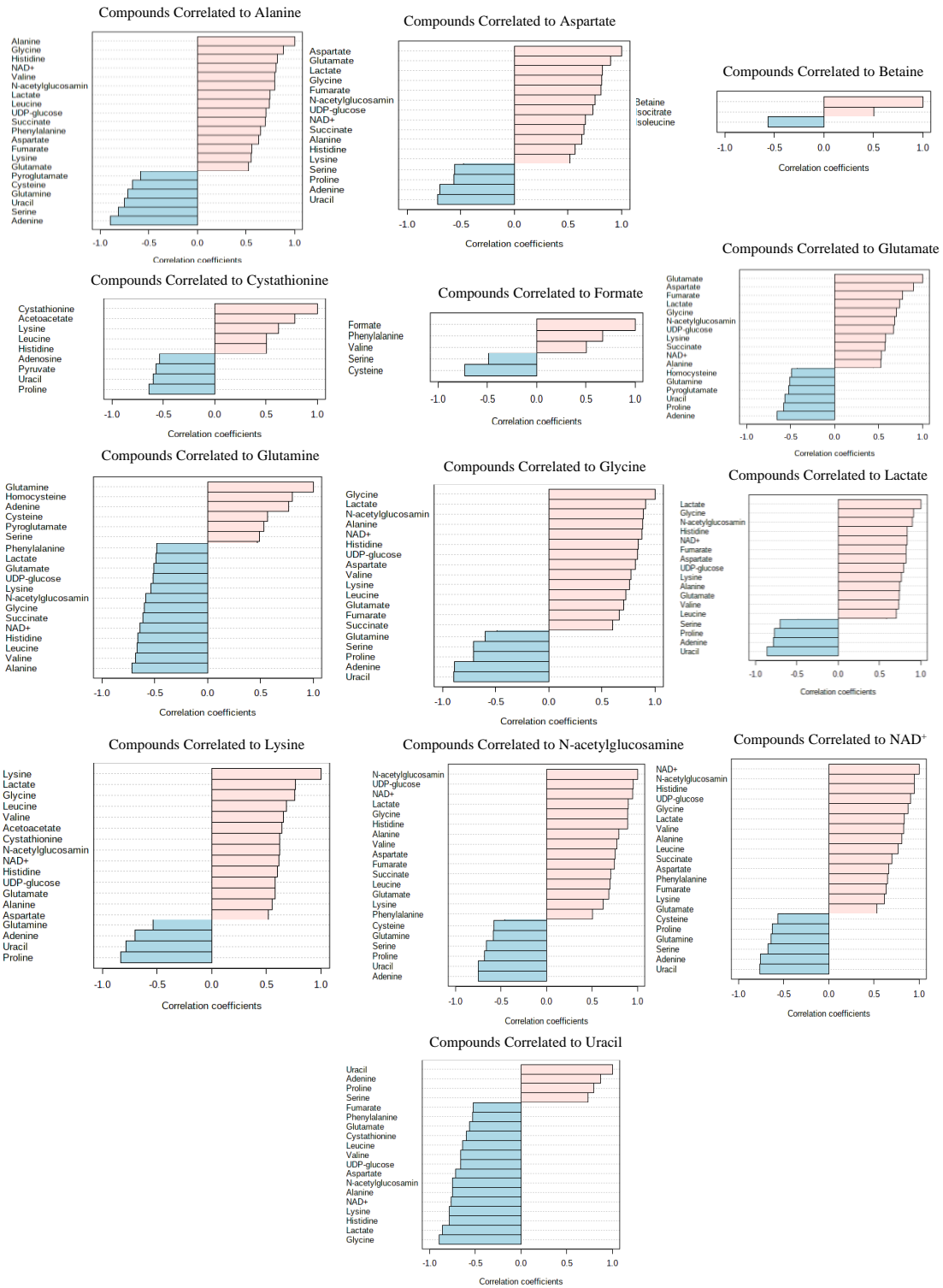


Figure B23. Pattern Hunter Correlations between Metabolites Observed in the Stationary Phase Comparison of Challenged Mutant and Unchallenged Wild Type Samples.

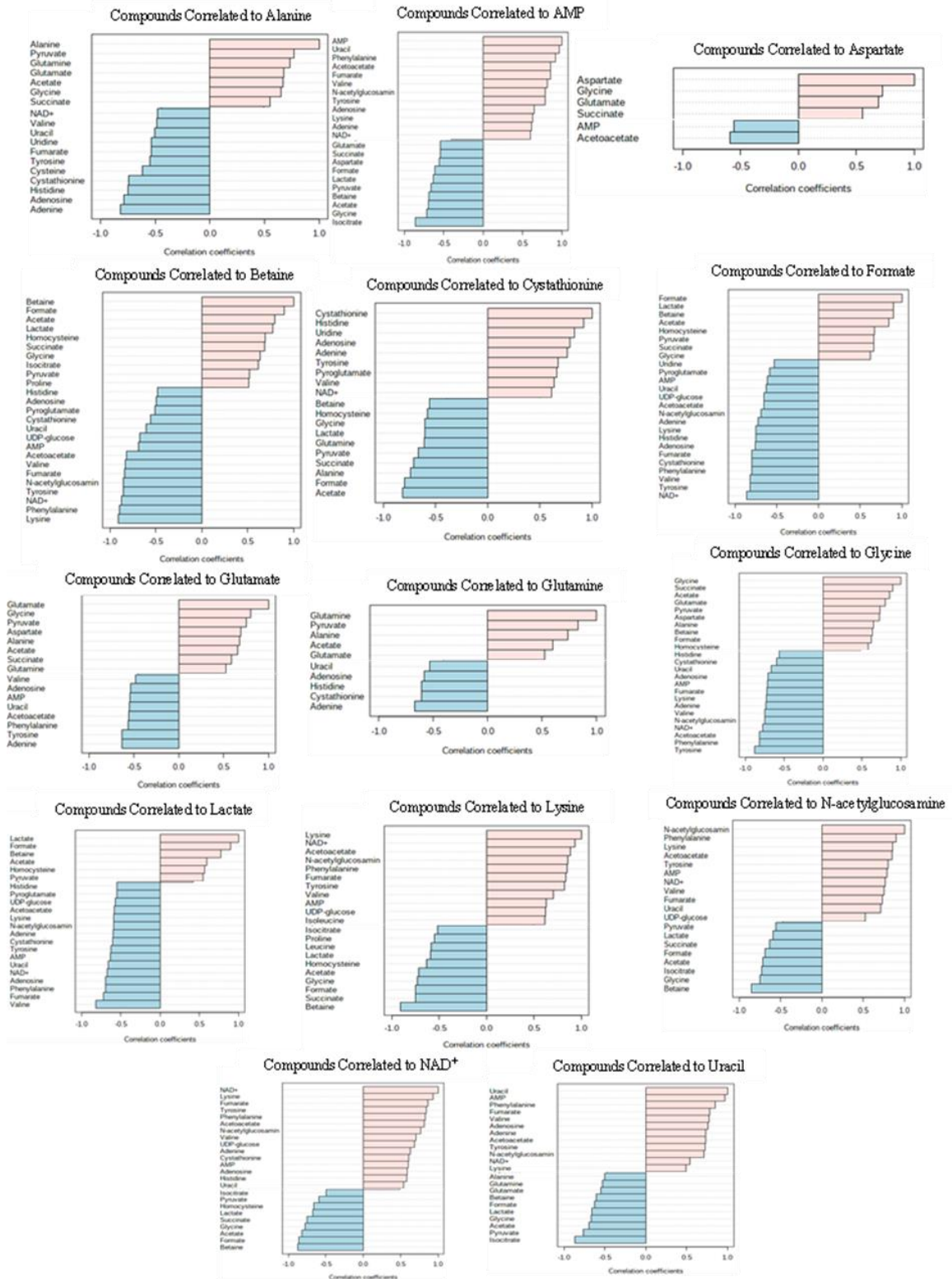


Figure B24. Pattern Hunter Correlations between Metabolites Observed in the Stationary Phase Comparison of Challenged Wild Type and Unchallenged Mutant Samples.

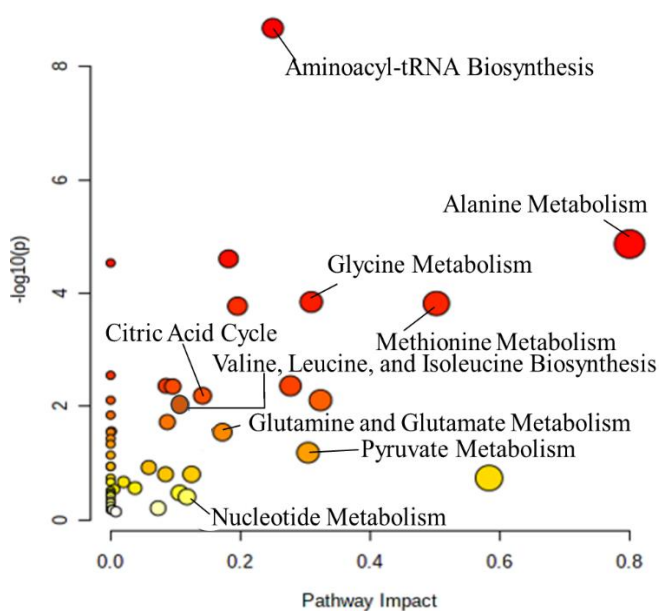


Figure B25. Top Impacted Pathways for Mid Log Phase Comparison of Unchallenged Mutant and Unchallenged Wild Type Samples. The larger and darker the circles are, the larger the impact the significant metabolites have on the listed pathway.

Table B2. The Identification Number Corresponding to Pathways Found in Pathway Analysis for Figures B26 – B36.

Identity Number	Pathways
1	Aminoacyl-tRNA Biosynthesis
2	Alanine Metabolism
3	Methionine Metabolism
4	Glycine Metabolism
5	Nucleotide Metabolism
6	Glutamine and Glutamate Metabolism
7	Valine, Leucine, and Isoleucine Biosynthesis
8	Acetyl-CoA Biosynthesis
9	Pyruvate Metabolism
10	Citric Acid Cycle

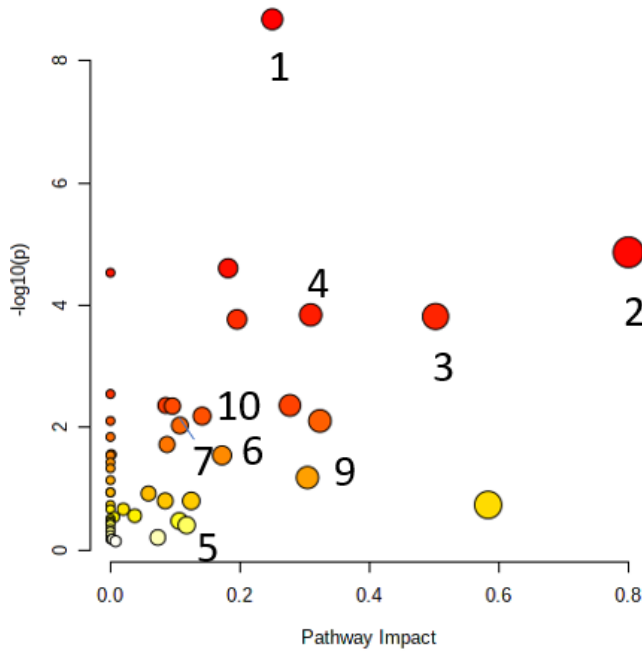


Figure B26. Top Impacted Pathways for Mid Log Phase Comparison of Challenged Mutant and Challenged Wild Type Samples. The larger and darker the circles are, the larger the impact the significant metabolites have on the listed pathway.

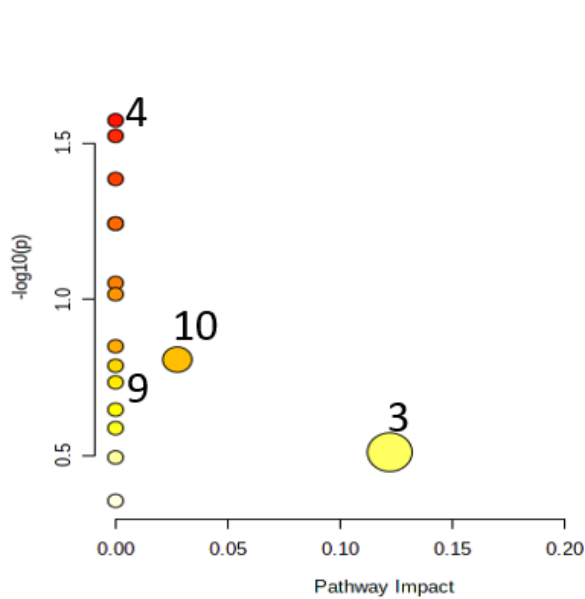


Figure B27. Top Impacted Pathways for Mid Log Phase Comparison of Challenged and Unchallenged Wild Type Samples. The larger and darker the circles are, the larger the impact the significant metabolites have on the listed pathway.

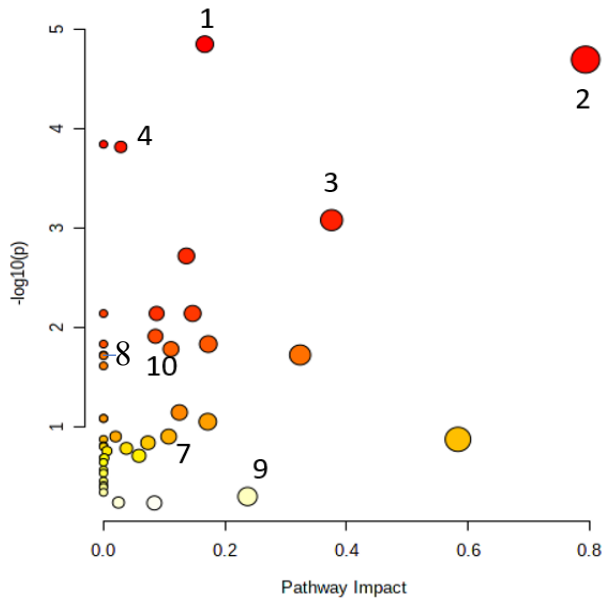


Figure B28. Top Impacted Pathways for Mid Log Phase Comparison of Challenged and Unchallenged Mutant Samples. The larger and darker the circles are, the larger the impact the significant metabolites have on the listed pathway.

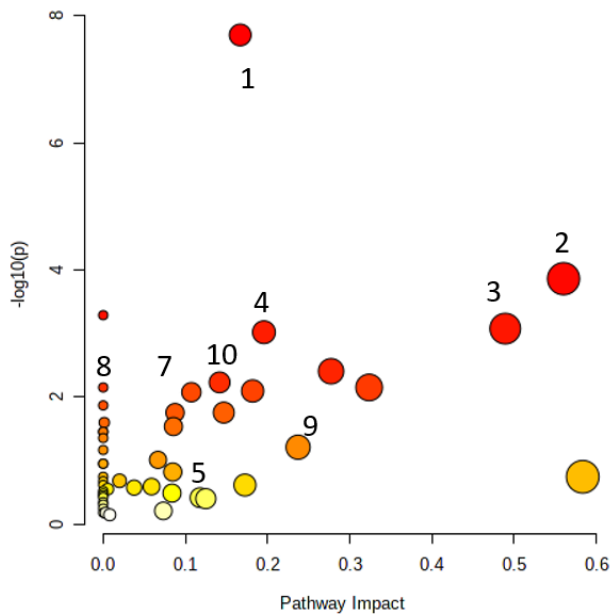


Figure B29. Top Impacted Pathways for Mid Log Phase Comparison of Challenged Mutant and Unchallenged Wild Type Samples. The larger and darker the circles are, the larger the impact the significant metabolites have on the listed pathway.

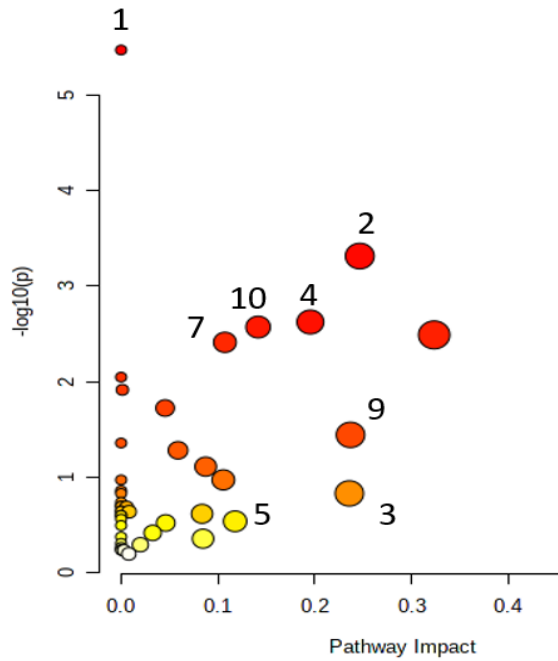


Figure B30. Top Impacted Pathways for Mid Log Phase Comparison of Challenged Wild Type and Unchallenged Mutant Samples. The larger and darker the circles are, the larger the impact the significant metabolites have on the listed pathway.

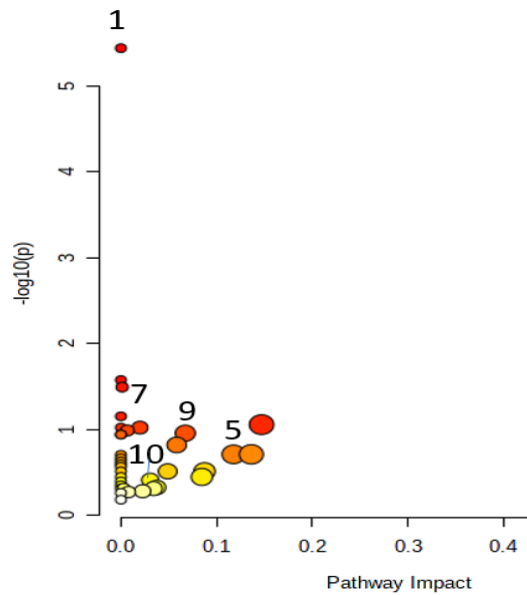


Figure B31. Top Impacted Pathways for Stationary Phase Comparison of Unchallenged Mutant and Unchallenged Wild Type Samples. The larger and darker the circles are, the larger the impact the significant metabolites have on the listed pathway.

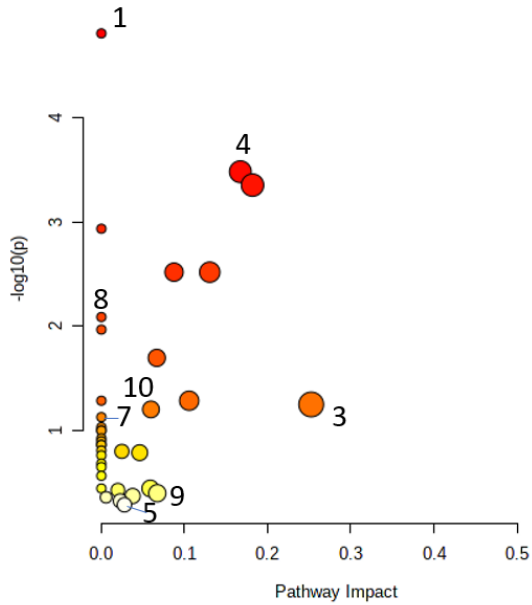


Figure B32. Top Impacted Pathways for Stationary Phase Comparison of Challenged Mutant and Challenged Wild Type Samples. The larger and darker the circles are, the larger the impact the significant metabolites have on the listed pathway.

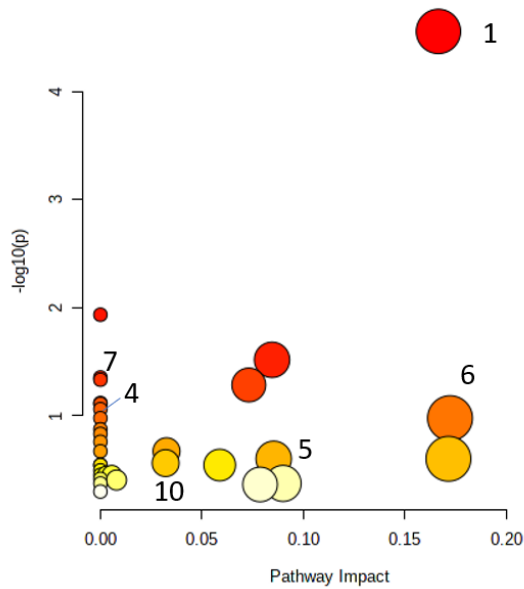


Figure B33. Top Impacted Pathways for Stationary Phase Comparison of Challenged and Unchallenged Wild Type Samples. The larger and darker the circles are, the larger the impact the significant metabolites have on the listed pathway.

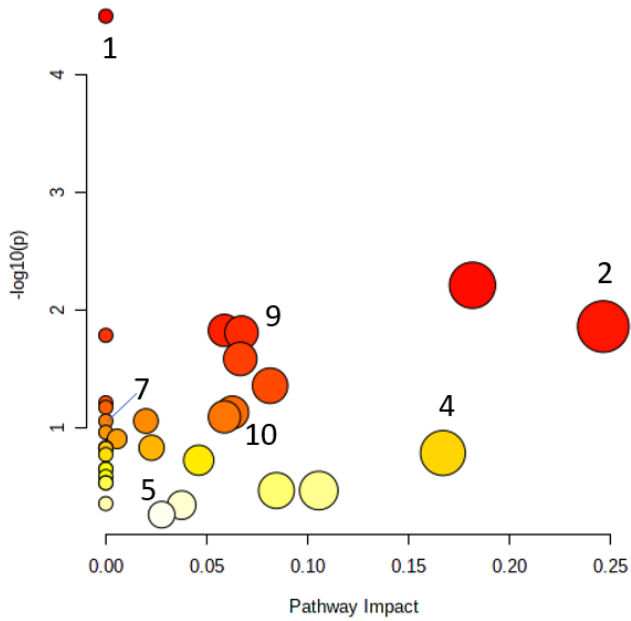


Figure B34. Top Impacted Pathways for Stationary Phase Comparison of Challenged and Unchallenged Mutant Samples. The larger and darker the circles are, the larger the impact the significant metabolites have on the listed pathway.

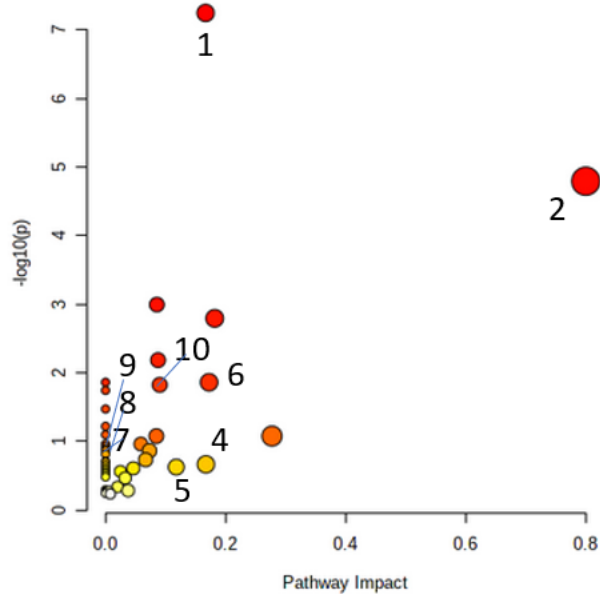


Figure B35. Top Impacted Pathways for Stationary Phase Comparison of Challenged Mutant and Unchallenged Wild Type Samples. The larger and darker the circles are, the larger the impact the significant metabolites have on the listed pathway.

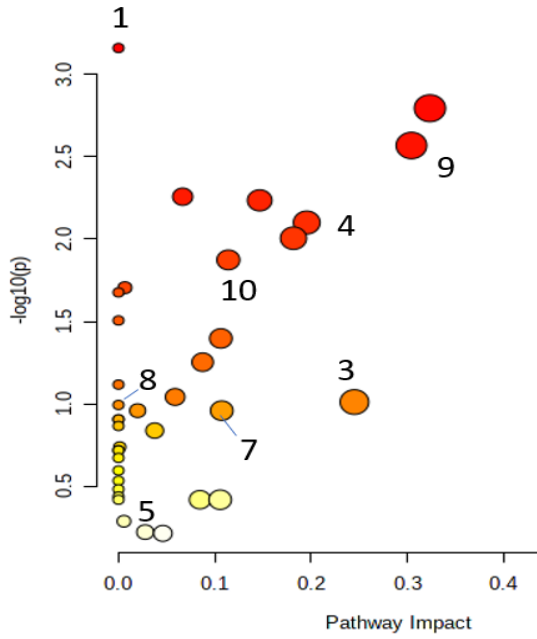
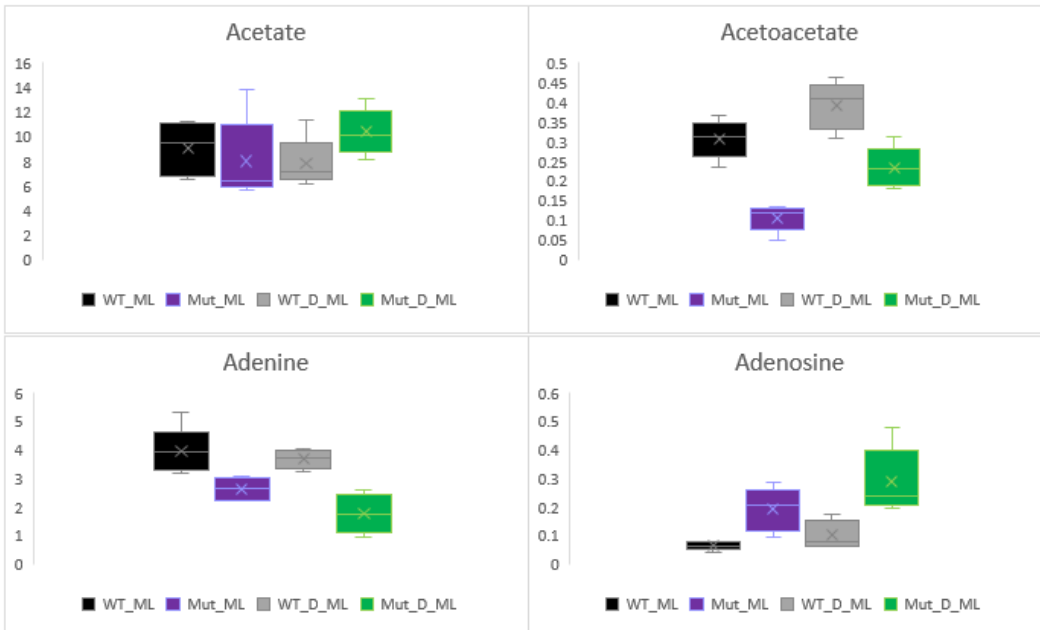
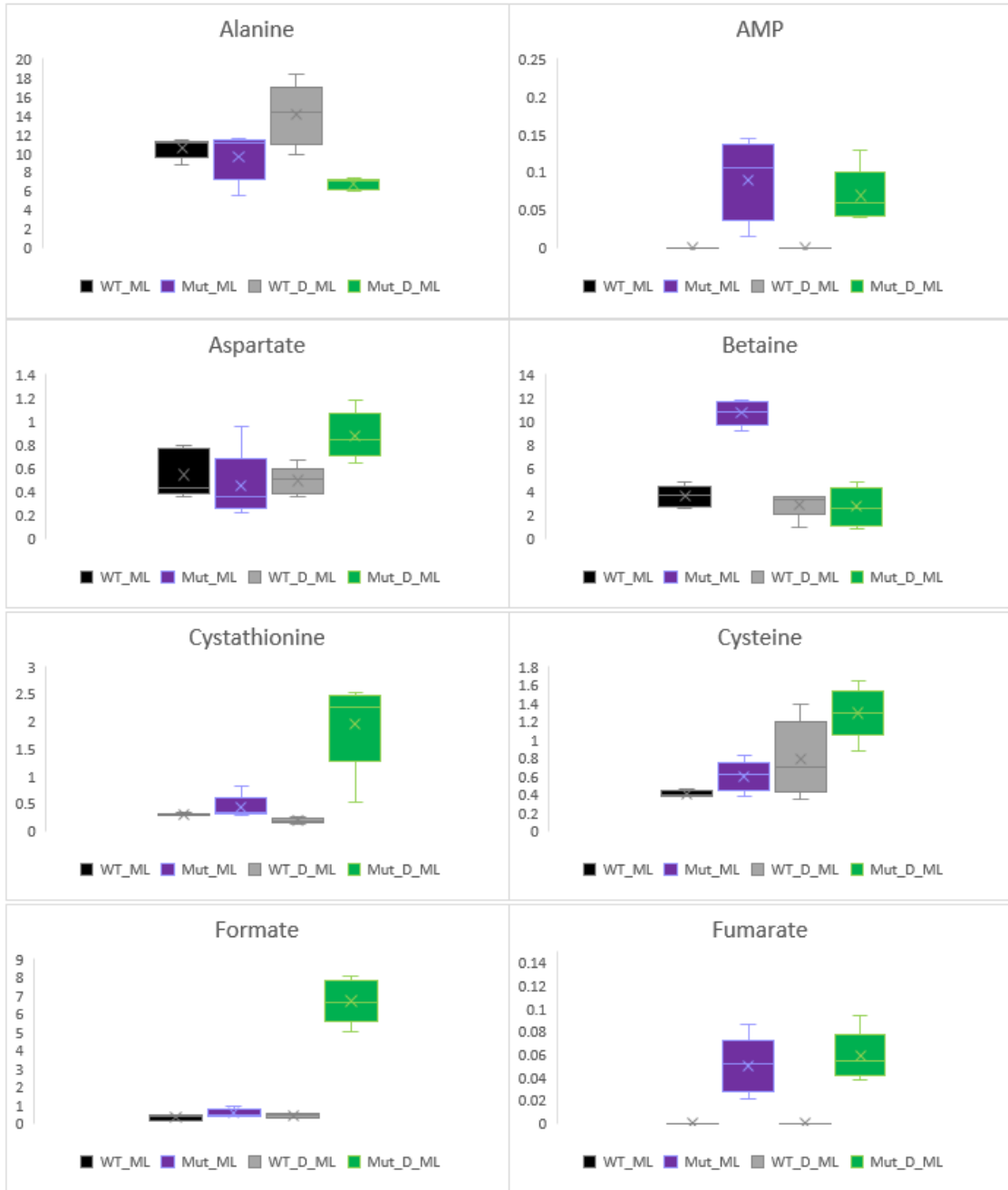
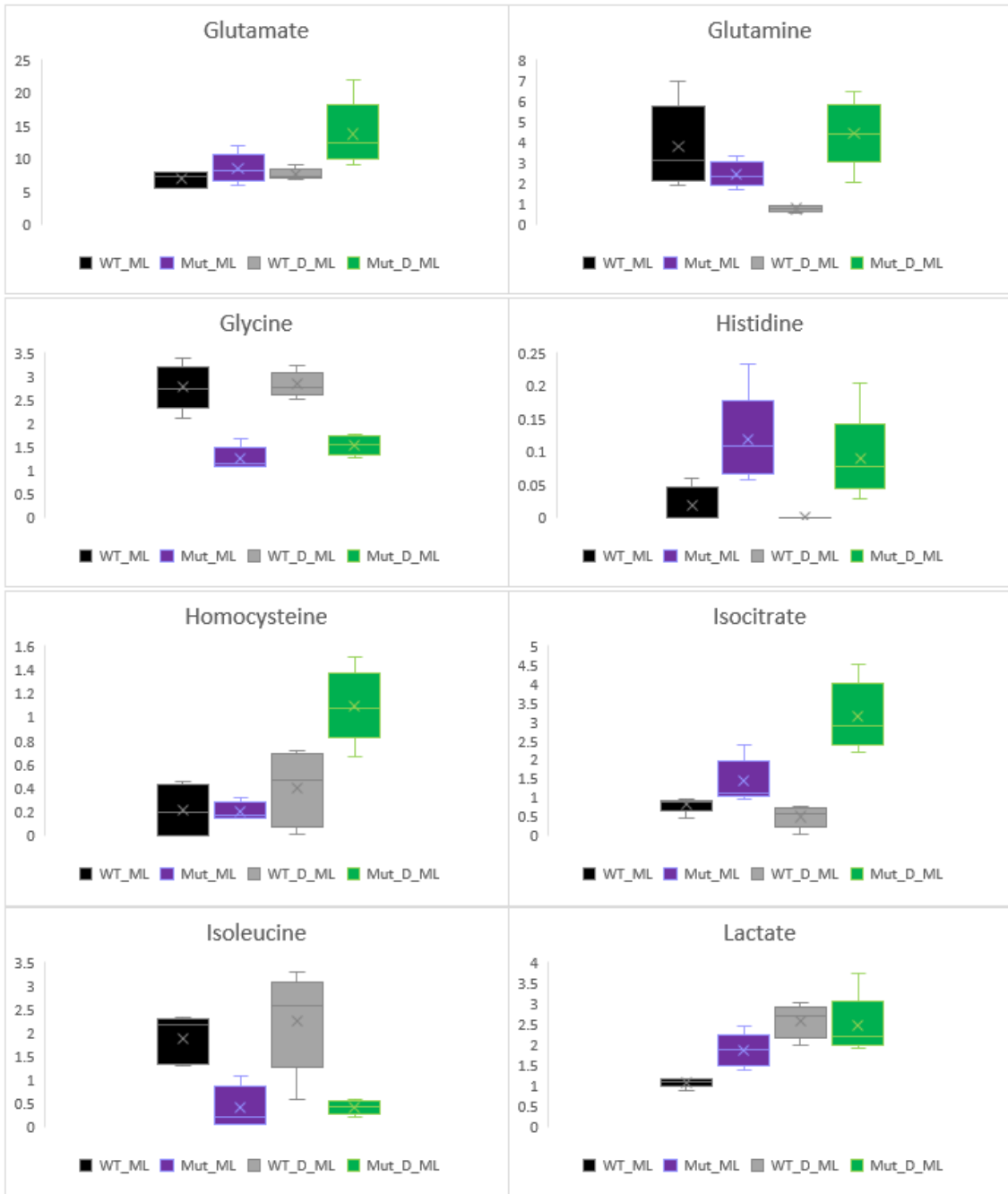


Figure B36. Top Impacted Pathways for Stationary Phase Comparison of Challenged Wild Type and Unchallenged Mutant Samples. The larger and darker the circles are, the larger the impact the significant metabolites have on the listed pathway.









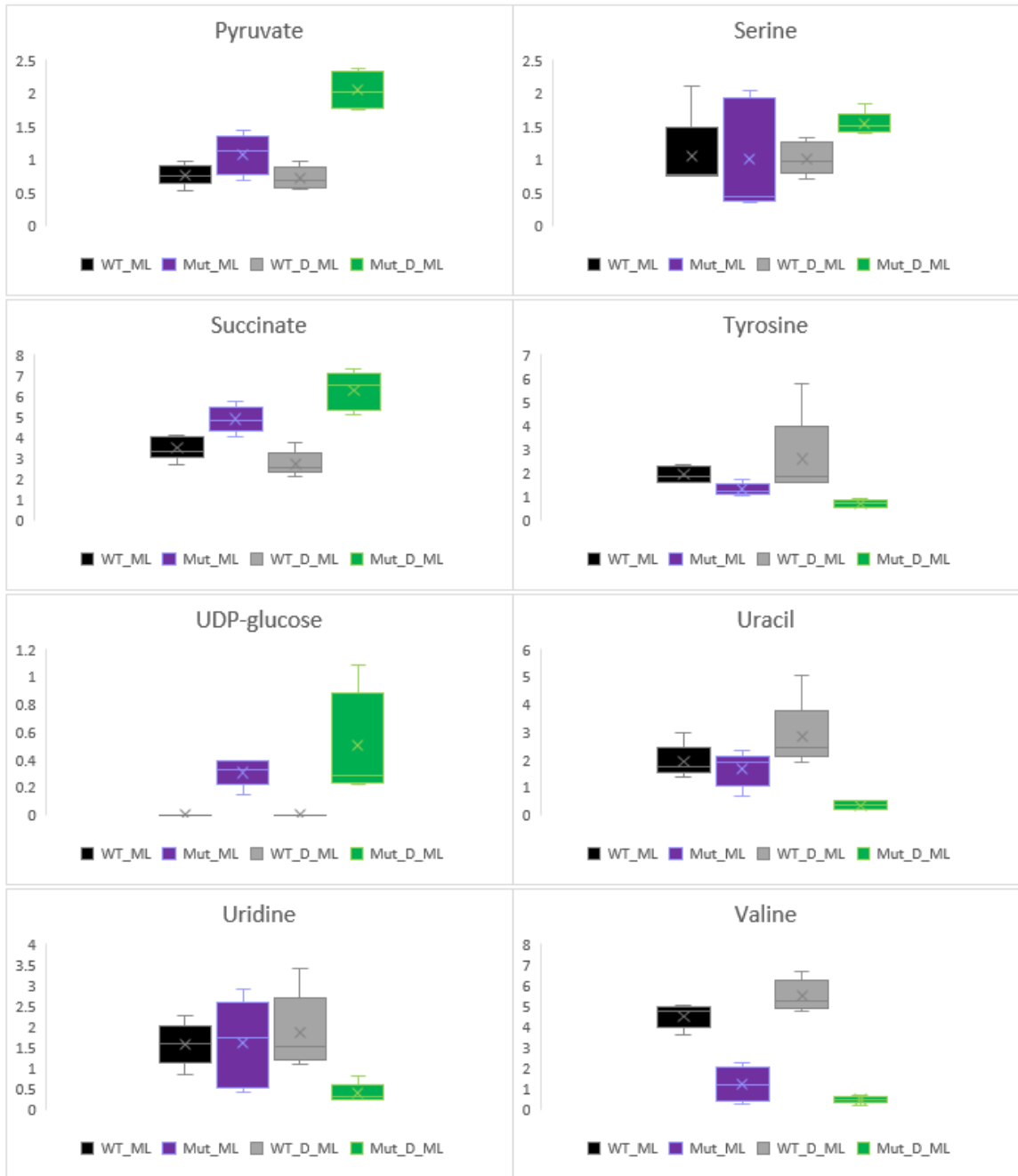
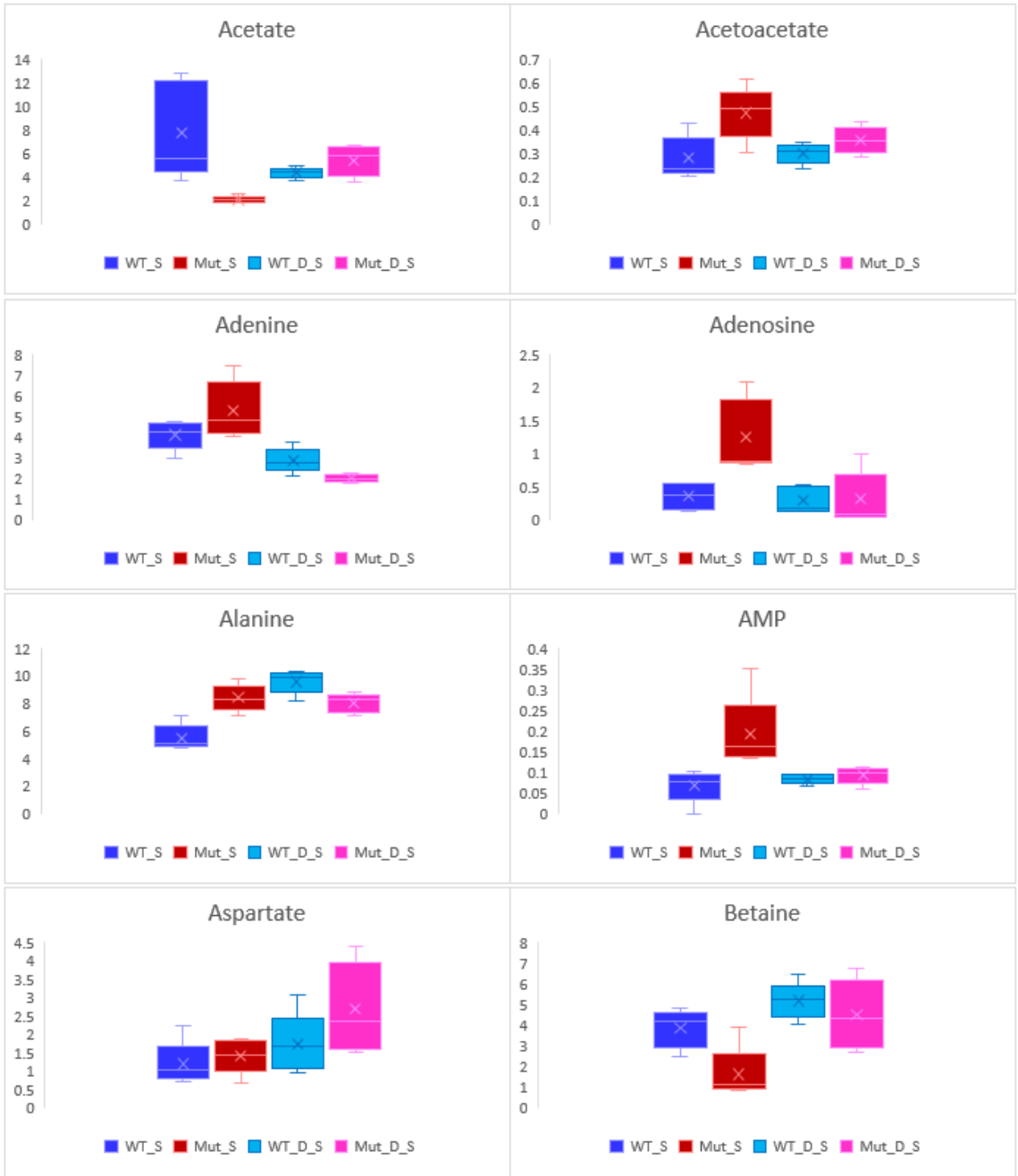
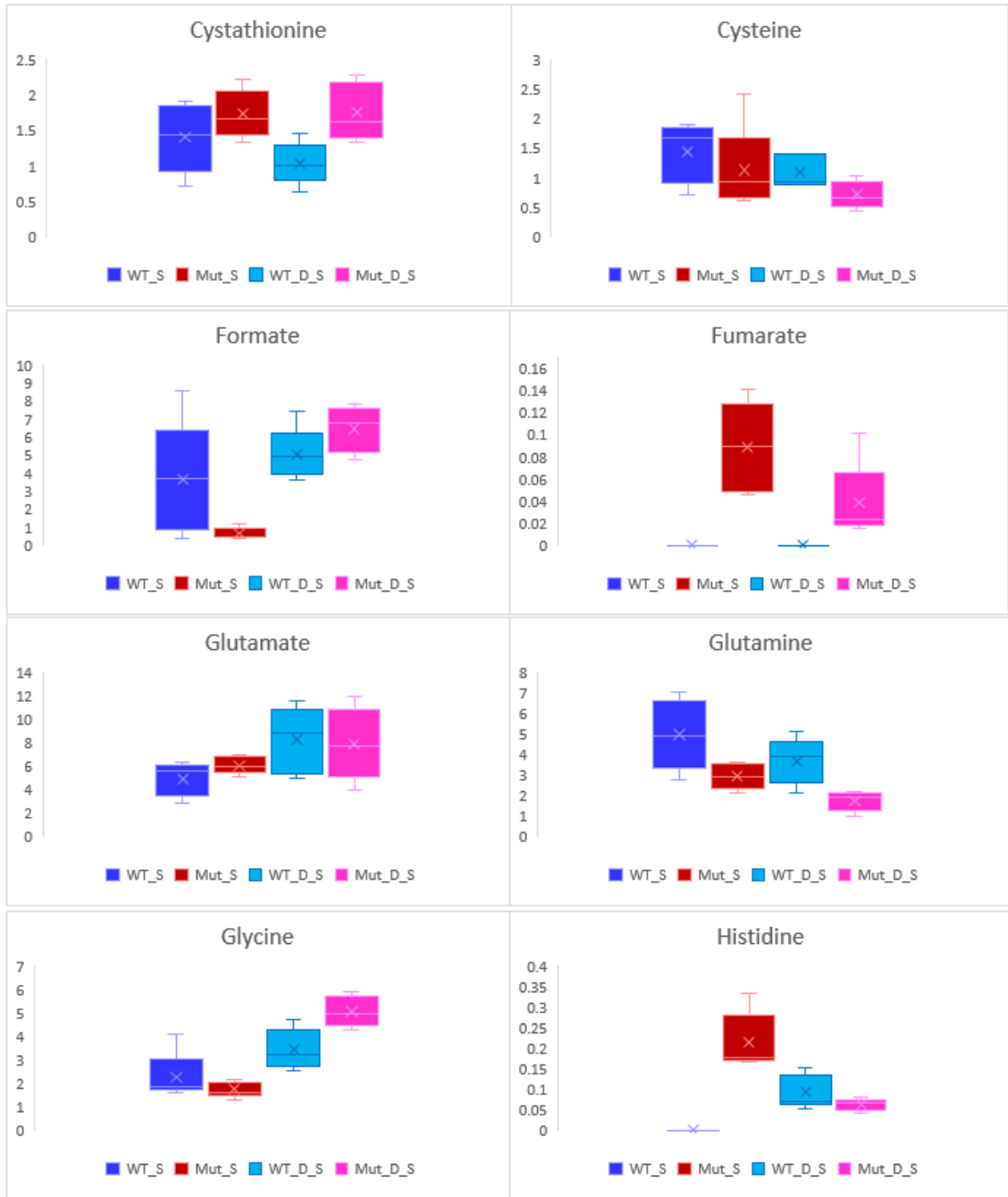
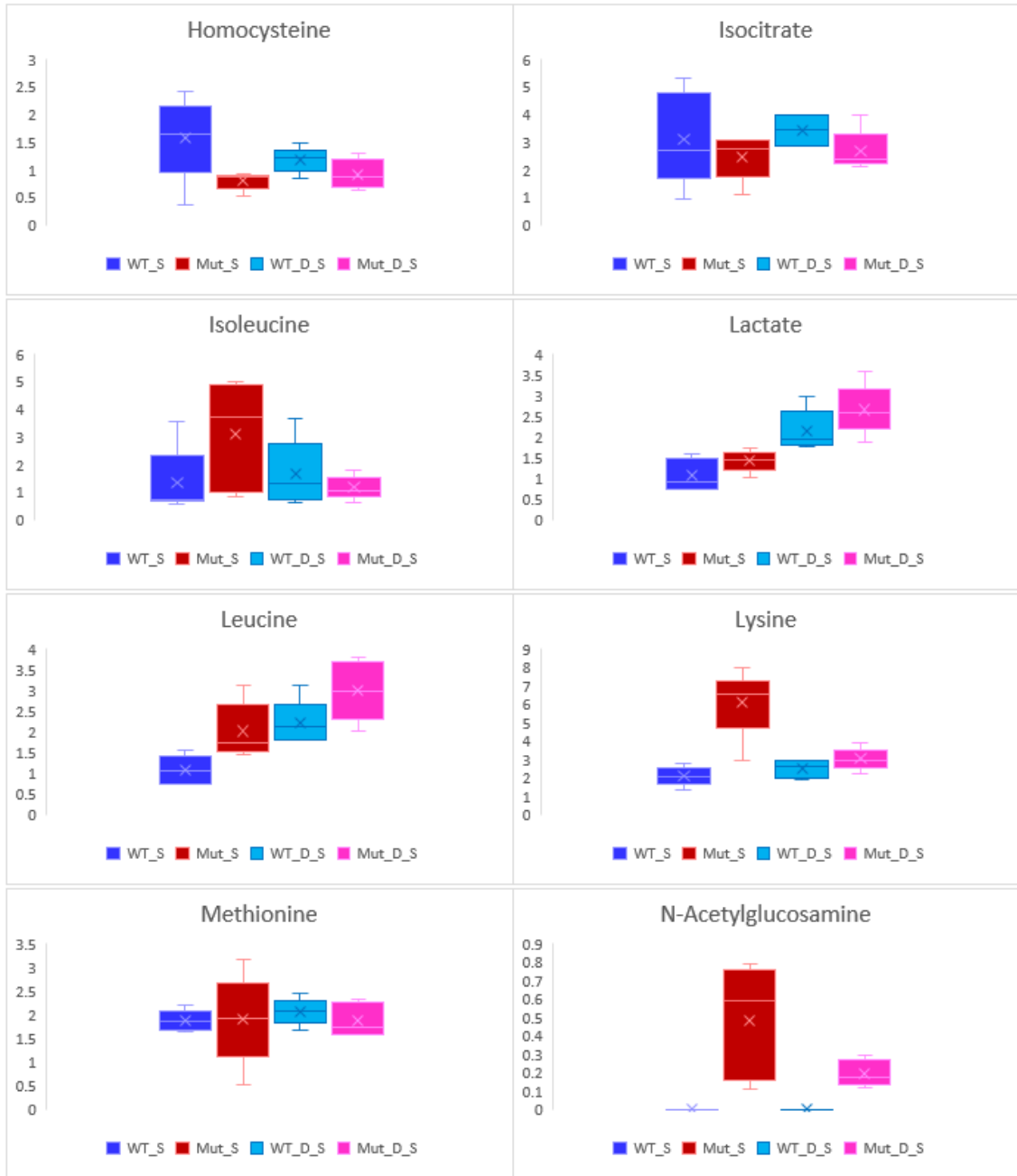
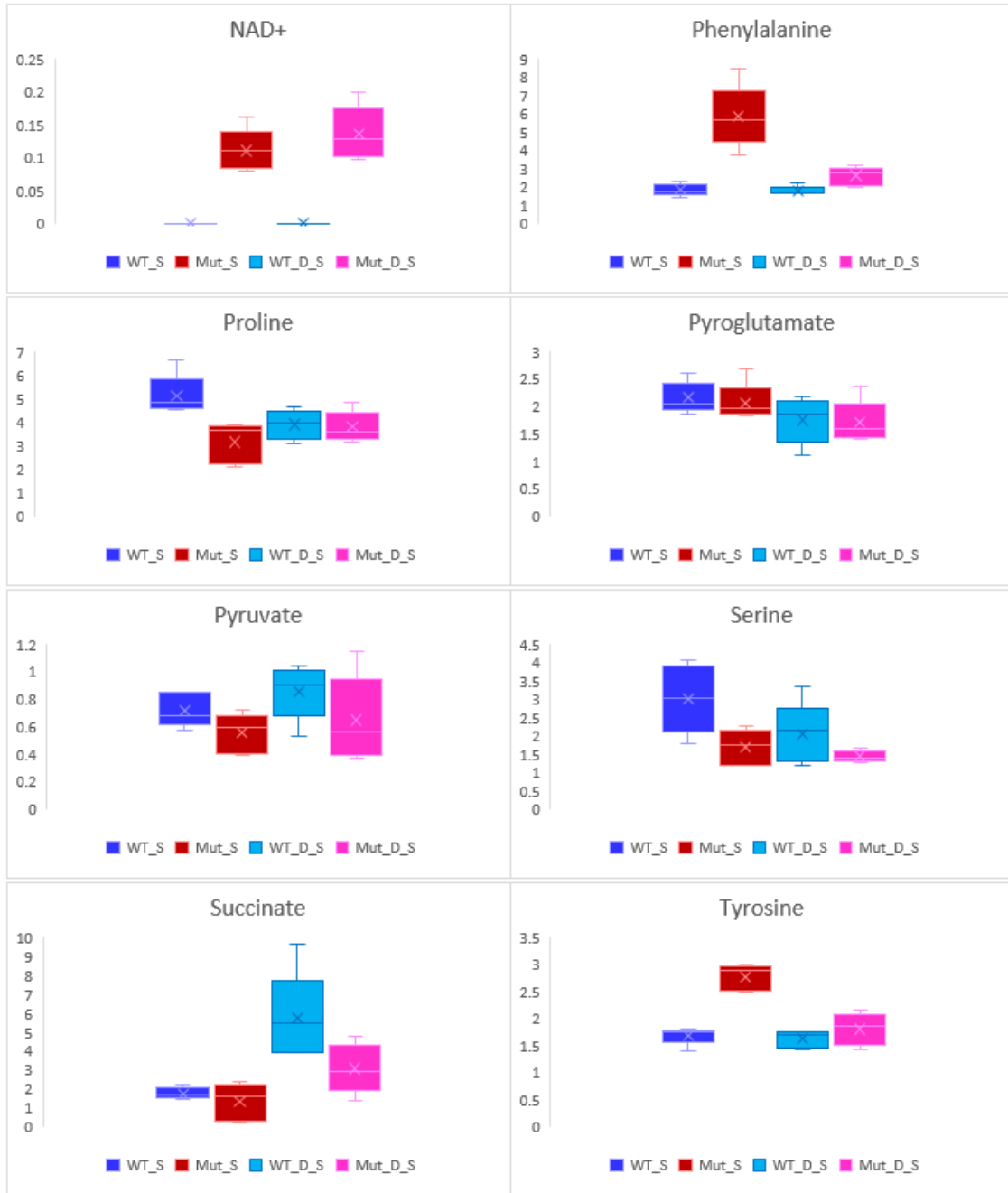


Figure B37. Mid Log Phase Metabolite Box and Whisker Plots. The ends of the whiskers are the minimum and maximum values, the center line is the median, the x is the mean, and the colored middle “box” encompasses the middle 50% of scores for the group.









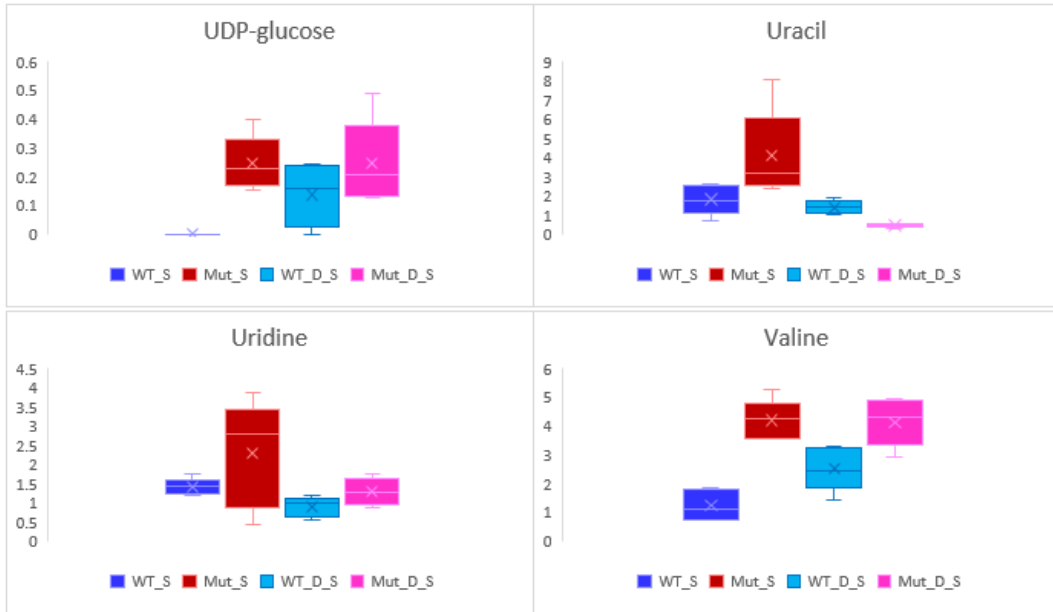
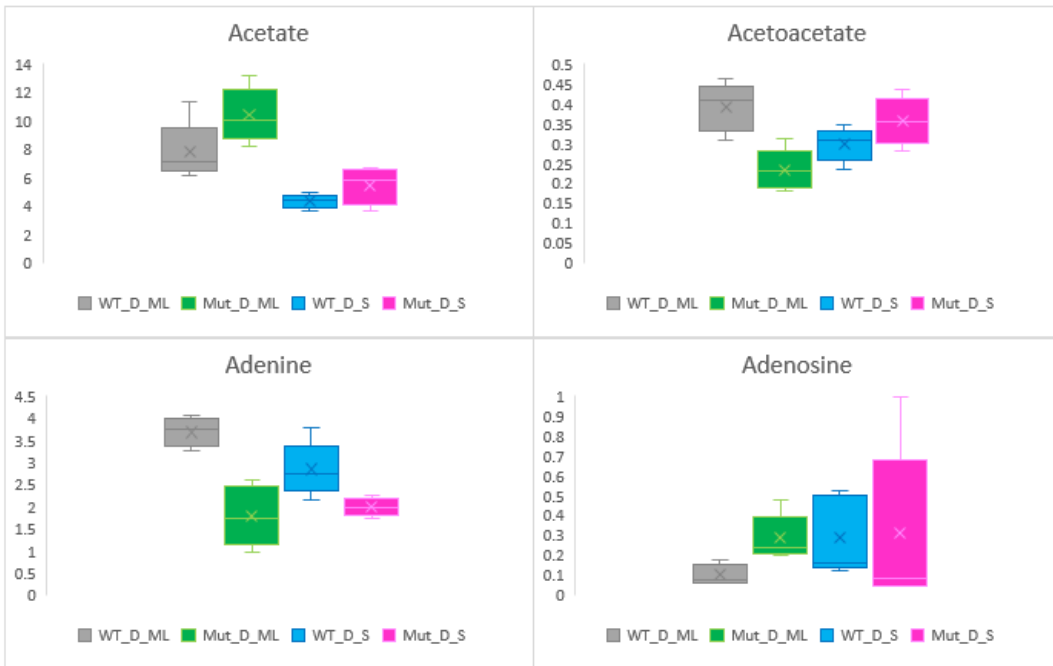
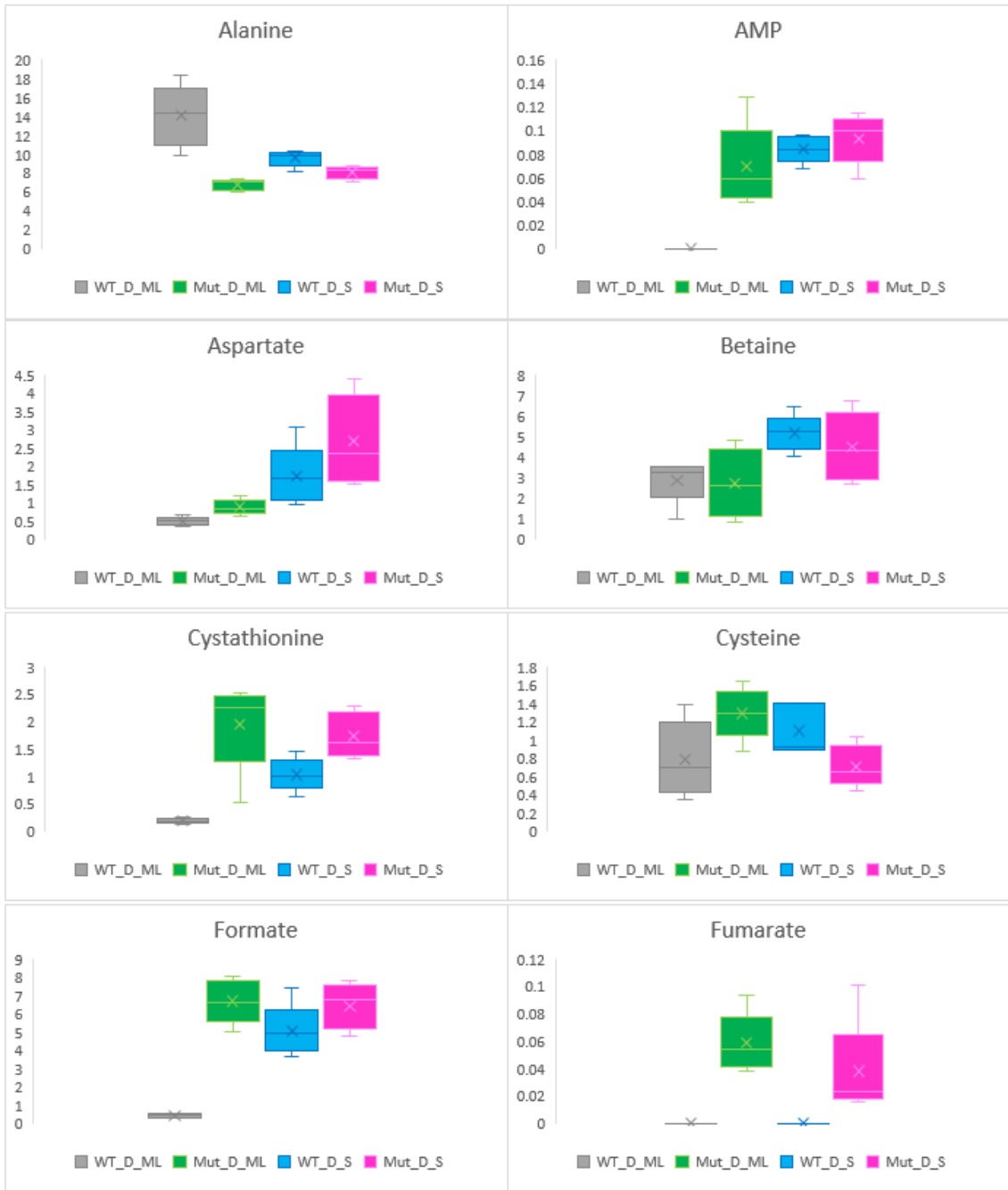


Figure B38. Stationary Phase Metabolite Box and Whisker Plots. The ends of the whiskers are the minimum and maximum values, the center line is the median, the x is the mean, and the colored middle “box” encompasses the middle 50% of scores for the group.









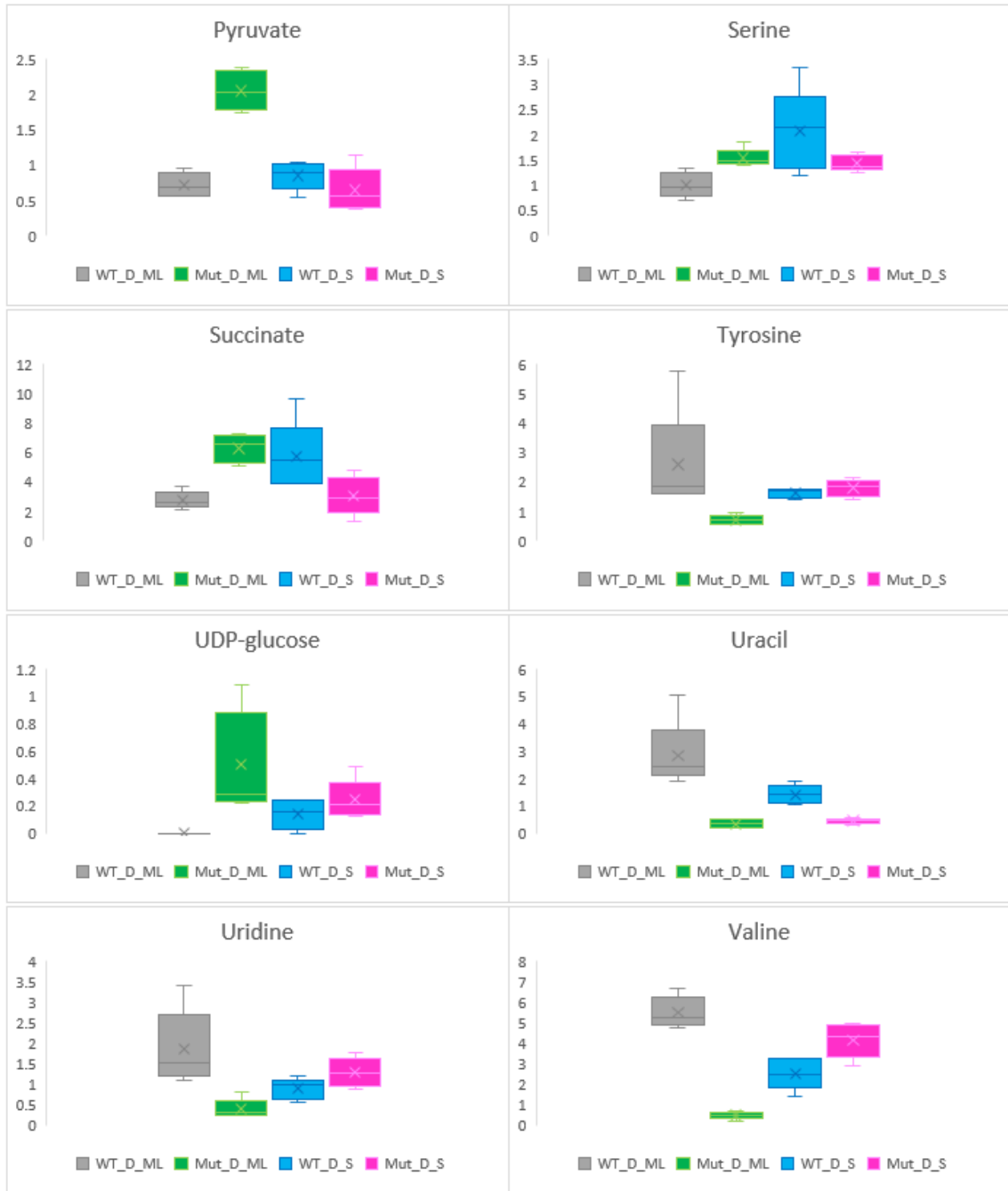
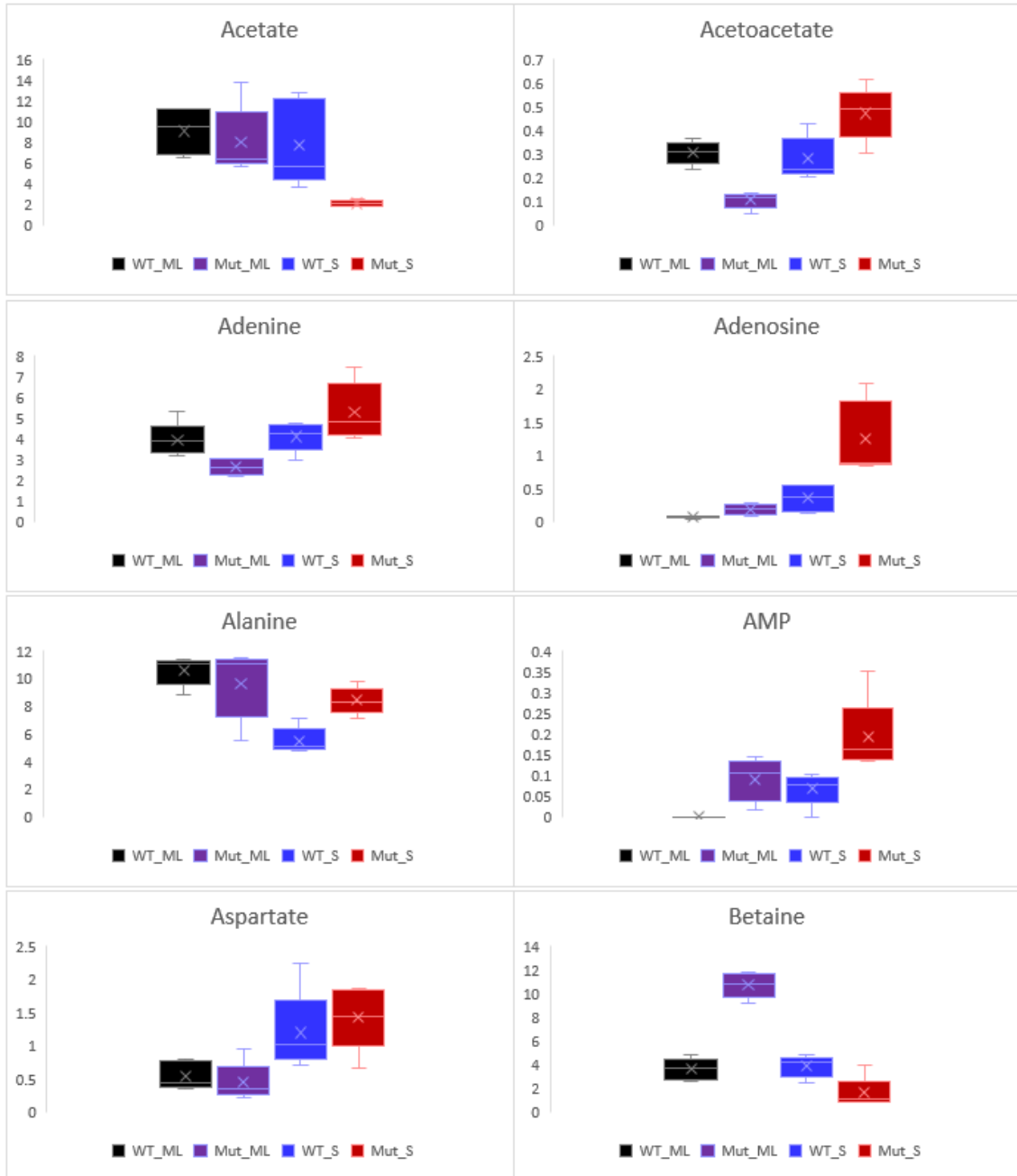
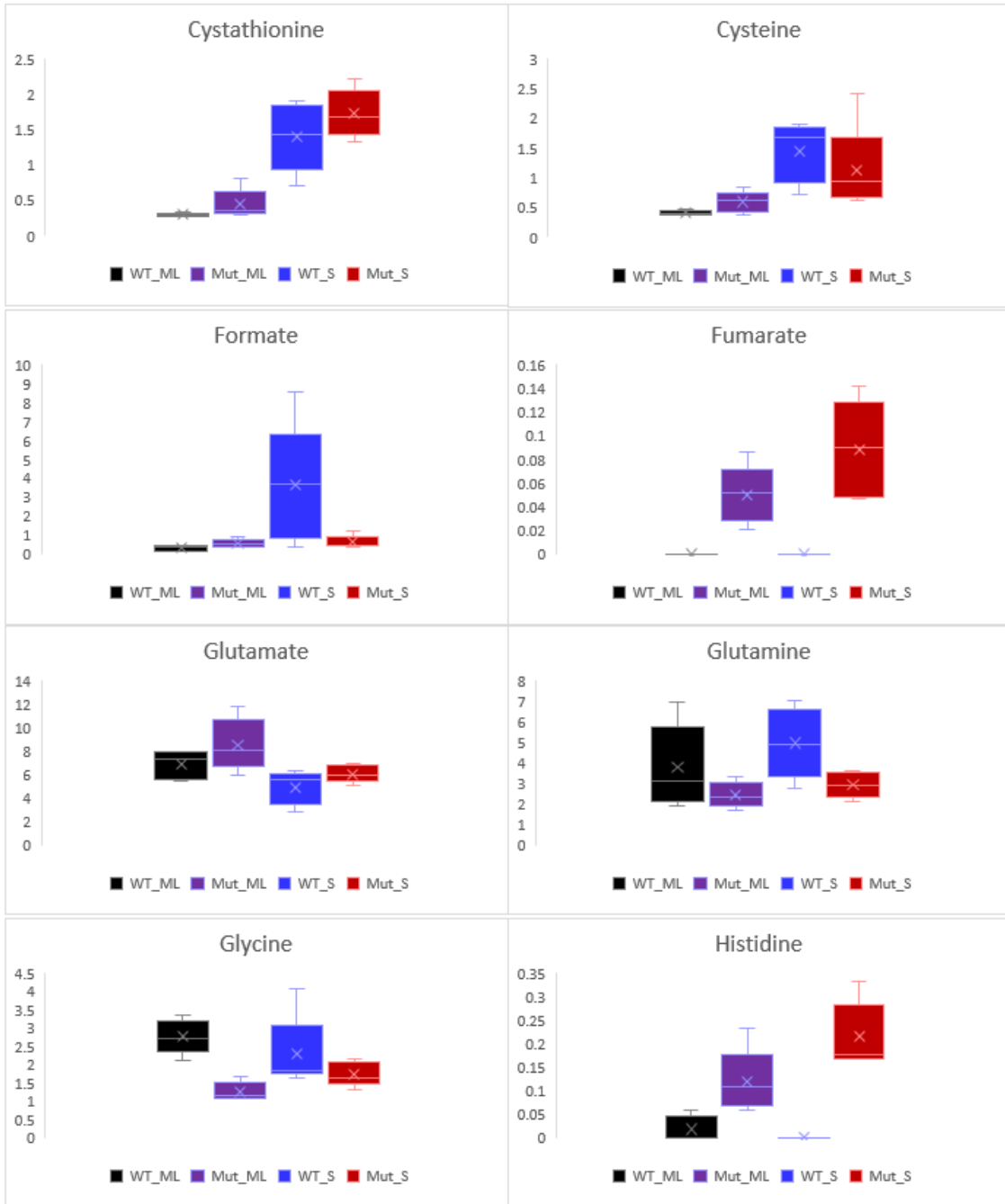
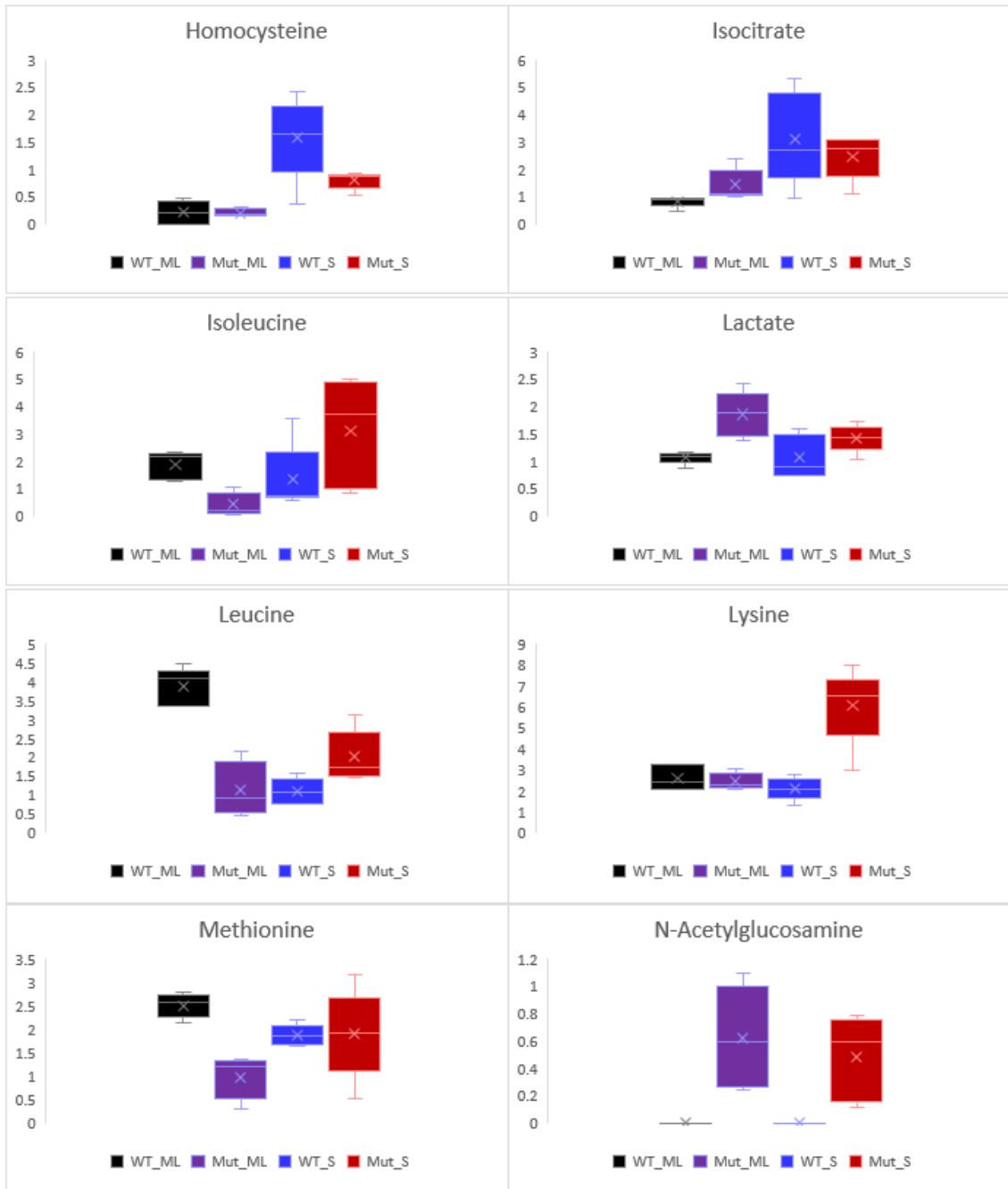
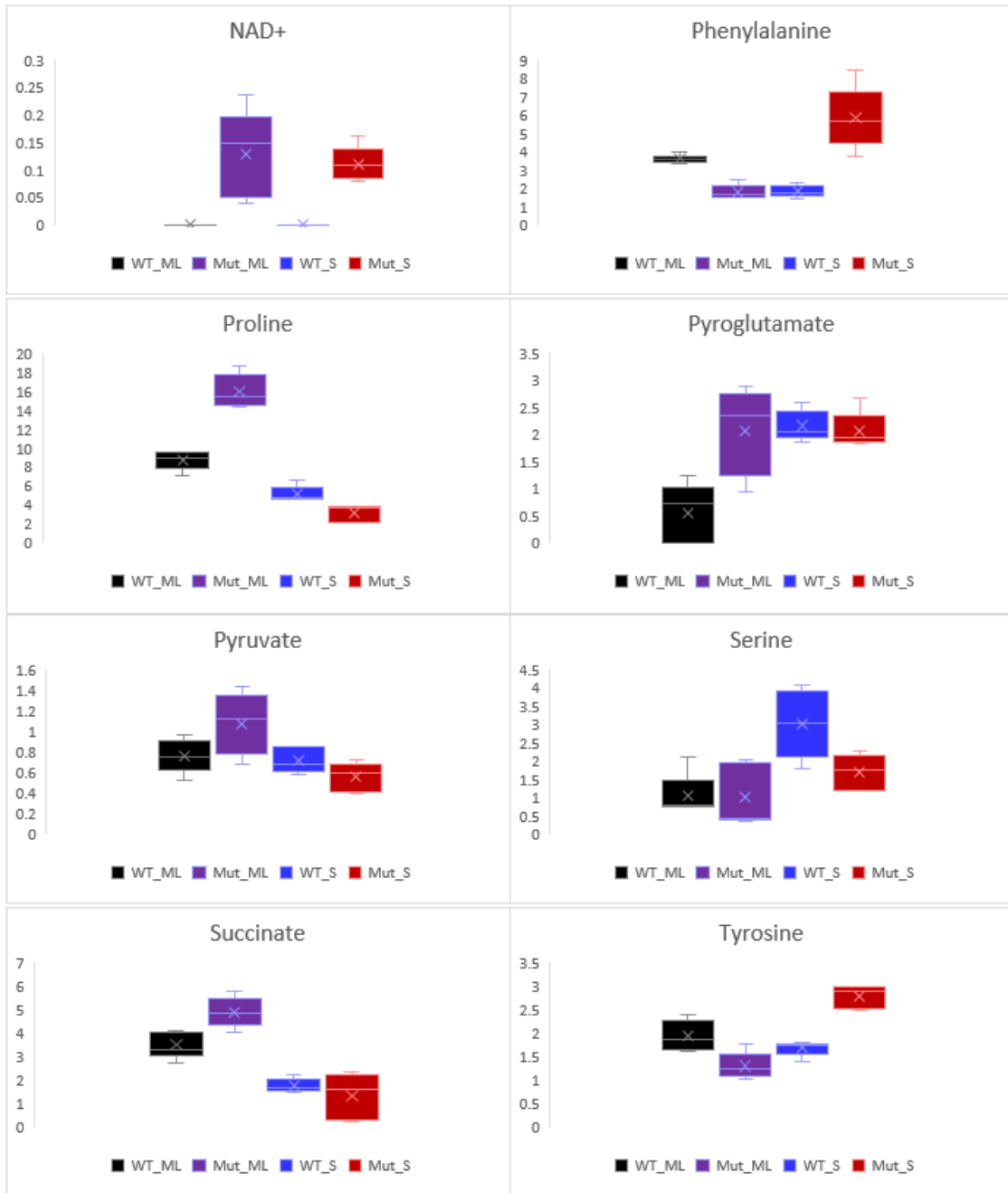


Figure B39. Challenged Sample Types Metabolite Box and Whisker Plots. The ends of the whiskers are the minimum and maximum values, the center line is the median, the x is the mean, and the colored middle “box” encompasses the middle 50% of scores for the group.









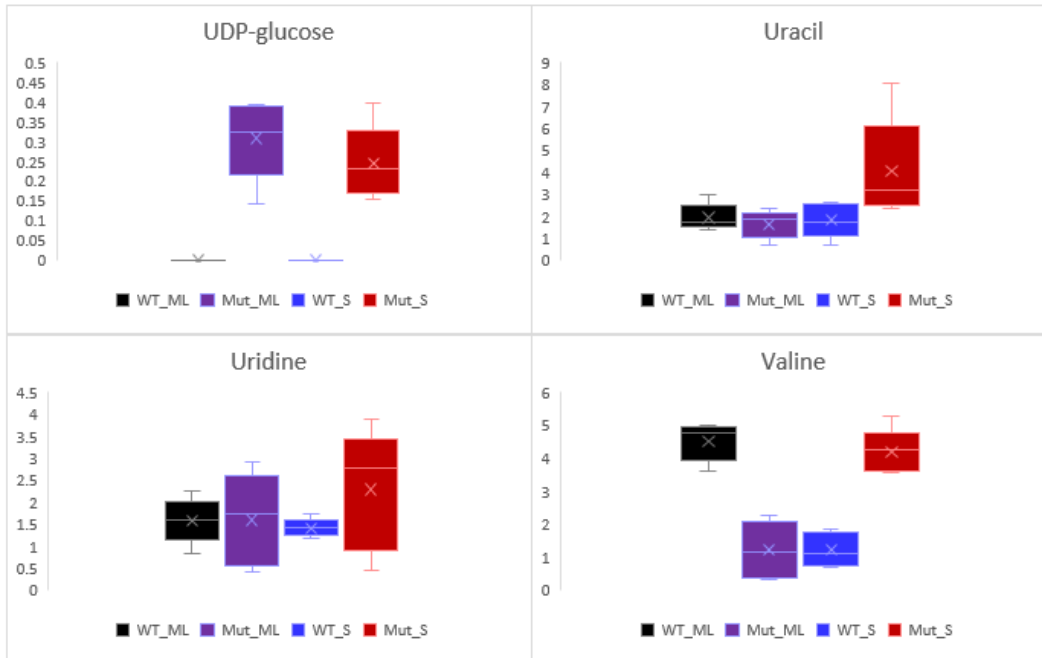
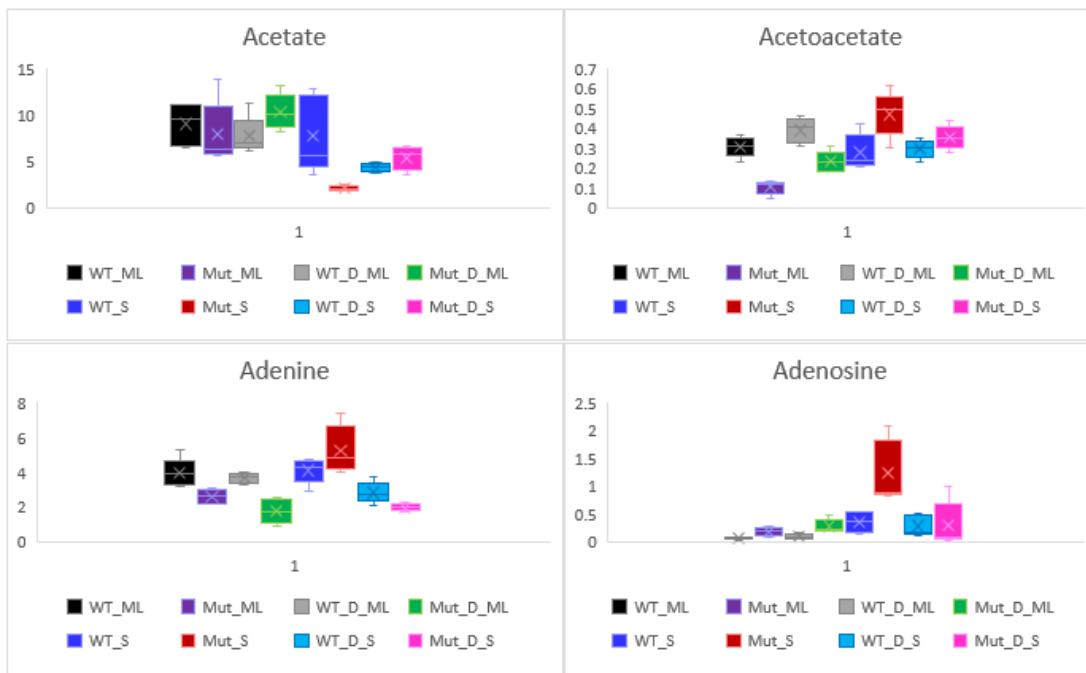
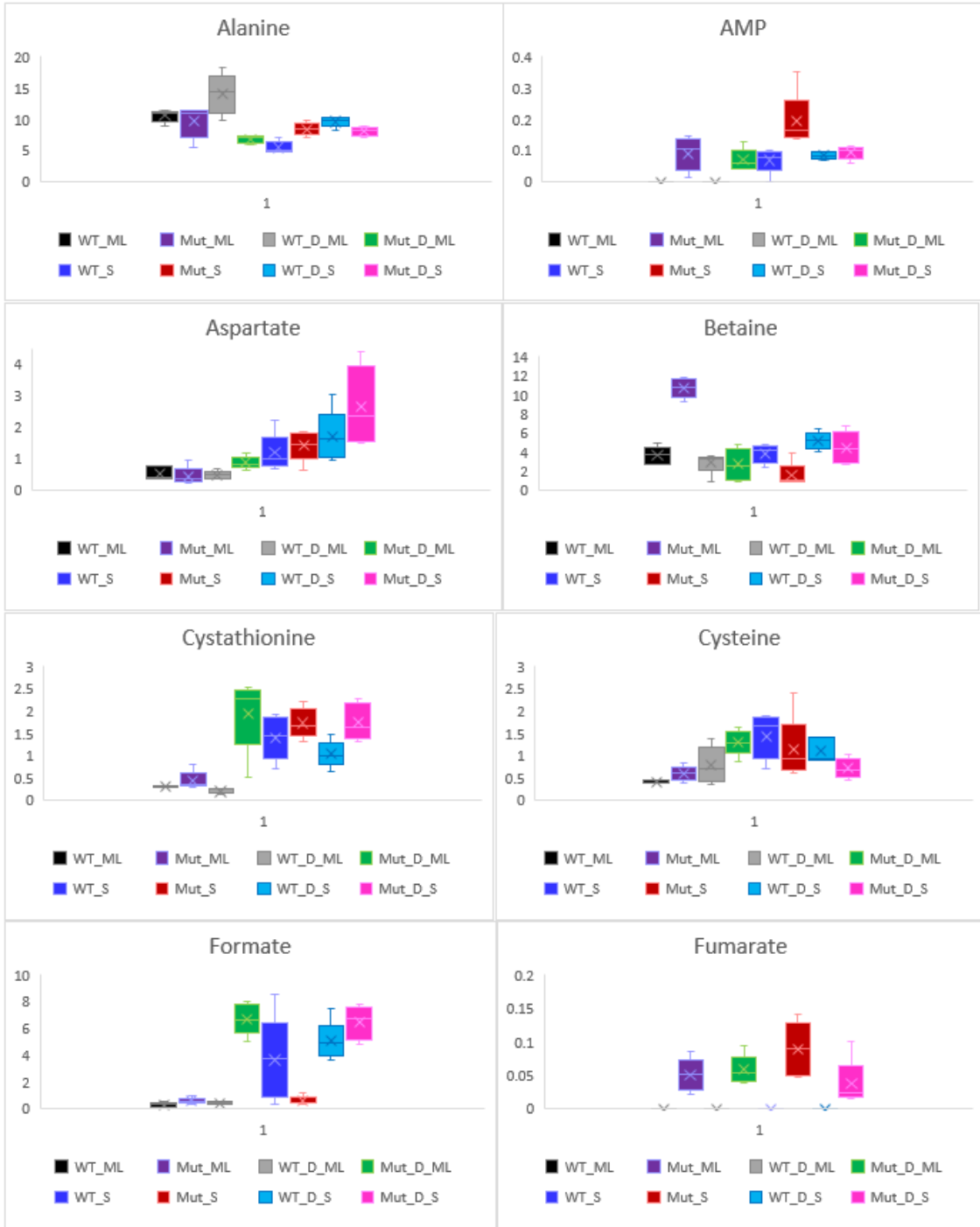
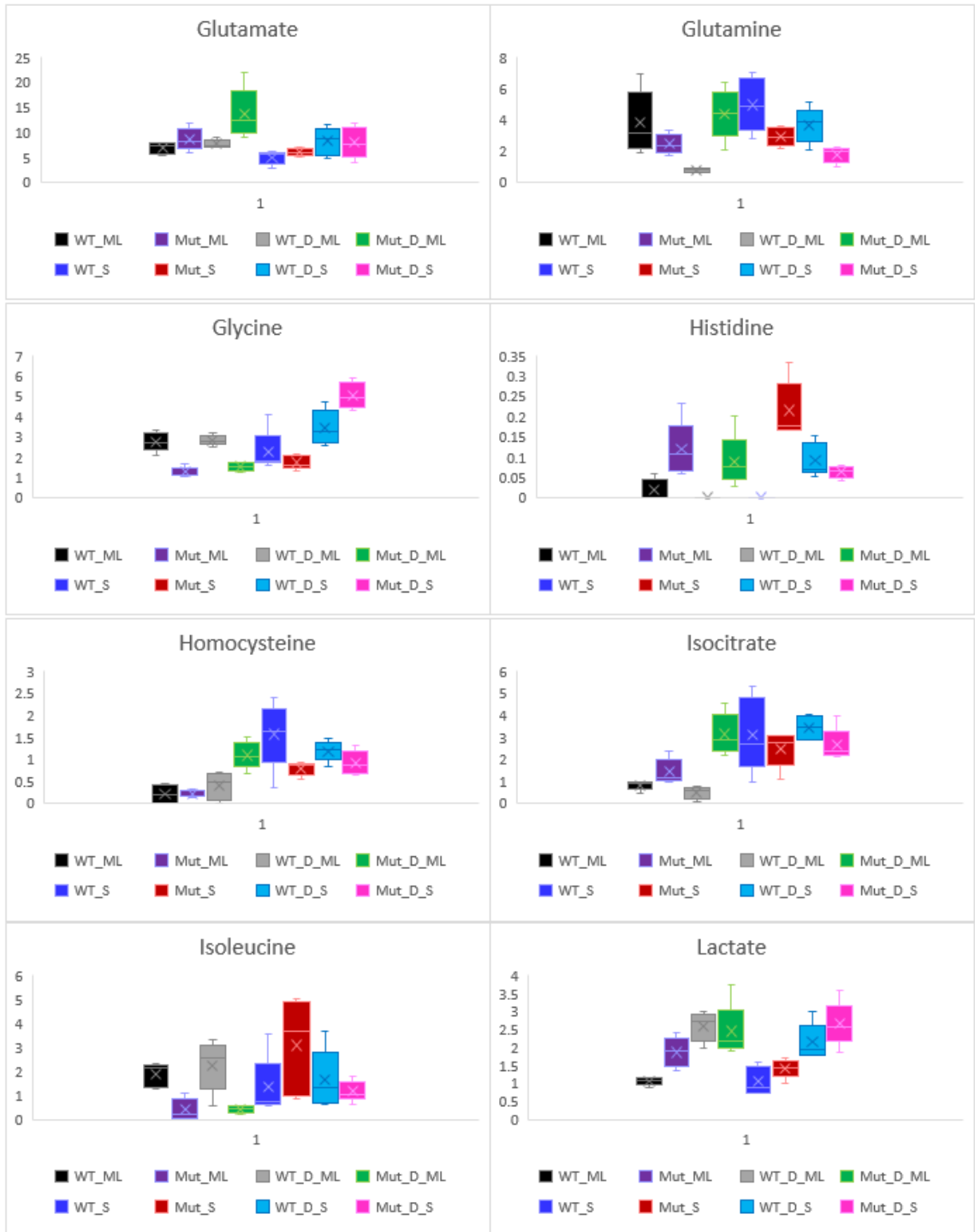
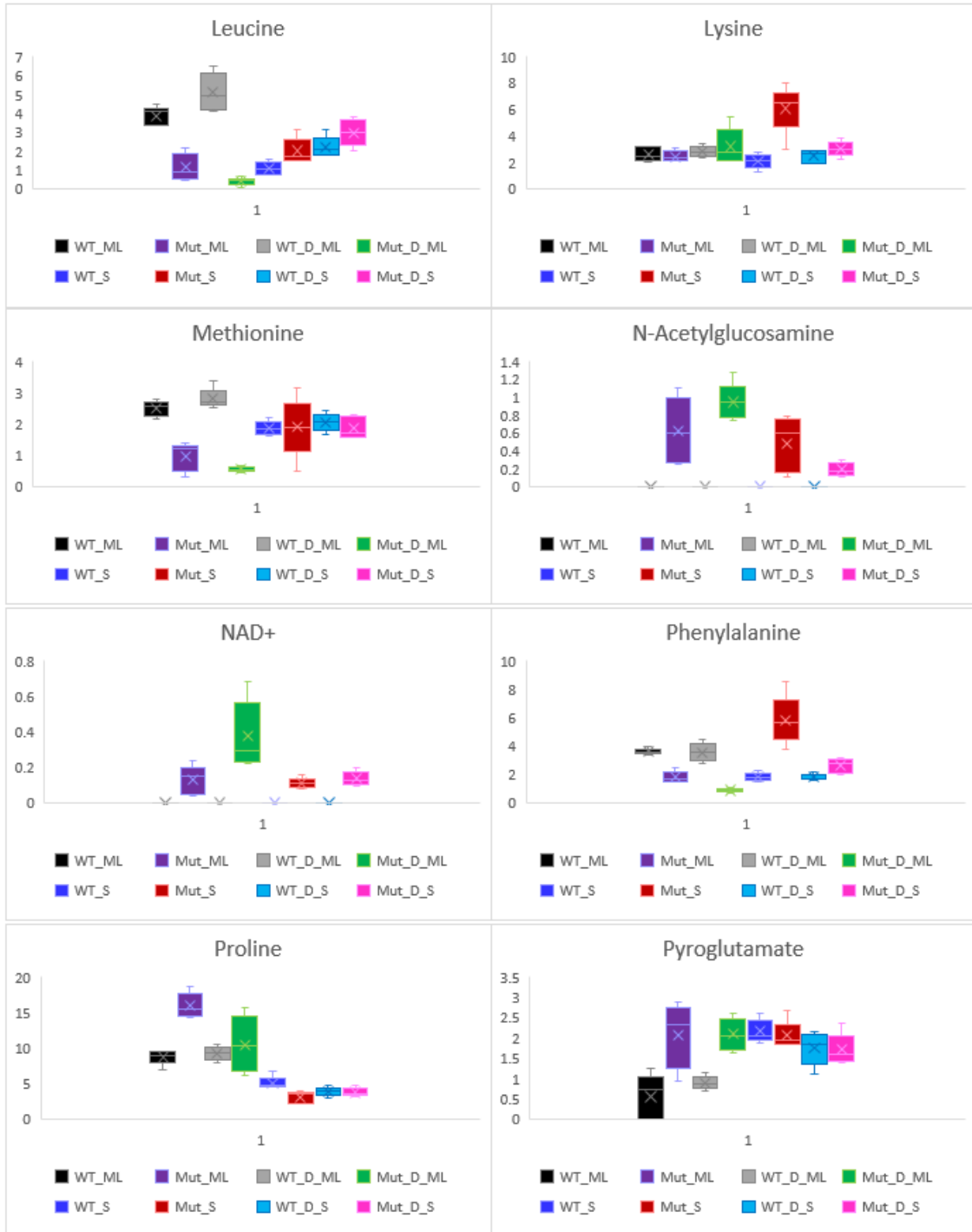


Figure B40. Unchallenged Sample Types Metabolite Box and Whisker Plots. The ends of the whiskers are the minimum and maximum values, the center line is the median, the x is the mean, and the colored middle “box” encompasses the middle 50% of scores for the group.









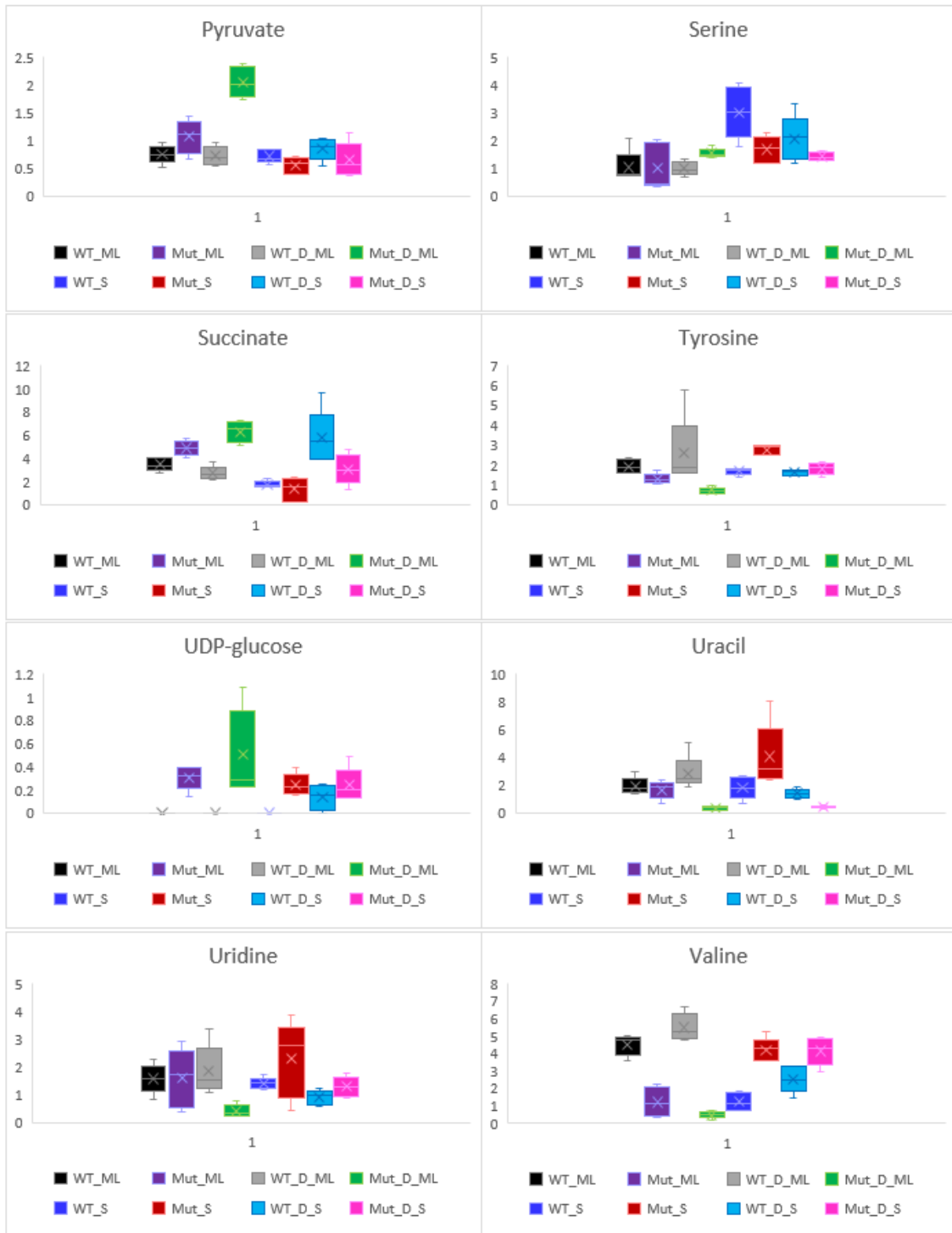


Figure B41. All Sample Type Metabolite Box and Whisker Plots. The ends of the whiskers are the minimum and maximum values, the center line is the median, the x is the mean, and the colored middle “box” encompasses the middle 50% of scores for the group.

References

- Ammons, MC. B., Tripet, B. P., Carlson, R. P., Kirker, K. R., Gross, M. A., Stanisich, J. J., Copié, V. (2014) Quantitative NMR Metabolite Profiling of Methicillin-Resistant and Methicillin-Susceptible *Staphylococcus aureus* Discriminates between Biofilm and Planktonic Phenotypes. *J Proteome Res*, 13, 2973-2985.
- Aries, M.L., Cloninger, M.J. (2020) NMR Metabolomic Analysis of Bacterial Resistance Pathways Using Multivalent Quaternary Ammonium Functionalized Macromolecules. *Metabolomics*, 16(82), 1-11. doi.org/10.1007/s11306-020-01702-1
- Wang, N. S. [Online] Experiment No. 9 °C Measurements of Cell Biomass Concentration. Department of Chemical and Biomolecular Engineering, University of Maryland, MD. <http://www.eng.umd.edu/~nsw/ench485/lab9c.htm>. (Accessed November 2019).

APPENDIX C
RNA PROJECT

RNA WORK OVERVIEW

The goal of this project was to compare RNA from the DABCOMD mutated samples to the RNA from the wild type samples. Coupled with the NMR metabolomic profiling, the RNA analysis could have advanced a more detailed description of the bacterial mutations that occur in the presence of DABCOMD. Unfortunately, this project was not completed because all critical samples were lost during a freezer failure. In this appendix, a description of the protocols that were developed for this project is provided to guide endeavors in this area should they be pursued by another researcher. The iterations of the RNA procedures, why changes were made to the procedures, and the results that were obtained are presented below. The process by which viable samples are identified is also described, and examples of data that show viable and nonviable RNA samples as well as what to look for when running the RNA samples are provided.

Figure C.1 shows the generic method used to ensure RNA purity and the steps taken toward analysis. Modifications to the procedures described below occurred during the step labeled “RNA Extraction”, which is the second step shown in Figure C1. The larger arrows going backward show when samples should be discarded, and the protocol should be repeated starting with cell pellet sample collection (please see Appendix A and B for sample collection procedures).

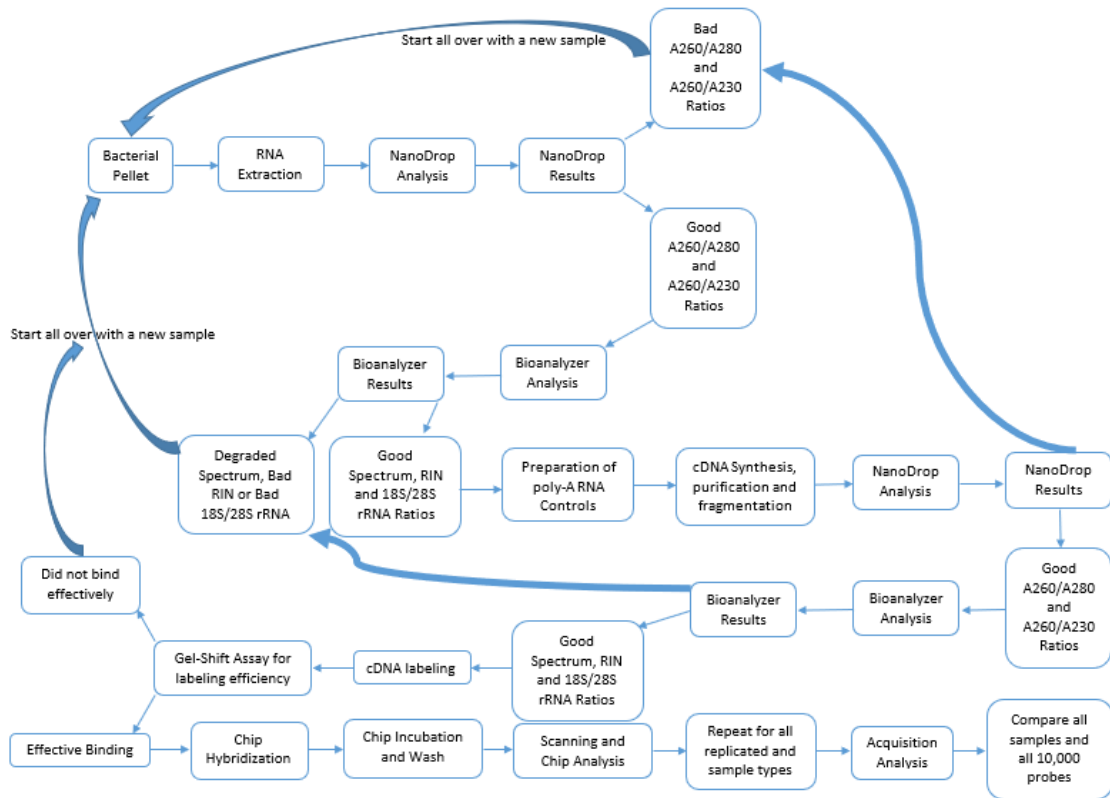


Figure C1. Procedures for the determination of RNA purity and results

After many trials to improve procedures, and after viable RNA was obtained, the -80°C freezer that was being used for sample storage failed. All of the samples in the freezer, including all the RNA samples for this project, were lost. Four sample types for the *E. coli* project (WT ML, WT S, Mut ML and Mut S) and eight sample types for the *B. cereus* project (WT ML, WT S, Mut ML, Mut S, WT D ML, WT D S, Mut D ML and Mut D S) were lost. At least nine replicates for each of sample set were fully extracted and ready for analysis when the freezer failure occurred (Figure C2). Because of the significant amount of time that would have been needed to reproduce the samples that were lost, work on this project was discontinued.



Figure C2. Shows the RNA samples (in Eppendorf tubes) ruined by freezer failure

After several iterations of the procedures for Zymo Research RNA extraction kit, viable samples were obtained, but the percentage of viable RNA obtained in each sample was not high enough. For this reason, the Qiagen RNeasy® RNA extraction kit was used. When using the Qiagen RNeasy® kit, each set of RNA extractions are performed separately, whereas Zymo Research completes several steps simultaneously (Qiagen 2014; Zymo Research 2015). Completing several steps concurrently appeared to result in fewer viable samples and a lower RNA yield for this project. Moreover, Zymo Research protocols indicate that an RNA purity of greater than 1.8 (A260/230 ratio) is acceptable (Zymo Research 2015), while other sources suggest that the ratio should be very close to 2.0 (NanoDrop 2007).

A NanoDrop® was used to observe RNA quality and concentration before the BioAnalyzer was used. For RNA, the A260/230 ratio should be between 2.0-2.2 for a pure sample (1.8 for pure DNA), the peak should be distinct without an oscillating center, and the concentration should be at least 50 ng/μL. If the A260/280 ratio is different, this difference could indicate the presence of protein, phenol, Tri Reagent, other contaminants or non-neutral pH (NanoDrop 2007; Williamson 2015).

2100 Agilent Technology RNA NanoChip Bioanalyzer was used to assess the quality and viability of the RNA samples. Everything below 200 nt was eliminated, because this is characteristic of small, fragmented pieces of RNA (degraded/junk). An RNA easy column can be used to eliminate all RNA under 200 nt. The 23S and 16S rRNA ratios are important, since the 23S peak should contain twice as much RNA as the 16S peak. The RNA integrity number (RIN) should be close to 10. (Biomedical Genomics 2016; Kishawi 2008; Williamson 2015)

Zymo Research RNA Extraction Procedures and Modifications

The entire protocol for the initial (unoptimized) and final (optimized) procedures are provided. Changes and rationales for the modifications are described. An explanation of the results of each modification, including whether the changes resulted in viable RNA, is described in italicized text below the listed changes to the procedures.

Starting Procedures (Zymo Research 2015)

- 40 mL of Microbiology Grade Ethanol was added to 160 mL of Direct-zol™
- RNA PreWash.
- 48 mL of Microbiology Grade Ethanol was added to 12 mL RNA Wash Buffer.
- Tri Reagent® was added in a 3:1 ratio to the cell pellet and incubated for 5 minutes on ice.
- An equal volume of Microbiology Grade Ethanol to Tri Reagent® was added and incubated for 5 minutes on ice.
- 0.7 mL was pipetted into a Zymo-Spin™ IIICG Column in a collection tube and centrifuged at 10,000 g force for 30 seconds. This was repeated until all of the sample was loaded on the column.
- The column was transferred to a new collection tube. The old collect tube and flow-through was discarded.
- A DNase I solution was mixed in a 1.5 mL RNase free Eppendorf tube.
 - 5 µL DNase I (6 U/µL)
 - 75 µL DNA Digestion Buffer
- 400 µL of RNA Wash Buffer was added and centrifuged at 10,000 g for 30 seconds.
- The column was treated with a DNase I solution and incubated at room temperature for 15 minutes.
- 400 µL Direct-zol™ RNA PreWash was added to the column and centrifuged at 10,000 g for 30 seconds.
- 700 µL RNA Wash Buffer was added and centrifuged at 10,000 g for 2 minutes.

- The column was transferred to an RNase-free 1.5 mL Eppendorf tube.
 - 50 μ L of DNase/RNase-Free Water was added to the column and centrifuged at 10,000 g for 30 seconds.
 - The samples were stored at -80 °C.
- ✚ *No viable RNA samples were obtained. RNA samples were not pure, and the sample concentrations were too low, as determined by the NanoDrop®. Figure C3 shows a nonviable NanoDrop® plot demonstrating the characteristic oscillating peak center that is indicative of a contamination, likely from the phenol reagent.*

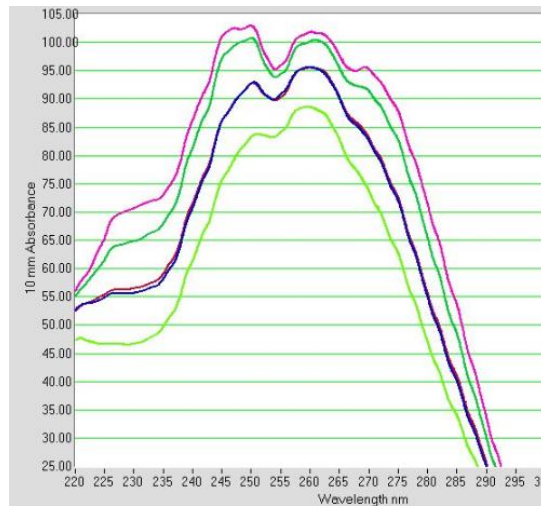


Figure C3. Nonviable RNA sample plot determined by the NanoDrop®.

First Set of Modifications

- Increased washes to help elute contaminants.
- Increased incubation time to help effectiveness of washes.
- Extra centrifuge step with a new tube at the end to help pull all moisture out of the column.

✚ *Cleaner RNA was obtained, but RNA samples were still not viable, as determined via NanoDrop®. The A260/280, A260/230 and concentration data obtained from the NanoDrop® showing nonviable data is shown in Table C1.*

Table C1. Concentration and absorbance NanoDrop® data demonstrating nonviable RNA

Sample ID	ng/μl	A260/280	A260/230	A260	A280
WT ML 1	75.67	1.75	1.06	1.89	1.08
WT ML 2	138.47	1.68	0.95	3.46	2.06
WT ML 3	113.74	1.67	0.98	2.84	1.70
WT ML 4	96.88	1.68	0.95	2.42	1.44
WT S 1	81.56	1.85	1.05	2.04	1.10
WT S 2	60.39	1.83	1.14	1.51	0.82
WT S 3	107.53	1.66	0.62	2.69	1.62
WT S 4	57.55	1.73	0.99	1.44	0.83
Mut ML 1	63.60	1.77	1.00	1.59	0.90
Mut ML 2	77.43	1.73	0.94	1.94	1.12
Mut ML 3	75.65	1.73	1.02	1.89	1.09
Mut ML 4	80.41	1.76	1.12	2.01	1.14
Mut S 1	62.97	1.68	0.98	1.57	0.94
Mut S 2	55.74	1.59	0.61	1.39	0.88
Mut S 3	29.03	1.51	0.36	0.73	0.48
Mut S 4	53.46	1.56	0.62	1.34	0.86

Second Set of Modifications

- Continued with the previous modified procedures.
- Lysozyme was added to increase cell lysis.

✚ *A higher RNA yield was obtained, but RNA samples were still not viable, as determined via NanoDrop®.*

Third Set of Modifications

- Continued with the previous modified procedures.
- Increased g force during centrifugation to help decrease contamination on the column.

- Phenol is in the Tri Reagent® and can contaminate the product; columns were switched twice to decrease contamination.

✚ *The cleanest RNA samples obtained up to this point were achieved, but the RNA samples were still not viable as determined via NanoDrop®.*

Fourth Set of Modifications

- Continued with the previous modified procedures.
- Heat was added to increase RNA yield and cell lysis.

✚ *A very high RNA yield was obtained, but still no viable RNA samples were obtained as determined via NanoDrop®. The results of the modifications show improved concentrations and absorbance ratios, indicating better yield of purer samples, but the RNA is still nonviable as shown in Table C2.*

Table C2. Demonstrates the improvement in concentration and more pure samples, but the RNA is still nonviable as determined by the NanoDrop®

Sample ID	ng/μl	260/280	260/230	A260	A280
WT ML 1	1550.09	1.57	1.09	3.88	2.48
WT ML 2	1301.11	1.68	1.08	3.28	1.95
WT S 1	1531.35	1.63	0.99	3.83	2.35
WT S 2	1036.04	1.66	1.00	3.40	2.05
Mut ML 1	2420.69	1.87	1.38	6.02	3.22
Mut ML 2	1674.20	1.60	0.83	4.18	2.62
Mut S 1	969.19	1.50	0.68	2.41	1.61
Mut S 2	1571.53	1.70	0.95	1.79	1.05

Fifth Set of Modifications

- Continued with the previous modified procedures.

- The Tri Reagent®/lysozyme/cell pellet sample was centrifuged to remove cellular debris (cloudiness) that was clogging up the column.
- ✚ *Viable RNA samples were obtained, as determined by using the NanoDrop®. These samples were run on the Bioanalyzer to check for RNA degradation. RNA degradation was identified.*

Sixth Set of Modifications

- Continued with the previous modified procedures.
- Minus the lysozyme step because possible RNA degradation due to the RNA stabilizing agent (Tri Reagent®) not being added until after this step.
- Added in Tri Reagent® then sonicated to break open cells with the RNA stabilizing agent present.
- ✚ *High quantities of pure RNA were obtained, as determined by the NanoDrop®. RNA was fragmented into small pieces, as determined by the Bioanalyzer. Since the majority of the RNA is below 200 nt, the 16S and 23S peaks are small and the ratio of 23S/16S is approximately 2, no viable RNA was obtained (Figure C4).*

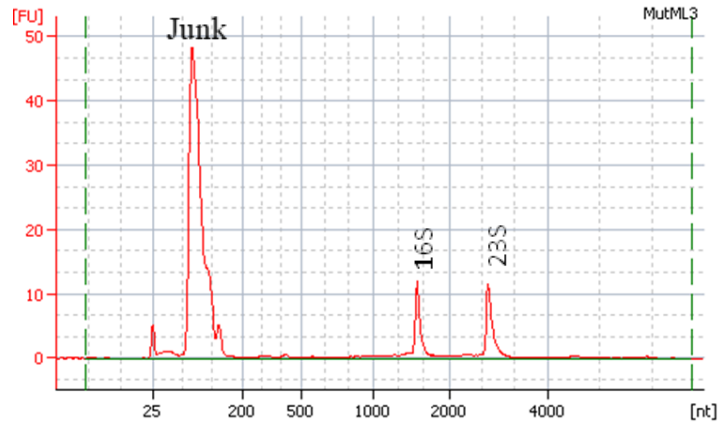


Figure C4. Bioanalyzer results showing degraded RNA.

Collection Procedures

➤ Metabolomics Procedures

- The samples were centrifuged at 2,500 rpms for 12 minutes. The supernatant was discarded and 5 mL cold sterile 1x PBS was added. Each tube was centrifuged at 2,500 rpms for 12 minutes. The supernatant was discarded, and the pellets were frozen at -80°C .

➤ New RNA Procedures

- The samples were centrifuged at 9,000 rpms for 2 minutes, the supernatant was discarded, and the pellet was frozen at -80°C .

Final Procedure Modifications

The parts of the procedure that were modified are in blue.

- 500 μL Lysozyme in TE Buffer (pH 8.0) 20 mg/mL was added to the cell pellet on ice for 2 minutes.
- 1 mL Tri Reagent® was added, and the tube was vortexed.

- Tri Reagent® was added in a 2:1 ratio to the cell pellet and incubated for 5 minutes at 70 °C. The sample was vortexed every minute.
- The sample was centrifuged at 14,000 g for 2 minutes. The pellet was discarded.
- The supernatant was transferred to 1.5 mL Eppendorf tubes.
- An equal volume of Microbiology Grade Ethanol to Tri Reagent® was added and incubated for 5 minutes on ice.
- 0.7 mL was pipetted into a Zymo-Spin™ IIIICG Column in a collection tube and centrifuged at 14,000 g force for 30 seconds. This was repeated until all of the sample was loaded on the column.
- The column was transferred to a new tube and centrifuged at 14,000 g for 30 seconds. The old collect tube and flow-through were discarded.
- The column was transferred to a new collection tube. The old collect tube and flow-through were discarded.
- A DNase I solution was mixed in a 1.5 mL RNase free Eppendorf tube.
 - 5 µL DNase I (6 U/µL)
 - 75 µL DNA Digestion Buffer
- 400 µL of RNA Wash Buffer was added and centrifuged at 14,000 g for 30 seconds.
- The column was treated with a DNase I solution and incubated at room temperature for 15 minutes.
- 500 µL Direct-zol™ RNA PreWash was added to the column and the column was incubated at room temperature for 30 seconds.
 - Centrifuged at 14,000 g for 30 seconds

- 500 μ L Direct-zol™ RNA PreWash was added to the column and centrifuged at 14,000 g for 30 seconds.
 - 700 μ L RNA Wash Buffer was added and the column was incubated at room temperature for 2 minutes.
 - Centrifuged at 14,000 g for 2 minutes
 - 500 μ L RNA Wash Buffer was added and the column was centrifuged at 14,000 g for 1 minute.
 - The column was put in a clean tube and centrifuged at 14,000 g for 2 minutes.
 - The column was transferred to an RNase-free 1.5 mL Eppendorf tube and incubated for 1 minute.
 - 50 μ L of DNase/RNase-Free Water was added to the column and centrifuged at 14,000 g for 1 minute.
 - The samples were stored at – 80 °C.
- ✚ *Viable RNA samples were obtained, as determined by the NanoDrop® and Bioanalyzer. All of the samples were deemed viable via the NanoDrop®, but only 60 % to 70 % were viable based on the Bioanalyzer. Small RNAs (200 nt or lower) not viable for cDNA production were present in too high of quantities in 30 % to 40 % of the samples. Some of those samples could be saved by running them through a size exclusion column. An example of viable RNA with a 23S/16S ratio and good RIN number but containing small RNA that needs to be removed with a size exclusion column is shown in Figure C5.*

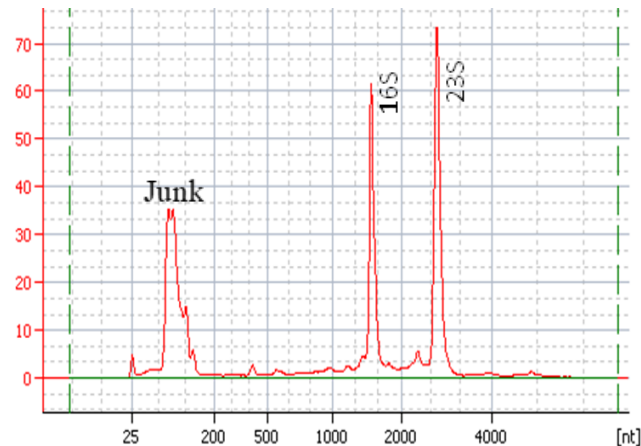


Figure C5. Bioanalyzer results showing viable RNA with a large quantity of small RNA.

cDNA Method Modification

- Long procedure
- Higher g force spins
- Slightly longer incubation times
- A few more washes
- Dry tubes were used for a second spin

✚ *Viable samples*

Conclusions on Final Method for the Zymo Research RNA Kit

- Clean and high yield RNA as determined by the NanoDrop®.
- 30 to 40 % of the samples were contaminated with small RNA as determined by the Bioanalyzer.
 - Some can be saved by using a size exclusion column.
- Switching to a different kit because a method with a higher percent yield of viable RNA samples (less small RNA) was needed.

- Qiagen RNeasy®
- Does not combine steps

Qiagen RNA Extraction Procedures and Modifications

The entire protocol for the initial (unoptimized) and final (optimized) procedures are provided. Changes and rationales for the modifications are described. An explanation of the results of each modification, including whether the changes resulted in viable RNA, is described in italicized text below the listed changes to the procedures.

Starting Procedures (Qiagen 2014)

- 10 μ L β -mercaptoethanol (β -ME) was added per 1 mL Buffer RLT Plus.
- A 4:1 ratio of ethanol to Buffer RPE was added and mix.
- The tube was flicked then 600 μ L Buffer RLT Plus was added.
- The solution was passed 6 times through a medical grade sterile 20 Gage needle.
- The solution was pipetted into a gDNA eliminator spin column in a 2 ml collection tube.
 - Centrifuged at 8,000 g for 30 seconds
 - Discarded the column
- An equal ratio (~600 μ L) of 70% ethanol was added to the solution in the collection tube.
 - It was pipetted up and down a few times to mix

- 700 μ L of the solution at a time was pipetted into a RNeasy spin column in a 2 mL collection tube.
 - Centrifuged at 8,000 g for 15 seconds
 - Discarded the flow-through
- The last step was repeated with the remaining volume of solution.
 - Discarded the flow-through
- 700 μ L Buffer RW1 was added to the RNeasy spin column.
 - Centrifuged at 8,000 g for 15 seconds
 - Discarded the flow-through
- 500 μ L Buffer RPE was added to the RNeasy spin column.
 - Centrifuged at 8,000 g for 15 seconds
 - Discarded the flow-through
- 500 μ L Buffer RPE was added to the RNeasy spin column.
 - Centrifuged at 8,000 g for 2 minutes
- The column was placed into a new 1.5 collection tube.
- 50 μ L RNase-free water was added to the spin column.
 - Centrifuged at 8,000 g for 1 minute
 - Discarded spin column
- The samples were stored at -80°C

✚ *No viable RNA samples were obtained. The samples were not pure, and the concentration of RNA was too low, as determined by the NanoDrop® as shown in*

Table C3. However, higher concentration and purity were obtained with this procedure than with the previous starting procedure.

Table C3. Demonstrates the RNA is nonviable as determined by the NanoDrop®

Sample ID	ng/μl	A260/280	A260/230	A260	A280
Mut ML	5011.28	1.50	1.50	100.23	67.02
WT ML	5118.74	1.31	1.33	102.38	78.17
Mut S	4527.46	1.84	1.90	90.55	49.19
WT S	4925.26	1.63	1.62	98.51	60.31

First Set of Modifications

- The starting solution was vortexed to increase cell lysis
- The solution was pipetted several times before expelling through a 20 Gage needle to increase homogenization.
- And extra centrifuge step was added with a new tube at the end to help pull all moisture out of the column.
- The time was increased to 30 seconds during the second Buffer RPE step to decrease contamination.

 *An increase in sample purity was observed, as determined by the NanoDrop®, but viable RNA samples were not obtained.*

Second Set of Modifications

- Continued with the previous modified procedures.
- The solution at the 70 % ethanol step was vortexed to increase homogenization.
- The g force was increased to 10,000 g to increase flow through and decrease contamination.

- A new column was used in between all centrifuging steps to increase homogenization.
- ✚ *The RNA quality was reduced. Vortexing the solution might have caused the problem. Viable RNA samples were not obtained.*

Third Set of Modifications

- Continued with the previous modified procedures
- Minus the vortexing steps
 - The solutions were pipetted instead.
 - Except for the starting pellet where it was still vortexed.
- Lysozyme was added to increase cell lysis.
- The solution was pipetted 15 times in the 70 % ethanol step to increase homogenization.
- The time was increased to 1 minute during the second Buffer RPE step to decrease contamination.
- The last Buffer RPE was column was placed into a new collection tube and centrifuged again for 1 minute to decrease contamination.
- ✚ *Viable RNA samples were collected, as determined by the NanoDrop® and Bioanalyzer as shown in Figures C6 – C8 and Table C4.*

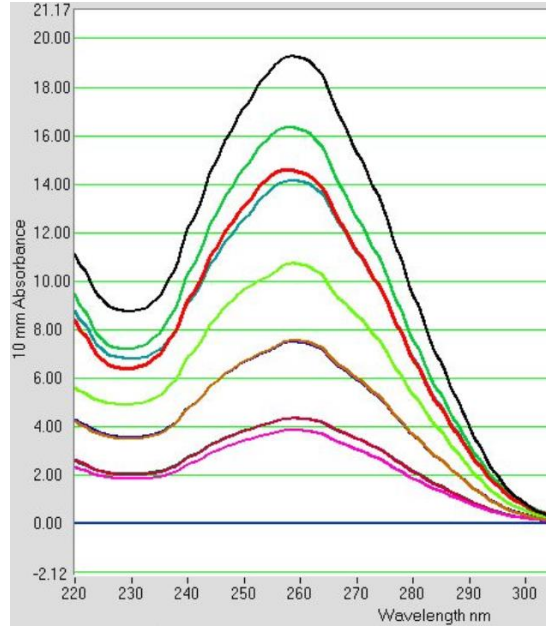


Figure C6. Shows the spectra of multiple viable RNA.

Table C4. Demonstrates viable RNA as determined by the NanoDrop®

Sample ID	ng/ μ l	260/280	260/230
WT ML 1	723.76	2.15	2.27
WT ML 2	190.6	2.10	2.11
WT ML 4	1197.04	2.03	2.05
WT S 1	811.47	2.15	2.26
WT S 2	372.33	2.06	2.11
WT S 3	704.35	2.07	2.08
Mut ML 2	215.05	2.05	2.17
Mut ML 3	214.9	2.03	2.13
Mut ML 4	959.69	2.04	2.20
Mut S 1	533.11	2.02	2.18
Mut S 2	375.09	2.07	2.16
Mut S 4	1474.94	2.06	2.23

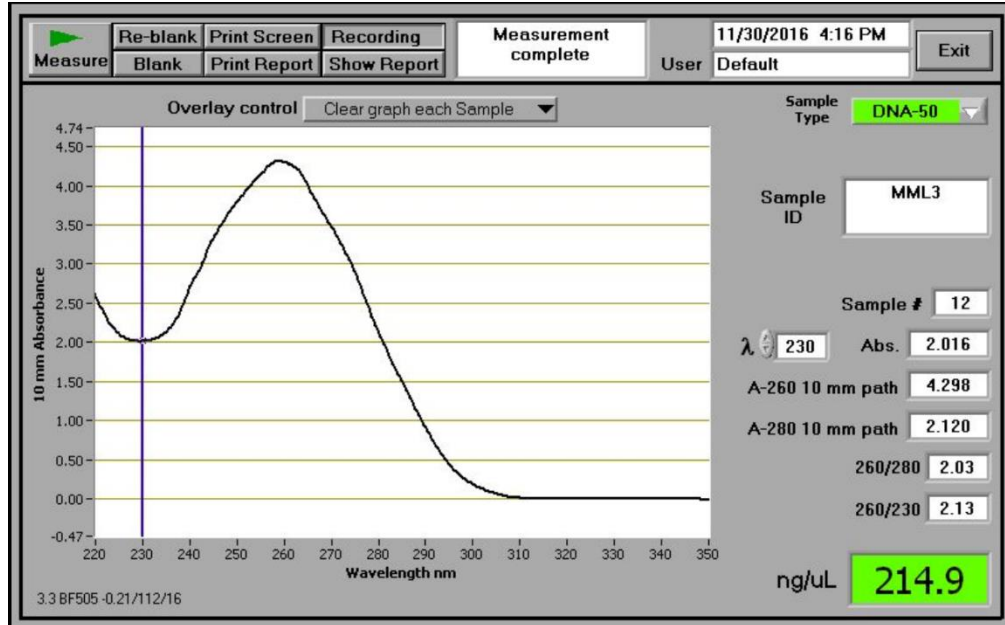


Figure C7. Displays the NanoDrop® screen showing the absorbance readings and ratios along with the concentration and spectrum of a viable sample.

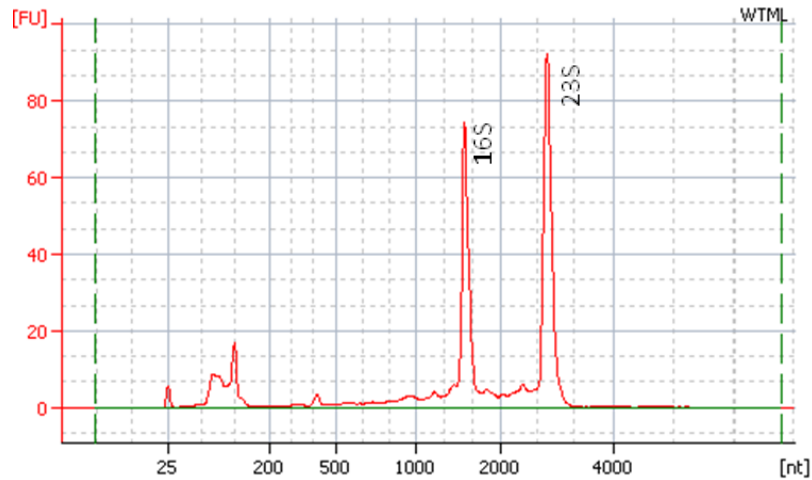


Figure C8. Bioanalyzer results showing viable RNA.

Final Procedure Modifications

The parts of the procedure that were modified are shown in blue.

- 10 μ L β -mercaptoethanol (β -ME) was added per 1 mL Buffer RLT Plus.

- About 1 months' worth at a time was mixed.
- A 4:1 ratio of ethanol to Buffer RPE was added and mix.
- 500 μ L Lysozyme in TE Buffer (pH 8.0) 20 mg/mL was added to the cell pellet on ice for 2 minutes.
 - The solution was vortexed.
- 600 μ L Buffer RLT Plus was added to the tube and pipetted up and down multiple times.
- The solution was pipetted multiple times before it was passed 6 times through a medical grade sterile 20 Gage needle.
- The solution was pipetted into a gDNA eliminator spin column in a 2 ml collection tube.
 - Centrifuged at 10,000 g for 30 seconds
- The column was centrifuged again at 10,000 g for 30 seconds.
 - The column was discarded.
- An equal ratio (~600 μ L) of 70% ethanol was added to the solution in the collection tube.
 - It was pipetted up and down 15 times to mix.
- 700 μ L of the solution at a time was pipetted into a RNeasy spin column in a 2 mL collection tube.
 - Centrifuged at 10,000 g for 15 seconds
 - Discarded the flow-through
- The last step was repeated with the remaining volume of solution.

- Discarded the flow-through
- The column was placed into a new 2 mL collection column.
 - Centrifuged at 10,000 g for 15 seconds
 - Discarded the flow-through
- 700 μ L Buffer RW1 was added to the RNeasy spin column.
 - Centrifuged at 10,000 g for 15 seconds
 - Discarded the flow-through
- The column was placed into a new 2 mL collection column.
 - Centrifuged at 10,000 g for 15 seconds
 - Discarded the flow-through
- 500 μ L Buffer RPE was added to the RNeasy spin column.
 - Centrifuged at 10,000 g for 1 minute
 - Discarded the flow-through
- The column was placed into a new 2 mL collection column.
- 500 μ L Buffer RPE was added to the RNeasy spin column.
 - Centrifuged at 10,000 g for 2 minutes
- The column was placed into a new 2 mL collection tube.
 - Centrifuged at 10,000 g for 1 minutes
- The column was placed into a new 1.5 collection tube.
- 50 μ L RNase-free water was added to the spin column.
 - Centrifuged at 10,000 g for 1 minute
 - Discarded spin column

- The samples were stored at – 80 °C.

cDNA Method Modifications

The cDNA procedures are quite a bit longer and were not included in entirety in this appendix. The RNA protocol was included as an example, and the same types of modifications to the cDNA procedure were made.

- Higher g force spins
- Slightly longer incubation times
 - Except for fragmentation steps
- A few more washes
- Dry tubes were used for a second spin

Viable samples

Affymetrix GeneChip® procedures are outlined in the 180-page instruction manual. There are 10,000 probes for all 20,366 genes in *E. coli* (Affymetrix 2012). A wavelength of 570 nm is used to determine the quantity of nRNA bound to each probe and labeled as the intensity. The data output results in a probe cell ID with intensity readings for all 10,000 probes. The IDs are looked up to obtain the pathways involved. The intensities and IDs would be compared for all 10,000 probes for all sample types (Affymetrix 2009). Unfortunately, the freezer failure ruined all of the prepared and viable RNA samples before the Affymetrix GeneChip® could be used, so no RNA information on the samples was obtained.

Acknowledgements

I would like to thank Professor Mike Franklin and the Franklin Lab for instruction and advice and for the use of their NanoDrop and Bioanalyzer. I would especially like to thank Kerry Williamson from the Franklin Lab for all of her help on how the NanoDrop and Bioanalyzer function and always being available for questions and for time when I was using the Bioanalyzer. I would like to thank Professor Ed Dratz and the Dratz lab for use of their RNA hood. I greatly appreciate the use of equipment and aid provided by Professor Franklin, the Franklin Lab, Kerry Williamson, Professor Dratz and the Dratz lab. This would not have been possible without them.

References

- Affymetrix (2009). GeneChip® Expression Analysis Technical Manual.
<http://affymetrix.com> Accessed October 2016
- Affymetrix (2012). Package Insert: GeneChip® *E. coli* Genome 2.0 Array.
- Biomedical Genomics, (2016). How the Agilent 2100 Bioanalyzer works.
http://biomedicalgenomics.org/How_does_Agilent_2100_Bioanalyzer_work.html
Accessed October 2016
- Kishawi, I. (2008). 2100 Bioanalyzer. Agilent Technologies.
<https://www.agilent.com/cs/library/posters/Public/BioAnalyzer.PDF> Accessed
October 2016
- NanoDrop (2007). NanoDrop Technologies Technical Support Bulletin: 260/280 and
260/230 Ratios. Thermo Scientific. <http://nanodrop.com>. Accessed October 2016
- Qiagen (2014). RNeasy® Plus Mini Handbook. <http://qiagen.com>. Accessed October
2016
- Williamson, K. Montana State University. Personal Communication. 2015
- Zymo Research (2015). Instruction Manual: Direct-zol™ RNA MinniPrep Plus.
<http://zymoresearch.com> Accessed October 2016

CUMULATIVE REFERENCES CITED

- Addinsoft (2021). XLSTAT Statistical and Data Analysis Solution. New York, USA.
<https://www.xlstat.com>.
- Affymetrix (2009). GeneChip® Expression Analysis Technical Manual.
<http://affymetrix.com> Accessed October 2016
- Affymetrix (2012). Package Insert: GeneChip® *E. coli* Genome 2.0 Array.
- Alanis, A. J. (2005) Review Article: Resistance to Antibiotics: Are we in the post-antibiotic era? *Archives of Medical Research*, 36, 697-705.
- Ammons, MC. B., Tripet, B. P., Carlson, R. P., Kirker, K. R., Gross, M. A., Stanisich, J. J., Copié, V. (2014) Quantitative NMR Metabolite Profiling of Methicillin-Resistant and Methicillin-Susceptible *Staphylococcus aureus* Discriminates between Biofilm and Planktonic Phenotypes. *Journal of Proteome Research*, 13, 2973-2985.
- Ammons, MC. B., Morrissey, K., Tripet, B. P., Van Leuven, J. T., Han, A., Lazarus, G. S., Zenilman, J. M., Stewart, P. S., James, G. A., Copié, V. (2015) Biochemical Association of Metabolic Profile and Microbiome in Chronic Pressure Ulcer Wounds. *PLOS one*, 10(5), 1-22. doi:10.1371/journal.pone.0126735.
- Anderson, R. J., Groundwater, P. W., Todd, A., Worsley, A. J. (2012). Microorganisms: In Antibacterial Agents: Chemistry, Mode of Action, Mechanisms of Resistance and Clinical Applications. (pp. 3-32). West Sussex, UK: Wiley.
- Anderson, R. J., Groundwater, P. W., Todd, A., Worsley, A. J. (2012). Glycopeptide Antibiotics: In Antibacterial Agents: Chemistry, Mode of Action, Mechanisms of Resistance and Clinical Applications. (pp. 305-318). West Sussex, UK: Wiley.
- Andre, S., Pieters R. J., Vrsaidas, I., Kaltner, H., Kuwabara, I., Liu, F-T., Liskamp, R. M. J., Gabius, H-J. (2001) Wedgelike Glycodendrimers as Inhibitors of Binding of Mammalian Galectins to Glycoproteins, Lactose Maxiclusters, and Cell Surface Glyconjugates. *ChemBioChem*, 2, 822-830.
- Aries, M.L., Cloninger, M.J. (2020) NMR Metabolomic Analysis of Bacterial Resistance Pathways Using Multivalent Quaternary Ammonium Functionalized Macromolecules. *Metabolomics*, 16(82), 1-11. doi.org/10.1007/s11306-020-01702-1
- Barding, G. A., Salditos, R., Larive, C.K. (2002) Quantitative NMR for Bioanalysis and Metabolomics. *Analytical Bioanalytical Chemistry*, 404, 1165-1179.

- Bertani, B., Ruiz, N. (2018) Function and Biogenesis of Lipopolysaccharides. *EcoSal Plus*, 8(1), 1-33. doi:10.1128/ecosalplus.ESP-0001-2018
- Biomedical Genomics, (2016). How the Agilent 2100 Bioanalyzer works. http://biomedicalgenomics.org/How_does_Agilent_2100_Bioanalyzer_work.html
Accessed October 2016
- Bottone, E.J. (2010) *Bacillus cereus*, a Volatile Human Pathogen. *Clinical Microbiology Reviews*, 23(2), 382-398.
- Brown, S., Santa Maria, J.P. Jr., Walker, S. (2013) Wall Teichoic Acids of Gram-Positive Bacteria. *Annual Review of Microbiology*, 67, 1-28. doi:10.1146/annurev-micro-092412-155620.
- Bundy, J.G., Willey, T.L., Castell, R.S., Ellar, D.J., Brindle, K.M. (2005) Discrimination of Pathogenic Clinical Isolates and Laboratory Strains of *Bacillus cereus* by NMR-Based Metabolomic Profiling. *FEMS Microbiology Letters*, 242, 127-136.
- Ceragiolo, M., Mols, M., Moezelaar, R., Ghelardi, E., Senesi, S., Abee, T. (2010) Comparative Transcriptomic and Phenotypic Analysis of the Responses of *Bacillus cereus* to Various Disinfectant Treatments. *Applied and Environmental Microbiology*, 76(10), 3352-3360.
- Chabre, Y., Roy, R. (2008) Recent Trends in Glycodendrimer Syntheses and Applications. *Current Topics in Medicinal Chemistry*, 8(14), 1237-1285.
- Chamorro, C., Boerman, M.A., Arnusch, C.J., Breukink, E., Pieters, R.J. (2012) Enhancing Membrane Disruption by Targeting and Multivalent Presentation of Antimicrobial Peptides. *Biochimica et Biophysica Acta*, 1818, 2171-2174.
- Chen, C. Z., Beck-Tan, N. C., Dhurjati, P., Van Dyk, T. K., LaRossa, R. A., Cooper, S. L. (2000) Quaternary Ammonium Functionalized Poly(propylene imine) Dendrimers as Effective Antimicrobials: Structure-Activity Studies, *Biomacromolecules*, 1, 473-480.
- Chen, A., Peng, H., Blakey, I., Whittaker, A.K. (2017) Biocidal Polymers: A Mechanistic Overview. *Polymer reviews*, 57(2), 276-310.
- Chenomx (2016) N.M.R. Suite 8.2. Edmonton: Chenomx Inc.
- Chenomx (2020) N.M.R. Suite 8.4. Edmonton: Chenomx Inc.

- Chong, J., Wishart, D. S., Xia, J. (2019) Using MetaboAnalyst 4.0 for Comprehensive and Integrative Metabolomics Data Analysis. *Current Protocols in Bioinformatics*, 68, e86.
- Cloninger, M. J. (2002) Biological Applications of Dendrimers. *Current Opinions in Chemical Biology*, 6, 742-748.
- Cox, E., Michalak, A., Pagentine, S., Seaton, P., Pokorny, A. (2014) Lysylated Phospholipids Stabilize Models of Bacterial Lipid Bilayers and Protect Against Antimicrobial Peptides. *Biochimica et Biophysica Acta*, 1838(9), 2198-2204.
- Denamur, E., Matic, I. (2006) Evolution of Mutation Rates in Bacteria. *Molecular Microbiology*, 60 (4), 820-827.
- Dettmer, K., Aronov, P. A., Hammock, B. D. (2007) Mass Spectrometry-Based Metabolomics. *Mass Spectrometry Review*, 26, 51-78.
- Emwas A-H., Saccenti, E., Gao, X., McKay, R.T., Martins dos Santos, V.A.P., Roy, R., Wishart, D.S. (2018) Recommend Strategies for Spectral Processing and Post-Processing of 1D ¹H-NMR Data of Biofluids with a Particular Focus on Urine. *Metabolomics*, 14(31), 1-23.
- Engel, R., Ghani, I., Montenegro, D., Thomas, M., Klaritch-Vrana, B., Castaño, A., Friedman, L., Leb, J., Rothman, L., Lee, H., Capodiferro, C., Ambinder, D., Cere, E., Awad, C., Sheikh, F., Rizzo, J.L., Nisbett, L-M., Testani, E., Melkonian, K. (2011) Polycationic Glycosides. *Molecules*, 16, 1508-1518.
- García-Gallego, S., Franci, G., Falanga, A., Gómez, R., Folliero, V., Galdiero, S., Javier de la Mata, F., Galdiero, M. (2017) Function Oriented Molecular Design: Dendrimers as Novel Antimicrobials. *Molecules*, 22, 1581-1610.
- Gerba, C.P. (2015) Quaternary Ammonium Biocides: Efficacy in Application. *Applied and Environmental Microbiology*, 81(2), 464-469.
- González-Bello, C. (2017) Antibiotic Adjuvants- A Strategy to Unlock Bacterial Resistance to Antibiotics. *Bioorganic and Medicinal Chemistry Letters*, 27, 4221-4228.
- Hammes, W., Schleifer, K. H., Kandler, O. (1973) Mode of Action of Glycine on the Biosynthesis of Peptidoglycan. *Journal of Bacteriology*, 116(2), 1029-1053.

- Hebecker, S., Krausze, J., Hasenkampf, T., Schneider, J., Groenewold, M., Reichelt, J., Jahn, D., Heinz, D.W., Moser, J. (2015) Structures of Two Bacterial Resistance Factors Mediating tRNA-Dependent Aminoacylation of Phosphatidylglycerol with Lysine or Alanine. *PNAS*, 112(34), 10691-10696.
- Hoerr, V., Duggan, G. E., Zbytnuik, L., Poon, K. K. H., Große, C., Neugebauer, U., Methling, K., Löffler, B., Vogel, H. J. (2016) Characterization and Prediction of the Mechanism of action of antibiotics through NMR Metabolomics. *BMC Microbiology*, 16(82), 1-14. doi:10.1186/s12866-016-0696-5
- Humann, J., Lenz, L. L. (2009) Bacterial Peptidoglycan Degrading Enzymes and their Impact on Host Muropeptide Detection. *Journal of Innate Immunity*, 1, 88-97.
- Hurdle J.G., O'Neill, A.J., Chopra, I., Lee, R.E. (2011) Targeting Bacterial Membrane Function: an Underexploited Mechanism of Treating Persistent Infections. *Nature Reviews Microbiology*, 9, 62-75.
- Jiao, Y., Niu, L-n., Ma, S., Li, J., Tay, F. R., Chen, J-h. (2017) Quaternary Ammonium-Based Biomedical Materials: State-of-the-Art, Toxicological Aspects and Antimicrobial Resistance. *Progress in Polymer Science*, 71, 53-90.
- Kanehisa, M., Goto, S. (2000) KEGG: Kyoto Encyclopedia of Genes and Genomes. *Nucleic Acid Research*, 28, 27-30.
- Kilcullen, K., Teunis, A., Popova, T.G., Popov, S.G. (2016) Cytotoxic Potential of *Bacillus cereus* Strains ATCC 11778 and 14579 against Human Lung Epithelial Cells under Microaerobic Growth Conditions. *Frontiers in Microbiology*, 7(69), 1-12.
- Kim, S.J., Chang, J., Singh, M. (2015) Peptidoglycan Architecture of Gram-Positive Bacteria by Solid-State NMR. *Biochimica et Biophysica Acta*, 1848, 350–362.
- Kishawi, I. (2008). 2100 Bioanalyzer. Agilent Technologies. <https://www.agilent.com/cs/library/posters/Public/BioAnalyzer.PDF> Accessed October 2016
- Kügler, R., Bouloussa, O., Rondelez, F. (2005) Evidence of Charge-Density Threshold for Optimum Efficiency of Biocidal Cationic Surfaces. *Microbiology*, 151, 1341-1349.

- Lämmerhofer, M., Weckwerth, W., Eds, (2013) NMR-Based Metabolomic Analysis: In Metabolomics in Practice: Successful Strategies to Generate and Analyze Metabolic Data. (pp. 209-233). Weinheim, Germany: Wiley-VCH.
- Lang, D.R., Lundgren, D.G. (1970) Lipid Composition of *Bacillus cereus* During Growth and Sporulation. *Journal of Bacteriology*, 101(2), 483-489.
- Lindon, J. C., Nicholson, J. K., Holmes, E. (2007). NMR Spectroscopic Techniques for Application to Metabonomics: In the Handbook of Metabolomics and Metabonomics. (pp. 55-112). Oxford, UK: Elsevier.
- Loskill, P., Pereira, P.M., Jung, P., Bischoff, M., Herrmann, M., Pinho, M.G., Jacobs, K. (2014) Reduction of the Peptidoglycan Crosslinking Causes a Decrease in the Stiffness of the *Staphylococcus aureus* Cell Envelope. *Biophysical Journal*, 107, 1082-1089.
- Lu, W., Pieters, R. J. (2019) Carbohydrate-Protein Interactions and Multivalency: Implications for the Inhibition of Influenza A Virus Infections. *Expert Opinion on Drug Discovery*, 14(4), 387-395.
- Mai-Prochnow, A., Clauson, M., Hong, J., Murphy, A.B. (2016) Gram-Positive and Gram-Negative Bacteria Differ in their Sensitivity to Cold Plasma. *Scientific Reports*, 6(38610), 1-11. doi:0.1038/srep38610
- Malanovic, N., Lohner K. (2016) Antimicrobial Peptides Targeting Gram-Positive Bacteria. *Pharmaceuticals*, 9(59), 1-33.
- Martinez, J. L., Baquero, F. (2000) Minireview: Mutation Frequency and Antibiotic Resistance. *Antimicrobial Agents and Chemotherapy*, 44(7), 1771-1777.
- Mengin-Lecreulx, D., Blanot, D., VanHeijenoort, J. (1994) Replacement of Diaminopimelic acid by Cystathionine or Lanthionine in the Peptidoglycan of *Escherichia coli*. *Journal of Bacteriology*, 176(14), 434-437.
- McDonnell, G., Russell, A. D. (1999) Antiseptics and Disinfectants: Activity, Action and Resistance. *Clinical Microbiology Review*, 12(1), 147-226.
- Metabolomics Workbench. (2020) <https://www.metabolomicsworkbench.org/StudyID/ST001351>. Accessed November 13, 2021.
- Metabolomics Workbench. (2021) <https://www.metabolomicsworkbench.org/StudyID/ST001966>. Accessed November 13, 2021.

- Mintzer, M. A., Dane, E. L., O'Toole, G. A., Grinstaff, M. W. (2011) Exploiting Dendrimer Multivalency to Combat Emerging and Reemerging Infectious Diseases. *Molecular Pharmaceutics*, 9, 342-354.
- NanoDrop (2007). NanoDrop Technologies Technical Support Bulletin: 260/280 and 260/230 Ratios. Thermo Scientific. <http://nanodrop.com>. Accessed October 2016
- Nguyen, L.T., Haney, E.F., Vogel, H.J. (2011) The Expanding Scope of Antimicrobial Peptide Structures and their Modes of Action. *Trend in Biotechnology*, 29(9), 464-472.
- Nikolaidis, I., Favini-Stabile, S., Dessen, A. (2014) Resistance to antibiotics targeted to the bacterial cell wall. *Protein Science*. 23, 243-259.
- Paleos, C. M., Tsiourvas, D., Sideratou Z., Tziveleka, L-A. (2010) Drug Delivery using Multifunctional Dendrimers and Hyperbranched Polymers. *Expert Opinion on Drug Delivery*, 7, 1387-1398.
- Pang, Z., Chong, J., Zhou, G., Morais D., Chang, L., Barrette, M., Gauthier, C., Jacques, PE., Li, S., and Xia, J. (2021) MetaboAnalyst 5.0: narrowing the gap between raw spectra and functional insights *Nucleic Acids Research* 49. doi: 10.1093/nar/gkab382
- Percy, M.G., Gründling, A. (2014) Lipoteichoic Acid Synthesis and Function in Gram-Positive Bacteria. *Annual Review of Microbiology*, 68, 81-100.
- Milo R., Phillips, R. (2015) Cell Biology by the Numbers. (pp. 88-91). Garland Science. <http://book.bionumbers.org/what-is-the-thickness-of-the-cell-membrane/> Accessed December 13, 2021.
- Perlin, M. H., Clark, D. R., McKenzie, C., Patel, H., Jackson, N., Kormanik, C., Powell, C., Bajorek, A., Myers, D. A., Dugatkin, L.A., Atlas, M. R. (2009) Protection of Salmonella by Ampicillin-Resistant Escherichia coli in the presence of otherwise Lethal Drug Concentrations. *Proceedings of the Royal Society B*, 276, 3759-3768.
- Pokhrel, S., Nagaraja, K. S., Varghese, B. (2004) Preparation, Characterization and X-ray Structure Analysis of 1,4-diazabicyclo-2,2,2-octane (DABCO) and Ammonium Cation with Tetrathiomolybdate Anion. *Journal of Structural Chemistry*, 45(5), 900-905.
- Pieters, R.J., Arnusch, C.J., Breukink, E. (2009) Membrane Permeabilization by Multivalent Anti-Microbial Peptides. *Protein & Peptide Letters*, 16 (7), 1-7.

- Qiagen (2014). RNeasy® Plus Mini Handbook. <http://qiagen.com>. Accessed October 2016
- Richard, C., Megin-Lecreulx, D., Pochet, S., Johnson, E.J., Cogen, G.N., Marlière, P. Directed Evolution of Biosynthetic Pathways. *The Journal of Biological Chemistry*, 268(36) 26827-26835.
- Richards, S-J., Isufi, K., Wilkins, L.E., Lipecki, J., Fullam, E., Gibson, M.I. (2018) Multivalent Antimicrobial Polymer Nanoparticles Target Mycobacteria and Gram-Negative Bacteria by Distinct Mechanisms. *Biomacromolecules*, 19, 256-264.
- Rowlett V.W., Mallampalli, V.K.P.S., Karlstaedt, A., Dowhan, W., Taegtmeier, H., Margolin, W., Vitrac, H. (2017) Impact of Membrane Phospholipid Alterations in *Escherichia coli* on Cellular Function and Bacterial Stress Adaptation. *Journal of Bacteriology*, 199(13), 1-22.
- Roy, R. (2003) A Decade of Glycodendrimer Chemistry. *Trends in Glycoscience and Glycotechnology*, 15(85), 291-310.
- Sabnis, A., Hagart, K.L.H., Klockner, A., Becce, M., Evan, L.E., Furniss, R.C.D., Despoina, A.I., Mavridou, D.A., Murphy, R., Stevens, M.M., Davies, J.C., Larrouy-Maumus, G.J., Clarke, T.B., Edwards, A.M., (2021) Colistin kills bacteria by targeting lipopolysaccharide in the cytoplasmic membrane. *eLife* 2021;10:e65836 DOI: 10.7554/eLife.65836
- Schleifer, K.H., Kandler, O. (1972) Peptidoglycan Types of Bacterial Cell Walls and their Taxonomic Implications. *Bacteriological Reviews*, 36(4), 407-477.
- Schneewind, O., Missiakas, D. (2014) Lipoteichoic Acids, Phosphate-containing Polymers in the Envelope of Gram-positive Bacteria. *Journal of Bacteriology*, 196(6), 1133-1142.
- Shepherd, J., Ibba, M. (2013) Direction of Aminoacylated transfer RNAs into Antibiotic Synthesis and Peptidoglycan-Mediated Antibiotic Resistance. *FEBS Letters*, 587(18), 2895-2904.
- Shulaev, V. (2006) Metabolomics technology and bioinformatics. *Briefings in Bioinformatics*, 7(2), 128-139.
- Soini, J., Ukkonen, K., Neubauer, P. (2008) High Cell Density Media for *Escherichia coli* are Generally Designed for Aerobic Cultivations – Consequences for Large-Scale bioprocesses and Shake Flask Cultures. *Microbial Cell Factors* 7, 26-36.

- Sreepereumbuduru, R. S., Abid, Z. M., Claunch, K. M., Chen, H. H., McGillivray, S. M., Simanek, E. E. (2016) Synthesis and Antimicrobial Activity of Triazine Dendrimers with DABCO Groups. *Royal Society of Chemistry Advances*, 6, 8806-8810.
- Tautenhahn, R., Cho, K., Uritboonthai, W., Zhu, Z., Patti, G.J., Siuzdak, G. (2012) An Accelerated Workflow for Untargeted Metabolomics using the METLIN Database. *Nature Biotechnology Correspondence*, 30(9), 826-828.
- Tiller, J.C., Liao, C-J., Lewis, K., Klivanov, A.M. (2001) Designing Surfaces that Kill Bacteria on Contact. *PNAS*, 98(11), 5981-5985.
- Timofeeva, L., Kleshcheva, N. (2011) Antimicrobial Polymers: Mechanism of Action, Factors of Activity, and Applications. *Applications in Microbiology and Biotechnology*, 89, 475-492.
- Todar, K., (2020). Textbook of Bacteriology (Online). University of Wisconsin, <http://textbookofbacteriology.net>. Accessed October 2021
- Turkoglu, O., Cital, A., Katar, C., Mert, I., Kumar, p., Yilmaz, A., Uygur, D.S., Erkata, S., Graham, S.F., Bahado-Singh, R.O. (2019) Metabolomic Identification of Novel Diagnostic Biomarkers in Ectopic Pregnancy. *Metabolomics*, 15(143), 1-11.
- VanKoten, H.W., Dlakic, W.M., Engel, R., Cloninger, M.J. (2016) Synthesis and Biological Activity of Highly Cationic Dendrimer Antibiotics. *Molecular Pharmaceutics* 13, 3827-3834. doi.org/10.1021/acs.molpharmaceut.6b00628
- Vembu, S., Pazhamalai, S., Gopalakrishnan, M. (2015) Potential Antibacterial Activity of Triazine Dendrimer: Synthesis and Controllable Drug Release Properties. *Bioorganic and Medicinal Chemistry*, 23, 4561-4566.
- Vollmer, W., Bertsche, U. (2008) Murein (peptidoglycan) Structure, Architecture and Biosynthesis in *Escherichia coli*. *Biochimica et Biophysica Acta*, 1778, 1714-1734.
- Vollmer, W., Blanot, D., de Pedro, M.A. (2008) Peptidoglycan Structure and Architecture. *FEMS Microbiology Review*. 32, 149-167.
- Wang, N. S. [Online] Experiment No. 9 °C Measurements of Cell Biomass Concentration. Department of Chemical and Biomolecular Engineering, University of Maryland, MD. <http://www.eng.umd.edu/~nsw/ench485/lab9c.htm>. (Accessed November 2019).

- Williamson, K. Montana State University. Personal Communication. 2015
- Wishart, D.S. (2008) Quantitative Metabolomics using NMR. *Trends in Analytical Chemistry*, 27(3), 228-237.
- Wolfenden, M., Cousin, J., Nangia-Makker, P., Raz, A., Cloninger, M. (2015) Glycodendrimers and Modified ELISAs: Tools to Elucidate Multivalent Interactions of Galectins 1 and 3. *Molecules*, 20, 7059-7096.
- Wrońska, N., Majoral, J. P., Appelhans, D., Bryszewska, M., Lisowska, K. (2019) Synergistic Effects of Anionic/Cationic Dendrimers and Levofloxacin on Antibacterial Activities. *Molecules*, 24, 2894-2905.
- Wu, X., Han, J., Gong, G., Koffas, M.A.G., Zha, J. (2021) Wall Teichoic Acids: Physiology and Applications. *FEMS Microbiology Reviews*, 45(4), 1-23.
- Xu, C., Lin, L., Ren, H., Zhang, Y., Wang, S., Peng, X. (2006) Analysis of Outer Membrane Proteome of *Escherichia coli* Related to Resistance to Ampicillin and Tetracycline. *Proteomics*, 6, 462-473.
- Xue, X., Chen, X., Mao, X., Hou, Z., Zhou, Y., Bai, H., Meng, J., Da, F., Sang, G., Wang, Y., Lou, X. (2013) Amino-Terminated Generation 2 Poly(amidoamine) Dendrimer as a Potential Broad-Spectrum, Nonresistance-Inducing Antibacterial Agent. *AAPS Journal*, 15, 132-142.
- Zhao, H., Roistacher, D.M., Helmann J.D. (2018) Aspartate Deficiency Limits Peptidoglycan Synthesis and Sensitizes Cells to Antibiotics Targeting Cell Wall Synthesis in *Bacillus subtilis*. *Molecular Microbiology*, 109(6), 826-844.
- Zymo Research (2015). Instruction Manual: Direct-zol™ RNA MinniPrep Plus. <http://zymoresearch.com> Accessed October 2016